



ISSN: 1696-2281
eISSN: 2013-8830
SORT 38 (2) July-December 2014

SORT

Statistics and Operations Research Transactions

Coediting institutions

*Universitat Politècnica de Catalunya
Universitat de Barcelona
Universitat de Girona
Universitat Autònoma de Barcelona
Universitat Pompeu Fabra
Universitat de Lleida
Institut d'Estadística de Catalunya*

Supporting institutions

*Spanish Region of the International Biometric Society
Societat Catalana d'Estadística*



Generalitat
de Catalunya
**Institut d'Estadística
de Catalunya**

SORT

Volume 38

Number 2

July-December 2014

ISSN: 1696-2281

eISSN: 2013-8830

Foreword

Articles

- Stochastic cash flows modeled by homogeneous and non-homogeneous discrete time backward semi-Markov reward processes 107
Fulvio Gismondi, Jacques Janssen, Raimondo Manca and Ernesto Volpe di Prignano
- Assessing the impact of early detection biases on breast cancer survival of Catalan women 139
Albert Roso-Llorach, Carles Forné, Francesc Macià, Jaume Galceran, Rafael Marcos-Gragera and Montserrat Rué
- Estimators for the parameter mean of Morgenstern type bivariate generalized exponential distribution using ranked set sampling 161
Saeid Tahmasebi and Ali Akbar Jafari
- Integrating network design and frequency setting in public transportation networks: a survey . . . 181
Francisco López-Ramos
- An extension of the slash-elliptical distribution 215
Mario A. Rojas, Heleno Bolfarine and Héctor W. Gómez
- New approaches in the chemometric analysis of infrared spectra of extra-virgin olive oils 231
María Isabel Sánchez-Rodríguez, Elena M. Sánchez-López, Alberto Marinas, José M^a Caridad, Francisco José Urbano and José M^a Marinas
- Exact prediction intervals for future current records and record range from any continuous distribution 251
Haroon Barakat, Elsayed Nigm and Ramy Aldallal
- Balancing properties: A need for the application of propensity score methods in estimation of treatment effects 271
Arantza Urkaregi, Lorea Martínez-Indart and José Ignacio Pijoán
- Untangling the influence of several contextual variables on the respondents' lexical choices. A statistical approach 285
Mónica Bécue-Bertaut, Jérôme Pagès and Belchin Kostov
- Selected article from *XIV Conferencia Española de Biometría 2013*
- Global hypothesis test to compare the likelihood ratios of multiple binary diagnostic tests with ignorable missing data 305
Ana Eugenia Marín-Jiménez and José Antonio Roldán-Nofuentes

Foreword

This issue is dedicated to the memory of M. Jesús Bayarri (Susie), who was a member of the Advisory Committee of SORT. The Editorial Committee of SORT expresses its deepest condolences to her family and colleagues from the *Universitat de València* and Duke University. We are immensely grateful for her contributions to our journal, and in particular for the discussion in the 2009 paper from Fuentes and Casella. Although she was busy and very selective with the projects in which she did participate, she continued with her support to SORT and felt sad because she could not be of more help.

Susie was well known for her many and deep contributions in Bayesian statistics, although her scope was broader and her influence has been enormous in many other topics such as computer models, model selection, decision theory and in the foundations of statistical inference. Many students and colleagues have learnt and benefitted from her knowledge, the discussions she engaged in and her passion for life. Susie's contributions raised the bar of statistics in Spain, and it is in good measure thanks to her that statistics in Spain got international visibility. Her active and generous participation in several scientific networks (in particular, the National Network of Biostatistics, Biostatnet), and Societies (she was President of the International Bayesian for Bayesian Analysis as well as the Spanish Region of the International Biometric Society) will always be remembered.



Stochastic cash flows modelled by homogeneous and non-homogeneous discrete time backward semi-Markov reward processes

Fulvio Gismondi¹, Jacques Janssen², Raimondo Manca³
and Ernesto Volpe di Prignano³

Abstract

The main aim of this paper is to give a systematization on the stochastic cash flows evolution. The tools that are used for this purpose are discrete time semi-Markov reward processes. The paper is directed not only to semi-Markov researchers but also to a wider public, presenting a full treatment of these tools both in homogeneous and non-homogeneous environment. The main result given in the paper is the natural correspondence of the stochastic cash flows with the semi-Markov reward processes. Indeed, the semi-Markov environment gives the possibility to follow a multi-state random system in which the randomness is not only in the transition to the next state but also in the time of transition. Furthermore, rewards permit the introduction of a financial environment into the model. Considering all these properties, any stochastic cash flow can be naturally modelled by means of semi-Markov reward processes. The backward case offers the possibility of considering in a complete way the duration inside a state of the studied system and this fact can be very useful in the evaluation of insurance contracts.

MSC: 60K15, 60K20, 91B28, 91B30.

Keywords: Stochastic cash flows, insurance contracts, discrete time backward semi-Markov processes, reward processes, homogeneous and non-homogeneous processes.

1. Introduction

By stochastic cash flow (SCF) we mean a financial operation (Janssen et al., 2009) in which the flow amount is stochastic. Furthermore, it is possible that the time of payments can be stochastic.

¹“Guglielmo Marconi” University.

²Solvay Business School, Université Libre de Bruxelles, Belgium. janssenwets.jacques@gmail.com

³Sapienza Università di Roma. Dipartimento di Metodi e Modelli per l'Economia, il Territorio e la Finanza. raimondo.manca@uniroma1.it; ernesto.volpe@gmail.com

Received: August 2012

Accepted: April 2014

More precisely, the discrete flow value in both cases can fluctuate within a time interval that we suppose being a subset of \mathbb{N} . Indeed in real life problems, the money amount is a discrete variable and the time of payments is a discrete variable. Under these assumptions, a SCF can be seen as an example of a bivariate discrete time stochastic process where the first variable is the time and the second the money amount.

The study of SCF has been particularly developed in a financial environment and in various aspects of insurance. Many papers were written on the evaluation of annuities with stochastic interest rates and/or on stochastic cash flow evaluation. In this environment, we recall the following papers: Artikis and Malliaris (1990), Artikis and Voudori (2000), Beekman and Fuelling (1991), Browne (1995), De Schepper and Goovaerts (1992), De Schepper et al. (1994), Donati-Martin et al. (2000), Duffie et al. (2000), Dufresne (2001), Halliwell (2003), Harrison (1977), Milevsky (1997), Milevsky and Posner (1998), Parker (1994), Perry and Stadje (2000, 2001), Pliska (1986), Sato and Yor (1998), Vanneste et al. (1994, 1997) and the books of Wolthuis (2003) and Yor (2001). All these papers and books face the problem of using the stochastic calculus tools under Markovian hypotheses with continuous states and continuous times. These hypotheses implies that the waiting time distribution functions (WTDF) are exponential, and furthermore that the duration inside the state cannot be considered in a Markov environment. In real life these hypotheses in the most cases are not verified.

Another way to evaluate a SCF was given by Wilkie (1986) and subsequently improved in Wilkie (1995). This model uses traditional time series tools. In this case, the model pointed to the study of future asset returns of an insurance company. This model cannot be considered a general model for the study of evolution of SCF and also in this case the duration inside the states cannot be considered.

As is well known, (see Janssen et al., 2009), financial operation is a set of financial supply (T_k, S_k) where S_k represents an amount and T_k the time of the payment of S_k . We can suppose that:

1. S_k depends on the state of a system and, usually, also on the time of the payment;
2. the change of state happens at a random time.

The introduction of this second random variable, as specified in Estes et al. (1989) complicates the calculation of the cash flow value at a given date.

If we suppose that, in a discrete time environment, the bivariate stochastic process future depends only on the present and not on the past history and that the WTDF between two transitions can be of any type, then we are in a semi-Markov process (SMP) environment (see Janssen and Manca, 2006 and 2007 and their references).

It is already known that the applications of the SMP to finance and insurance problems assume great relevance and in the literature these applications were given, for example, in Janssen (1966), Hoem (1972), CMIR (1991), Carravetta et al. (1981), Balcer and Sahin (1979, 1986), Swishchuck (1995), De Medici et al. (1995), Janssen and Manca (1997, 1998), Janssen et al. (2004) and in the book Janssen and Manca (2007).

In the study of cash flow evolution and the related evaluation, the present value and the “accumulated value” assume great relevance. The association of an amount of money to a state of the system and/or to a state transition can be done by attaching a reward structure to the process. This structure can be thought of as a random variable associated with the state occupancies and/or the transitions, see Howard (1971) in which is given a nice presentation of Homogeneous Semi-Markov ReWard Processes (HSMRWP).

Non-homogeneous semi-Markov reward processes (NHSMRWP) were defined in De Dominicis and Manca (1986), and we recall more recent papers (Papadopoulou et al., 2012 and Papadopoulou, 2013) that applied this tool in other fields.

The rewards can be of different kinds but, in a financial environment, it makes sense to consider only amounts of money as rewards. These amounts can be positive for the system if they can be seen as a benefit and negative if they can be considered as a cost.

SMRWP is a very important tool for applications, and most relevant when it is necessary to consider the random evolution of a multi-state system in which amounts of money are involved in this evolution. Despite these considerations, these kinds of processes, as far as the authors know, have not yet been fully dealt with in the financial and actuarial literature.

The main aim of this paper is showing how natural is modelling SCF by means of SMRWP. For these reasons, the paper is directed not only to semi-Markov experts but, in general, to financial practitioners and in particular to actuaries. Furthermore in the paper, new evolution equations are presented that give more application possibilities to this powerful tool.

A good description of HSMRWP appeared in Howard (1971), although not all the relevant aspects that could have been dealt with were outlined.

A complete description of the homogeneous and non-homogeneous SMRWP and a general presentation of SMP in homogeneous and non-homogeneous cases can be found in Janssen and Manca (2006, 2007).

In the semi-Markov environment, a backward time represents the time spent in a state before the valuation point of the system. In the first book on semi-Markov (Silvestrov, 1980) the SMP evolution equations were presented only taking into account backward times. In this case, the transition probabilities are also conditioned by the time of entrance into a given state. Instead in a semi-Markov process, when backward times are not considered then we are in the hypothesis that the entrance time was just at the valuation point. Backwards times give the possibility to take into account in a complete way the duration inside a state. In a Markov environment, backward time cannot be considered and also in Wilkie’s models this aspect was not considered.

A detailed description of homogeneous backward semi-Markov processes is reported in Limnios and Oprüsan (2001). The discrete time non-homogeneous semi-Markov reward processes with backward recurrence time were described in Stenberg et al. (2007).

In the second section of the paper, the reward notations will be introduced. In Sections 3 and 4 the Discrete Time Homogeneous and Non-Homogeneous semi-Markov

processes (DTHSMRP, DTNHSMRP) will be introduced before in the simplest way and after with the initial backward recurrence time. After, the Discrete Time Homogeneous and Non-Homogeneous Semi-Markov ReWard Process (DTHSMRWP, DTNHSMRWP) relations will be given. In addition, the related backward semi-Markov Reward Process will be presented. Section 5 will give matrix notations for the DTHSMRWP, DTNHSMRWP and the second moments of these processes as defined in Stenberg et al. (2006, 2007). Section 6 will present how it is possible to follow and to evaluate, in a natural way, the evolution of SCFs by means of the presented stochastic processes. Furthermore, in this section generalizations of the models given in Stenberg et al. (2006, 2007) will also be presented. Section 7 presents a real data application of these processes that describes the construction of an insurance disability model. The last section will highlight the main results presented in the paper and the addresses of future works.

2. Rewards notation

The association of a sum of money to a state of the system and to a state transition assumes great relevance in the study of financial phenomena. This can be done by attaching a reward structure to a stochastic process. This structure can be thought as a random variable associated with state occupancies and transitions (Howard, 1971).

In the homogeneous case, the time evolution of the system is function of the duration that the system is in a state after a transition.

In the non-homogeneous environment the time evolution of the system is a function of two times: the arriving time in a state and the time of the subsequent transition. For these reasons, the rewards can be a function of the duration time in the homogeneous case, whereas, in the non-homogeneous environment they can also be function of both the starting time and the ending time. In the two different environments, the same differences can also hold for the financial variables.

There are two kinds of rewards; one that is paid or received because of remaining in a state (permanence rewards), the other that is paid or received because of a transition (transition rewards). In the literature, *permanence reward* and *transition reward* are also called respectively *rate reward* and *impulse reward* (see Qureshi and Sanders, 1994).

In the non-homogeneous process, it is possible to take into account the fact that the interest rates can change as a function of the starting time of the financial operation.

For this reason, the variable interest rate could change as a function of the duration of the financial operation (homogeneous variable interest rate) and/or because of the start and the end times of the financial operation (non-homogeneous variable interest rate). It may also be possible to consider a stochastic interest rate (see Janssen Manca, 2002).

In NHSMRWP, non-homogeneity makes it possible to take into account the rewards that change because of both the times s and t .

$$\psi_{i,j}, \psi_{i,j}(t), \psi_{i,j}(s, t)$$

denote the reward that is given for the transition from the i^{th} state:

- the first the cases in which the payment flow in the state i is constant in time, changing only in function of the state,
- the second when the payment is a function of the state and of the time,
- the third when the rate rewards change because of starting and arriving times, in this case we say that there is a non-homogenous payment (the cash flow is function of the state, the time of entrance into the state and the time of payment).

For each state, usually, there is a different reward and ψ , $\psi(t)$, $\psi(s, t)$ represents the vector of these rewards respectively in case of constant rewards, rewards that change because of running time and non-homogeneous rewards. It should be mentioned that it may also be possible to consider permanence rewards that change because of the next transition (see Howard, 1971, Janssen and Manca, 2006, Papadopoulou and Tsaklidis, 2007), but in this paper we will not present the related evolution equations because, in a financial environment, they would not make sense.

Let γ_{ij} , $\gamma_{ij}(t)$, $\gamma_{ij}(s, t)$ denote the reward that is given for the transition from the i^{th} state to to the j^{th} one (impulse reward); the difference between the three symbols is the same as in the previous cases. \bar{A} is the matrix of the transition rewards. The different kinds of ψ rewards represent a stochastic money discrete time flow that is paid or received because of staying in a state. On the other hand, γ represents lump sums that are paid at the instant of transition.

As far as the impulse reward γ concerned, in the case of discounting, it is only necessary to compute the present value of the lump sum paid at the moment of the related transition.

Reward structure can be considered a very general structure attached to the problem being studied. This random variable evolves together with the stochastic process to which it is linked. When the studied system, that evolves dynamically in a random way, is in a state then a reward of ψ type can be paid; once there is a transition, a reward of γ type could be paid.

This behaviour is particularly efficient in the construction of models which are useful for following the dynamic evolution of insurance problems. Indeed, permanence in a state involves the payment of a premium or the receipt of a claim. In addition, the transition from one state to another can often bring about some cost or benefit.

3. DTSMP with a finite state set

In this section, DTHSMP and DTNHSMP will be described following the SMP notation given in Janssen and Manca (2006) and (2007).

Given the complete filtered probability space $(\Omega, \mathfrak{F}, \mathfrak{F}_t, P)$ in which the following two sequences of random variables (r.v.s) are

1. $J_n : \Omega \rightarrow I = \{1, 2, \dots, m\}$, $n \in \mathbb{N}$ representing the state at the n^{th} transition.
2. $T_n : \Omega \rightarrow \mathbb{N}$ representing the time of the n^{th} transition.

We suppose that (J_n, T_n) is a homogeneous (non-homogeneous) Markov renewal process of kernel $\mathbf{Q} = [Q_{ij}(t)]$ ($\mathbf{Q} = [Q_{ij}(s, t)]$), where:

$$\begin{aligned} Q_{ij}(t) &\equiv P[J_{n+1} = j, T_{n+1} - T_n \leq t | \sigma(J_a, T_a), 0 \leq a < n, J_n = i] \\ &= P[J_{n+1} = j, T_{n+1} - T_n \leq t | J_n = i]. \end{aligned}$$

$$\left(\begin{aligned} Q_{ij}(s, t) &\equiv P[J_{n+1} = j, T_{n+1} \leq t | \sigma(J_a, T_a), 0 \leq a < n, J_n = i, T_n = s] \\ &= P[J_{n+1} = j, T_{n+1} \leq t | J_n = i, T_n = s]. \end{aligned} \right)$$

Furthermore we define

$$X_n = T_n - T_{n-1}.$$

X_n represents the so called *inter-arrival time*, i.e. the time spent between two subsequent transitions.

We know also that:

$$p_{ij} = P[J_{n+1} = j | J_n = i] = \lim_{t \rightarrow \infty} Q_{ij}(t); i, j \in I, t \in \mathbb{N}$$

$$p_{ij}(s) = P[J_{n+1} = j | J_n = i, T_n = s] = \lim_{t \rightarrow \infty} Q_{ij}(s, t); i, j \in I, s, t \in \mathbb{N}$$

where $\mathbf{P} = [p_{ij}]$ and $\mathbf{P}(s) = [p_{ij}(s)]$ are the transition matrices of the embedded homogeneous and non-homogeneous Markov chain respectively. It is also necessary to introduce the probability that the process will leave state i in a time t :

$$H_i(t) \equiv P[T_{n+1} - T_n \leq t | J_n = i],$$

$$H_i(s, t) \equiv P[T_{n+1} \leq t | J_n = i, T_n = s].$$

Obviously, it results that:

$$H_i(t) = \sum_{j=1}^m Q_{ij}(t),$$

$$H_i(s, t) = \sum_{j=1}^m Q_{ij}(s, t),$$

where $H_i(t)$ and $H_i(s, t)$ are distribution functions (d.f.); then:

$$\lim_{t \rightarrow \infty} H_i(t) = 1, \quad \forall i,$$

$$\lim_{t \rightarrow \infty} H_i(s, t) = 1, \quad \forall i.$$

Now the d.f. WTDF for each state i can be defined, given that the state successively occupied is known:

$$F_{ij}(t) = P[T_{n+1} - T_n \leq t | J_n = i, J_{n+1} = j],$$

$$F_{ij}(s, t) = P[T_{n+1} \leq t | J_n = i, J_{n+1} = j, T_n = s].$$

The difference between Markov and semi-Markov processes is mainly in these d.f. Indeed, in the discrete time Markov case, these d.f. can only be geometric distribution whereas in the semi-Markov case they could be of any type.

The related probabilities can be obtained by means of the following relations:

$$F_{ij}(t) = \begin{cases} Q_{ij}(t)/p_{ij} & \text{if } p_{ij} \neq 0 \\ U_1(t) & \text{if } p_{ij} = 0 \end{cases}$$

$$F_{ij}(s, t) = \begin{cases} Q_{ij}(s, t)/p_{ij}(s) & \text{if } p_{ij}(s) \neq 0 \\ U_1(s, t) & \text{if } p_{ij}(s) = 0 \end{cases}$$

where:

$$U_1(t) = \begin{cases} 0 & \text{if } 0 > t \\ 1 & \text{if } 0 \leq t. \end{cases} \quad \text{and} \quad U_1(s, t) = \begin{cases} 0 & \text{if } s > t \\ 1 & \text{if } s \leq t. \end{cases}$$

In a discrete time environment, it is necessary to define the following probabilities:

$$b_{ij}(t) = P[J_{n+1} = j, T_{n+1} - T_n = t | J_n = i],$$

$$b_{ij}(s, t) = P[J_{n+1} = j, T_{n+1} = t | J_n = j, T_n = s].$$

resulting in:

$$b_{ij}(t) = \begin{cases} 0 & \text{if } t = 0 \\ Q_{ij}(t) - Q_{ij}(t-1) & \text{if } t > 0 \end{cases}$$

$$b_{ij}(s, t) = \begin{cases} 0 & \text{if } s = t \\ Q_{ij}(s, t) - Q_{ij}(s, t-1) & \text{if } t > s \end{cases}$$

Fixed:

$$N(t) = \sup \{n | T_n \leq t\}, \quad \forall t \in \mathbb{N}$$

the DTHSMP and DTNHSMP $Z = (Z_t, t \in \mathbb{N})$ can be defined. where $Z(t) = J_{N(t)}$ represents, for each time t , the state occupied by the process. In the non-homogeneous case, supposing that s is a transition time, the transition probabilities are defined in the following way:

$$\begin{aligned} \phi_{ij}(t) &= P[Z_t = j | Z_0 = i] \\ \phi_{ij}(s, t) &= P[Z_t = j | Z_s = i] \end{aligned}$$

They are obtained solving the following evolution equations:

$$\phi_{ij}(t) = \delta_{ij}(1 - H_i(t)) + \sum_{\beta=1}^m \sum_{\vartheta=1}^t b_{i\beta}(\vartheta) \phi_{\beta j}(t - \vartheta), \quad (1)$$

$$\phi_{ij}(s, t) = \delta_{ij}(1 - H_i(s, t)) + \sum_{\beta=1}^m \sum_{\vartheta=s+1}^t b_{i\beta}(s, \vartheta) \phi_{\beta j}(\vartheta, t), \quad (2)$$

where δ_{ij} represents the Kronecker symbol.

Both (1) and (2) can be obtained by means of a simple probabilistic argument using the regenerative property of the Markov renewal process (see Janssen and Manca, 2006 and 2007).

With the aim of clarification the meaning of the parts of (2) is given:

$$\delta_{ij}(1 - H_i(s, t))$$

represents the probability of remaining in the state i without any transition from the time s up to time t , and it only makes sense if $i = j$; this is the reason for the Kronecker delta.

$$\sum_{\vartheta=s+1}^t b_{i\beta}(s, \vartheta) \phi_{\beta j}(\vartheta, t)$$

represents the probabilities of all the possible trajectories that can be followed going from state i at time s to state j at time t .

In Figure 1 a typical trajectory of a semi-Markov process is shown.

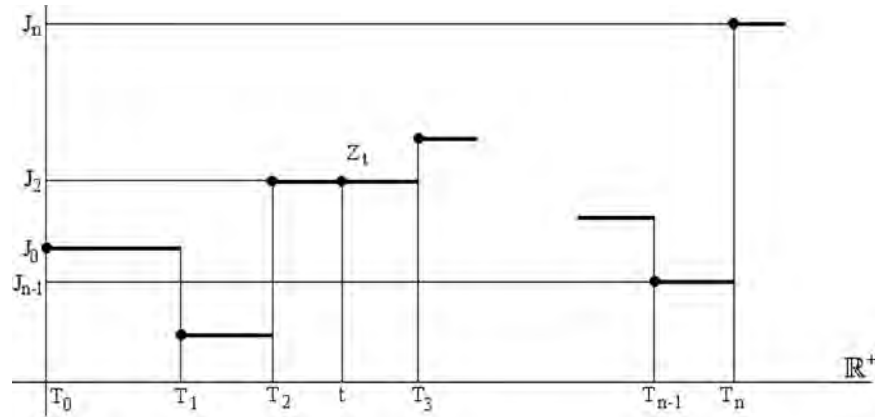


Figure 1: Trajectory of a SMP.

Now the backward recurrence process will be introduced. To explain the meaning of backward time, we present Figure 2 and Figure 3 in which homogeneous and non-homogeneous cases are shown.

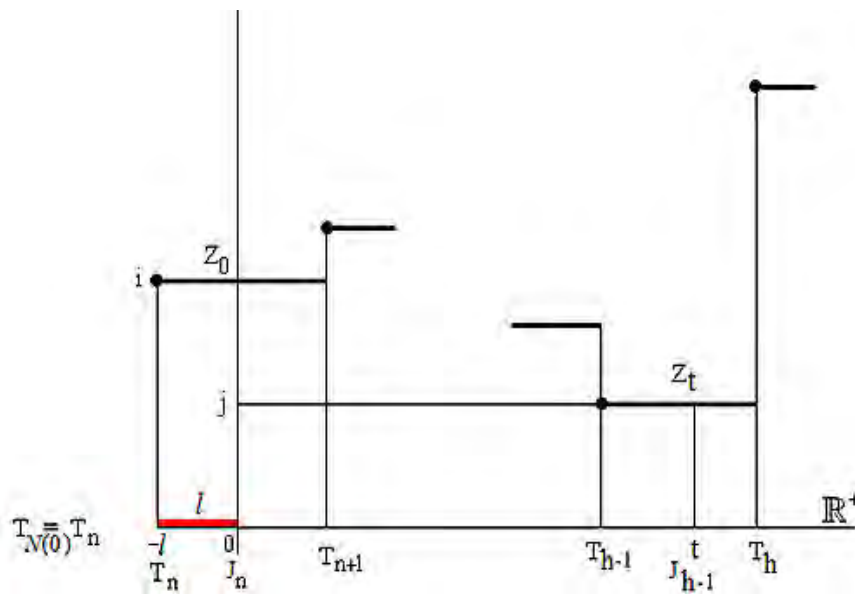


Figure 2: Trajectory of a HSMP with recurrence backward time.

We follow the system from time s up time t , but, this time, we consider in a non-homogeneous environment that the system entered the state i at time $s - u$ and that the system does not move from i for a period of time u that is the recurrence backward time.

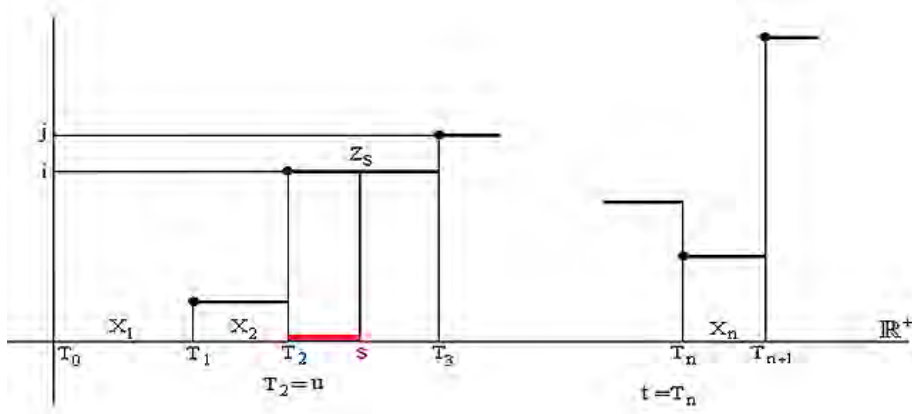


Figure 3: Trajectory of a NHSMP with recurrence backward time.

In order to take into account the backward time, it is necessary to condition the system to remain for a time u inside the state i .

Under the backward assumptions, the relations 1 and 2 become respectively:

$${}^b\phi_{ij}(u;t) = \delta_{ij} \frac{(1 - H_i(t+u))}{(1 - H_i(u))} + \sum_{\beta=1}^m \sum_{\vartheta=1}^t \frac{b_{i\beta}(\vartheta+u)}{(1 - H_i(u))} \phi_{\beta j}(0;t-\vartheta),$$

$${}^b\phi_{ij}(u,s;t) = \delta_{ij} \frac{(1 - H_i(u,t))}{(1 - H_i(u,s))} + \sum_{\beta=1}^m \sum_{\vartheta=s+1}^t \frac{b_{i\beta}(u,\vartheta)}{(1 - H_i(u,s))} \phi_{\beta j}(0,\vartheta;t),$$

where

$${}^b\phi_{ij}(u,t) = \mathbb{P} [Z(t) = j | Z(0) = i, T_{N(0)} = -u]$$

$${}^b\phi_{ij}(u,s;t) = \mathbb{P} [Z(t) = j | Z(s) = i, T_{N(s)} = u]$$

In the homogeneous case it is supposed that the system arrived a time u before 0 in the state i and it does not move from the arriving time up to 0. In the non-homogeneous case, it is supposed that the system arrived at time u in the state i and does not move from this state up to the time s .

4. The semi-Markov reward process with backward time

In this part, the DTHSMRWP and DTNHSMRWP will be introduced.

As in the previous section, before presenting the backward relations the SMRWP evolution equations will be given. This is to point out that the SMRWP are a class of stochastic processes, in the sense that, depending on the problem to be faced, a different

evolution equation will be obtained. A classification of DTSMRWP was given in Janssen and Manca (2007).

In DT two general cases should be considered the DTSMRWP-immediate and the DTSMRWP-due. In the following we give two different evolution equations, one homogeneous and one non-homogeneous, the first for the due and the other for the immediate. The first case has the time-variable permanence and impulse rewards and variable rate of interest. The non-homogeneous case has non-homogeneous rate of interest and rewards.

For each case we present in (3) and (5) the reward process and in (4) and (6) the related semi-Markov reward evolution equations that are the mean of the process, as it is proved in Stenberg et al. (2006, 2007) and more recently in a more general case in D'Amico et al. (2013).

$$\begin{aligned}
\ddot{\xi}_i(t) &\equiv 1_{\{T_{N(0)+1} > t | J_{N(0)} = i\}} \left(\sum_{\tau=1}^t \psi_i(\tau) \nu(\tau-1) \right) \\
&+ \sum_{k=1}^m \sum_{\vartheta=1}^t 1_{\{J_{N(0)+1} = k, T_{N(0)+1} = \vartheta | J_{N(0)} = i\}} \left(\sum_{\tau=1}^{T_{N(0)+1}} \psi_i(\tau) \nu(\tau-1) \right) \\
&+ \sum_{k=1}^m \sum_{\vartheta=1}^t 1_{\{J_{N(0)+1} = k, T_{N(0)+1} = \vartheta | J_{N(0)} = i\}} \nu(T_{N(0)+1}) \gamma_{iJ_{N(0)+1}}(T_{N(0)+1}) \\
&+ \sum_{k=1}^m \sum_{\vartheta=1}^t 1_{\{J_{N(0)+1} = k, T_{N(0)+1} = \vartheta | J_{N(0)} = i\}} \ddot{\xi}_{J_{N(0)+1}}(t - T_{N(0)+1})
\end{aligned} \tag{3}$$

$$\begin{aligned}
\dot{V}_i(t) &= (1 - H_i(t)) \sum_{\theta=1}^t \psi_i(\theta) \nu(\theta-1) + \sum_{k=1}^m \sum_{\vartheta=1}^t b_{ik}(\vartheta) \sum_{\theta=1}^{\vartheta} \psi_i(\theta) \nu(\theta-1) \\
&+ \sum_{k=1}^m \sum_{\vartheta=1}^t b_{ik}(\vartheta) \nu(\vartheta) \gamma_{ik}(\vartheta) + \sum_{k=1}^m \sum_{\vartheta=1}^t b_{ik}(\vartheta) \nu(\vartheta) \dot{V}_k(t - \vartheta),
\end{aligned} \tag{4}$$

$$\begin{aligned}
\xi_i(s, t) &\equiv 1_{\{T_{N(s)+1} > t | J_{N(s)} = i, T_{N(s)} = s\}} \left(\sum_{\tau=s+1}^t \psi_i(s, \tau) \nu(s, \tau) \right) \\
&+ \sum_{k=1}^m \sum_{\vartheta=s+1}^t 1_{\{J_{N(s)+1} = k, T_{N(s)+1} = \vartheta | J_{N(s)} = i, T_{N(s)} = s\}} \left(\sum_{\tau=s+1}^{T_{N(s)+1}} \psi_i(s, \tau) \nu(s, \tau) \right) \\
&+ \sum_{k=1}^m \sum_{\vartheta=s+1}^t 1_{\{J_{N(s)+1} = k, T_{N(s)+1} = \vartheta | J_{N(s)} = i, T_{N(s)} = s\}} \nu(s, T_{N(s)+1}) \gamma_{iJ_{N(s)+1}}(s, T_{N(s)+1}) \\
&+ \sum_{k=1}^m \sum_{\vartheta=s+1}^t 1_{\{J_{N(s)+1} = k, T_{N(s)+1} = \vartheta | J_{N(s)} = i, T_{N(s)} = s\}} \nu(s, T_{N(s)+1}) \xi_{J_{N(s)+1}}(T_{N(s)+1}; t)
\end{aligned} \tag{5}$$

$$\begin{aligned}
V_i(s, t) = & (1 - H_i(s, t)) \sum_{\theta=s+1}^t \psi_i(s, \theta) v(s, \theta) + \sum_{k=1}^m \sum_{\vartheta=s+1}^t b_{ik}(s, \vartheta) \sum_{\theta=s+1}^{\vartheta} \psi_i(s, \theta) v(s, \theta) \\
& + \sum_{k=1}^m \sum_{\vartheta=s+1}^t b_{ik}(s, \vartheta) v(s, \vartheta) \gamma_{ik}(s, \vartheta) + \sum_{k=1}^m \sum_{\vartheta=s+1}^t b_{ik}(s, \vartheta) v(s, \vartheta) V_k(\vartheta, t) \quad (6)
\end{aligned}$$

where:

$$\begin{aligned}
v(t) &= \begin{cases} 1 & \text{if } t = 0 \\ \prod_{\tau=1}^t (1 + r(\tau))^{-1} & \text{if } t > 0 \end{cases}; \\
v(s, t) &= \begin{cases} 1 & \text{if } t = s \\ \prod_{\tau=s+1}^t (1 + r(s, \tau))^{-1} & \text{if } t > s \end{cases} \\
1_{\{T_{N(0)+1} > t | J_{N(0)} = i\}} &:= \begin{cases} 1 & \text{if } T_{N(0)+1}(\omega) > t \quad \omega \in \Omega(i, 0) \\ 0 & \text{otherwise,} \end{cases} \\
\Omega(i, 0) &= \{\omega \in \Omega : J_{N(s)}(\omega) = i, T_{N(s)}(\omega) = 0\}.
\end{aligned}$$

For a deeper understanding, the interested reader can refer to D'Amico et al. (2013)

- both permanence (or rate) and transition (or impulse) rewards are considered,
- the rewards in (3) and (4) are homogeneous in time and (5) and (6) non-homogeneous,
- the interest rates are in (3) fixed, in (4) and (6) variable in time and in (5) non-homogeneous.

Remark 4.1. *The introduction of stochastic interest rate does not present any difficulties (see Janssen et al., 2002).*

The interested reader can find other cases in the Janssen and Manca (2006, 2007) books.

Now we present a homogenous and a non-homogenous case with backward times. The homogeneous is in an immediate environment, the non-homogeneous in a due. As before we present before the reward processes and after the related evolution equations. The first time index gives the backward time. The hypotheses on interest rates and on rewards are the same of the relations given in (3) and (5).

In the homogeneous case the backward time is negative because it is supposed to begin following the system, after each transition, at time 0. The non-homogeneous backward relations, in which the first index time gives the backward, the second the starting horizon time and the third the ending time are the following:

$$\begin{aligned}
{}^b \ddot{\xi}_i(u, s; t) &\equiv 1_{\{T_{N(s)+1} > t | J_{N(s)} = i, T_{N(s)} = u, T_{N(s)+1} > s\}} \left(\sum_{\tau=s+1}^t \psi_i(s, \tau) \nu(s, \tau - 1) \right) \\
&+ \sum_{k=1}^m \sum_{\vartheta=s+1}^t 1_{\{J_{N(s)+1} = k, T_{N(s)+1} = \vartheta | J_{N(s)} = i, T_{N(s)} = u, T_{N(s)+1} > s\}} \left(\sum_{\tau=s+1}^{T_{N(s)+1}} \psi_i(s, \tau) \nu(s, \tau - 1) \right) \quad (7) \\
&+ \sum_{k=1}^m \sum_{\vartheta=s+1}^t 1_{\{J_{N(s)+1} = k, T_{N(s)+1} = \vartheta | J_{N(s)} = i, T_{N(s)} = u, T_{N(s)+1} > s\}} \nu(s, T_{N(s)+1}) \gamma_{iJ_{N(s)+1}}(s, T_{N(s)+1}) \\
&+ \sum_{k=1}^m \sum_{\vartheta=s+1}^t 1_{\{J_{N(s)+1} = k, T_{N(s)+1} = \vartheta | J_{N(s)} = i, T_{N(s)} = u, T_{N(s)+1} > s\}} \nu(s, T_{N(s)+1}) \ddot{\xi}_{J_{N(s)+1}}(T_{N(s)+1}, T_{N(s)+1}; t)
\end{aligned}$$

$$\begin{aligned}
\dot{V}_i(u, s; t) &= \frac{(1 - H_i(u, t))}{(1 - H_i(u, s))} \sum_{\theta=s+1}^t \psi_i(s, \theta) \nu(s, \theta) \\
&+ \sum_{k=1}^m \sum_{\vartheta=s+1}^t \frac{b_{ik}(u, \vartheta)}{(1 - H_i(u, s))} \sum_{\theta=s+1}^{\vartheta} \psi_i(s, \theta) \nu(s, \theta) \quad (8) \\
&+ \sum_{k=1}^m \sum_{\vartheta=s+1}^t \frac{b_{ik}(u, \vartheta)}{(1 - H_i(u, s))} \gamma_{ik}(s, \vartheta) \nu(s, \vartheta) \\
&+ \sum_{k=1}^m \sum_{\vartheta=s+1}^t \frac{b_{ik}(u, \vartheta)}{(1 - H_i(u, s))} \dot{V}_k(0, \vartheta; t) \nu(s, \vartheta).
\end{aligned}$$

$$\begin{aligned}
{}^b \xi_i(-u; t) &\equiv 1_{\{T_{N(0)+1} > t | J_{N(0)} = i, T_{N(0)} = -u, T_{N(0)+1} > 0\}} \left(\sum_{\tau=1}^t \psi_i(\tau) \nu(\tau) \right) \\
&+ \sum_{k=1}^m \sum_{\vartheta=1}^t 1_{\{J_{N(0)+1} = k, T_{N(0)+1} = \vartheta | J_{N(0)} = i, T_{N(0)} = -u, T_{N(0)+1} > 0\}} \left(\sum_{\tau=s+1}^{T_{N(s)+1}} \psi_i(\tau) \nu(\tau) \right) \quad (9) \\
&+ \sum_{k=1}^m \sum_{\vartheta=1}^t 1_{\{J_{N(0)+1} = k, T_{N(0)+1} = \vartheta | J_{N(0)} = i, T_{N(0)} = -u, T_{N(0)+1} > 0\}} \nu(T_{N(0)+1}) \gamma_{iJ_{N(s)+1}}(T_{N(0)+1}) \\
&+ \sum_{k=1}^m \sum_{\vartheta=1}^t 1_{\{J_{N(0)+1} = k, T_{N(0)+1} = \vartheta | J_{N(0)} = i, T_{N(0)} = -u, T_{N(0)+1} > 0\}} \nu(T_{N(0)+1}) \xi_{J_{N(0)+1}}(0; t - T_{N(0)+1})
\end{aligned}$$

$$\begin{aligned}
V_i(u; t) &= \frac{(1 - H_i(t + u))}{(1 - H_i(u))} \sum_{\theta=1}^t \psi_i(\theta) \nu(\theta) + \sum_{k=1}^m \sum_{\vartheta=1}^t \frac{b_{ik}(\vartheta + u)}{(1 - H_i(u))} \sum_{\theta=1}^{\vartheta} \psi_i(\theta) \nu(\theta) \quad (10) \\
&+ \sum_{k=1}^m \sum_{\vartheta=1}^t \frac{b_{ik}(\vartheta + u)}{(1 - H_i(u))} \nu(\vartheta) \gamma_{ik}(\vartheta) + \sum_{k=1}^m \sum_{\vartheta=1}^t \frac{b_{ik}(\vartheta + u)}{(1 - H_i(u))} \nu(\vartheta) V_k(0; t - \vartheta).
\end{aligned}$$

Now we explain the meaning of (8), the meaning of the other relations is similar and can be easily understood. The first part of (8)

$$\frac{(1 - H_i(u, t))}{(1 - H_i(u, s))} \sum_{\theta=s+1}^t \psi_i(s, \theta) v(s, \theta) \quad (11)$$

can be seen as a discrete time annuity with non-homogeneous variable instalments $\psi_i(s, \theta)$ discounted by means of a non-homogeneous interest rate that is calculated from time s up to time $t - 1$. (11) is conditioned in function of the arrival time in the state i at time u .

The second part

$$\sum_{k=1}^m \sum_{\vartheta=s+1}^t \frac{b_{ik}(u, \vartheta)}{(1 - H_i(u, s))} \sum_{\theta=s+1}^{\vartheta} \psi_i(s, \theta) v(s, \theta)$$

represents the rewards that were paid up to the moment of the first transition, still with the same conditioning.

The third and fourth parts

$$\sum_{k=1}^m \sum_{\vartheta=s+1}^t \frac{b_{ik}(u, \vartheta)}{(1 - H_i(u, s))} \check{V}_k(0, \vartheta; t) v(s, \vartheta) + \sum_{k=1}^m \sum_{\vartheta=s+1}^t \frac{b_{ik}(u, \vartheta)}{(1 - H_i(u, s))} \gamma_{ik}(s, \vartheta) v(s, \vartheta)$$

explain what happened at the transition moments. Indeed, $\gamma_{ik}(s, \vartheta)$ represents the transition reward that is paid at the transition instant and $\check{V}_k(0, \vartheta; t)$ the mean present value of all the payments made from time ϑ up to time t . Both sums are evaluated at time ϑ so it is necessary to discount them at time s , thus the presence of the discount factor. In this case, the conditioning to arrive at time u in the state i is also considered.

The algorithm to solve the discrete time homogeneous and non-homogeneous backward case are given in Stenberg et al. (2006, 2007) respectively.

Remark 4.2. *The choice between the homogeneous and non-homogeneous cases depends on the available data. Non-homogeneity is closer to real life problems in the case of time that depends on age or seniority is certainly better to use it (insurance problems) but, in order to apply it, a great quantity of data is necessary. If the database is not huge it can be better to remain in a homogeneous environment.*

Remark 4.3. *The backward times are fundamental in the evaluation of many insurance contracts (in our opinion any insurance contract is a SCF). For example, if we have to consider the disability in an insurance contract the dead probability of a disabled person is different from the dead probability of a healthy person. But this difference decreases as a function of the time distance from the beginning of the disability time (see D'Amico et al., 2009b).*

5. The risk estimation

The evolution equation of the reward processes gives the mean present value of the stochastic financial operation. But in a stochastic environment it remains fundamental also the evaluation of the risk, i.e. the estimation of the variability. In Stenberg et al. (2006, 2007) the formulas for the higher moments of the reward processes were presented. We will report only the second order moment formula, the calculation of variance and of standard deviation.

The relation (6), in matrix form can be rewritten in the following way:

$$\mathbf{V}(u; t) = \mathbf{D}(u; t) \cdot \mathbf{A}(t) * \mathbf{1}_m + \sum_{\vartheta=1}^t (\mathbf{B}(u; \vartheta) \cdot \tilde{\mathbf{A}}(\vartheta)) * \mathbf{1}_m + \sum_{\vartheta=1}^t (\mathbf{B}(u; \vartheta) * \mathbf{V}(0; t - \vartheta)) \nu(\vartheta),$$

where:

* represents the row-column matrix product,

· represents the element by element (Hadamard) matrix product,

$\mathbf{D}(u; t)$ is a diagonal matrix whose elements in the main diagonal are $\frac{(1 - H_i(u, t))}{(1 - H_i(u, s))}$

$\mathbf{A}(t)$ is a diagonal matrix whose elements in the main diagonal are $\sum_{\theta=1}^t \psi_i(\theta) \nu(\theta)$

$$\mathbf{B}(u; \vartheta) = \left[\left(\frac{b_{ik}(\vartheta + u)}{(1 - H_i(u))} \right)_{ik} \right] \quad (12)$$

$$\tilde{\mathbf{A}}(\vartheta) = \left[\left(\sum_{\theta=1}^{\vartheta} \psi_i(\theta) \nu(\theta) + \nu(\vartheta) \gamma_{ik}(\vartheta) \right)_{ik} \right] \quad (13)$$

$\mathbf{1}$ is the sum vector.

Remark 5.1. The relations (12) and (13) denote the general element of the respective matrices.

(8) can be rewritten in the following matrix form:

$$\begin{aligned} \check{\mathbf{V}}(u, s; t) &= \mathbf{D}(u, s; t) \cdot \check{\mathbf{A}}(s, t) * \mathbf{1}_m + \sum_{\vartheta=1}^t (\mathbf{B}(u, s; \vartheta) \cdot \check{\check{\mathbf{A}}}(s, \vartheta)) * \mathbf{1}_m + \\ &+ \sum_{\vartheta=1}^t (\mathbf{B}(u, s; \vartheta) * \check{\mathbf{V}}(0, \vartheta; t)) \nu(s, \vartheta), \end{aligned}$$

where:

$\mathbf{D}(u, s; t)$ is a diagonal matrix whose elements in the main diagonal are $\frac{(1 - H_i(u, t))}{(1 - H_i(u, s))}$

$$\mathbf{B}(u, s; \vartheta) = \left[\left(\frac{b_{ik}(u, \vartheta)}{(1 - H_i(u, s))} \right)_{ik} \right]$$

$\tilde{\mathbf{A}}(s, t)$ is a diagonal matrix whose elements in the main diagonal are $\sum_{\theta=s}^{t-1} \psi_i(s, \theta) \nu(s, \theta)$

$$\tilde{\tilde{\mathbf{A}}}(s, \vartheta) = \left[\left(\sum_{\theta=s+1}^{\vartheta} \psi_i(s, \theta) \prod_{\tau=s}^{\theta-1} (1 + r(s, \tau))^{-1} + \gamma_{ik}(s, \vartheta) \prod_{\tau=s+1}^{\vartheta} (1 + r(s, \tau))^{-1} \right)_{ik} \right].$$

Now we will present the matrix form of the evolution equations of the second order moments of our two examples

1. Homogeneous immediate case:

$$\begin{aligned} \mathbf{V}^{(2)}(u; t) &= \mathbf{D}(u; t) \cdot \mathbf{A}^{(2)}(t) * \mathbf{1}_m + \sum_{\vartheta=1}^t \left(\mathbf{B}(u; \vartheta) \cdot \tilde{\mathbf{A}}^{(2)}(\vartheta) \right) * \mathbf{1}_m \quad (14) \\ &+ \sum_{\vartheta=1}^t \left(\mathbf{B}(u; \vartheta) \cdot \tilde{\mathbf{A}}(\vartheta) \right) 2\nu(s, \vartheta) * \mathbf{V}(0; t - \vartheta) + \sum_{\vartheta=1}^t \left(\mathbf{B}(u; \vartheta) * \mathbf{V}^{(2)}(0; t - \vartheta) \right) \nu(s, \vartheta)^2, \end{aligned}$$

2. Non-homogeneous due case:

$$\begin{aligned} \tilde{\mathbf{V}}^{(2)}(u, s; t) &= \mathbf{D}(u, s; t) \cdot \tilde{\mathbf{A}}^{(2)}(s, t) * \mathbf{1}_m + \sum_{\vartheta=s+1}^t \left(\mathbf{B}(u, s; \vartheta) \cdot \tilde{\tilde{\mathbf{A}}}^{(2)}(s, \vartheta) \right) * \mathbf{1}_m \\ &+ \sum_{\vartheta=s+1}^t \left(\mathbf{B}(u, s; \vartheta) \cdot \tilde{\tilde{\mathbf{A}}}(s, \vartheta) \right) * \tilde{\mathbf{V}}(0, \vartheta; t) 2 \prod_{\tau=s+1}^{\vartheta} (1 + r(s, \tau))^{-1} \quad (15) \\ &+ \sum_{\vartheta=s+1}^t \left(\mathbf{B}(u, s; \vartheta) * \tilde{\mathbf{V}}^{(2)}(0, \vartheta; t) \right) \prod_{\tau=s+1}^{\vartheta} (1 + r(s, \tau))^{-2}, \end{aligned}$$

where $\mathbf{V}^{(2)}(u; t)$ and $\tilde{\mathbf{V}}^{(2)}(u, s; t)$ are the second order moment of stochastic processes (7) and (9) respectively.

The proof of relations similar to (14) and (15) can be found in Stenberg et al. (2006, 2007) respectively.

Remark 5.2. *The DTSMRWP and DTNHSRWP presented In Stenberg et al. (2006, 2007) did not consider the differences between immediate and due models. These differences are fundamental in the model construction for applications.*

Remark 5.3. *As already outlined the reward processes are a class of stochastic processes. The consideration of backward times increases the number of the different kinds of processes.*

Once that the first and the second moments are known it is possible to calculate in a very simple way the variance and the standard deviation (see Stenberg et al., 2006, 2007).

6. SCF and semi-Markov reward processes

A deterministic cash flow is a finite or countable vector

$$\mathbf{O} = ((S_1, T_1), (S_2, T_2), \dots)$$

whose elements are couples (S_i, T_i) where S_i is a sum and T_i is the time in which S_i is paid (negative value) or cashed (positive value). A cash flow is fair at a given time t if its value is equal 0.

A SCF is always a vector of couples but this time the first element of the couples is always a random variables and the time in some cases but not always is random. The vector could also have a finite or infinite order.

Remark 6.1. *The time of transition rewards is always random. Permanence rewards can be paid or cashed at each time period or randomly. For this reason the time can sometimes be considered deterministic. It is also possible that in some state the permanence rewards should not be computed. In this last case we can consider for all the period of staying in the state without permanence rewards that are equal to 0.*

Our hypotheses are:

1. $J_n \in I, I \subset \mathbb{R}, |I| \in \mathbb{N}$ or $|I| = |\mathbb{N}|$ where $|A|$ represents the cardinality of A .
2. $T_n \in \mathbb{N}$
- 3.a $\mathbb{P}[J_{n+1} = j, T_{n+1} - T_n \leq t - T_{n+1} < T_{n+2} - T_{n+1} | (J_n, T_n), (J_{n-1}, T_{n-1}), \dots, (J_0, T_0)]$
 $= \mathbb{P}[J_{n+1} = j, T_{n+1} - T_n \leq t - T_{n+1} < T_{n+2} - T_{n+1} | J_n].$ (16)

in the homogeneous environment and

- 3.b $\mathbb{P}[J_{n+1} = j, T_{n+1} \leq t < T_{n+2} | (J_n, T_n), (J_{n-1}, T_{n-1}), \dots, (J_0, T_0)]$
 $= \mathbb{P}[J_{n+1} = j, T_{n+1} \leq t < T_{n+2} | (J_n, T_n)]$ (17)

in non-homogeneous case.

4. The horizon time is given by:

$$[0, T], T \in \mathbb{N} \text{ if the horizon is limited,}$$

$$[0, +\infty) \text{ if the horizon is infinite}$$

Remark 6.2. (16) and (17) describe what happens to the SCF at each time of transition. The state of the system at time t is j . If there are permanence rewards they will be paid between two subsequent transitions. More precisely we know that $T_n - T_{n-1} = X_n$ and X_n rate rewards, one for each period, will be paid or received in case of deterministic permanence rewards. These rewards will be paid or cashed at the beginning of the period in the due case and at the end in the immediate case. In case of existence of transition rewards at the transition time an impulse reward will be paid or cashed.

Supposing that:

1. at time the system start in the state i ,
2. at transition time the system arrive at state j ,
3. there are both permanence and transition rewards,
4. the permanence and the transition rewards change because of running time.

This financial operation in the immediate case can be described in the following way:

$$\mathbf{O} = ((\psi_i(1), 1), (\psi_i(2), 2), \dots, (\psi_i(X_1), X_1), (\gamma_{ik_1}, T_1), (\psi_{k_1}(T_1 + 1), T_1 + 1),$$

$$(\psi_{k_1}(T_1 + 2), T_1 + 2), \dots, (\psi_{k_1}(T_1 + X_2), T_1 + X_2), (\gamma_{k_1k_2}, T_2), (\psi_{k_2}(T_2 + 1), T_2 + 1),$$

$$\dots, (\psi_{k_2}(T_2 + X_3), T_2 + X_3), (\gamma_{k_2k_3}, T_3), \dots, (\gamma_{k_{n-1}k_n}, T_n), (\psi_{k_n}(T_n + 1), T_n + 1), \dots,$$

$$(\psi_{k_n}(T_n + X_n), T_n + X_n), (\gamma_{k_nj}, T_{n+1}), \dots),$$

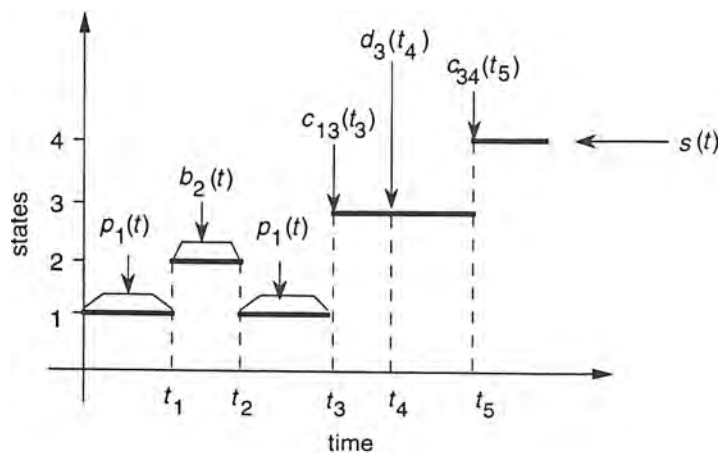


Figure 4: Insurance contract as shown in Haberman and Pitacco (1999) [20].

Under the 4 hypotheses it is evident that the stochastic evolution of this process can be naturally followed by means of a SMP.

The main SCF problem is the evaluation of the mean present value. Another important issue is the evaluation of the risk that, as is well-known, can be calculated knowing the second order moment and consequently the variance or the sigma square.

Remark 6.3. *Most of the insurance contracts can be modelled taking into account these four hypotheses. Indeed an insurance contract, as specified for example in Haberman and Pitacco (1999), is a stochastic cash flow. In some cases (see Janssen and Manca, 1997) it is necessary to introduce other time random variables generalizing the SMP but, de facto, also these generalized SMRWP model a more complex SCF. Figure 4 represents the trajectory of a general insurance contract as shown in Haberman and Pitacco (1999), and is the perfect reproduction of a trajectory of a SMRWP. Indeed, $p_1(t)$ and $b_2(t)$ represent respectively a premium and a benefit they are paid or received in function of the state in which the insured is. They represent permanence rewards in the SMRWP environment. The first is an entrance and the second is a cost for the insurance company $c_{13}(t_3)$ and $c_{34}(t_5)$ represent two transition rewards. $d_3(t_4)$ is a reward that is given in function of the staying of a time $t_4 - t_3$ in the state 3. Clearly, the time $t_4 - t_3$ is a backward time. This fact implies that we have to define also the SMRWP with backward permanence rewards.*

Remark 6.4. *In the discrete time SCF evaluation the instant of payments assumes great relevance. The distinction between immediate and due DTSMRWP is fundamental.*

6.1. The relations of SMRWP with backward time rewards

In this subsection the homogeneous and non-homogeneous SMRWP with rewards and interest rates depending on the backward time will be presented. In this paper the backward time given on the permanence rewards is pointed out. Indeed, the possibility of considering the rewards and interest rates that changes as a function of backward time is an important issue in insurance contracts. It is to outline, for example, that in a disability insurance framework it is well known that the grade of disability can decrease in function of the time spent from the disability event (see D'Amico et al., 2009b). In this case the consideration of rewards that depend on backward time can really be important in the calculation of the benefits and the premium of the insurance contract. Furthermore, in the management of a SCF with a term structure of interest rate it can happen that the interest rates of the SCF can change in function of the elapsed time between the stipulation of contract and the beginning of the financial operation. The consideration of interest rates that depends on backward time can take into consideration this other aspect of financial contracts.

We consider, in (15) and (16), at the same time both these aspects. It is clear that it is possible the writing of relations that point out only one of the two problems.

$$\begin{aligned}
V_i(u; t) &= \frac{(1 - H_i(t + u))}{(1 - H_i(u))} \sum_{\theta=1}^t \psi_i(u; \theta) v(u; \theta) \\
&+ \sum_{k=1}^m \sum_{\vartheta=1}^t \frac{b_{ik}(\vartheta + u)}{(1 - H_i(u))} \sum_{\theta=1}^{\vartheta} \psi_i(u; \theta) v(u; \theta) \\
&+ \sum_{k=1}^m \sum_{\vartheta=1}^t \frac{b_{ik}(\vartheta + u)}{(1 - H_i(u))} v(u; \vartheta) \gamma_{ik}(u; \vartheta) \\
&+ \sum_{k=1}^m \sum_{\vartheta=1}^t \frac{b_{ik}(\vartheta + u)}{(1 - H_i(u))} v(u; \vartheta) V_k(0; t - \vartheta).
\end{aligned} \tag{15}$$

$$\begin{aligned}
\dot{V}_i(u, s; t) &= \frac{(1 - H_i(u, t))}{(1 - H_i(u, s))} \sum_{\theta=s+1}^t \psi_i(u, s; \theta) v(u, s; \theta) \\
&+ \sum_{k=1}^m \sum_{\vartheta=s+1}^t \frac{b_{ik}(u, \vartheta)}{(1 - H_i(u, s))} \sum_{\theta=s+1}^{\vartheta} \psi_i(u, s; \theta) v(u, s; \theta) \\
&+ \sum_{k=1}^m \sum_{\vartheta=s+1}^t \frac{b_{ik}(u, \vartheta)}{(1 - H_i(u, s))} \dot{V}_k(0, \vartheta; t) v(u, s; \vartheta) \\
&+ \sum_{k=1}^m \sum_{\vartheta=s+1}^t \frac{b_{ik}(u, \vartheta)}{(1 - H_i(u, s))} \gamma_{ik}(u, s; \vartheta) v(u, s; \vartheta).
\end{aligned} \tag{16}$$

We would outline that it is the first time that are presented reward processes in which it is possible taking into consideration the reward and interest rates depending on backward times.

Remark 6.5. *It is clear that it is possible to write the matrix relations as in the previous case. A studious reader can try to write them.*

6.2. A mixed due and immediate SMRWP with backward recurrence times

There are insurance contracts in which the premium are paid at beginning of the period and the insured benefit at the end of the period. In these cases, it is necessary to define a SMRWP that can take into account this *mixed* situation.

(17) and (18) give the homogeneous and non-homogeneous SMRWP evolution equations in the case of rewards paid or cashed at the beginning or at the end of the period.

$$\begin{aligned}
\bar{V}_i(u; t) &= \frac{(1 - H_i(t + u))}{(1 - H_i(u))} \sum_{\theta=1}^t \psi_i(u; \theta) \prod_{\tau=sw(i)}^{\theta+sw(i)-1} (1 + r(u; \tau))^{-1} \\
&+ \sum_{k=1}^m \sum_{\vartheta=1}^t \frac{b_{ik}(\vartheta + u)}{(1 - H_i(u))} \sum_{\theta=1}^{\vartheta} \psi_i(u; \theta) \prod_{\tau=sw(i)}^{\theta+sw(i)-1} (1 + r(u; \tau))^{-1} \\
&+ \sum_{k=1}^m \sum_{\vartheta=1}^t \frac{b_{ik}(\vartheta + u)}{(1 - H_i(u))} \prod_{\tau=1}^{\vartheta} (1 + r(u; \tau))^{-1} \gamma_{ik}(\vartheta) \\
&+ \sum_{k=1}^m \sum_{\vartheta=1}^t \frac{b_{ik}(\vartheta + u)}{(1 - H_i(u))} \prod_{\tau=1}^{\vartheta} (1 + r(u; \tau))^{-1} \bar{V}_k(0; t - \vartheta).
\end{aligned} \tag{17}$$

$$\begin{aligned}
\bar{V}_i(u, s; t) &= \frac{(1 - H_i(u, t))}{(1 - H_i(u, s))} \sum_{\theta=s}^t \psi_i(u, s; \theta) \prod_{\tau=s+sw(i)}^{\theta+sw(i)-1} (1 + r(u, s; \tau))^{-1} \\
&+ \sum_{k=1}^m \sum_{\vartheta=s+1}^t \frac{b_{ik}(u, \vartheta)}{(1 - H_i(u, s))} \sum_{\theta=s}^{\vartheta} \psi_i(u, s; \theta) \prod_{\tau=s+sw(i)}^{\theta+sw(i)-1} (1 + r(u, s; \tau))^{-1} \\
&+ \sum_{k=1}^m \sum_{\vartheta=s+1}^t \frac{b_{ik}(u, \vartheta)}{(1 - H_i(u, s))} \gamma_{ik}(s, \vartheta) \prod_{\tau=s+1}^{\vartheta} (1 + r(u, s; \tau))^{-1} \\
&+ \sum_{k=1}^m \sum_{\vartheta=s+1}^t \frac{b_{ik}(u, \vartheta)}{(1 - H_i(u, s))} V_k(0, \vartheta; t) \prod_{\tau=s+1}^{\vartheta} (1 + r(u, s; \tau))^{-1}.
\end{aligned} \tag{18}$$

Remark 6.6. *The trick in the relations (17) and (18) consists in the usage of a vector of binary variable sw of order m that will assume at the i th element value 1 if the permanence reward is paid at the end of the period and 0 if it is paid at the beginning of the period.*

Remark 6.7. *The two relations (17) and (18) are the most general that can be given respectively in the homogeneous and non-homogeneous SMRWP for the calculation of the mean present value of a SCF.*

7. A quasi real data example

In this part we present results both for both homogeneous and non-homogeneous environments. The raw data are the same as were used in Stenberg et al. (2006, 2007) papers but the models are different. We speak of quasi real data because we truncated the Waiting Time Distribution Function (WTDF) at 10. Indeed interest rates and benefits that change because of backward recurrence times were used. Furthermore, in the model the benefits of the first state are paid at beginning of the period, instead of the benefits of the other states at the end of the period. It is the first time that a model of a SCF

considers this possibility. Having data of only disabled people all the considered rewards are paid by the INAIL (Istituto Nazionale Assistenza Infortuni sul Lavoro), which is a public assistance institute and pays for the working accidents.

The historical data give the disability history of 840 people that had silicosis problems and lived in Campania, an Italian region. Each individual with silicosis will be examined by a doctor. The doctor will determine the degree of disability in the form of a percentage for each patient, ranging from 0% to 100%. Depending on the degree of disability the policy maker has determined five possible states, categorized in Table 1.

Table 1: Disability states.

1	[0 %, 10%)
2	[10 %, 30%)
3	[30 %, 50%)
4	[50 %, 70%)
5	[70 %, 100%)

This subdivision is the same as the ones used in Yntema (1962), Janssen (1966) that were the first to apply respectively Markov and semi-Markov environment to disability problems.

Transition between states occurs after a visit to the doctor that can be seen as the check to decide in which state the disabled person is in. This leads naturally to an example where virtual transitions are possible, i.e., the individual has become neither sufficiently better nor worse to change state. In the table we have introduced 5 different states, $E = 1, 2, 3, 4, 5$, one for each reward policy.

In Figure 5 the graph of the transitions is reported.

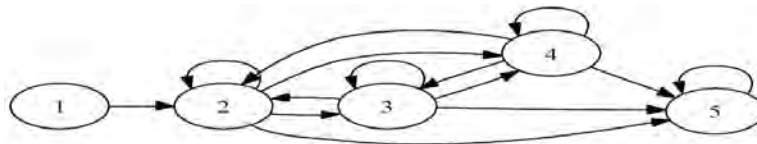


Figure 5: Graph of Markov transition matrix.

From the graph of Figure 5 it results:

- there is one absorbing state,
- the states 2, 3 and 4 are interconnected (they form a class of states),
- the state 5 is an absorbing state that forms the only absorbing class.

Under these conditions both homogeneous and non-homogeneous embedded Markov chains are mono-unireducible, see D'Amico et al. (2009a). These matrices were constructed by the real data.

Given the five states defined previously, we attached a reward policy to the disability degree. The reward that is given to construct the example represents the money amount that is paid for each time period to the disabled person with respect to the degree of illness. We did not have these data so we did not use real data values. The same was done for the evaluation of the interest rates. The data that we used were not sufficient for the evaluation of waiting time cumulated distribution functions. We construct these functions by means of random number extraction. Given that the applications have a horizon time of 10 years we truncate the waiting time distribution function in the way that the 10^{th} value is included between 0.9 and 1.

Transition rewards are not provided. Resuming, the hypothesis of the models that we apply are the following:

1. the evolution equations have only permanence rewards,
2. the rewards are all of the same sign (it is a disability insurance that is paid by social assistance),
3. the first state is paid at the beginning of the period the others at the end (we put this hypothesis to show the potential of our model).

Our hypothesis implies different evolution equations and we report them in (19) and (20) in homogeneous and non-homogeneous case respectively.

$$\begin{aligned}
\bar{V}_i(u; t) &= \frac{(1 - H_i(t + u))}{(1 - H_i(u))} \sum_{\theta=1}^t \psi_i(u; \theta) \prod_{\tau=sw(i)}^{\theta+sw(i)-1} (1 + r(u; \tau))^{-1} \\
&+ \sum_{k=1}^m \sum_{\vartheta=1}^t \frac{b_{ik}(\vartheta + u)}{(1 - H_i(u))} \sum_{\theta=1}^{\vartheta} \psi_i(u; \theta) \prod_{\tau=sw(i)}^{\theta+sw(i)-1} (1 + r(u; \tau))^{-1} \\
&+ \sum_{k=1}^m \sum_{\vartheta=1}^t \frac{b_{ik}(\vartheta + u)}{(1 - H_i(u))} \prod_{\tau=1}^{\vartheta} (1 + r(u; \tau))^{-1} \bar{V}_k(u; t - \vartheta).
\end{aligned} \tag{19}$$

$$\begin{aligned}
\bar{V}_i(u; t) &= \frac{(1 - H_i(t + u))}{(1 - H_i(u))} \sum_{\theta=1}^t \psi_i(u; \theta) \prod_{\tau=sw(i)}^{\theta+sw(i)-1} (1 + r(u; \tau))^{-1} \\
&+ \sum_{k=1}^m \sum_{\vartheta=1}^t \frac{b_{ik}(\vartheta + u)}{(1 - H_i(u))} \sum_{\theta=1}^{\vartheta} \psi_i(u; \theta) \prod_{\tau=sw(i)}^{\theta+sw(i)-1} (1 + r(u; \tau))^{-1} \\
&+ \sum_{k=1}^m \sum_{\vartheta=1}^t \frac{b_{ik}(\vartheta + u)}{(1 - H_i(u))} \prod_{\tau=1}^{\vartheta} (1 + r(u; \tau))^{-1} \bar{V}_k(u; t - \vartheta).
\end{aligned} \tag{20}$$

7.1. The results

7.1.1. Homogeneous case

In this real data example we cover an horizon time of 10 years. The inputs of the program are the embedded Markov chain and the waiting time d.f.s

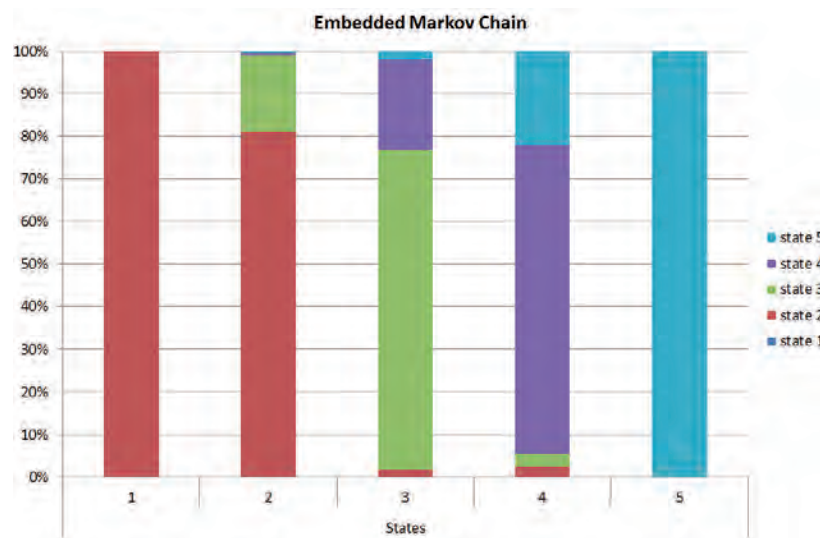


Figure 6: The Markov chain embedded in the homogeneous process.

In Figure 6 the matrix of the embedded Markov chain is reported. Each starting state is represented by a rectangle of the histogram. The transition probabilities are represented by different colors, for example the state 1 can go only in the state 2.

Figure 7 shows the waiting time d.f.'s. We would like to remember that a waiting time d.f. is given for each possible transition.

In Figure 8 the mean present values of rewards with no backward time, 3 years and 5 years of backward are given. We observe that with different backward and similar durations are obtained different results.

Finally Figure 9 shows the variance values. We would like to comment on the calculation of variance gives the possibility to have a measure of the risk. It is to observe that the variance has, by far, higher values of the reward values and this means a high risk in the financial operation.

7.1.2. Non-homogeneous case

In this subsection the results of the non-homogeneous case are reported.

In Figure 10 the non-homogeneous embedded Markov chains at time 1, 3 and 5 are shown. As it is possible to observe that at different times the embedded Markov chains have different transition probabilities.

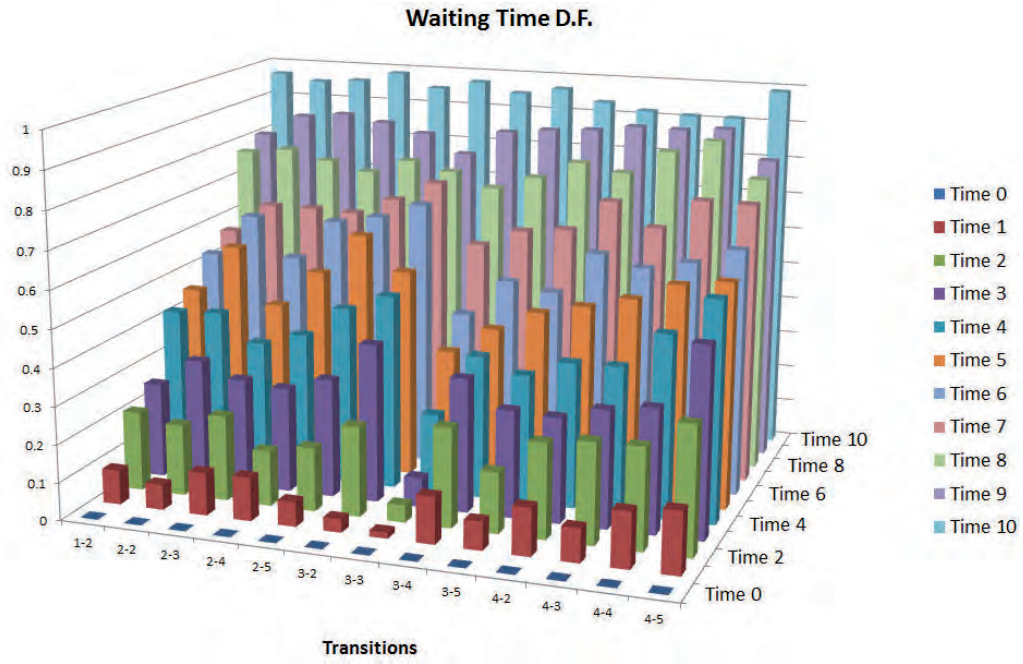


Figure 7: The waiting time d.f.

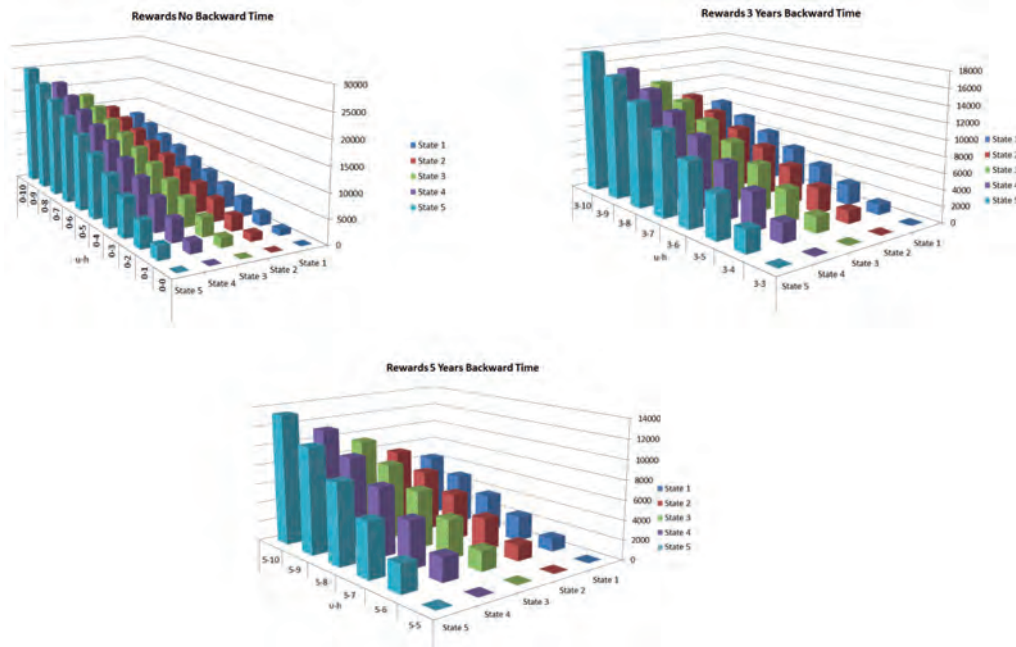


Figure 8: Reward mean present value (backward time 0, 3, 5).

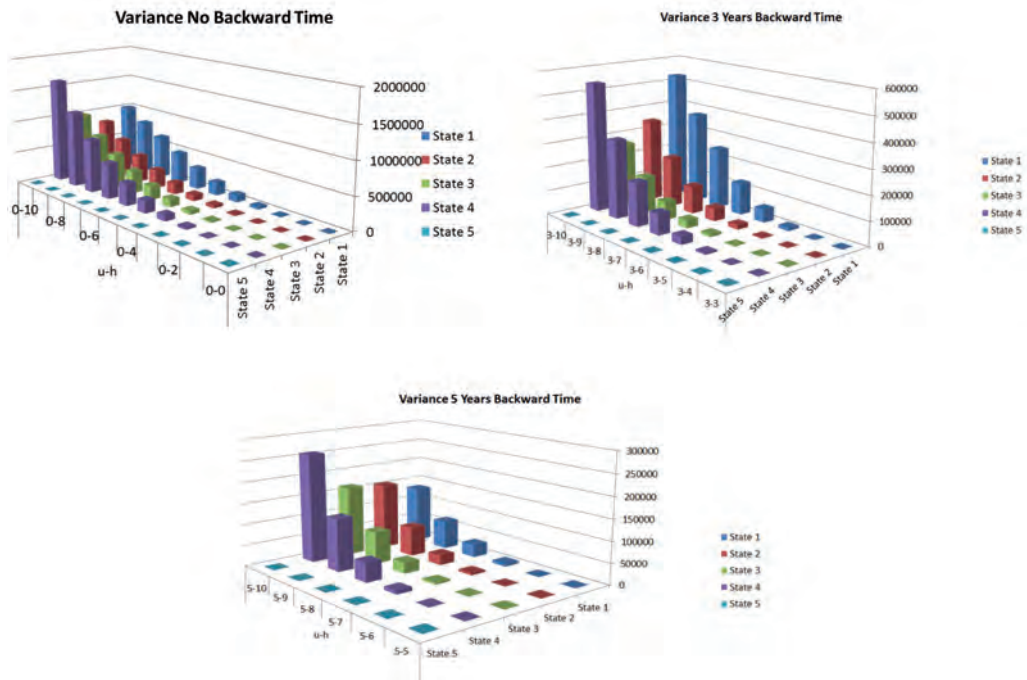


Figure 9: Variance values (backward time 0, 3, 5).

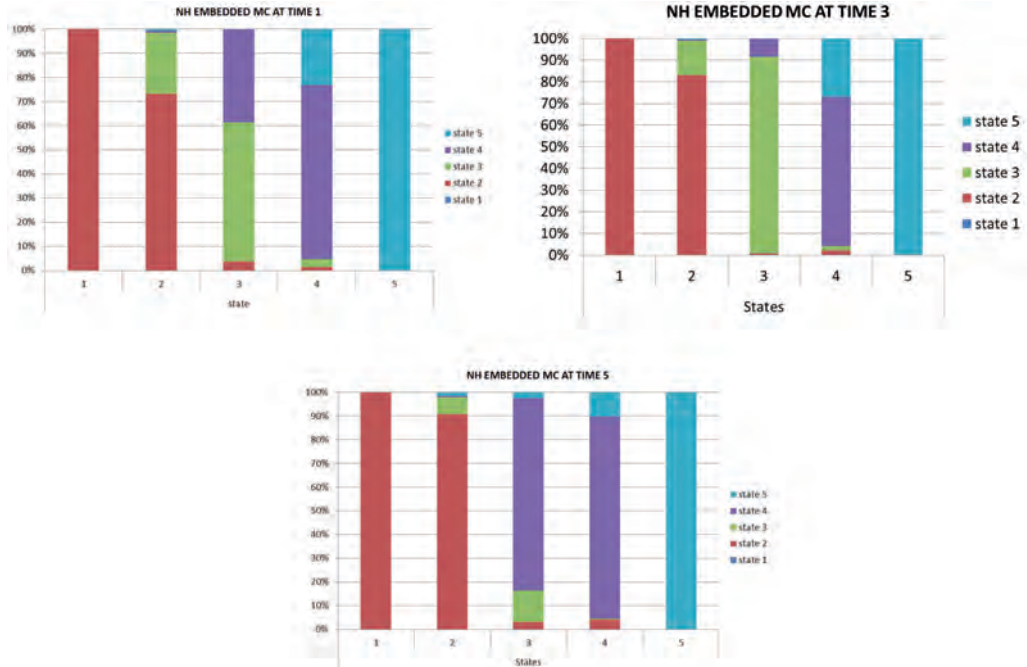


Figure 10: Non-homogeneous embedded Markov chain at time 1, 3, 5.

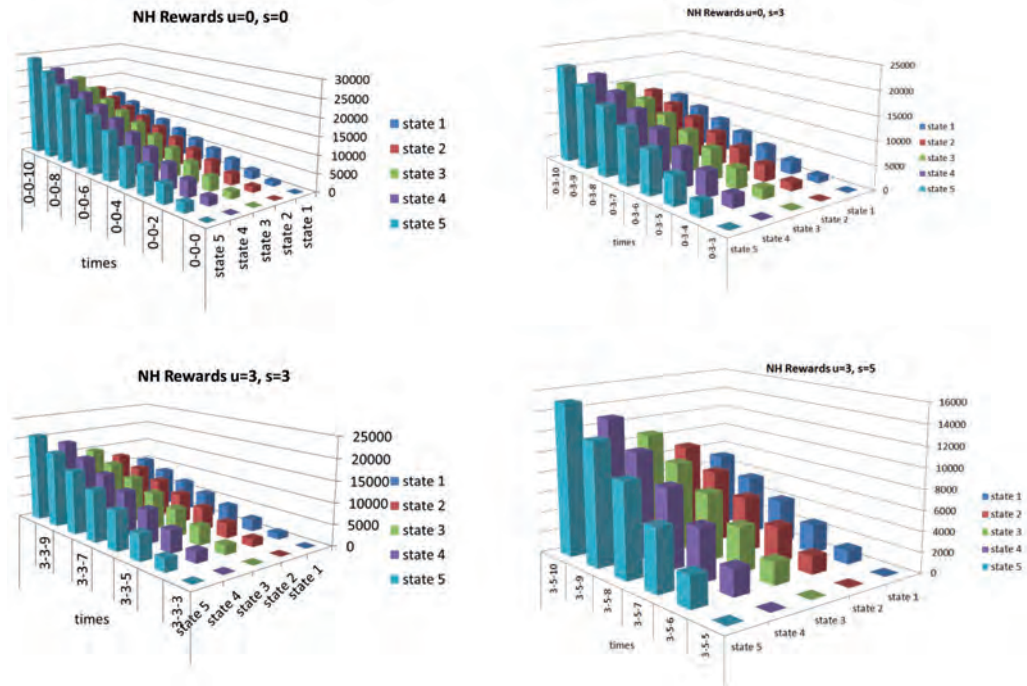


Figure 11: Non-homogenous reward mean present values (back time 0 start time 0,3, 3; back time 3 start time 3,5).

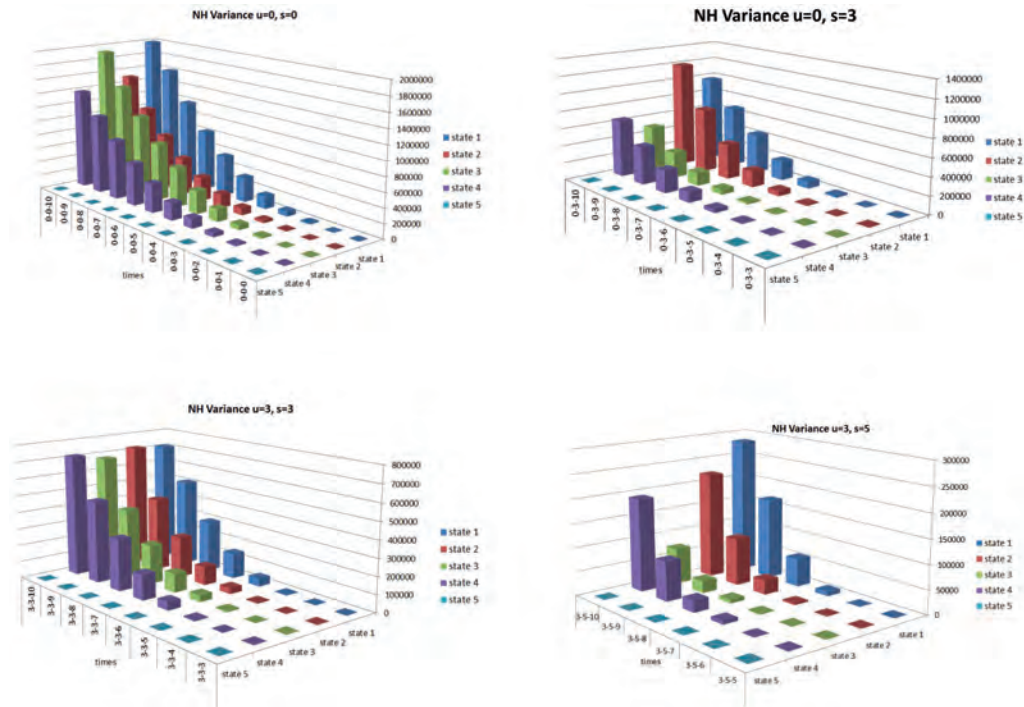


Figure 12: Non-homogenous variance values (back time 0 start time 0,3, 3; back time 3 start time 3,5).

In Figure 11 the non-homogeneous reward present values are given. The first two images report the values obtained without backward recurrence time with starting time equal to 0 and 3. The other two images report the results with backward recurrence time 3 and with starting time 3 and 5. It is interesting to observe that both non-homogeneity and backward time influence the result in substantial way.

Finally Figure 12 presents the variance values corresponding to the reward results that were given previously. We should point out that they are bigger by far than the mean values of our process. This means an over-dispersion of starting data and that our financial operation has a high risk.

8. Conclusions

The paper presented how to apply DTSMRWP in both the homogeneous and non-homogeneous case with backward recurrence time for calculation of the evolution and of the evaluation of SCFs. The model gives the possibility to take into account permanence rewards that are immediate, due and also a mixture of the two cases. Another important result presented is given by the calculation of the second order moment and gives the possibility to calculate the variance and consequently the sigma square, obtaining in this way an evaluation of the risk of the studied SCF.

It is the first time that the evaluation of a SCF by means of a DTSMRWP is presented and we retain that this new approach at this problem gives an important step in the study in general of SCF and more specifically of the most part of insurance contracts.

In the paper, for the first time the possibility is presented to construct a model in which some rewards are paid at the beginning of the period and others at the end of the period. This simple new approach gives the possibility to evaluate in the right way many insurance contracts, because frequently the premium of insurance contracts are paid at the beginning of the periods and the benefits at the end. Furthermore, for the first time SMRWP evolution equations with rewards and interest rates that depend on backward times have been presented.

The authors believe that recurrence times processes attached to a semi-Markov environment can be of great relevance in the study of finance and insurance problems. It is well known that SCF are a fundamental tool for the evaluation of financial and insurance contract and this paper proposes a model that solves the problem.

The presented relations are in discrete time and discrete state but in a future work we will give also the continuous version of these models and the inter-correlations between the discrete and the continuous cases.

The main aim of the paper was to show that a discrete time SCF can be studied naturally by means of a semi-Markov reward process. Furthermore, by means of the semi-Markov approach, it is possible to overcome all the difficulties regarding the study of SCFs that are highlighted in the literature.

Acknowledgments

The authors would like to thank the friends and colleagues Guglielmo D'Amico and Filippo Petroni for the discussions and suggestions that they gave during the drawing up of this paper. Furthermore, they are grateful to the two anonymous referees who with their comments and suggestions improved substantially the paper.

References

- Artikis, T. P. and Malliaris, A. G. (1990). Discounting certain random sums. *Scandinavian Actuarial Journal*, 1-2, 34–38.
- Artikis, T. and Voudouri, A. (2000). A stochastic integral arising in discounting continuous cash flows and certain transformed characteristic functions. *Applied Mathematical Letters*, 13, 87–90.
- Balcer, Y. and Sahin, I. (1979). Stochastic models for a pensionable service. *Operations Research*, 27, 888–903.
- Balcer, Y. and Sahin, I. (1986). *Pension accumulation as a semi-Markov reward process, with applications to pension reform. Semi-Markov models*. Plenum N.Y.
- Beekman, J. A. and Fuelling, C. P. (1991). Extra randomness in certain annuity models. *Insurance Mathematics and Economics*, 10, 275–287.
- Browne, S. (1995). Optimal investment policies for a firm with a random risk process: exponential utility and minimizing the probability of ruin. *Mathematics of Operations Research*, 20, 937–958.
- Carravetta, M., De Dominicis, R. and Manca, R. (1981). Semi-Markov stochastic processes in social security problems. *Cahiers du C.E.R.O.*, 23, 333–339.
- CMIR12 (1991). (Continuous Mortality Investigation Report, number 12). *The analysis of permanent health insurance data*. The Institute of Actuaries and the Faculty of Actuaries.
- D'Amico, G., Guillen, M. and Manca, R. (2009). Full backward non-homogeneous semi-Markov processes for disability insurance models: A Catalunya real data application. *Insurance: Mathematics and Economics*, 45, 173–179.
- D'Amico, G., Guillen, M. and Manca, R. (2013). Semi-Markov Disability Insurance Models. *Communications in Statistics-Theory and Methods*, 42, 2172–2188.
- D'Amico, G., Janssen, J. and Manca, R. (2009a). The dynamic behavior of single unireducible non-homogeneous Markov and semi-Markov chains. In *Networks: Topology and Dynamic. Lectures Notes in Economic and Mathematical Systems*, (A. Naimzada, S. Stefani and A. Torriero, eds.). Springer, 195–211.
- De Dominicis, R. and Manca, R. (1986). Some new results on the transient behaviour of semi-Markov reward processes. *Methods of Operations Research*, 53, 387–397.
- De Medici, G., Janssen, J. and Manca, R. (1995). Financial operation evaluation: a semi-Markov approach. *Proc. VAFIR Symposium Brussels*, vol. 3 bis. Janssen J. Ed. CESIAF, Bruxelles.
- De Schepper, A. and Goovaerts, M. (1992). Some further results on annuities certain with random interest rate. *Insurance Mathematics and Economics*, 11, 283–290.
- De Schepper, A., Teunen, M. and Goovaerts, M. (1994). An analytical inversion of a Laplace transform related to annuities certain. *Insurance Mathematics and Economics*, 14, 33–37.
- Donati-Martin, C., Matsumoto, H. and Yor, M. (2000). On positive and negative moments of the integral of geometric Brownian motions. *Statistics and Probability Letters*, 49, 45–52.
- Duffie, D., Pan, J. and Singleton, K. (2000). Transform analysis and asset pricing for affine jump-diffusions. *Econometrica*, 68, 1343–1376.

- Dufresne, D. (2001). The integral of geometric Brownian motion. *Advances in Applied Probability*, 33, 223–241.
- Estes, J. H., Moor, W. C. and Rollier, D. A. (1989). Stochastic cash flow evaluation under conditions of uncertain timing. *Engineering Costs and Production Economics*, 18, 65–70.
- Haberman, S. and Pitacco, E. (1999). *Actuarial Models for Disability Insurance*, Chapman & Hall.
- Halliwell, L. J. (2003). The Valuation of Stochastic Cash Flows. *CAS Forum*, (Reinsurance Call Papers, Spring 2003), 1-68, available on line at: www.casact.org/pubs/forum/03spforum/03spf001.pdf.
- Harrison, M. J. (1977). Ruin problems with compounding assets. *Stochastic Processes and their Applications*, 5, 67–79.
- Hoem, J. M. (1972). Inhomogeneous semi-Markov processes, select actuarial tables, and duration-dependence in demography. In *Population, Dynamics*, ed. T.N.E. Greville Academic Press, 251–296.
- Howard, R. (1971). *Dynamic probabilistic systems*, vol II, Wiley.
- Janssen, J. (1966). Application des processus semi-markoviens à un problème d'invalidité. *Bulletin de l'Association Royale des Actuaraires Belges*, 63, 35–52.
- Janssen, J. and Manca, R. (1997). A realistic non-homogeneous stochastic pension funds model on scenario basis. *Scandinavian Actuarial Journal*, 113–137.
- Janssen, J. and Manca, R. (1998). Non-homogeneous stochastic pension fund model: an algorithmic approach. *Transactions of the 26th ICA Birmingham Vol. V*, 216–238.
- Janssen, J. and Manca, R. (2002). General actuarial models in a semi-Markov environment. *Proceedings of 27th ICA 2002, Cancun*, available on line at <http://www.actuaries.org/EVENTS/Congresses/Cancun/astin subject/astin 78 janssen manca.pdf>.
- Janssen, J. and Manca, R. (2006). *Applied semi-Markov Processes*, Springer.
- Janssen, J. and Manca, R. (2007). *Semi-Markov Risk Models for Finance, Insurance and Reliability*, Springer.
- Janssen, J. and Manca, R. and Volpe di Prignano, E. (2002). Non homogeneous interest rate structure in a semi-Markov framework. *Proceedings of 27th ICA 2002, Cancun*, available on line at <http://www.actuaries.org/EVENTS/Congresses/Cancun/afir subject/afir 47 janssen manca volpe.pdf>.
- Janssen, J. and Manca, R. and Volpe di Prignano, E. (2004). Continuous Time Non Homogeneous Semi-Markov a. Reward Processes And Multi-State Insurance Application. *Proceedings IME 2004 Roma*.
- Janssen, J. and Manca, R. and Volpe di Prignano, E. (2009). *Mathematical Finance, Deterministic and Stochastic models*, ISTE Wiley.
- Limnios, N. and Oprisan, G. (2001). *Semi-Markov Processes and Reliability*, Birkhäuser, Boston.
- Marocco, P. and Pitacco, E. (1998). Longevity risk and life annuity reinsurance. *Transactions of the 26th ICA Birmingham, vol VI*, 453–479.
- Milevsky, M. (1997). The present value of a stochastic perpetuity and the gamma distribution. *Insurance Mathematics and Economics*, 20, 243–250.
- Milevsky, M. and Posner, E. (1998). Asian options, the sum of lognormals and the reciprocal gamma distribution. *Journal of Financial and Quantitative Analysis*, 33, 409–422.
- Papadopoulou, A. A. (2013). Some results on modeling biological sequences and web navigation with a semi-Markov chain. *Communications in statistics-Theory and Methods*, 42, 2153–2171.
- Papadopoulou, A. A. and Tsaklidis, G. M. (2007). Some reward paths in semi-Markov models with stochastic selection of the transition probabilities. *Methodology and Computing in Applied Probability*, 9, 399–411.
- Papadopoulou, A. A., Tsaklidis, G., McClean, S. and Garg, L. (2012). On the moments and the distribution of the cost of a semi-Markov model for healthcare systems. *Methodology and Computing in Applied Probability*, 14 717–737.
- Parker, G. (1994). Limiting distribution of the present value of a portfolio. *Astin Bulletin*, 24, 47–60.

- Perry, D. and Stadje, W. (2000). Risk analysis for a stochastic cash management model with two types of customers. *Insurance Mathematics and Economics*, 26, 25–36.
- Perry, D. and Stadje, W. (2001). Function space integration for annuities. *Insurance Mathematics and Economics*, 29, 73–82.
- Pitacco, E. and Olivieri, A. (1997). *Introduzione alla teoria attuariale delle assicurazioni di persone*, Quaderno UMI, 42.
- Pliska, S. R. (1986). A stochastic calculus model of continuous trading. *Mathematics of Operations Research*, 11, 371–382.
- Qureshi, M. A. and Sanders, H. W. (1994). Reward model solution methods with impulse and rate rewards: an algorithmic and numerical results. *Performance Evaluation*, 20, 413–436.
- Papadopoulou, A. A., Tsaklidis, G., McClean, S. and Garg, L. (2012). On the moments and the distribution of the cost of a semi-Markov model for healthcare systems. *Methodology and Computing in Applied Probability*, 14, 717–737.
- Sato, S. and Yor, M. (1998). Computation of moments for discounted Brownian additive functional. *Journal of Mathematics of Kyoto University*, 38, 475–486.
- Silvestrov, D. S. (1980). *Semi-Markov Processes with a Discrete State Space*, Sovetske Radio, Moskow (Russian).
- Stenberg, F., Manca, R. and Silvestrov, D. (2006). Semi-Markov reward models for insurance. *Theory of Stochastic Processes*, 12, 239–254.
- Stenberg, F., Manca, R. and Silvestrov, D. (2007). An algorithmic approach to discrete time non-homogeneous backward semi-Markov reward processes with an application to disability insurance. *Methodology and Computing in Applied Probability*, 9, 497–519.
- Swishchuk, A. V. (1995). Hedging of options under mean-square criterion and with semi-Markov volatility. *Ukrainian Mathematic Journal*, 47, 1119–1127.
- Vanneste, M., Goovaerts, M. J., De Schepper, A. and Dhaene, J. (1997). A straightforward analytical calculation of the distribution of an annuity certain with stochastic interest rate *Insurance Mathematics and Economics*, 15, 37–48.
- Vanneste, M., Goovaerts, M. J. and Labie, E. (1994). The distribution of annuities. *Insurance Mathematics and Economics*, 15, 37–48.
- Wilkie, A. D. (1986). A stochastic investment model for actuarial use. *Transactions of the Faculty of Actuaries*, 39, 341–403.
- Wilkie, A. D. (1995). The risk premium on ordinary shares (with discussion). *British Actuarial Journal*, 1, 251–293.
- Wolthuis, H. (2003). *Life Insurance Mathematics (the Markovian Model)*, II edition, Peeters Publishers, Herent, XI, 288.
- Yntema, L. (1962). A markovian treatment of silicosis. *Acta III Conferencia Int. De Actuarios y Estadísticos de la Seguridad Social*, Madrid.
- Yor, M. (2001). *Exponential Functionals of Brownian Motion and Related Processes*, Springer.

Assessing the impact of early detection biases on breast cancer survival of Catalan women

Albert Roso-Llorach^{1,2}, Carles Forné^{3,4}, Francesc Macià^{5,6},
Jaume Galceran⁷, Rafael Marcos-Gragera⁸ and Montserrat Rué^{6,9,*}

Abstract

Survival estimates for women with screen-detected breast cancer are affected by biases specific to early detection. Lead-time bias occurs due to the advance of diagnosis, and length-sampling bias because tumors detected on screening exams are more likely to have slower growth than tumors symptomatically detected. Methods proposed in the literature and simulation were used to assess the impact of these biases. If lead-time and length-sampling biases were not taken into account, the median survival time of screen-detected breast cancer cases may be overestimated by 5 years and the 5-year cumulative survival probability by between 2.5 to 5 percent units.

MSC: 62N02; 62P10.

Keywords: Breast cancer, early detection, screening, lead time bias, length bias, survival.

1. Introduction

Some types of cancer can be detected before they cause symptoms. The primary goal of cancer screening programs is to reduce mortality. Screening tests, such as mam-

* Corresponding author e-mail: montse.rue@cmb.udl.cat

¹ Unitat de Suport a la Recerca Terres de l'Ebre, Institut Universitari d'Investigació en Atenció Primària Jordi Gol (IDIAP Jordi Gol), Tortosa, Spain.

² Universitat Autònoma de Barcelona, Bellaterra (Cerdanyola del Vallès), Spain.

³ Dept. Ciències Mèdiques Bàsiques, IRBLLEIDA-Universitat de Lleida, Spain.

⁴ Oblikue Consulting, Barcelona, Spain.

⁵ Servei d'Epidemiologia i Avaluació, Hospital del Mar-Parc de Salut Mar, Barcelona, Spain.

⁶ Red de Investigación en Servicios de Salud y Enfermedades Crónicas (REDISSEC).

⁷ Registre de Càncer de Tarragona, Fundació Lliga per a la Investigació i Prevenció del Càncer, Reus, IISPV, RTICC, Spain.

⁸ Unitat d'Epidemiologia i Registre de Càncer de Girona (UERCg), Pla Director d'Oncologia. Departament de Salut. Institut d'Investigació Biomèdica de Girona (IdIBGi), Spain.

⁹ Dept. Ciències Mèdiques Bàsiques, IRBLLEIDA-Universitat de Lleida, Avgda. Rovira Roure 80, 25198-Lleida, Spain.

Received: September 2013

Accepted: April 2014

mography, can detect cancer at an earlier stage compared to symptomatic diagnosis. It is expected that an early diagnosis will be associated with a better prognosis and consequently, with an increase of survival time. However, measuring the benefit of early detection as survival time from the date of diagnosis is confounded by two screening-specific biases: lead-time and length-sampling biases (Zelen and Feinleib, 1969).

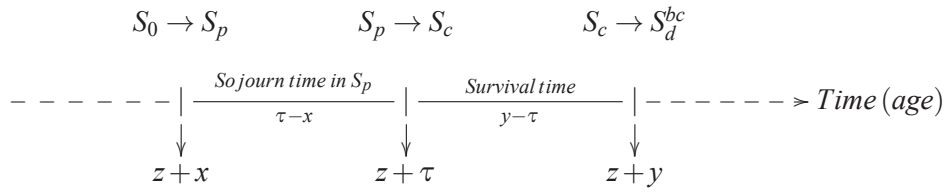
For a screen-detected cancer, the lead-time is defined as the time gained by diagnosing the disease before the patient experiences symptoms. Even if early diagnosis and early treatment had no benefit, the survival of early detected cancer cases would be longer than the survival of clinical cases (see Figure A.1 in the Appendix). Length-sampling bias arises because screen-detected cancers are more likely to have slower growth than non-screen detected cancers. It seems reasonable to assume that the clinical course of the disease is positively correlated with its pre-clinical course. Thus, patients with screen-detected cancers survive longer in part because their tumors are less aggressive. Therefore the difference in survival cannot be only attributed to the early detection (see Figure A.1 in the Appendix). Different authors have studied the effect of these biases in the survival functions of women with screen-detected breast cancer (BC) and have proposed several corrections (Walter and Stitt, 1987; Xu and Prorok, 1995; Xu, Fagerstrom and Prorok, 1999; Duffy et al., 2008 and Mahnken et al., 2008). The goals of this study are: 1) To review the methods of bias correction for BC; 2) To obtain bias-corrected survival estimates of the screen-detected cases; and 3) To evaluate the impact of the lead-time and length-sampling biases. The rest of the paper is organized as follows. Section 2 reviews the existing methods in the literature for bias correction and describes the statistical methods used, including a simulation study. Section 3 presents the results, and Section 4 is a general discussion.

2. Methods

2.1. Breast cancer early detection model

As defined by Zelen and Feinleib (1969), the progress of BC can be characterized as a stochastic process, assuming that each individual in a specific population is in one of these three states: disease-free (S_0); the pre-clinical or asymptomatic state (S_p), when the disease can be diagnosed by a special exam; and the clinical or symptomatic state (S_c). Sometimes an absorbing state (S_d^{bc}) referring to death from BC can be added.

Based on this early work, Lee and Zelen (LZ) proposed a stochastic model for predicting the mortality of the early detection programs as a function of the characteristics of the early detection scenario (Lee and Zelen, 1998, 2008). The assumptions of the LZ model are: (1) progressive disease; (2) age-dependent transitions into the different states, $S_0 \rightarrow S_p \rightarrow S_c \rightarrow S_d^{bc}$; (3) age-dependent examination sensitivity; (4) age-dependent sojourn times in each state; and (5) exam-diagnosed cases have a stage-shift in the direction of more favorable prognosis relative to the distribution of stages in symptomatic detection.



Note that the transition $S_0 \rightarrow S_p$ is never observed and the transition $S_p \rightarrow S_c$ refers to the disease incidence. If the early detection exam does diagnose the disease in the pre-clinical state, the transition $S_p \rightarrow S_c$ will never be observed.

The LZ model considers:

- n screening exams at times $t_0 < t_1 < \dots < t_{n-1}$. It is assumed that $t_0 = 0$ and $z = \text{age}$ at t_0 .
- Three chronological times (see above schema):
 - x : time at entering S_p , $z+x$: age when entering S_p . The time x is not observed but can be derived from the incidence function and the distribution of sojourn time in the S_p state. x takes a negative value if the transition to S_p occurs before the age at first exam, z .
 - τ : time at entering S_c , $z+\tau$: age at entering S_c . The time τ can not be observed in cases detected by exam, only in the clinically detected cases. For cases detected by exam, τ can be estimated.
 - y : time at death, $z+y$: age at death. Then $x < \tau < y$
- Sojourn time in S_p : $\tau - x$
- Sojourn time in S_c : $y - \tau$

The LZ basic model calculates the cumulative probability of death for the cohort group exposed to any screening program after T years of follow-up. Similarly, the cumulative probability of death for the cohort group not exposed to screening can be calculated. These probabilities are used to calculate the possible reduction in mortality from an early detection program after T years of follow-up and can be obtained as follows.

Survival distributions for exam-diagnosed, interval, and control cases are assumed to be conditional on the stage at diagnosis and treatment, but are not dependent on the mode of diagnosis. The LZ model assumes k disease stages which describe the severity of a person's cancer based on the size and/or extent of the tumor. If $\phi_s(j)$, $\phi_i(j)$ and $\phi_c(j)$ represent the probability of being diagnosed at stage j , $j = 1, \dots, k$ for exam-diagnosed, interval and control cases, respectively, and $f_j(t|z+\tau)$ is the probability density function (pdf) of survival time t among subjects who would have been clinically diagnosed at stage j in the absence of screening, then the survival time *pdfs* of the exam-diagnosed, interval and control cases are the mixtures:

$$g_s(t|z + \tau) = \sum_{j=1}^k \phi_s(j) f_j(t|z + \tau), \quad g_i(t|z + \tau) = \sum_{j=1}^k \phi_i(j) f_j(t|z + \tau)$$

and

$$g_c(t|z + \tau) = \sum_{j=1}^k \phi_c(j) f_j(t|z + \tau),$$

respectively. In other words, the g density functions are obtained by weighting the f functions by the distribution of disease stages at diagnosis. Since screening will appear to increase survival time, the LZ model controls for *lead-time* bias by setting the origin of survival time for the screened, interval, and clinical cases at the time of clinical diagnosis. Consequently, there is an implied *guarantee time* for disease-specific survival, that is, the cases diagnosed earlier would have been alive at the time the disease would have been clinically diagnosed. This guarantee time, also called *lead-time*, is a random variable and is incorporated into the equations of the model. Explicitly, the lead-time is $\tau - t_r$, where τ is the time at which the individual enters the clinical state and t_r is the time at which the r detection exam, when the disease is diagnosed, is given.

2.2. Methods for correcting the biases specific to early detection

After reviewing the literature, we selected the methods of Walter and Stitt (1987), Xu and Prorok (1995), Xu et al. (1999) and Duffy et al. (2008). All these authors assume the progressive disease model aforementioned with an exponential distribution of the sojourn time in the pre-clinical state. The observed survival time, Z , after diagnosis by screening is defined as $Z = X + Y$, Y is the lead-time, and X the post-lead survival time (the time from clinical detection to death or the end of study). X is the time of interest, free of biases.

2.2.1. The Walter and Stitt method

Walter and Stitt (1987) developed a model for the survival of screen-detected cases, with a hazard function that depends on an individual's lead-time, Y , the duration of the sojourn time in the pre-clinical state and the time since diagnosis, Z . Their main assumptions were that the hazard function considers a guarantee time from the screening detection until when the disease would become clinical and an exponential distribution for the lead-time, Y (Walter and Day, 1983). The authors showed that if the post-lead-time, X , can be assumed to have an exponential distribution, the corresponding parameter can be estimated by maximum likelihood using life-table methods.

2.2.2. *The Xu and Prorok method*

Xu and Prorok (1995) developed a model under the assumption of an exponential distribution for the lead-time and independence between the lead-time and post-lead-time. They presented a method to estimate the survival function of the post-lead time, X , of screen-detected cancer cases based on the observed total survival time, Z . The authors relaxed the parametric assumption for the post-lead-time and obtained the non-parametric maximum likelihood estimator (NPMLE) of the survival function of the post-lead time, X .

2.2.3. *The Xu et al. method*

As Xu and Prorok mentioned, it seems biologically reasonable that the lead-time and the post-lead-time are positively correlated. Xu et al. (1999) introduced a new model that involved dependence between the lead- and post-lead-time through nuisance variables to ensure positive correlation. Several levels of correlation were studied. They applied the Xu and Prorok method on the new model to obtain the NPMLE of the post-lead-time survival function.

2.2.4. *The Duffy et al. method*

Duffy et al. (2008) proposed a simple correction for lead time, assuming an exponential distribution of the sojourn time in the pre-clinical state. The additional follow-up due to lead-time is estimated individually for each patient with a screen-detected cancer as the expected lead-time conditional on its being less than the observed survival time or time to last follow-up. The expression of the expected lead-time depends on whether the patient died of BC or not. The corrected survival time, for screen-detected cases, is obtained subtracting the expected lead-time from the observed survival time.

2.3. *Data*

BC survival data were obtained from the Girona and Tarragona population-based cancer registries (PCR) in Catalonia (both provinces representing 20% of the total Catalan population and covering either urban or rural areas). Data from Girona were provided directly by the Girona Cancer Registry and data from Tarragona was obtained through the Foundation League for the Research and Prevention of Cancer (FUNCA). Given that the BC incidence and mortality rates in the Girona and Tarragona registries were similar, both datasets were merged. The PCR sample included 1,221 women residing in the province of Girona and diagnosed between 2002 and 2006, and 2,149 women residing in the province of Tarragona and diagnosed between 2000 and 2005.

We also obtained BC survival data from the hospital cancer registry of Parc de Salut Mar (HCR-PSMAR) in the city of Barcelona. The HCR-PSMAR included BC tumours from women attending an early detection program (screen-detected or not) and also

BC tumours from other women living in the hospital area. The HCR-PSMAR sample included 1,704 women diagnosed with BC between 1996 and 2006. BC cases in this study refer to invasive BC. Ductal carcinoma in situ (DCIS) cases were not included.

2.4. Statistical analysis

2.4.1. Survival analysis

First, we estimated the biased BC specific survival using the Kaplan-Meier method, assuming that BC was the single cause of death. We considered death from BC as the event of interest. Deaths from other causes (OC) or lost to follow-up (either dropouts or withdrawals) were treated as right-censored observations. Censoring was assumed to be non-informative. Survival time was calculated as the difference between the date of diagnosis and the minimum of time to the event and censored time. Then, we applied the methods described in Section 2.2 in order to correct the BC-specific survival of screen-detected cases. We assumed an exponential distribution with scale parameter 0.25 for the lead-time. This assumption was based on the values proposed by Lee and Zelen (2006) for the mean sojourn time in the pre-clinical state, the previous work of Zelen and Feinleib (1969), the age at diagnosis distribution of the studied cases, and the simulation study described in 2.4.2. For the method of Xu et al. (1999), we considered a dependence parameter 0.5 corresponding to a moderate dependence between lead-time and post-lead-time. All analyses were performed with R version 3.0.1 (R Core Team, 2013).

2.4.2. Simulation study

Since the observed data were characterized by heavy right censoring, we conducted a simulation study. The main goal of the simulation study was to estimate the lead-time and length biases under different screening strategies and to compare the results with those obtained using the correction methods described in Section 2.2. The simulation reproduces the individual life histories of women initially in the disease-free state. Our simulation model considered the Lee and Zelen model inputs for Catalonia (Vilapinyo et al., 2008, 2009; Martinez-Alonso et al., 2010) and additional assumptions described below. For simplicity, in the following sections t refers to chronological time or age.

Initial parameters We used observed or predicted data on BC incidence and mortality for the cohort of Catalan women born in 1950. We assumed a sample size of $n = 100,000$ women. The time horizon was 0-85 years of age, we only considered BC incident cases before age 85 and stopped the follow-up at age 85. We grouped the data by age, considering J yearly disjoint intervals $(a_{j-1}, a_j]$ for $j = 1, \dots, J$, where $a_0 = 0$. We assumed the values proposed by Lee and Zelen (2006) for the age-dependent examination sensitivity, $\beta(t)$, and the exponential distribution with age-dependent mean, $m(t)$, for sojourn time in S_p . The $m(t)$ in years was: 2 for women 40 years old or younger,

4 for women older than 50 years and the linear interpolation $m(t) = -6 + 0.2 * age$ for women aged 40-50 years. The periodicity of the exams was annual or biennial. The initial ages of screening schedules were 40 and 50 years, while the ages at the last examination were 68 years for biennial and 69 years for annual strategies, resulting in four screening strategies. Bivariate correlated data of sojourn times in S_p and S_c were simulated using copula models (Trivedi and Zimmer, 2007). We chose the Clayton's Archimedean copula because it has some interesting features. For example, it is adequate for positive associations between times. Under the Clayton's copula model, three different dependence parameters were chosen, $\alpha \in \{1, 5/4, 3/2\}$; they represent values for Kendall's tau of $\tau_K \in \{0, 1/9, 1/5\}$ ranging from no association to moderate association.

Death from causes other than breast cancer The age-specific death rates from OC for Catalan women, by birth cohort, were used as the hazard function in a survival process where failure was death from OC. Then, ages at death from OC were sampled using the inverse transformation of the cumulative survival function.

Generation of the pre-clinical cases We used Catalan BC incidence rates, estimated assuming no screening for BC (Martinez-Alonso et al., 2010), to obtain the transition probabilities to the pre-clinical state using the method described by Lee and Zelen (1998). We considered these transition probabilities as the hazard in a survival process, where failure consists of entering S_p . Using the same reasoning as for OC, an age when entering S_p was generated for each simulated woman.

Generation of the age at entering the clinical state S_c Some authors have provided evidence that the sojourn time in the pre-clinical state is exponentially distributed (Zelen and Feinleib, 1969; Walter and Day, 1983). A sojourn time in S_p was sampled assuming an age-dependent exponential distribution with mean $m(t)$. Then an age when entering S_c was generated adding the sojourn time to the age at entering S_p , for each simulated woman that transitioned to S_p .

Generation of the screen-detected and the interval cancer cases For women that entered S_p , we considered that their BC could be screen-detected if they received screening exams during their sojourn time in S_p . To decide whether the result of an exam was positive or negative we used a Bernoulli random variable with success probability the sensitivity of the exam, $\beta(t)$. The cases diagnosed at the interval between two exams were considered as interval cases.

Death from breast cancer We used the Clayton's copula, as described in Trivedi and Zimmer (2007), to generate a survival time from the BC diagnosis, using the Catalan age-specific survival functions for BC (Vilapriyo et al., 2009). The survival time was correlated with the sojourn time in S_p through the copula function.

For screen-detected cases, we considered two assumptions for the survival time: with and without benefit of early detection. When survival benefit was assumed, the survival *pdfs* for screen-detected, interval, and clinical cases were obtained weighting the age- and stage-specific survival *pdfs* by the distribution of disease stages at diagnosis. (See Section 2.1 for more details). The distribution of disease stages at diagnosis for screen-detected, interval and clinical BC cases is shown in Table A.1 in the Appendix.

The no-survival benefit assumption was based on a systematic review that reported a non-statistically significant reduction in BC mortality for trials with adequate randomization (Gotzsche and Nielsen, 2009). When no-survival benefit from screening was assumed, we used the clinical stages distribution for screen-detected, interval and clinical cases.

Once the survival time was generated, the age of death from BC was obtained adding the survival time to the age when entering the clinical state S_c for the screened, interval and clinical cases. In that way, there is no lead-time bias for the screen-detected cases.

Age at death We obtained the age of death as the minimum between age at BC death and age at OC death, assuming that both events were independent. A total of 24 scenarios were analysed considering the two assumptions for the survival benefit of early detection, the four screening strategies and the three copula parameters.

The simulation code was developed in R version 3.0.1 (R Core Team, 2013). For each scenario, to generate one dataset, the algorithm ran for approximately 45 seconds on a MacBook Pro machine with 2.4 Ghz Intel Core 2 Duo processor with 4 GB of RAM memory. For each scenario $B = 100$ datasets were generated.

2.4.3. *Estimation of the lead-time and length-sampling biases for screen-detected cases*

The lead-times for the screen-detected cases were obtained as the difference between the age at entering the clinical state and the age at detection. To estimate the mean lead-time of each scenario, first we obtained the mean lead-time within each dataset and then we calculated the mean and the empirical standard error of the 100 dataset means.

To estimate the length bias, first we obtained the median survival time of screen detected cases corrected by the lead-time bias. Then we obtained the median survival time of the background scenario (no screening). Finally, the difference of the two median survival times was considered the length bias effect on the median survival time of screen-detected cases. For the scenarios with no benefit of screening and independence between sojourn time in the pre-clinical state and survival time, the expected length bias would be zero.

2.4.4. Comparison of the methods of bias correction

We calculated the root mean square error (RMSE) between the simulated unbiased cumulative survival and the corrected cumulative survival for the different methods of bias correction. The RMSE gives the standard deviation of the model prediction errors. A smaller value indicates a better model performance. To compute the RMSE we considered the first 25 years of follow-up. The mean RMSE over the 100 simulations was obtained for each scenario (Burton et al., 2006).

2.4.5. Validation

We have compared our results with results in the literature on cumulative incidence and BC cumulative survival. In addition, we have compared a) the frequencies of screen-detected and interval cancer, by age-group; and b) the sensitivity of the program, with the results of the INterval CANcer (INCA) study in Spain, which included 645,764 women aged 45/50 to 69 years that participated biennially in seven population-based screening programs, from January 2000 to December 2006 (Blanch et al., 2014 and Domingo et al., 2014). The cohort was followed until June 2009 for breast cancer identification, resulting in 5,309 cases screen-diagnosed and 1,653 interval cancers. The sensitivity of the program was defined as the ratio of the number of tumors detected in the screening exams between all the detected tumors.

3. Results

3.1. Observed and corrected cumulative survival.

Data from the cancer registries

Table 1 presents the median follow-up time and the censoring percentage for screen-detected and clinical cases, according to BC survival status. Both the PCR and HCR-PSMAR samples presented a large percentage of right censoring, which was around 95% or higher for screen-detected cases. The median follow-up time was shorter for the PCR sample.

Table 1: Follow-up time and survival status for the two studied samples.

	Population Cancer Registries Girona and Tarragona		Hospital Cancer Registry PSMAR	
	No BC death	BC death	No BC death	BC death
Screen-detected cases (<i>n</i>)	633	19	463	27
Median of follow-up (years)	5.46	3.82	7.19	4.31
Percent (%)	97.1	2.9	94.5	5.5
Clinical cases (<i>n</i>)	2284	434	988	226
Median of follow-up (years)	5.10	2.31	6.43	3.10
Percent (%)	84.0	16.0	81.4	18.6

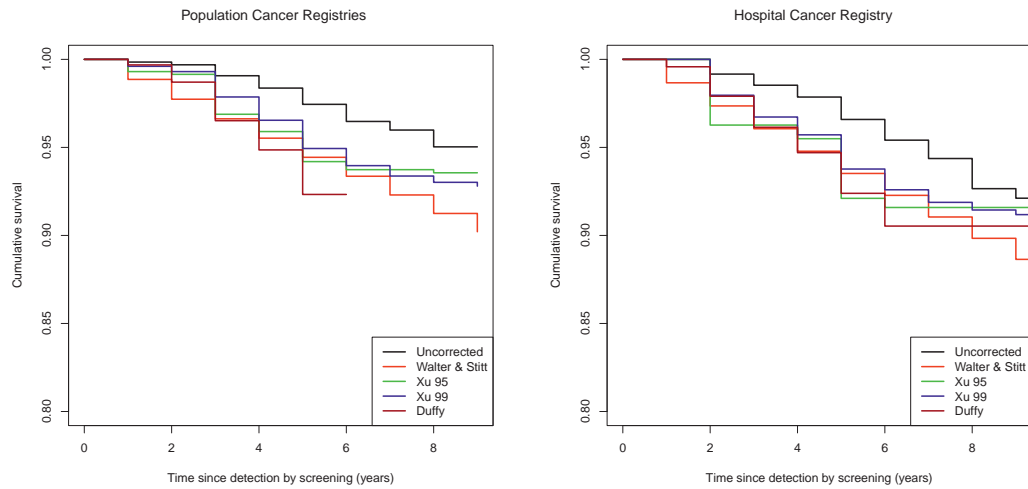


Figure 1: Observed (black) and corrected survival (colours) for each method of correction, for screen-detected cases.

Figure 1 shows the observed and corrected BC survival of screen-detected cases, using the methods described in Section 2.2, for both studied samples. The corrected cumulative survival curves grouped together below the observed survival curve. Table 2 presents the observed and corrected cumulative survival rates at five years after BC detection. Differences of observed and corrected cumulative survival varied from 2.5 to 5.1% units. Observed cumulative survival rate at 5 years around 97% decreased to 94 or 92% after correction. The higher difference was observed for the Duffy method in the PCR sample (5.1%) followed by the Xu and Prorok (4.5%) and the Duffy methods in the HCR-PSMAR sample (4.2%).

Table 2: Observed and corrected survival rates at five years after breast cancer detection.

Cumulative Survival	Population Cancer Registries Girona and Tarragona	Hospital Cancer Registry PSMAR
Observed (uncorrected)	97.44	96.59
Walter and Stitt	94.44	93.52
Xu and Prorok	94.19	92.11
Xu et al.	94.94	93.77
Duffy et al.	92.33	92.39

3.2. Simulation study

The detailed simulation results for all the 24 scenarios can be found in the Appendix (Tables A.2, A.3, A.4 and A.5 and Figure A.2).

Table 3 describes the lead-time (mean and standard error of the 100 simulated datasets for each of the 24 scenarios), overall and stratified by age at entering S_p , for

Table 3: Estimated lead-time (years) for screen-detected cases, overall and by age at entering the pre-clinical state. Mean and standard error (S.E.) of the 100 simulated datasets for each screening strategy.

Strategy	Age at entering the pre-clinical state							
	Overall		< 40 yrs		40 – 49 yrs		≥ 50 yrs	
	Mean	S.E.	Mean	S.E.	Mean	S.E.	Mean	S.E.
A4069	3.67	0.06	1.98	0.26	3.17	0.14	3.83	0.07
B4068	3.69	0.07	1.98	0.27	3.22	0.15	3.85	0.08
A5069	3.81	0.06	1.73	1.60	3.56	0.22	3.84	0.07
B5068	3.81	0.07	1.63	1.59	3.56	0.22	3.84	0.08

A4069: Annual exams in the age interval 40-69 years. B4068: Biennial exams in the age interval 40-68 years.
 A5069: Annual exams in the age interval 50-69 years. B5068: Biennial exams in the age interval 50-68 years.

the four screening strategies. Mean lead-times for all the strategies, by age group, were similar, with an increasing trend by age at entering S_p . It is important to notice that the mean lead-times correspond to screen-detected cancers only.

Figure 2 shows the cumulative observed (solid) and corrected (dashed) BC survival after diagnosis of BC for screen-detected cases, for biennial screening strategies. The figure corresponds to one of the 100 simulated datasets for $\alpha = 1.25$ with (left) and without (right) survival benefit. The separation of the curves is more marked in the assumption of no survival benefit, mainly for the 5 to 10 years follow-up time interval.

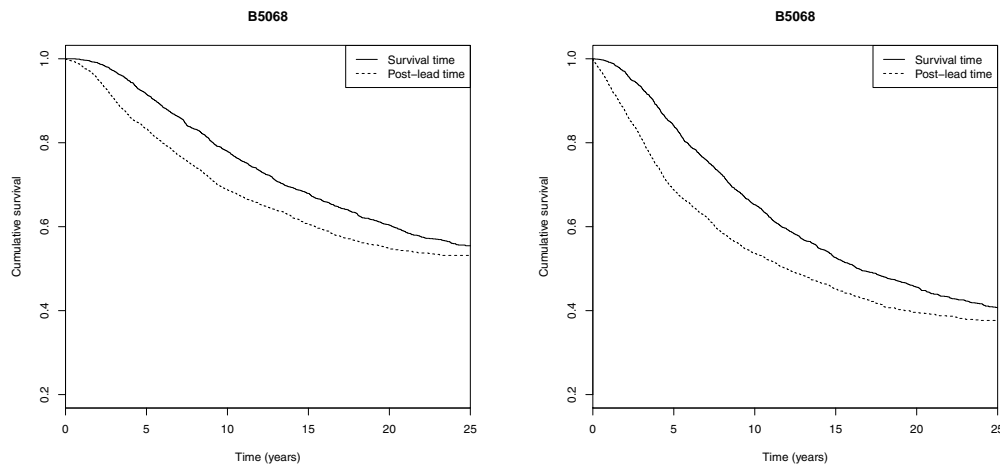


Figure 2: BC cause-specific survival of screen-detected cases. B5068: Biennial exams in the age interval 50-68 years. $\alpha = 1.25$, left: with screening benefit, right: without screening benefit.

Table 4 presents the mean and standard error estimates of the median survival time and the median post-lead-time for the screen-detected cases with the assumption of no benefit. The lead-time and length biases are also summarized. For each screening strategy, both the survival time and post-lead-time increase as α increases. This result is

Table 4: Median total survival time (biased), median post-lead-time (corrected) and early detection biases for screen-detected cases, without benefit of screening. Different assumptions (values of α) of correlation between time in S_p and survival time.

Without benefit of screening									
$\alpha = 1$	Median survival time		Median post-lead time		Median lead-time bias		Median length bias		Strategy
	Mean	S.E.	Mean	S.E.	Mean	S.E.	Mean	S.E.	
A4069	15.83	0.43	11.20	0.44	4.63	0.23	-0.03	0.31	
B4068	15.83	0.48	11.20	0.49	4.63	0.26	-0.03	0.35	
A5069	15.69	0.43	10.92	0.42	4.76	0.21	-0.31	0.31	
B5068	15.66	0.48	10.92	0.46	4.75	0.27	-0.31	0.38	
$\alpha = 1.25$	Median survival time		Median post-lead time		Median lead-time bias		Median length bias		Strategy
	Mean	S.E.	Mean	S.E.	Mean	S.E.	Mean	S.E.	
A4069	16.09	0.52	11.74	0.45	4.35	0.23	1.11	0.34	
B4068	16.69	0.59	12.32	0.53	4.38	0.25	1.69	0.41	
A5069	15.99	0.48	11.50	0.45	4.49	0.23	0.87	0.34	
B5068	16.49	0.59	12.01	0.53	4.48	0.24	1.38	0.44	
$\alpha = 1.5$	Median survival time		Median post-lead time		Median lead-time bias		Median length bias		Strategy
	Mean	S.E.	Mean	S.E.	Mean	S.E.	Mean	S.E.	
A4069	16.40	0.54	12.23	0.46	4.17	0.20	2.00	0.36	
B4068	17.71	0.70	13.37	0.64	4.34	0.27	3.13	0.53	
A5069	16.35	0.51	12.03	0.45	4.31	0.26	1.80	0.35	
B5068	17.45	0.65	13.03	0.57	4.42	0.27	2.79	0.48	

A4069: Annual exams in the age interval 40-69 years. B4068: Biennial exams in the age interval 40-68 years.

A5069: Annual exams in the age interval 50-69 years. B5068: Biennial exams in the age interval 50-68 years.

consistent with the facts: 1) screen-detected tumors have a longer sojourn time in S_p ; and 2) higher values of α indicate higher correlation between time in S_p and survival time, therefore, longer sojourn times will have more chances of being followed by longer survival times and post-lead times. Median lead-time is higher than 4 years in all the screening strategies and decreases as α increases. In contrast, the median length bias is near zero for $\alpha = 1$ and increases with α . For $\alpha = 1.25$, which indicates moderate correlation between sojourn time in S_p and survival time, the median length bias takes values around 1 year. While the lead-time is similar in annual and biennial strategies, the length bias is higher in biennial than annual strategies.

Table 5 provides the RMSE mean between the simulated and predicted survival when the bias correction methods were used, for each screening scenario. For all scenarios, the Xu and Prorok and the Duffy et al. methods outperformed the other methods in terms of mean RMSE. The Walter and Stitt method obtained the worst mean RMSE in all

Table 5: Root mean square error (RMSE) $\times 10^{-2}$ obtained using the bias correction methods described in section 2.2.

	$\alpha = 1$			$\alpha = 1.25$			$\alpha = 1.5$					
	A4069	B4068	A5069	B5068	A4069	B4068	A5069	B5068	A4069	B4068	A5069	B5068
With survival												
benefit	A4069	B4068	A5069	B5068	A4069	B4068	A5069	B5068	A4069	B4068	A5069	B5068
Walter and Stitt	4.44	4.75	3.47	3.88	4.28	4.53	3.29	3.62	4.13	4.28	3.15	3.39
Xu and Prorok	1.23	1.35	1.31	1.41	0.89	0.99	0.94	1.04	1.14	1.23	1.19	1.29
Xu et al.	2.27	2.44	2.44	2.61	1.75	1.85	1.80	1.90	1.63	1.68	1.57	1.64
Duffy et al.	1.52	1.68	1.61	1.78	1.02	1.10	1.18	1.25	0.92	0.94	1.12	1.13
Without survival												
benefit	A4069	B4068	A5069	B5068	A4069	B4068	A5069	B5068	A4069	B4068	A5069	B5068
Walter and Stitt	7.22	7.16	6.28	6.32	6.99	6.84	6.00	5.96	6.74	6.52	5.70	5.60
Xu and Prorok	1.89	1.93	1.95	1.99	1.21	1.26	1.27	1.31	1.46	1.48	1.56	1.57
Xu et al.	4.04	4.03	4.31	4.29	3.20	3.11	3.35	3.26	2.81	2.70	2.87	2.75
Duffy et al.	3.15	3.16	3.34	3.34	2.25	2.19	2.46	2.38	1.71	1.61	1.95	1.83

A4069: Annual exams in the age interval 40-69 years.

B4068: Biennial exams in the age interval 40-68 years.

A5069: Annual exams in the age interval 50-69 years.

B5068: Biennial exams in the age interval 50-68 years.

scenarios and the Xu and Prorok method performed better in scenarios with moderate association; on the other hand the Xu et al. method performed better in moderate or strong association scenarios and with survival benefit.

3.3. Validation

Our cumulative incidence estimate in the 0-85 age interval was 7.81% for the cohort of Catalan women born in 1950 (Table A.2 in the Appendix). The results are consistent with cross-sectional estimates in the 0-74 age-interval of 7.01% in 1995 and 7.89% in 2002, for Catalan women (Borras et al., 2008). Moreover, the Catalan survival rate at five years was 80.9 for women diagnosed with BC in the period 1995-1999 (Galceran et al., 2008). The corresponding estimate in our simulation study, assuming that there was a screening benefit, is somewhat lower, 76.1%.

Our simulated results show that around 40 to 50% of women diagnosed with BC are expected to die of the disease (Table A.5 in the Appendix). These results are comparable with those obtained by Bush et al. who reported that non-BC deaths accounted for almost half of deaths among BC patients in the 15 years following diagnosis (Bush et al., 2010).

Our simulated data estimated percentages of interval cases among all BC cases equal to 30.6% and 28.7% in the age groups 50-59 and 60-69 years, respectively, for the scenario B50-68. Corresponding data for the INCA study were 36% and 26%, respectively (data not published).

Our estimated overall program sensitivity for B50-68 was 70.5%. This value in the INCA study was 68.1% (data not published).

4. Discussion

4.1. Principal findings

This study used BC registry data and simulations to correct BC survival estimates and to assess the impact of lead-time and length sampling biases on survival estimates of screen-detected BC. When the observed survival estimates from the PCR or the HCR-PSMAR were corrected for lead-time bias, the cumulative survival estimates at 5 years decreased between 2.5 to 5.1 percent units, depending on the correction method used. The simulation results showed that, except the Walter and Stitt method, the other three methods for correcting biases performed without major differences. Furthermore, the most accurate correction for the survival estimate was obtained with one or another method depending on different settings. In addition, the simulation results also showed that: 1) screening for BC annually or biennially after 40 years of age brings the age at diagnosis for screen detected cancers forward by more than 3 years; 2) median survival time of screen-detected cases may be overestimated by more than 4 years due to lead-time bias; and 3) assuming a moderate correlation between sojourn time in the pre-

clinical state and survival time (parameter $\alpha = 1.25$), women with screen-detected BC may have a median survival time (already corrected by lead-time) around 1 year or more longer than non-screened women due to length bias. Overall, median survival of screen-detected cases might have been overestimated by 5 years if no corrections for these biases were made.

4.2. Comparison with other studies

Some authors, such as Kafadar and Prorok (2009), have assumed that the benefit of screening is zero to be able to estimate the length bias. According to Kafadar and Prorok, since survival time for screen-detected cases confounds the effects of lead-time, benefit time, and length-sampling bias, studies that use survival time to evaluate screening programs need to take account of these effects.

Shen et al. (2005) found an apparent survival benefit beyond stage shift for patients with screen-detected BC compared with patients with BC detected otherwise. They concluded that method of detection is an important prognostic factor for BC survival, even after adjusting for known tumor characteristics. This result is consistent with our results which indicate a non-negligible length bias effect.

Lehtimaki et al. (2011) performed a multivariate analysis to assess the effect of methods of detection on BC survival, adjusted by tumor size, node involvement, differentiation grade, hormonal status and ductal type. The method of detection was an independent prognostic factor, with a hazard ratio of 1.69 (95% confidence interval = 1.06 to 2.70) between patients whose tumors were detected outside screening and those whose tumors were screen-detected. The authors conclude that survival differences could not be explained completely by lead-time and length bias-related variables, although they may have not completely corrected these biases when adjusting by known risk factors.

4.3. Limitations

This study has several limitations. First, data from the PCR and the HCR-PSMAR presented a large percentage of right censoring, that hindered the application of the methods of bias correction and interpretation of the results. Our simulation study tried to overcome this limitation by extending the follow-up and therefore increasing the number of events. Second, our model relies on data and assumptions that may be not correct. For instance, a) the older age-specific BC incidence and mortality rates for the studied 1950 cohort were projected using an age-period-cohort model. b) The distribution of disease stages at diagnosis for annual or biennial strategies or for screen-detected, clinical or interval cases was taken from US data due to non-availability of annual screening data from the Catalan or Spanish registries. c) We assumed independence between death from BC and other causes. d) We could not test the appropriateness of the copula parameters that correlate both sojourn and survival times. Thus, we used several values compatible with low, medium or high correlation assumptions between the sojourn times. In any

case, many of the simulated results are consistent with the literature and the trends observed are compatible with the studied screening scenarios, therefore we think that our estimates of lead-time and length sampling biases are reliable.

4.4. Conclusion

Survival estimates of screen-detected BC cases are affected by the lead-time and length-sampling biases. The size of these biases depends on the starting age and periodicity of the screening exams. If lead-time and length-sampling bias were not taken into account, the median survival time of screen-detected BC cases may be overestimated by 5 years and the cumulative survival at 5 years may be overestimated between 2.5 to 5 percent. Our results illustrate the importance of correcting or controlling these biases when assessing the benefit of screening mammography. The Xu and Prorok, Duffy et al. and Xu et al. methods for correcting biases outperformed the Walter and Stitt method, with slight differences depending on the scenarios' assumptions.

Acknowledgements

In Memory of Professor Marvin Zelen, without whose enormous contributions to the field of statistics this article would not have been possible.

This study was funded by grant PS09/01340 from the Health Research Fund (Fondo de Investigación Sanitaria) of the Spanish Ministry of Health. We are also indebted to the INCA Study Group for providing data that was used to validate our simulation study and to the research group Grup de Recerca en Anàlisi Estadística de la Supervivència (GRASS) for fruitful discussions. We also thank the reviewers of this paper for their valuable comments on a preliminary version of the manuscript and JP Glutting for review and editing.

Appendix

Table A.1: Distribution of stages at diagnosis of BC.

Age (years)	Stages ¹				
	I	II-	II+	III	IV
	Background ^{1,2}				
40-49	0.3008	0.2277	0.3091	0.0999	0.0625
50-59	0.2868	0.2176	0.3111	0.1021	0.0825
60-69	0.3028	0.2225	0.2713	0.0974	0.1061
70-79	0.3157	0.2671	0.2227	0.0983	0.0961

Table A.1 (cont): Distribution of stages at diagnosis of BC.

Annual screening. Screen-detected cases ^{1,3}					
40-49	0.6200	0.1131	0.2141	0.0436	0.0092
50-59	0.6669	0.1057	0.1935	0.0296	0.0043
60-69	0.7641	0.0739	0.1412	0.016	0.0047
70-79	0.7821	0.0875	0.1067	0.0165	0.0072
Annual screening. Interval cases ^{1,3}					
40-49	0.4644	0.1903	0.2598	0.0667	0.0188
50-59	0.4501	0.1744	0.2976	0.0665	0.0113
60-69	0.5417	0.1532	0.2320	0.0591	0.0141
70-79	0.5446	0.2345	0.1583	0.0496	0.013
Biennial screening. Screen-detected cases ^{1,3}					
40-49	0.5839	0.1217	0.2360	0.0438	0.0146
50-59	0.6210	0.1472	0.1734	0.0423	0.0161
60-69	0.6563	0.1295	0.1830	0.0246	0.0067
70-79	0.7287	0.1311	0.1128	0.0137	0.0137
Biennial screening. Interval cases ^{1,3}					
40-49	0.3673	0.2246	0.3099	0.0819	0.0164
50-59	0.2945	0.2609	0.2648	0.1166	0.0632
60-69	0.4077	0.2231	0.2672	0.0744	0.0275
70-79	0.4336	0.2885	0.1770	0.0673	0.0336

¹ American Joint Committee on Cancer (AJCC) stage distribution.

² From Surveillance, Epidemiology, and End Results (SEER).

³ From Breast Cancer Surveillance Consortium (BCSC).

Table A.2: Pre-clinical state summary and cumulative incidence. Background scenario. One hundred simulated scenarios for each screening strategy. Time horizon 0-85 years.

Parameter	Mean	S.E.
Cumulative transition to S_p (%)	9.08	0.09
Cumulative incidence (%)	7.81	0.08
Mean sojourn time in S_p (years)	3.24	0.04
Mean sojourn time in $S_p \leq 40$ (years)	2.00	0.11
Mean sojourn time in S_p 40 – 50 (years)	3.16	0.13
Mean sojourn time in $S_p > 50$ (years)	4.01	0.05

Table A.3: Screening summary. One hundred simulated scenarios for each screening strategy. Time horizon 0-85 years.

Strategy ¹	Mean sojourn time SD ²		Mean sojourn time I ²		Program sensitivity ³		Cumulative incidence ³	
	Mean	S.E.	Mean	S.E.	Mean	S.E.	Mean	S.E.
A4069	4.40	0.06	0.66	0.02	47.40	0.62	7.87	0.08
B4068	4.91	0.07	1.12	0.03	37.39	0.56	7.85	0.08
A5069	4.67	0.06	0.72	0.03	41.49	0.60	7.86	0.08
B5068	5.15	0.08	1.19	0.03	33.15	0.56	7.85	0.08

¹ A4069: Annual exams in the age interval 40-69 years.

B4068: Biennial exams in the age interval 40-68 years.

A5069: Annual exams in the age interval 50-69 years.

B5068: Biennial exams in the age interval 50-68 years.

² SD: Screen-detected cases, I: Interval cases.

³ Expressed as percentage.

Table A.4: Median survival summary for interval cancer cases. One hundred simulated scenarios for each screening strategy. Time horizon 0-85 years.

Survival time for interval cancer cases				
$\alpha = 1$	With benefit of screening		Without benefit of screening	
	Mean	S.E.	Mean	S.E.
Strategy ¹				
A4069	18.79	2.01	11.55	1.01
B4068	14.24	0.95	11.40	0.70
A5069	17.55	2.03	10.86	1.00
B5068	13.41	1.05	10.86	0.81
$\alpha = 1.25$	With benefit of screening		Without benefit of screening	
	Mean	S.E.	Mean	S.E.
Strategy ¹				
A4069	13.52	1.16	8.70	0.66
B4068	11.13	0.63	8.99	0.52
A5069	12.99	1.07	8.26	0.67
B5068	10.62	0.71	8.60	0.60
$\alpha = 1.5$	With benefit of screening		Without benefit of screening	
	Mean	S.E.	Mean	S.E.
Strategy ¹				
A4069	10.92	0.74	7.07	0.51
B4068	9.40	0.49	7.57	0.42
A5069	10.65	0.75	6.74	0.51
B5068	8.98	0.55	7.24	0.47

¹ A4069: Annual exams in the age interval 40-69 years. B4068: Biennial exams in the age interval 40-68 years. A5069: Annual exams in the age interval 50-69 years. B5068: Biennial exams in the age interval 50-68 years.

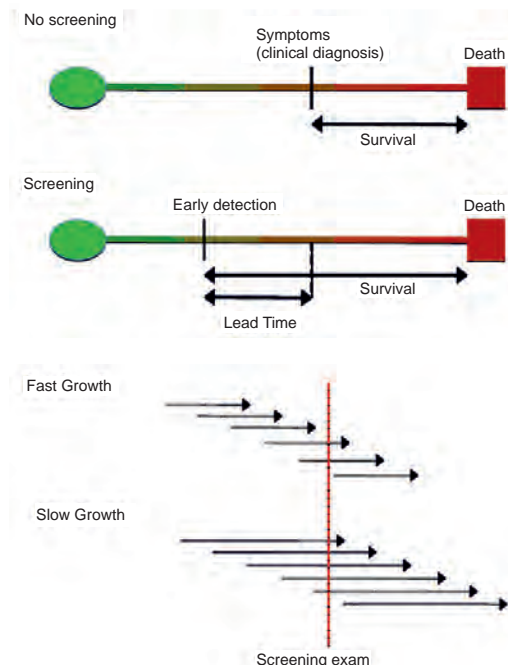


Figure A.1: Lead-time (top) and length bias (bottom).

Table A.5: *Mortality summary. One hundred simulated scenarios for each screening strategy. Time horizon 0-85 years.*

With benefit of screening									
$\alpha = 1$	Cumulative mortality		Deaths by BC		Deaths by BC SD ²		Deaths by BC I ²		
Strategy ¹	Mean	S.E.	Mean	S.E.	Mean	S.E.	Mean	S.E.	
A4069	3.04	0.05	38.90	0.59	40.82	0.82	51.03	1.74	
B4068	3.24	0.05	41.53	0.57	43.12	0.93	55.89	1.25	
A5069	3.10	0.05	39.71	0.61	40.02	0.87	51.40	1.96	
B5068	3.29	0.05	42.10	0.58	42.60	0.97	56.63	1.66	
$\alpha = 1.25$	Cumulative mortality		Deaths by BC		Deaths by BC SD ²		Deaths by BC I ²		
Strategy ¹	Mean	S.E.	Mean	S.E.	Mean	S.E.	Mean	S.E.	
A4069	3.13	0.05	40.10	0.60	40.06	0.88	57.47	1.80	
B4068	3.34	0.05	42.73	0.60	41.36	0.95	61.32	1.31	
A5069	3.19	0.05	40.92	0.61	39.17	0.91	57.85	1.99	
B5068	3.38	0.05	43.30	0.60	40.84	0.98	62.19	1.62	
$\alpha = 1.5$	Cumulative mortality		Deaths by BC		Deaths by BC SD ²		Deaths by BC I ²		
Strategy ¹	Mean	S.E.	Mean	S.E.	Mean	S.E.	Mean	S.E.	
A4069	3.19	0.05	40.88	0.61	39.24	0.88	62.60	1.72	
B4068	3.40	0.05	43.54	0.62	39.79	0.97	65.73	1.22	
A5069	3.25	0.05	41.69	0.61	38.26	0.88	63.00	1.90	
B5068	3.44	0.05	44.10	0.62	39.24	0.97	66.66	1.59	
Without benefit of screening									
$\alpha = 1$	Cumulative mortality		Deaths by BC		Deaths by BC SD ²		Deaths by BC I ²		
Strategy ¹	Mean	S.E.	Mean	S.E.	Mean	S.E.	Mean	S.E.	
A4069	3.72	0.05	47.65	0.59	57.88	0.81	59.78	1.73	
B4068	3.72	0.05	47.65	0.59	58.10	0.90	59.97	1.23	
A5069	3.72	0.05	47.65	0.59	57.93	0.86	60.78	1.91	
B5068	3.72	0.05	47.65	0.59	58.23	0.97	60.88	1.53	
$\alpha = 1.25$	Cumulative mortality		Deaths by BC		Deaths by BC SD ²		Deaths by BC I ²		
Strategy ¹	Mean	S.E.	Mean	S.E.	Mean	S.E.	Mean	S.E.	
A4069	3.80	0.05	48.72	0.57	56.78	0.80	66.40	1.73	
B4068	3.80	0.05	48.72	0.57	55.96	0.88	65.50	1.28	
A5069	3.80	0.05	48.72	0.57	56.74	0.83	67.34	1.79	
B5068	3.80	0.05	48.72	0.57	56.07	0.96	66.46	1.60	
$\alpha = 1.5$	Cumulative mortality		Deaths by BC		Deaths by BC SD ²		Deaths by BC I ²		
Strategy ¹	Mean	S.E.	Mean	S.E.	Mean	S.E.	Mean	S.E.	
A4069	3.86	0.05	49.49	0.58	55.89	0.77	71.71	1.67	
B4068	3.86	0.05	49.49	0.58	54.22	0.85	69.96	1.17	
A5069	3.86	0.05	49.49	0.58	55.76	0.83	72.72	1.65	
B5068	3.86	0.05	49.49	0.58	54.27	0.90	71.07	1.45	

¹ A4069: Annual exams in the age interval 40-69 years. B4068: Biennial exams in the age interval 40-68 years.

A5069: Annual exams in the age interval 50-69 years. B5068: Biennial exams in the age interval 50-68 years.

² SD: Screen-detected cases, I: Interval cases.

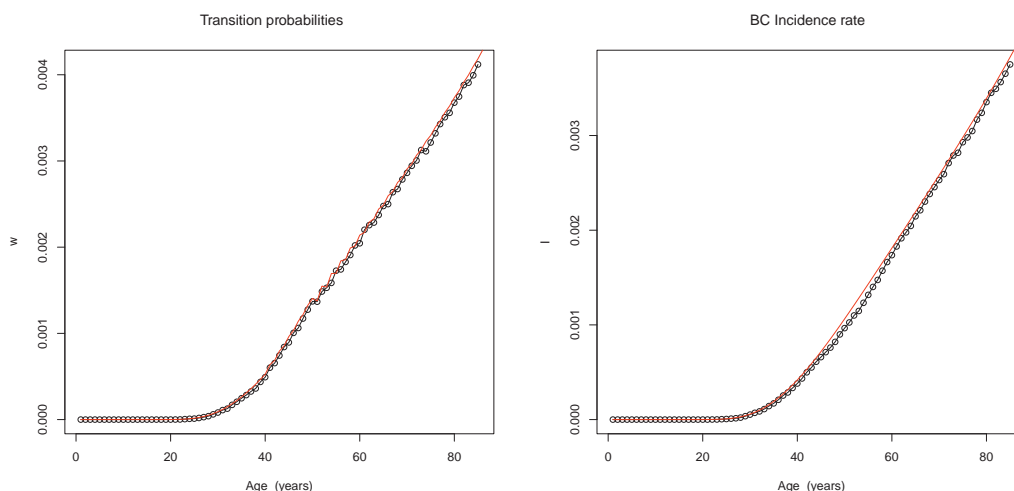


Figure A.2: Mean simulated (black dots) and observed (red line) BC transition to *Sp* and incidence rates. One hundred simulated scenarios for each screening strategy. Time horizon 0–85 years.

References

- Blanch, J., Sala, M., Ibáñez, J., Domingo, L., Fernandez, B., Otegi, A., Barata, T., Zubizarreta, R., Ferrer, J., Castells, X., Rué, M. and Salas, D. (2014). Impact of risk factors on different interval cancer subtypes in a population-based breast cancer screening programme. *PLoS One*, 9(10): e110207.
- Borras, J., Ameijide, A., Vilardell, L., Valls, J., Marcos-Gragera, R. and Izquierdo, A. (2008). Trends in cancer incidence in Catalonia, 1985–2002. *Medicina Clínica (Barcelona)*, 131 Suppl 1, 11–18.
- Burton, A., Altman, D. G., Royston, P. and Holder, L. (2006). The design of simulation studies in medical statistics. *Statistics in Medicine*, 25, 4279–4292.
- Bush, D., Smith, B., Younger, J. and Michaelson, J. S. (2010). The non-breast-cancer death rate among breast cancer patients. *Breast Cancer Research and Treatment*.
- Domingo, L., Salas, D., Zubizarreta, R., Baré, M., Sarriugarte, G., Barata, T., Ibáñez, J., Blanch, J., Puig-Vives, M., Fernández, A., Castells, X. and Sala, M. (2014). Tumor phenotype and breast density in distinct categories of interval cancer: results of population-based mammography screening in Spain. *Breast Cancer Research*, 16: R3.
- Duffy, S. W., Nagtegaal, I. D., Wallis, M., Cafferty, F. H., Houssami, N., Warwick, J., Allgood, P. C., Kearins, O., Tappenden, N., O’Sullivan, E. and Lawrence, G. (2008). Correcting for lead time and length bias in estimating the effect of screen detection on cancer survival. *American Journal of Epidemiology*, 168, 98–104.
- Galceran, J., Puigdefabregas, A., Ribas, G., Izquierdo, A., Pareja, L. and Marcos-Gragera, R. (2008). Cancer survival trends in Catalonia and comparison with Europe. *Medicina Clínica (Barcelona)*, 131 Suppl 1, 19–24.
- Gotzsche, P. C. and Nielsen, M. (2009). Screening for breast cancer with mammography. *Cochrane Database of Systematic Reviews*, (4), CD001877.
- Kafadar, K. and Prorok, P. C. (2009). Effect of length biased sampling of unobserved sojourn times on the survival distribution when disease is screen detected. *Statistics in Medicine*, 28, 2116–2146.

- Lee, S. and Zelen, M. (2006). A stochastic model for predicting the mortality of breast cancer. *Journal of the National Cancer Institute Monographs*, 79–86.
- Lee, S. J. and Zelen, M. (1998). Scheduling periodic examinations for the early detection of disease: applications to breast cancer. *Journal of the American Statistical Association*, 93, 1271–1281.
- Lee, S. J. and Zelen, M. (2008). Mortality modeling of early detection programs. *Biometrics*, 64, 386–395.
- Lehtimäki, T., Lundin, M., Linder, N., Sihto, H., Holli, K., Turpeenniemi-Hujanen, T., Kataja, V., Isola, J., Joensuu, H. and Lundin, J. (2011). Long-term prognosis of breast cancer detected by mammography screening or other methods. *Breast Cancer Research and Treatment*, 13, R134.
- Mahnken, J. D., Chan, W., Jr Freeman, D. H. and Freeman, J. L. (2008). Reducing the effects of lead-time bias, length bias and over-detection in evaluating screening mammography: a censored bivariate data approach. *Statistical Methods in Medical Research*, 17, 643–663.
- Martinez-Alonso, M., Vilapriño, E., Marcos-Gragera, R. and Rue, M. (2010). Breast cancer incidence and overdiagnosis in Catalonia (Spain). *Breast Cancer Research and Treatment*, 12, R58.
- R Core Team (2013). *R: A Language and Environment for Statistical Computing*. R Foundation for Statistical Computing, Vienna, Austria.
- Shen, Y., Yang, Y., Inoue, L. Y., Munsell, M. F., Miller, A. B. and Berry, D. A. (2005). Role of detection method in predicting breast cancer survival: analysis of randomized screening trials. *Journal of the National Cancer Institute*, 97, 1195–1203.
- Trivedi, P. K. and Zimmer, D. M. (2007). Copula modeling: an introduction for practitioners. *Foundation and trends in Econometrics*, 1, 1–111.
- Vilapriño, E., Gispert, R., Martinez-Alonso, M., Carles, M., Pla, R., Espinas, J. A. and Rue, M. (2008). Competing risks to breast cancer mortality in Catalonia. *BMC Cancer*, 8, 331.
- Vilapriño, E., Rue, M., Marcos-Gragera, R. and Martinez-Alonso, M. (2009). Estimation of age- and stage-specific Catalan breast cancer survival functions using US and Catalan survival data. *BMC Cancer*, 9, 98.
- Walter, S. D. and Day, N. E. (1983). Estimation of the duration of a pre-clinical disease state using screening data. *American Journal of Epidemiology*, 118, 865–886.
- Walter, S. D. and Stitt, L. W. (1987). Evaluating the survival of cancer cases detected by screening. *Statistics in Medicine*, 6, 885–900.
- Xu, J. L., Fagerstrom, R. M. and Prorok, P. C. (1999). Estimation of post-lead-time survival under dependence between lead-time and post-lead-time survival. *Statistics in Medicine*, 18, 155–162.
- Xu, J. L. and Prorok, P. C. (1995). Non-parametric estimation of the post-lead-time survival distribution of screen-detected cancer cases. *Statistics in Medicine*, 14, 2715–2725.
- Zelen, M. and Feinleib, M. (1969). On the theory of screening for chronic diseases. *Biometrika*, 56, 601–614.

Estimators for the parameter mean of Morgenstern type bivariate generalized exponential distribution using ranked set sampling

Saeid Tahmasebi¹ and Ali Akbar Jafari²

Abstract

In situations where the sampling units in a study can be more easily ranked based on the measurement of an auxiliary variable, ranked set sampling provides unbiased estimators for the mean of a population that are more efficient than unbiased estimators based on simple random sampling. In this paper, we consider the Morgenstern type bivariate generalized exponential distribution and obtain several unbiased estimators for the mean parameter of its marginal distribution, based on different ranked set sampling schemes. The efficiency of all considered estimators are evaluated and several numerical illustrations are given.

MSC: 62D05; 62F07;62G30.

Keywords: Concomitants of order statistics, Morgenstern type bivariate generalized exponential distribution, ranked set sampling.

1. Introduction

Ranked set sampling (RSS) was first suggested by McIntyre (1952) for estimating mean pasture and forage yields. RSS is applicable whenever ranking of a set of sampling units can be done easily by a judgement method with respect to the variable of interest. Later, Takahasi and Wakimoto (1968) provided the statistical foundation and necessary mathematical properties of the method. They indicated that in situations where the sampling units in a study can be more easily ranked based on the measurement of an auxiliary

* Corresponding author e-mail: aajafari@yazd.ac.ir

¹ Department of Statistics, Persian Gulf University, Bushehr, Iran.

² Department of Statistics, Yazd University, Yazd, Iran.

Received: August 2013

Accepted: May 2014

variable, RSS provides unbiased estimators for the mean of a population, and these estimators are more efficient than unbiased estimators based on simple random sampling (SRS).

The RSS technique is composed of two stages in a sample selection procedure: At the first stage, n simple random samples of size n are drawn from a population and each sample is called a set. Then, each of the units are ranked from the smallest to the largest according to a variable of interest, say Y , in each set based on a low-level measurement such as a concomitant variable or previous experience. At the second stage, the first unit from the first set, the second unit from the second set and going on like this till the n th unit from the n th set are taken and measured according to the variable Y . The obtained sample is called a RSS. It can be noted that the units of this sample are independent order statistics but not identically distributed. The reader can refer to the book of Chen et al. (2004) for details of RSS and its applications.

Other schemes and modifications of RSS were investigated in the literature: A modified RSS procedure is introduced by Stokes (1980) and only the largest or the smallest judgment ranked unit is chosen for quantification in each set. In estimating the population mean, Samawi et al. (1996) suggested the extreme ranked set sampling (ERSS), Muttlak (1997) suggested the median RSS, Jemain and Al-Omari (2006) suggested double quartile ranked set samples, and Al-Odat and Al-Saleh (2001) suggested moving extreme ranked set sampling (MERSS). Yu and Tam (2002) considered the problem of estimating the mean of a population based on RSS with censored data. Al-Saleh and Al-Kadiri (2000) considered double RSS (DRSS), and Al-Saleh and Al-Omari (2002) generalized the DRSS to the multistage ranked set sampling (MSRSS) method. For the mean normal or exponential, Sinha et al. (1996) used median ranked set sampling (MRSS) to modify the RSS estimators Muttlak (2003) introduced percentile ranked set sampling (PRSS). Al-Nasser (2007) proposed a generalized robust sampling method called L ranked set sampling (LRSS) and showed that the estimator for the mean based on the LRSS is unbiased if the underlying distribution is symmetric. A robust extreme ranked set sampling (RERSS) is proposed by Al-Nasser and Mustafa (2009) for estimating the population mean.

RSS and its modifications are applied for estimating a parameter in a bivariate population (X, Y) , where Y is the variable of interest and X is a concomitant variable that is not of direct interest but is relatively easy to measure or to order by judgment: Stokes (1977) studied RSS with concomitant variables. Barnett and Moore (1997) derived the best linear unbiased estimator (BLUE) for the mean of Y , based on a ranked set sample obtained using an auxiliary variable X . Al-Saleh and Al-Ananbeh (2007) estimated the means of the bivariate normal distribution using moving extremes RSS. Chacko and Thomas (2008) and Al-Saleh and Diab (2009) considered estimation of a parameter of Morgenstern type bivariate exponential distribution and Downton's bivariate exponential distribution, respectively. Tahmasebi and Jafari (2012) assumed the Morgenstern type bivariate uniform distribution and obtained several estimators for a scale parameter.

The distribution function of a Morgenstern type bivariate generalized exponential distribution (MTBGED) is defined as

$$F_{X,Y}(x,y) = (1 - e^{-\theta_1 x})^{\alpha_1} (1 - e^{-\theta_2 y})^{\alpha_2} [1 + \lambda(1 - (1 - e^{-\theta_1 x})^{\alpha_1})(1 - (1 - e^{-\theta_2 y})^{\alpha_2})], \quad (1)$$

$$x, y > 0, \quad -1 \leq \lambda \leq 1, \quad \alpha_1, \alpha_2, \theta_1, \theta_2 > 0,$$

with the corresponding probability density function (pdf)

$$f_{X,Y}(x,y) = \alpha_1 \alpha_2 \theta_1 \theta_2 e^{-\theta_1 x - \theta_2 y} (1 - e^{-\theta_1 x})^{\alpha_1 - 1} (1 - e^{-\theta_2 y})^{\alpha_2 - 1} \\ \times \left\{ 1 + \lambda [2(1 - e^{-\theta_1 x})^{\alpha_1} - 1][2(1 - e^{-\theta_2 y})^{\alpha_2} - 1] \right\}. \quad (2)$$

Note that when (X, Y) has MTBGED, the marginal distribution of X and Y is the generalized exponential distribution with the expected values

$$\mu_x = \frac{B(\alpha_1)}{\theta_1}, \quad \mu_y = \frac{B(\alpha_2)}{\theta_2},$$

respectively, where $B(\alpha) = \psi(\alpha + 1) - \psi(1)$ and $\psi(\cdot)$ is the digamma function. Also, the correlation coefficient between X and Y is obtained as (see Tahmasebi and Jafari, 2013)

$$\rho = \frac{\lambda D(\alpha_1) D(\alpha_2)}{\sqrt{C(\alpha_1) C(\alpha_2)}} = \lambda g(\alpha_1) g(\alpha_2), \quad (3)$$

where $D(\alpha) = B(2\alpha) - B(\alpha)$, $C(\alpha) = \psi'(1) - \psi'(\alpha + 1)$, $\psi'(\cdot)$ is the derivative of the digamma function, and $g(\alpha) = \frac{D(\alpha)}{\sqrt{C(\alpha)}}$.

In this paper, we consider estimation of the parameter μ_y when α_2 is known, and propose several estimator based on the RSS idea. Also, we suggest some improved version of these estimators. In Section 2, we present unbiased estimators for the parameter μ_y in MTBGED based on the RSS, LRSS, ERSS, MERSS, and MSRSS methods. We evaluate the efficiency of all considered estimators in Section 3.

2. Unbiased estimators for μ_y based on different RSS schemes

Suppose that the random variable (X, Y) has a MTBGED as defined in (1). In this section, we find unbiased estimators for the parameter μ_y based on different sampling schemes. In each case, first the general pattern of sampling is presented, and then an unbiased estimator with its variance is given for the parameter μ_y . Also, the efficiency of the proposed estimators are obtained.

2.1. RSS estimation

The procedure of RSS is described by Stokes (1977) for a bivariate random variable by the following steps:

Step 1. Randomly select n independent bivariate samples, each of size n .

Step 2. Rank the units within each sample with respect to variable X together with the Y variate associated.

Step 3. In the r th sample of size n , select the unit $(X_{(r)r}, Y_{[r]r})$, $r = 1, 2, \dots, n$, where $X_{(r)r}$ is the measured observation on the variable X in the r th unit and $Y_{[r]r}$ is the corresponding measurement made on the study variable Y of the same unit.

Therefore, $Y_{[r]r}$, $r = 1, 2, 3, \dots, n$, are the RSS observations made on the units of the RSS regarding the study variable Y which is correlated with the auxiliary variable X . Therefore, clearly $Y_{[r]r}$ is the concomitant of r th order statistic arising from the r th sample.

From Scaria and Nair (1999) the pdf of $Y_{[r]r}$ for $1 \leq r \leq n$ is given by

$$h_{[r]r}(y) = \alpha_2 \theta_2 e^{-\theta_2 y} (1 - e^{-\theta_2 y})^{\alpha_2 - 1} [1 + \delta_r (1 - 2(1 - e^{-\theta_2 y})^{\alpha_2})], \quad 1 \leq r \leq n, \quad (4)$$

where $\delta_r = \frac{\lambda(n-2r+1)}{n+1}$ and its mean and variance of $Y_{[r]r}$ are obtained by Tahmasebi and Jafari (2013) as

$$E[Y_{[r]r}] = \frac{1}{\theta_2} [B(\alpha_2) - \delta_r D(\alpha_2)], \quad \text{Var}[Y_{[r]r}] = \frac{1}{\theta_2^2} [C(\alpha_2) + \delta_r (C(2\alpha_2) - C(\alpha_2))]. \quad (5)$$

Since $Y_{[r]r}$ and $Y_{[s]s}$ for $r \neq s$ are drawn from two independent samples, so we have

$$\text{Cov}(Y_{[r]r}, Y_{[s]s}) = 0, \quad r \neq s.$$

Theorem 1 Based on the RSS procedure, an unbiased estimator for μ_y is given by

$$\hat{\mu}_{RSS} = \frac{1}{n} \sum_{r=1}^n Y_{[r]r},$$

and its variance is

$$\text{Var}(\hat{\mu}_{RSS}) = \frac{C(\alpha_2)}{n\theta_2^2}. \quad (6)$$

Proof. Since $\sum_{r=1}^n \delta_r = \sum_{r=1}^n \frac{\lambda(n-2r+1)}{n+1} = 0$, using (5)

$$E(\hat{\mu}_{\text{RSS}}) = \frac{1}{n} \sum_{r=1}^n E(Y_{[r]r}) = \frac{1}{n\theta_2} \sum_{r=1}^n (B(\alpha_2) - \delta_r D(\alpha_2)) = \frac{B(\alpha_2)}{\theta_2} = \mu_y,$$

and

$$\begin{aligned} \text{Var}(\hat{\mu}_{\text{RSS}}) &= \frac{1}{n} \sum_{r=1}^n \text{Var}(Y_{[r]r}) = \frac{1}{n^2\theta_2^2} \sum_{r=1}^n [C(\alpha_2) + \delta_r(C(2\alpha_2) - C(\alpha_2))] \\ &= \frac{1}{n^2\theta_2^2} \sum_{r=1}^n [C(\alpha_2) + \delta_r(C(2\alpha_2) - C(\alpha_2))] = \frac{C(\alpha_2)}{n\theta_2^2}. \quad \square \end{aligned}$$

Now, we study the efficiency of $\hat{\mu}_{\text{RSS}}$ relative to the BLUE of μ_y , $\tilde{\mu}$, based on $Y_{[r]r}$, $r = 1, 2, 3, \dots, n$, for MTBGED, when λ is known. From David and Nagaraja (2003, p. 185) the BLUE of μ_y is derived as

$$\tilde{\mu} = \sum_{r=1}^n a_r Y_{[r]r},$$

where

$$a_r = \frac{H(\alpha_2, r)}{W(\alpha_2, r)} \left(\sum_{j=1}^n \frac{[H(\alpha_2, j)]^2}{W(\alpha_2, j)} \right)^{-1}, \quad r = 1, 2, 3, \dots, n,$$

$H(\alpha_2, r) = 1 - \frac{\delta_r D(\alpha_2)}{B(\alpha_2)}$ and $W(\alpha_2, r) = C(\alpha_2) + \delta_r [C(2\alpha_2) - C(\alpha_2)]$. The variance of $\tilde{\mu}$ is

$$\text{Var}[\tilde{\mu}] = \frac{v_2}{\theta_2^2},$$

where $v_2 = \left(\sum_{r=1}^n \frac{[H(\alpha_2, r)]^2}{W(\alpha_2, r)} \right)^{-1}$, and therefore, the relative efficiency of $\hat{\mu}_{\text{RSS}}$ to $\tilde{\mu}$ is given by

$$e_1 = e(\tilde{\mu} | \hat{\mu}_{\text{RSS}}) = \frac{C(\alpha_2)}{n} \sum_{r=1}^n \frac{[H(\alpha_2, r)]^2}{W(\alpha_2, r)}.$$

In Section 3, we calculate the relative efficiency of $\hat{\mu}_{\text{RSS}}$ to $\tilde{\mu}$, e_1 , for some values of the parameters and sample size.

Remark 2 We know that the correlation coefficient between X and Y in MTBGED is $\lambda g(\alpha_1)g(\alpha_2)$. So when α_1 and α_2 are known, by using the sample correlation coefficient q of the RSS observations $(X_{(r)r}, Y_{[r]r})$, $r = 1, 2, 3, \dots, n$ an estimator for λ is given by

$$\hat{\lambda} = \begin{cases} -1 & q < -g(\alpha_1)g(\alpha_2) \\ \frac{q}{g(\alpha_1)g(\alpha_2)} & -g(\alpha_1)g(\alpha_2) \leq q \leq g(\alpha_1)g(\alpha_2) \\ 1 & g(\alpha_1)g(\alpha_2) < q \end{cases}$$

Sometimes, k units of observations are censored in the RSS schemes. Let $Y_{[m_r]m_r}$, $r = 1, 2, \dots, n-k$, be the ranked set sample observations on the study variable Y , which results from censoring and ranking on the auxiliary variable X . We can represent the ranked set sample observations on the study variate Y as $p_1 Y_{[1]1}, p_2 Y_{[2]2}, \dots, p_n Y_{[n]n}$, where $p_r = 0$ if the r th unit is censored, and $p_r = 1$ otherwise. Consider k units are censored. Hence $\sum_{r=1}^n p_r = n-k$. if we write $m_r, r = 1, 2, \dots, n-k$, as the integers such that $1 \leq m_1 < m_2 < \dots < m_{n-k} \leq n$ and $p_{m_r} = 1$, then

$$E\left(\frac{\sum_{r=1}^n p_r Y_{[r]r}}{n-k}\right) = \frac{1}{\theta_2} \left(B(\alpha_2) - \frac{D(\alpha_2)}{n-k} \sum_{r=1}^{n-k} \delta_{m_r} \right),$$

Therefore, the ranked set sample mean in the censored case is not an unbiased estimator for μ_y . However, we can construct an unbiased estimator based on this expected value.

Theorem 3 An unbiased estimator for μ_y based on the censored RSS is given by

$$\hat{\mu}_{CRSS} = \frac{1}{w} \sum_{r=1}^{n-k} Y_{[m_r]m_r},$$

where $w = n-k + \left(1 - \frac{B(2\alpha_2)}{B(\alpha_2)}\right) \sum_{r=1}^{n-k} \delta_{m_r}$, and its variance is

$$\text{Var}(\hat{\mu}_{CRSS}) = \frac{v_3}{\theta_2^2},$$

where $v_3 = \frac{1}{w^2} \sum_{r=1}^{n-k} [C(\alpha_2) + \delta_{m_r}(C(2\alpha_2) - C(\alpha_2))]$.

Proof

$$E(\hat{\mu}_{CRSS}) = \frac{1}{w} \sum_{r=1}^{n-k} E(Y_{[m_r]m_r}) = \frac{\sum_{r=1}^{n-k} (B(\alpha_2) - \delta_{m_r} D(\alpha_2))}{(n-k - \frac{D(\alpha_2)}{B(\alpha_2)} \sum_{r=1}^{n-k} \delta_{m_r}) \theta_2} = \frac{B(\alpha_2)}{\theta_2} = \mu_y,$$

and $\text{Var}(\hat{\mu}_{CRSS})$ can be easily obtained from (5). □

2.2. LRSS estimation

Al-Nasser (2007) proposed a generalized robust sampling method called L ranked set sampling (LRSS) for estimating population mean. The procedure of LRSS with a concomitant variable is as follows:

- Step 1.** Randomly select n independent bivariate samples, each of size n .
- Step 2.** Rank the units within each sample with respect to variable X together with the Y variate associated.
- Step 3.** Select the LRSS coefficient, $k = [n\gamma]$, such that $0 \leq \gamma < .5$, where $[x]$ is the largest integer value less than or equal to x .
- Step 4.** For each of the first $k+1$ ranked samples of size n , select the unit $(X_{(k+1)r}, Y_{[k+1]r})$, $r = 1, 2, \dots, k$.
- Step 5.** For each of the last $k+1$ ranked samples of size n , i.e., the $(n-k)$ th to the n th ranked sample, select the unit $(X_{(n-k)r}, Y_{[n-k]r})$, $r = n-k+1, \dots, n$.
- Step 6.** For $j = k+2, \dots, n-k-1$, select the unit $(X_{(j)r}, Y_{[j]r})$, $r = k+1, \dots, n-k$.

Note that this LRSS scheme leads to the RSS when $k = 0$, and to the traditional MRSS when $k = \lfloor \frac{n-1}{2} \rfloor$. Also, the PRSS could be considered as a special case of this scheme.

Theorem 4 An unbiased estimator of μ_y in MTBGED based on LRSS scheme is given by

$$\hat{\mu}_{LRSS} = \frac{1}{n} \left(\sum_{r=1}^k Y_{[k+1]r} + \sum_{r=k+1}^{n-k} Y_{[r]r} + \sum_{r=n-k+1}^n Y_{[n-k]r} \right),$$

with variance

$$\text{Var}(\hat{\mu}_{LRSS}) = \text{Var}(\hat{\mu}_{RSS}) = \frac{C(\alpha_2)}{n\theta_2^2}. \quad (7)$$

Proof. Since

$$\begin{aligned} \sum_{r=1}^k \delta_{k+1} &= \frac{\lambda}{n+1} \sum_{r=1}^k (n - 2(k+1) + 1) = \frac{\lambda k}{n+1} (n - 2k - 1), \\ \sum_{r=1}^k \delta_{n-k} &= \frac{\lambda}{n+1} \sum_{r=n-k+1}^n (n - 2(n-k) + 1) = \frac{\lambda k}{n+1} (-n + 2k + 1), \\ \sum_{r=k+1}^{n-k} \delta_r &= \frac{\lambda}{n+1} \sum_{r=k+1}^{n-k} (n - 2r + 1) = 0, \end{aligned}$$

we have

$$E(\hat{\mu}_{LRSS}) = \frac{1}{n} \left(\frac{kB(\alpha_2)}{\theta_2} - \frac{D(\alpha_2)}{\theta_2} \frac{\lambda k}{n+1} (n-2k-1) + \frac{kB(\alpha_2)}{\theta_2} - \frac{D(\alpha_2)}{\theta_2} \frac{\lambda k}{n+1} (-n+2k+1) + \frac{(n-2k)B(\alpha_2)}{\theta_2} \right) = \frac{B(\alpha_2)}{\theta_2} = \mu_y,$$

and

$$\begin{aligned} Var(\hat{\mu}_{LRSS}) &= \frac{1}{n^2} \left(\frac{kC(\alpha_2)}{\theta_2^2} - \frac{C(2\alpha_2) - C(\alpha_2)}{\theta_2} \frac{\lambda k}{n+1} (n-2k-1) + \frac{kC(\alpha_2)}{\theta_2^2} - \frac{C(2\alpha_2) - C(\alpha_2)}{\theta_2^2} \frac{\lambda k}{n+1} (-n+2k+1) + \frac{(n-2k)C(\alpha_2)}{\theta_2^2} \right) = \frac{C(\alpha_2)}{n\theta_2^2}. \end{aligned} \quad \square$$

2.3. ERSS estimation

The extreme ranked set sampling (ERSS) method with concomitant variable, introduced by Samawi et al. (1996), can be described as follows:

Step 1. Select n random samples each of size n bivariate units from the population.

Step 2. If the sample size n is even, then select from $\frac{n}{2}$ samples the smallest ranked unit X together with the associated Y and from the other $\frac{n}{2}$ samples the largest ranked unit X together with the associated Y . These selected observations $(X_{(1)1}, Y_{[1]1}), (X_{(n)2}, Y_{[n]2}), (X_{(1)3}, Y_{[1]3}), \dots, (X_{(1)n-1}, Y_{[1]n-1}), (X_{(n)n}, Y_{[n]n})$ can be denoted by ERSS₁.

Step 3. If n is odd then select from $\frac{n-1}{2}$ samples the smallest ranked unit X together with the associated Y and from the other $\frac{n-1}{2}$ samples the largest ranked unit X together with the associated Y and from one sample the median of the sample for actual measurement. In this case the selected observations $(X_{(1)1}, Y_{[1]1}), (X_{(n)2}, Y_{[n]2}), (X_{(1)3}, Y_{[1]3}), \dots, (X_{(n)n-1}, Y_{[n]n-1}), (\frac{X_{(1)n} + X_{(n)n}}{2}, \frac{Y_{[1]n} + Y_{[n]n}}{2})$ can be denoted ERSS₂ and $(X_{(1)1}, Y_{[1]1}), (X_{(n)2}, Y_{[n]2}), (X_{(1)3}, Y_{[1]3}), \dots, (X_{(n)n-1}, Y_{[n]n-1}), (X_{(\frac{n+1}{2})n}, Y_{[(\frac{n+1}{2})n]})$ can be denoted by ERSS₃.

Theorem 5 (i) if n is even, then an unbiased estimator for μ_y using ERSS₁ is defined as

$$\hat{\mu}_{ERSS_1} = \frac{1}{n} \sum_{r=1}^{n/2} (Y_{[1]2r-1} + Y_{[n]2r}),$$

with variance

$$\text{Var}(\hat{\mu}_{ERSS_1}) = \text{Var}(\hat{\mu}_{RSS}) = \frac{C(\alpha_2)}{n\theta_2^2}.$$

(ii) If n is odd then unbiased estimators for μ_y using $ERSS_2$ and $ERSS_3$ are obtained as

$$\hat{\mu}_{ERSS_2} = \frac{1}{n} \sum_{r=1}^{(n-1)/2} (Y_{[1]2r-1} + Y_{[n]2r}) + \frac{Y_{[1]n} + Y_{[n]n}}{2n},$$

$$\hat{\mu}_{ERSS_3} = \frac{1}{n} \sum_{r=1}^{(n-1)/2} (Y_{[1]2r-1} + Y_{[n]2r}) + \frac{Y_{[\frac{n+1}{2}]n}}{n},$$

with variance

$$\text{Var}(\hat{\mu}_{ERSS_2}) = \frac{v_4}{\theta_2^2}, \quad (8)$$

$$\text{Var}(\hat{\mu}_{ERSS_3}) = \text{Var}(\hat{\mu}_{ERSS_1}) = \frac{C(\alpha_2)}{n\theta_2^2}, \quad (9)$$

respectively, where $v_4 = \frac{1}{2n^2} \{ (2n-1)C(\alpha_2) + \frac{4\lambda^2 D^2(\alpha_2)}{(n+1)^2(n+2)} \}$.

Proof. (i) Since

$$\sum_{r=1}^{n/2} \delta_1 = \frac{\lambda n(n-1)}{2(n+1)}, \quad \sum_{r=1}^{n/2} \delta_n = \frac{\lambda n(-n+1)}{2(n+1)},$$

we have

$$E(\hat{\mu}_{ERSS_1}) = \frac{1}{n} \left(\frac{nB(\alpha_2)}{2\theta_2} - \frac{D(\alpha_2)}{\theta_2} \frac{\lambda n(n-1)}{2(n+1)} + \frac{nB(\alpha_2)}{2\theta_2} - \frac{D(\alpha_2)}{\theta_2} \frac{\lambda n(-n+1)}{2(n+1)} \right) = \frac{B(\alpha_2)}{\theta_2},$$

$$\text{Var}(\hat{\mu}_{ERSS_1}) = \frac{1}{n^2} \left(\frac{nC(\alpha_2)}{2\theta_2^2} + \frac{C(2\alpha_2) - C(\alpha_2)}{\theta_2^2} \frac{\lambda n(n-1)}{2(n+1)} + \frac{nC(\alpha_2)}{2\theta_2^2} \right. \\ \left. + \frac{C(2\alpha_2) - C(\alpha_2)}{\theta_2^2} \frac{\lambda n(-n+1)}{2(n+1)} \right) = \frac{C(\alpha_2)}{n\theta_2^2}.$$

(ii) In the estimator $\hat{\mu}_{ERSS_2}$, it is easy to see that $Y_{[1]1}, Y_{[n]2}, Y_{[1]3}, \dots, Y_{[n]n-1}$ are independent of $Y_{[1]n}$ and $Y_{[n]n}$, but the random variables $Y_{[1]n}$ and $Y_{[n]n}$ are dependent. From Scaria and Nair (1999) the joint density function of $(Y_{[1]n}, Y_{[n]n})$ is given by

$$h_{[1],n}(z, w) = (\alpha_2 \theta_2)^2 e^{-\theta_2(z+w)} [(1 - e^{-\theta_2 z})(1 - e^{-\theta_2 w})]^{\alpha_2 - 1} \left\{ 1 + \frac{2\lambda(n-1)}{n+1} [(1 - e^{-\theta_2 w})^{\alpha_2} - (1 - e^{-\theta_2 z})^{\alpha_2}] + \delta_{1,n} [1 - 2(1 - e^{-\theta_2 w})^{\alpha_2}] [1 - 2(1 - e^{-\theta_2 z})^{\alpha_2}] \right\},$$

where $\delta_{1,n} = \frac{\lambda^2(-n^2+n+2)}{(n+1)(n+2)}$. Therefore,

$$\begin{aligned} \text{Cov}(Y_{[1]n}, Y_{[n]n}) &= E[Y_{[1]n}Y_{[n]n}] - E[Y_{[1]n}]E[Y_{[n]n}] = \frac{D^2(\alpha_2)}{\theta_2^2} [\delta_{1,n} - \delta_1 \delta_n] \\ &= \frac{\lambda^2 D^2(\alpha_2)}{\theta_2^2} \left[\frac{-n^2+n+2}{(n+1)(n+2)} + \left(\frac{n-1}{n+1}\right)^2 \right] = \frac{4\lambda^2 D^2(\alpha_2)}{(n+1)^2(n+2)\theta_2^2}. \end{aligned}$$

Also, $Y_{[1]1}, Y_{[n]2}, Y_{[1]3}, \dots, Y_{[n]n-1}$ and $Y_{[\frac{n+1}{2}]n}$ are all independent in $\hat{\mu}_{\text{ERSS}_3}$. Since

$$\sum_{r=1}^{(n-1)/2} \delta_1 = \frac{\lambda(n-1)^2}{2(n+1)}, \quad \sum_{r=1}^{(n-1)/2} \delta_n = \frac{-\lambda(n-1)^2}{2(n+1)}, \quad \delta_{(n+1)/2} = 0,$$

we have

$$\begin{aligned} E(\hat{\mu}_{\text{ERSS}_2}) &= \frac{1}{n} \left(\frac{(n-1)B(\alpha_2)}{2\theta_2} - \frac{D(\alpha_2)\lambda(n-1)^2}{\theta_2 2(n+1)} + \frac{(n-1)B(\alpha_2)}{2\theta_2} + \frac{D(\alpha_2)\lambda(n-1)^2}{\theta_2 2(n+1)} \right. \\ &\quad \left. + \frac{B(\alpha_2)}{2\theta_2} - \frac{D(\alpha_2)\lambda(n-1)}{2\theta_2(n+1)} + \frac{B(\alpha_2)}{2\theta_2} + \frac{D(\alpha_2)\lambda(n-1)}{2\theta_2(n+1)} \right) = \frac{B(\alpha_2)}{\theta_2}, \\ E(\hat{\mu}_{\text{ERSS}_3}) &= \frac{1}{n} \left(\frac{(n-1)B(\alpha_2)}{2\theta_2} - \frac{D(\alpha_2)\lambda(n-1)^2}{\theta_2 2(n+1)} + \frac{(n-1)B(\alpha_2)}{2\theta_2} \right. \\ &\quad \left. + \frac{D(\alpha_2)\lambda n(n-1)^2}{\theta_2 2(n+1)} + \frac{B(\alpha_2)}{\theta_2} \right) = \frac{B(\alpha_2)}{\theta_2}, \\ \text{Var}(\hat{\mu}_{\text{ERSS}_2}) &= \frac{1}{n^2} \left(\frac{(n-1)C(\alpha_2)}{2\theta_2^2} + \frac{C(2\alpha_2) - C(\alpha_2)\lambda(n-1)^2}{\theta_2^2 2(n+1)} + \frac{(n-1)C(\alpha_2)}{2\theta_2^2} \right. \\ &\quad - \frac{C(2\alpha_2) - C(\alpha_2)\lambda(n-1)^2}{\theta_2^2 2(n+1)} + \frac{C(\alpha_2)}{4\theta_2^2} + \frac{C(2\alpha_2) - C(\alpha_2)\lambda(n-1)}{4\theta_2^2 2(n+1)} \\ &\quad \left. + \frac{C(\alpha_2)}{4\theta_2^2} - \frac{C(2\alpha_2) - C(\alpha_2)\lambda(n-1)}{4\theta_2^2 2(n+1)} + \frac{1}{2} \text{Cov}(Y_{[1]n}, Y_{[n]n}) \right) \\ &= \frac{1}{2\theta_2^2 n^2} \left\{ (2n-1)C(\alpha_2) + \frac{4\lambda^2 D^2(\alpha_2)}{(n+1)^2(n+2)} \right\}, \end{aligned}$$

$$\begin{aligned} \text{Var}(\hat{\mu}_{\text{ERSS}_3}) &= \frac{1}{n^2} \left(\frac{(n-1)C(\alpha_2)}{2\theta_2^2} + \frac{C(2\alpha_2) - C(\alpha_2)}{\theta_2^2} \frac{\lambda(n-1)^2}{2(n+1)} + \frac{(n-1)C(\alpha_2)}{2\theta_2^2} \right. \\ &\quad \left. - \frac{C(2\alpha_2) - C(\alpha_2)}{\theta_2^2} \frac{\lambda(n-1)^2}{2(n+1)} + \frac{C(\alpha_2)}{\theta_2^2} \right) = \frac{C(\alpha_2)}{n\theta_2^2}. \quad \square \end{aligned}$$

By using (6) and (8) the efficiency of $\hat{\mu}_{\text{RSS}}$ relative to the estimator $\hat{\mu}_{\text{ERSS}_2}$ is given by

$$e_2 = e(\hat{\mu}_{\text{ERSS}_2} | \hat{\mu}_{\text{RSS}}) = \frac{2nC(\alpha_2)}{(2n-1)C(\alpha_2) + \frac{4\lambda^2 D^2(\alpha_2)}{(n+1)^2(n+2)}}.$$

Note that e_2 decreases with respect to $|\lambda|$ for fixed n . Also, $\lim_{n \rightarrow \infty} e_2 = 1$. In Section 3, we calculate the relative efficiency of $\hat{\mu}_{\text{ERSS}_2}$ to $\hat{\mu}_{\text{RSS}}$, e_2 , for some values of the parameters and sample size.

2.4. MERSS estimation

Al-Odat and Al-Saleh (2001) suggested the MERSS, and Al-Saleh and Al-Ananbeh (2007) used the concept of MERSS with concomitant variable for the estimation of the means of the bivariate normal distribution. The procedure of MERSS with concomitant variable in MTBGED is as follows:

Step 1. Select n units each of size n from the population using SRS. Identify by judgment the minimum of each set with respect to the variable X together with the associated Y .

Step 2. Repeat step 1, but for the maximum.

Note that the $2n$ pairs of set $\{(X_{(1)r}, Y_{[1]r}), (X_{(n)r}, Y_{[n]r}); r = 1, 2, \dots, n\}$ that are obtained using the above procedure, are independent but not identically distributed.

Theorem 6 An unbiased estimator for μ_y based on MERSS is given by

$$\hat{\mu}_{\text{MERSS}} = \frac{1}{2n} \sum_{r=1}^n (Y_{[1]r} + Y_{[n]r}),$$

and its variance is

$$\text{Var}(\hat{\mu}_{\text{MERSS}}) = \frac{C(\alpha_2)}{2n\theta_2^2} = \frac{1}{2} \text{Var}(\hat{\mu}_{\text{RSS}}).$$

Proof. The proof is similar to proof of Theorem 5, part (i). \square

2.5. MSRSS estimation

Al-Saleh and Al-Kadiri (2000) have considered DRSS to increase the efficiency of the RSS estimator without increasing the set size n . Al-Saleh and Al-Omari (2002) generalized DRSS to MSRSS. The MSRSS scheme can be described as follows:

- Step 1.** Randomly selected n^{l+1} sample units from the population, where l is the number of stages, and n is the set size.
- Step 2.** Allocate the n^{l+1} selected units randomly into n^{l-1} sets, each of size n^2 .
- Step 3.** For each set in Step 2, apply the procedure of ranked set sampling method with respect to variable X to obtain a (judgment) ranked set, of size n ; this step yields n^{l-1} (judgment) ranked sets, of size n each.
- Step 4.** Without doing any actual quantification on these ranked sets, repeat Step 3 on the n^{l-1} ranked sets to obtain n^{l-2} second stage (judgment) ranked sets, of size n each.
- Step 5.** This process is continued, without any actual quantification, until we end up with the l th stage (judgement) ranked set of size n .
- Step 6.** Finally, the n identified in step 5 are now quantified for the variable X together with the associated Y . Show the value measured for (X, Y) on the units selected at the r th stage of the MSRSS by $(X_{(r)}^{(l)}, Y_{[r]}^{(l)})$, $r = 1, \dots, n$.

For $\lambda > 0$, let $Y_{[n]r}^{(l)}$, $r = 1, 2, \dots, n$, be the value measured on the units selected at the r th stage of the unbalanced MSRSS (Similar to suggestion by Chacko and Thomas, 2008). It is easily to see that each $Y_{[n]r}^{(l)}$ is the concomitant of the largest order statistic of n^l independently and identically distributed bivariate random variables with MTBGED, and therefore, the pdf of $Y_{[n]r}^{(l)}$ is given by

$$h_{[n]r}^{(l)}(y) = \alpha_2 \theta_2 e^{-\theta_2 y} (1 - e^{-\theta_2 y})^{\alpha_2 - 1} \left[1 + \frac{\lambda(n^l - 1)}{n^l + 1} (2(1 - e^{-\theta_2 y})^{\alpha_2} - 1) \right].$$

Thus the mean and variance of $Y_{[n]r}^{(l)}$ for $r = 1, 2, \dots, n$, are given as

$$E[Y_{[n]r}^{(l)}] = \mu_y \xi_{n^l}, \quad \text{Var}[Y_{[n]r}^{(l)}] = \frac{\gamma_{n^l}}{\theta_2^2}, \quad (10)$$

respectively, where $\xi_{n^l} = 1 + \lambda \frac{(n^l - 1)D(\alpha_2)}{(n^l + 1)B(\alpha_2)}$ and $\gamma_{n^l} = C(\alpha_2) + \lambda \frac{(n^l - 1)}{n^l + 1} (C(\alpha_2) - C(2\alpha_2))$.

Theorem 7 If α_2 and λ are known then the BLUE of μ_y is

$$\hat{\mu}_{MSRSS} = \frac{1}{n\xi_{n^l}} \sum_{r=1}^n Y_{[n]r}^{(l)}, \quad (11)$$

with variance

$$\text{Var}(\hat{\mu}_{MSRSS}) = \frac{\gamma_{n^l}}{n\xi_{n^l}^2 \theta_2^2}. \quad (12)$$

Proof. It can easily be proved using (10). \square

If we take $l = 1$ in (11) and (12), then we get the BLUE of μ_y based the usual single stage unbalanced RSS (URSS) as

$$\hat{\mu}_{URSS} = \frac{1}{n\xi_n} \sum_{r=1}^n Y_{[n]r},$$

where its variance is given as

$$\text{Var}(\hat{\mu}_{URSS}) = \frac{\gamma_n}{n\xi_n^2 \theta_2^2}. \quad (13)$$

If we let $l \rightarrow \infty$ in the MSRSS method described above, then $Y_{[n]r}^{(\infty)}$, $r = 1, 2, \dots, n$ are unbalanced steady-state ranked set samples (USSRSS) of size n with the following pdf (Al-Saleh, 2004):

$$h_{[n]r}^{(\infty)}(y) = \alpha_2 \theta_2 e^{-\theta_2 y} (1 - e^{-\theta_2 y})^{\alpha_2 - 1} [1 + \lambda(2(1 - e^{-\theta_2 y})^{\alpha_2} - 1)].$$

The mean and variance of $Y_{[n]r}^{(\infty)}$ are obtained as

$$E[Y_{[n]r}^{(\infty)}] = \mu_y Z(\alpha_2, \lambda), \quad \text{Var}[Y_{[n]r}^{(\infty)}] = \frac{I(\alpha_2, \lambda)}{\theta_2^2}, \quad (14)$$

where $Z(\alpha_2, \lambda) = 1 + \lambda \frac{D(\alpha_2)}{B(\alpha_2)}$ and $I(\alpha_2, \lambda) = C(\alpha_2) + \lambda(C(\alpha_2) - C(2\alpha_2))$.

Theorem 8 The BLUE of μ_y based on USSRSS is given by

$$\hat{\mu}_{USSRSS} = \frac{1}{nZ(\alpha_2, \lambda)} \sum_{r=1}^n Y_{[n]r}^{(\infty)},$$

with variance

$$\text{Var}(\hat{\mu}_{USSRSS}) = \frac{I(\alpha_2, \lambda)}{n(Z(\alpha_2, \lambda))^2 \theta_2^2}. \quad (15)$$

Proof. It can easily be proved using (14). \square

From (6), (13), and (15), we get efficiency of unbiased estimators $\hat{\mu}_{USSRSS}$ and $\hat{\mu}_{URSS}$ relative to $\hat{\mu}_{RSS}$ as

$$e_3 = e(\hat{\mu}_{URSS} | \hat{\mu}_{RSS}) = \frac{C(\alpha_2) \xi_n^2}{\gamma_n},$$

$$e_4 = e(\hat{\mu}_{USSRSS} | \hat{\mu}_{RSS}) = \frac{C(\alpha_2)(Z(\alpha_2, \lambda))^2}{I(\alpha_2, \lambda)}.$$

Note that e_4 does not depend on the value of n . In Section 3, we calculate the relative efficiencies of estimators for μ_y based on the MSRSS scheme to $\hat{\mu}_{RSS}$ for some values of the parameters and sample size.

3. Efficiency of estimators

In this section, we compare the efficiency of the proposed estimators in Section 2 for μ_y based on different RSS schemes; usual RSS, ERSS, and MSRSS. These evaluations are based numerical computation, and we did not consider LRSS and MERSS schemes. Here, we consider $n = 2(2)10(5)25$, $\alpha_2 = 0.8, 1.0, 2.0, 5$, and $\lambda = \pm.25, \pm.5, \pm.75, \pm 1$.

In Table 1, we calculate the relative efficiency e_1 of $\hat{\mu}_{RSS}$ to $\tilde{\mu}$, and we can conclude that i) $\tilde{\mu}$ is more efficient than $\hat{\mu}_{RSS}$, ii) the efficiency increases with respect to $|\lambda|$ for fixed n and α , iii) the efficiency increases with respect to n for fixed λ and α , and iv) the efficiency decreases with respect to α for fixed λ and n .

In Table 1, we calculate the relative efficiency e_2 of $\hat{\mu}_{ERSS_2}$ to $\hat{\mu}_{RSS}$, and we can conclude that i) $\hat{\mu}_{ERSS_2}$ is more efficient than $\hat{\mu}_{RSS}$, ii) the efficiency decreases with respect to $|\lambda|$ and α for fixed n , iii) the efficiency decreases with respect to n for fixed λ and α , iv) the efficiency closes to one for very large n , and v) the efficiency decreases with respect to α for fixed λ and n . Also, $\hat{\mu}_{ERSS_2}$ is more efficient than $\tilde{\mu}$.

In Tables 2 and 3, for different values for l , we calculate the relative efficiency of $\hat{\mu}_{MSRSS}$ to $\hat{\mu}_{RSS}$,

$$e_5 = e(\hat{\mu}_{MRRSS} | \hat{\mu}_{RSS}) = \frac{C(\alpha_2) \xi_{n^l}^2}{\gamma_{n^l}}.$$

Table 1: Comparing the efficiency of estimations.

		α_2							
		0.8		1.0		2.0		5.0	
n	λ	e_1	e_2	e_1	e_2	e_1	e_2	e_1	e_2
2	0.25	1.0049	1.3326	1.0039	1.3326	1.0019	1.3325	1.0008	1.3325
2	0.50	1.0195	1.3304	1.0157	1.3303	1.0077	1.3300	1.0032	1.3298
2	0.75	1.0440	1.3267	1.0353	1.3264	1.0174	1.3258	1.0073	1.3255
2	1.00	1.0786	1.3216	1.0629	1.3211	1.0310	1.3200	1.0130	1.3194
4	0.25	1.0088	1.1428	1.0070	1.1428	1.0035	1.1428	1.0015	1.1428
4	0.50	1.0353	1.1426	1.0283	1.1426	1.0139	1.1426	1.0058	1.1425
4	0.75	1.0801	1.1423	1.0640	1.1422	1.0314	1.1422	1.0131	1.1422
4	1.00	1.1443	1.1418	1.1149	1.1418	1.0561	1.1417	1.0234	1.1416
6	0.25	1.0104	1.0909	1.0084	1.0909	1.0041	1.0909	1.0017	1.0909
6	0.50	1.0421	1.0908	1.0337	1.0908	1.0166	1.0908	1.0069	1.0908
6	0.75	1.0958	1.0908	1.0764	1.0908	1.0375	1.0908	1.0156	1.0907
6	1.00	1.1731	1.0907	1.1375	1.0907	1.0669	1.0906	1.0278	1.0906
8	0.25	1.0114	1.0667	1.0091	1.0667	1.0045	1.0667	1.0019	1.0667
8	0.50	1.0459	1.0666	1.0367	1.0666	1.0181	1.0666	1.0076	1.0666
8	0.75	1.1045	1.0666	1.0834	1.0666	1.0408	1.0666	1.0170	1.0666
8	1.00	1.1893	1.0666	1.1501	1.0666	1.0729	1.0666	1.0303	1.0666
10	0.25	1.0120	1.0526	1.0096	1.0526	1.0048	1.0526	1.0020	1.0526
10	0.50	1.0483	1.0526	1.0386	1.0526	1.0190	1.0526	1.0080	1.0526
10	0.75	1.1101	1.0526	1.0878	1.0526	1.0430	1.0526	1.0179	1.0526
10	1.00	1.1996	1.0526	1.1582	1.0526	1.0767	1.0526	1.0319	1.0526
15	0.25	1.0128	1.0345	1.0103	1.0345	1.0051	1.0345	1.0021	1.0345
15	0.50	1.0517	1.0345	1.0414	1.0345	1.0204	1.0345	1.0085	1.0345
15	0.75	1.1180	1.0345	1.0940	1.0345	1.0460	1.0345	1.0192	1.0345
15	1.00	1.2142	1.0345	1.1696	1.0345	1.0821	1.0345	1.0341	1.0345
20	0.25	1.0132	1.0256	1.0106	1.0256	1.0053	1.0256	1.0022	1.0256
20	0.50	1.0535	1.0256	1.0428	1.0256	1.0211	1.0256	1.0088	1.0256
20	0.75	1.1221	1.0256	1.0973	1.0256	1.0475	1.0256	1.0198	1.0256
20	1.00	1.2219	1.0256	1.1756	1.0256	1.0849	1.0256	1.0353	1.0256
25	0.25	1.0135	1.0204	1.0108	1.0204	1.0054	1.0204	1.0022	1.0204
25	0.50	1.0546	1.0204	1.0436	1.0204	1.0215	1.0204	1.0090	1.0204
25	0.75	1.1247	1.0204	1.0993	1.0204	1.0485	1.0204	1.0202	1.0204
25	1.00	1.2267	1.0204	1.1793	1.0204	1.0866	1.0204	1.0360	1.0204
30	0.25	1.0137	1.0169	1.0110	1.0169	1.0054	1.0169	1.0023	1.0169
30	0.50	1.0553	1.0169	1.0442	1.0169	1.0218	1.0169	1.0091	1.0169
30	0.75	1.1264	1.0169	1.1007	1.0169	1.0492	1.0169	1.0205	1.0169
30	1.00	1.2299	1.0169	1.1818	1.0169	1.0878	1.0169	1.0365	1.0169

Table 2: Comparing the efficiency of estimations.

		$\alpha = 0.8$					$\alpha = 1.0$				
		l					l				
n	λ	1	2	5	13	∞	1	2	5	13	∞
2	0.25	1.120	1.223	1.365	1.392	1.392	1.108	1.201	1.327	1.350	1.350
2	0.50	1.250	1.482	1.827	1.894	1.894	1.225	1.430	1.728	1.785	1.786
2	0.75	1.392	1.784	2.410	2.539	2.540	1.350	1.691	2.220	2.326	2.327
2	1.00	1.546	2.133	3.151	3.372	3.373	1.485	1.988	2.823	2.999	3.000
4	0.25	1.223	1.340	1.391	1.392	1.392	1.201	1.305	1.349	1.350	1.350
4	0.50	1.482	1.765	1.892	1.894	1.894	1.430	1.675	1.784	1.786	1.786
4	0.75	1.784	2.293	2.536	2.540	2.540	1.691	2.122	2.323	2.327	2.327
4	1.00	2.133	2.954	3.366	3.373	3.373	1.988	2.665	2.994	3.000	3.000
6	0.25	1.270	1.368	1.392	1.392	1.392	1.242	1.329	1.350	1.350	1.350
6	0.50	1.592	1.834	1.894	1.894	1.894	1.525	1.734	1.785	1.786	1.786
6	0.75	1.977	2.424	2.539	2.540	2.540	1.856	2.231	2.326	2.327	2.327
6	1.00	2.437	3.174	3.372	3.373	3.373	2.242	2.842	2.999	3.000	3.000
8	0.25	1.296	1.378	1.392	1.392	1.392	1.265	1.338	1.350	1.350	1.350
8	0.50	1.655	1.860	1.894	1.894	1.894	1.580	1.756	1.786	1.786	1.786
8	0.75	2.092	2.473	2.540	2.540	2.540	1.953	2.272	2.327	2.327	2.327
8	1.00	2.622	3.259	3.373	3.373	3.373	2.395	2.909	3.000	3.000	3.000
10	0.25	1.313	1.383	1.392	1.392	1.392	1.280	1.342	1.350	1.350	1.350
10	0.50	1.697	1.872	1.894	1.894	1.894	1.616	1.767	1.786	1.786	1.786
10	0.75	2.168	2.497	2.540	2.540	2.540	2.017	2.291	2.327	2.327	2.327
10	1.00	2.746	3.299	3.373	3.373	3.373	2.496	2.941	3.000	3.000	3.000
15	0.25	1.337	1.388	1.392	1.392	1.392	1.302	1.347	1.350	1.350	1.350
15	0.50	1.757	1.884	1.894	1.894	1.894	1.668	1.777	1.786	1.786	1.786
15	0.75	2.279	2.521	2.540	2.540	2.540	2.110	2.311	2.327	2.327	2.327
15	1.00	2.930	3.340	3.373	3.373	3.373	2.645	2.974	3.000	3.000	3.000
20	0.25	1.350	1.389	1.392	1.392	1.392	1.313	1.348	1.350	1.350	1.350
20	0.50	1.789	1.889	1.894	1.894	1.894	1.695	1.781	1.786	1.786	1.786
20	0.75	2.339	2.529	2.540	2.540	2.540	2.160	2.318	2.327	2.327	2.327
20	1.00	3.030	3.354	3.373	3.373	3.373	2.726	2.985	3.000	3.000	3.000
25	0.25	1.358	1.390	1.392	1.392	1.392	1.320	1.349	1.350	1.350	1.350
25	0.50	1.809	1.891	1.894	1.894	1.894	1.712	1.783	1.786	1.786	1.786
25	0.75	2.376	2.533	2.540	2.540	2.540	2.191	2.321	2.327	2.327	2.327
25	1.00	3.093	3.361	3.373	3.373	3.373	2.777	2.990	3.000	3.000	3.000
30	0.25	1.363	1.391	1.392	1.392	1.392	1.325	1.349	1.350	1.350	1.350
30	0.50	1.822	1.892	1.894	1.894	1.894	1.724	1.784	1.786	1.786	1.786
30	0.75	2.402	2.535	2.540	2.540	2.540	2.213	2.323	2.327	2.327	2.327
30	1.00	3.137	3.365	3.373	3.373	3.373	2.812	2.993	3.000	3.000	3.000

Table 3: Comparing the efficiency of estimations.

		$\alpha = 2.0$					$\alpha = 5.0$				
		l					l				
n	λ	1	2	5	13	∞	1	2	5	13	∞
2	0.25	1.078	1.144	1.231	1.247	1.247	1.053	1.096	1.153	1.163	1.163
2	0.50	1.161	1.301	1.496	1.533	1.533	1.107	1.198	1.320	1.342	1.342
2	0.75	1.247	1.473	1.799	1.862	1.862	1.163	1.305	1.500	1.537	1.537
2	1.00	1.338	1.659	2.144	2.240	2.240	1.221	1.418	1.696	1.748	1.748
4	0.25	1.144	1.216	1.247	1.247	1.247	1.096	1.143	1.163	1.163	1.163
4	0.50	1.301	1.462	1.532	1.533	1.533	1.198	1.299	1.342	1.342	1.342
4	0.75	1.473	1.741	1.860	1.862	1.862	1.305	1.466	1.536	1.537	1.537
4	1.00	1.659	2.056	2.237	2.240	2.240	1.418	1.647	1.747	1.748	1.748
6	0.25	1.173	1.233	1.247	1.247	1.247	1.115	1.154	1.163	1.163	1.163
6	0.50	1.365	1.500	1.533	1.533	1.533	1.238	1.322	1.342	1.342	1.342
6	0.75	1.577	1.806	1.862	1.862	1.862	1.369	1.504	1.537	1.537	1.537
6	1.00	1.813	2.154	2.240	2.240	2.240	1.508	1.701	1.748	1.748	1.748
8	0.25	1.189	1.239	1.247	1.247	1.247	1.126	1.158	1.163	1.163	1.163
8	0.50	1.401	1.514	1.533	1.533	1.533	1.261	1.331	1.342	1.342	1.342
8	0.75	1.638	1.830	1.862	1.862	1.862	1.405	1.518	1.537	1.537	1.537
8	1.00	1.902	2.191	2.240	2.240	2.240	1.560	1.721	1.748	1.748	1.748
10	0.25	1.199	1.242	1.247	1.247	1.247	1.133	1.160	1.163	1.163	1.163
10	0.50	1.424	1.521	1.533	1.533	1.533	1.275	1.335	1.342	1.342	1.342
10	0.75	1.677	1.842	1.862	1.862	1.862	1.429	1.525	1.537	1.537	1.537
10	1.00	1.960	2.208	2.240	2.240	2.240	1.593	1.731	1.748	1.748	1.748
15	0.25	1.214	1.245	1.247	1.247	1.247	1.142	1.162	1.163	1.163	1.163
15	0.50	1.458	1.528	1.533	1.533	1.533	1.296	1.339	1.342	1.342	1.342
15	0.75	1.734	1.853	1.862	1.862	1.862	1.462	1.532	1.537	1.537	1.537
15	1.00	2.045	2.226	2.240	2.240	2.240	1.641	1.741	1.748	1.748	1.748
20	0.25	1.222	1.246	1.247	1.247	1.247	1.147	1.163	1.163	1.163	1.163
20	0.50	1.476	1.530	1.533	1.533	1.533	1.307	1.340	1.342	1.342	1.342
20	0.75	1.764	1.857	1.862	1.862	1.862	1.480	1.534	1.537	1.537	1.537
20	1.00	2.090	2.232	2.240	2.240	2.240	1.666	1.744	1.748	1.748	1.748
25	0.25	1.227	1.246	1.247	1.247	1.247	1.150	1.163	1.163	1.163	1.163
25	0.50	1.486	1.531	1.533	1.533	1.533	1.314	1.341	1.342	1.342	1.342
25	0.75	1.782	1.859	1.862	1.862	1.862	1.491	1.535	1.537	1.537	1.537
25	1.00	2.118	2.235	2.240	2.240	2.240	1.682	1.746	1.748	1.748	1.748
30	0.25	1.230	1.247	1.247	1.247	1.247	1.152	1.163	1.163	1.163	1.163
30	0.50	1.494	1.532	1.533	1.533	1.533	1.318	1.341	1.342	1.342	1.342
30	0.75	1.795	1.860	1.862	1.862	1.862	1.498	1.536	1.537	1.537	1.537
30	1.00	2.138	2.237	2.240	2.240	2.240	1.692	1.746	1.748	1.748	1.748

Note that e_5 is the relative efficiency of $\hat{\mu}_{\text{USSRSS}}$ to $\hat{\mu}_{\text{RSS}}$, i.e. e_4 , when $l = \infty$. We can conclude that i) $\hat{\mu}_{\text{MSRSS}}$ is more efficient than $\hat{\mu}_{\text{RSS}}$, ii) the efficiency increases with respect to $\lambda > 0$ for fixed n and α , iii) the efficiency increases with respect to n for fixed λ and α , and iv) the efficiency decreases with respect to α for fixed λ and n . Also, the efficiency increases when the number of stages, l , increases, and $\hat{\mu}_{\text{USSRSS}}$ is more efficient than $\hat{\mu}_{\text{MSRSS}}$ for all l .

Acknowledgements

The authors would like to thank an anonymous reviewer of this journal for many constructive suggestions and comments for improving this manuscript.

References

- Al-Nasser, A. D. (2007). L ranked set sampling: A generalization procedure for robust visual sampling. *Communications in Statistics-Simulation and Computation*, 36, 33–43.
- Al-Nasser, A. D. and Mustafa, A. B. (2009). Robust extreme ranked set sampling. *Journal of Statistical Computation and Simulation*, 79, 859–867.
- Al-Odat, M. and Al-Saleh, M. F. (2001). A variation of ranked set sampling. *Journal of Applied Statistical Science*, 10, 137–146.
- Al-Saleh, M. F. (2004). Steady-state ranked set sampling and parametric estimation. *Journal of Statistical Planning and Inference*, 123, 83–95.
- Al-Saleh, M. F. and Al-Ananbeh, A. M. (2007). Estimation of the means of the bivariate normal using moving extreme ranked set sampling with concomitant variable. *Statistical Papers*, 48, 179–195.
- Al-Saleh, M. F. and Al-Kadiri, M. A. (2000). Double-ranked set sampling. *Statistics and Probability Letters*, 48, 205–212.
- Al-Saleh, M. F. and Al-Omari, A. I. (2002). Multistage ranked set sampling. *Journal of Statistical Planning and Inference*, 102, 273–286.
- Al-Saleh, M. F. and Diab, Y. A. (2009). Estimation of the parameters of Downton's bivariate exponential distribution using ranked set sampling scheme. *Journal of Statistical Planning and Inference*, 139, 277–286.
- Barnett, V. and Moore, K. (1997). Best linear unbiased estimates in ranked-set sampling with particular reference to imperfect ordering. *Journal of Applied Statistics*, 24, 697–710.
- Chacko, M. and Thomas, P. Y. (2008). Estimation of a parameter of Morgenstern type bivariate exponential distribution by ranked set sampling. *Annals of the Institute of Statistical Mathematics*, 60, 301–318.
- Chen, Z., Bai, Z. and Sinha, B. (2004). *Lecture Notes in Statistics, Ranked Set Sampling: Theory and Applications*. Springer, New York.
- David, H. A. and Nagaraja, H. (2003). *Order Statistics*. John Wiley and Sons.
- Jemain, A. A. and Al-Omari, A. I. (2006). Double quartile ranked set samples. *Pakistan Journal of Statistics*, 22, 217–228.
- McIntyre, G. A. (1952). A method for unbiased selective sampling, using ranked sets. *Australian Journal of Agricultural Research*, 3, 385–390.
- Muttlak, H. A. (1997). Median ranked set sampling. *Journal of Applied Statistical Sciences*, 6, 245–255.
- Muttlak, H. A. (2003). Modified ranked set sampling methods. *Pakistan Journal of Statistics*, 19, 315–324.

- Samawi, H. M., Ahmed, M. S. and Abu-Dayyeh, W. (1996). Estimating the population mean using extreme ranked set sampling. *Biometrical Journal*, 38, 577–586.
- Scaria, J. and Nair, N. U. (1999). On concomitants of order statistics from Morgenstern family. *Biometrical Journal*, 41, 483–489.
- Sinha, B. K., Sinha, B. K. and Purkayastha, S. (1996). On some aspects of ranked set sampling for estimation of normal and exponential parameters. *Statistics and Decisions*, 14, 223–240.
- Stokes, S. L. (1977). Ranked set sampling with concomitant variables. *Communications in Statistics-Theory and Methods*, 6, 1207–1211.
- Stokes, S. L. (1980). Inferences on the correlation coefficient in bivariate normal populations from ranked set samples. *Journal of the American Statistical Association*, 75, 989–995.
- Tahmasebi, S. and Jafari, A. A. (2012). Estimation of a scale parameter of Morgenstern type bivariate uniform distribution by ranked set sampling. *Journal of Data Science*, 10, 129–141.
- Tahmasebi, S. and Jafari, A. A. (2013). Concomitants of order statistics and record values from Morgenstern type bivariate generalized exponential distribution. *Bulletin of the Malaysian Mathematical Sciences Society*, (Accepted for publication).
- Takahasi, K. and Wakimoto, K. (1968). On unbiased estimates of the population mean based on the sample stratified by means of ordering. *Annals of the Institute of Statistical Mathematics*, 20, 1–31.
- Yu, P. L. and Tam, C. Y. (2002). Ranked set sampling in the presence of censored data. *Environmetrics*, 13, 379–396.

Integrating network design and frequency setting in public transportation networks: a survey

Francisco López-Ramos*

Abstract

This work reviews the literature on models which integrate the network design and the frequency setting phases in public transportation networks. These two phases determine to a large extent the service for the passengers and the operational costs for the operator of the system. The survey puts emphasis on modelling features, i.e., objective cost components and constraints, as well as on algorithmic aspects. Finally, it provides directions for further research.

MSC: 90B06.

Keywords: Public transport, network design, frequency setting, integrating.

1. Introduction

Rapid population growth in cities has led to traffic congestion. To alleviate this effect, transport agencies have designed public transportation systems, with their operating frequencies and resource capacities continuously being revised. Because of the high cost of construction and exploitation of these resources, it is important to pay attention to issues affecting effectiveness in different planning stages. For instance, the design of the layout of the lines must consider infrastructure budgetary restrictions and coverage demand satisfaction, whereas the line frequencies must be set so that passenger trip requirements are satisfied at reasonable operative costs while not exceeding resource capacities.

Traditionally, both planning phases have been solved sequentially, i.e., when the design of the layout of the lines is determined, the frequencies are assigned to these layouts. This approach may lead the public transportation system to operate in an inefficient manner because the network design phase assigns the demand to the lines without con-

* Pontificia Universidad Católica de Valparaíso, ITRA, 2147 Brasil Avenue, 2362804 Valparaíso, Chile.
francisco.lopez.r@ucv.cl

Received: April 2014

Accepted: May 2014

sidering resource capacities. Therefore, suboptimal designs and congestion are highly likely to be produced. However, an integrated approach may overcome this drawback.

State-of-the-art reviews on public transportation issues (Desaulniers and Hickman, 2007; Guihaire and Hao, 2008; Kepaptsoglou and Karlaftis, 2009; Farahani, Miandoabchi and Szeto, 2013) do not attach the proper importance to optimization approaches that integrate the network design and the frequency setting phases. Moreover, they do not cover the main modelling and solving features involved in these phases. The present review aims at fulfilling these gaps and suggesting lines for further research for both modelling and solving issues.

The rest of the paper is organized as follows. Section 2 defines the planning stages covered in this review. Section 3 reviews all the works which consider some modelling features from both planning stages. Finally, Section 4 presents the conclusions and lines for further research.

2. The transit planning process

The complete transit planning process is made up of the following five phases: network design, frequency setting, timetable development, vehicle scheduling and crew scheduling (Ceder and Wilson, 1986). Traditionally, the five phases have been solved sequentially due to the inefficiency of solving them simultaneously for large-sized networks. The two first phases (i.e., the network design and the frequency setting) determine to a large extent the service for the passengers and the operational costs for the operator of the system. Therefore, state-of-the-art research on transit planning processes has been mainly focused on these two phases.

2.1. The Network Design Problem

The Network Design Problem (*NDP*) involves the allocation of the new public transportation infrastructure, i.e., new stations and its interconnections following a pre-specified network layout design rules. This problem considers the construction costs of the new infrastructure, i.e, the new stations, and also its interconnections for railway-based systems. Additionally, the number of new resources to be constructed is limited by an infrastructure budget. Finally, the existence of a network already in operation is considered, in the sense that infrastructure costs are not taken into consideration. Under these assumptions, the aim of the *NDP* is to cover as much demand as possible at reasonable infrastructure construction costs.

2.2. The Frequency Setting Problem

The Frequency Setting Problem (*FSP*) assigns a certain number of vehicles and its services to the existing lines plus the constructed lines so that the expected demand

is covered. The term “service” refers to a complete line cycle performed by a vehicle halting at some or all of the stations on the line. This problem considers the costs and the capacities of the planning resources (vehicles, platform stations, stations and stretches). The costs of the planning resources involve the power consumption costs of the vehicles, the costs of acquisition and maintenance of the vehicles and the salaries of its drivers, mainly. The capacities of the planning resources are related to the maximum number of passengers that a vehicle can hold, the number of available vehicles (fleet size), the maximum number of passengers that a platform station can hold, while they are waiting to board a vehicle, the maximum number of services per unit of time that a station can hold, and the number of vehicles per unit of time that can go through a stretch.

2.3. The passenger transit assignment model

The integration of the *NDP* and *FSP* problems requires a passenger transit assignment model. This model determines how the passengers use the constructed plus the existing lines through a detailed representation of the network. This representation considers in-vehicle traveling time, boarding and alighting from the vehicle times, at-station waiting time, in-vehicle waiting time and walking time. An economical cost is associated with each type of time previously cited so that the total passenger trip time can be compared with the operator costs.

3. Review on the network design and frequency setting problem

The literature on the integration of the network design and frequency setting phases is scant when considering the time elapsed from the first works Lampkin and Saalmans (1967), Silman, Barzily and Passy (1974) and the last work López (2014). Moreover, the research is not well developed because some important modelling features have been discarded and all the modelling features encountered are not considered in the same work. Finally and not least, the solving approaches are either inefficient or unreliable because the goodness of the solution is not guaranteed. In the following subsections, the review will focus the attention on these issues, leaving aside the modelling features not considered in any paper. The later issue will be analysed in Section 4.

3.1. Objective function costs

Tables 1-2 show the main objective function costs considered by the literature works. They are divided into two parts: the costs related to the operator and the costs associated with the users. The operator costs comprise the Infrastructure Resources and the Planning Resources (they are shown in columns 3 and 4), whereas user costs consist of the Travel Times, At-Station Waiting, In-vehicle Waiting, Transfer times, Vehicle Occupancy and Mode Disutility (they are hold on columns 5 to 11). The coloured tick

marks indicate that the paper considers the feature partially (orange coloured tick mark) or totally (green coloured tick mark). In some papers, there are question marks denoting that it is unknown whether the feature is considered. This problem occurs when the author(s) do(es) not mention its use explicitly. In the following subsections, the reader can find the explanation of each cost with references to the literature works that considered these costs. Additionally, the alternative implementations of these costs are described if any.

3.1.1. Infrastructure resource costs

Infrastructure resources are related to line segments (also called stretches in the context of a railway based system) and stations. The costs of the stretches and the stations represent a great amount of the operational costs of the system operator. To mention one of them, the construction of one kilometer of stretch in the Spanish commuter train network (*RENFE*) costs between 1-1.6 M€ and is amortized between 30-60 years (Ferropedia, 2014a). So, it costs around 3.8-6 €/km-h. Moreover, if it is an underground system, we must also consider the construction of a tunnel whose value, according to *RENFE*, is significantly higher (around 30 M€/km). However, it is amortized in a larger period of time, 100 years, so it costs 34.25 €/km-h. Despite the importance of these costs, there are few works in the literature that consider the construction and/or maintenance costs of the stretches and stations of the new network infrastructure (Bielli, Carotenuto and Confessore, 1998; Bielli, Caramia and Carotenuto, 2002; Borndörfer, 2007; López, 2014).

3.1.2. Planing resource costs

The planning resources are associated with the public transportation vehicles and the drivers that control these vehicles. The costs of the vehicles and the drivers represent the same order of magnitude as the costs of the network infrastructure. For the *RENFE*, they costs around 26 €/train-km (Ferropedia, 2014b) and comprise the power consumption costs of the public transportation vehicles, the costs of acquisition and maintenance of these vehicles and the salaries of the drivers, mainly. Planning resource costs have been partially considered in the works of Agrawai and Mathew (2004), Barra et al. (2007), Baaj and Mahmassani (1990), Baaj and Mahmassani (1991), Baaj and Mahmassani (1995), Bielli et al. (1998), Bielli et al. (2002), Fan and Machemehl (2006), Fan and Machemehl (2008), Wan and Hong (2003), Marwah et al. (1993), Ceder and Wilson (1986), van Oudheusden et al. (1987), Israeli and Ceder (1989), Ngamchai and Lovell (1993), Pattnaik et al. (1998), Rao, Muralidhar and Dhingra (2000), Shih and Mahmassani (1994), Soehodho and Koshi (1999), Fan and Machemehl (2004), Fernández, de Cea and Malbran (2008), Mauttone (2011), Shimamoto, Schmöcker and Kurauchi (2012), Tom and Mohan (2003), and fully considered in López (2014), Marín, Mesa and Perea (2009), Cipriani et al. (2012), Zhao and Zeng (2007), Cipriani et

al. (2005), Petrelli (2004), Chien, Yang and Hou (2001), Shih, Mahmassani and Baaj (1998). The cost of acquisition and maintenance of vehicles are considered in the vast majority of the works; however, salaries and power consumption costs have been seldom considered. Additionally, there are some works which do not specify whether they use planning resource costs or which planning resource costs are used (Borndörfer, 2007; Fusco, Gori and Petrelli, 2002; Rao et al., 2000).

3.1.3. Unsatisfied demand

Urban public transportation networks aims at covering as much demand as possible. To penalize the uncovered demand, the vast majority of authors use a penalization weight in the objective function that increments the value of the objective function as the amount of unsatisfied demand increases (Barra et al., 2007; Bussieck et al., 1996; Cipriani et al., 2005 and 2012; Fan and Machemehl, 2004, 2006 and 2008; Marín et al., 2009). However, in López (2014) a pedestrian network that connects the O-D demand pairs directly is used. So the unsatisfied O-D pairs go through these links, with a high travel time costs. There are some additional works which do not specify whether they include some uncovered demand costs (Caramia, Carotenuto and Confessore, 2001; Fusco et al., 2002).

3.1.4. Travel time costs

Travel time costs refer to the in-vehicle and the boarding and alighting from the vehicle passenger times. These times are considered in the vast majority of works except in van Oudheusden et al. (1987), van Nes, Hamerslag and Immer (1988) and, possibly, in Caramia et al. (2001), Fusco et al. (2002). The last works do not specify whether they use the travel time costs. The travel times are generally computed using a time value associated with the network link that is expressed in units of time per person and the total amount of passengers going through the link. The overall time is weighted by a constant term which represents the passenger time cost perception. This constant plays an important role on the quality of the solution because it determines the importance of the main passenger costs in the optimum with respect to the operator costs. However, scant literature address that issue.

Mauttone (2011) has study the effect of the time weight by applying the interactive multi-objective optimization method (Ehrgott and Gandibleux, 2002). This method determines a set of non-dominated solutions which approximates to the optimal pareto front. A solution S1 dominates another solution S2, if S1 is no worse than S2 in all objectives and S1 is strictly better than S2 in at least one objective. So, in the study models, it means that all non-dominated solutions have passenger and operators costs which are equal or less than the ones of the dominated solutions and, the operator costs or the passengers costs of the non-dominated solutions are strictly less than the ones of the dominated solutions.

The conference presentation of Codina et al. (2008) also deals with multi-objective analysis but the aim was to determine a value to the cost of time such that all passengers will want to use the available network resources, no matter which operator cost is. Therefore, the authors did not seek for a set of non-dominated solutions but for a set of solutions where passenger costs have much more importance than operator costs.

3.1.5. At-station waiting costs

Waiting at a station is a very unpleasant situation for a user of the public transportation system. On average, the perception cost of the waiting time for a user is three times the time perception costs of the travel times. Thus, it is very important to consider at-station waiting times. Non-exact approaches have implemented these times because the module that evaluates them, assumes a fixed route configuration (i.e., its stretches, stations and operating frequencies are already determined) and, thus, the model is linear. However, in (quasi)-exact approaches the mathematical programming program formulated copes with some non-linearities. For instance, in the absence of congestion and link capacities (see Subsection 3.2.4), there is the product of frequencies and waiting times in particular constraints (Spiess and Florian, 1989). This fact discourages the authors of these works to face to waiting times. The reader is referred to Table 3 to see the distinct approaches of the literature works.

3.1.6. In-vehicle waiting costs

Passengers also experience some waiting when they are in a vehicle that is serving at a station, different from the station where they have boarded or alighted. This waiting time is increasingly significant as the vehicle takes more time in serving other passengers at the station. It is also influenced by the number of intermediate stations between the passenger boarding station and the passenger alighting station. Consequently, this waiting time component merits some consideration. There are just a few works in which this waiting time component is considered (López, 2014; Shimamoto et al., 1993). In both works, the number of passengers waiting in the vehicle are weighted by an average passenger time value per person and then the overall waiting time is penalized by a time cost that represents the passenger cost perception of waiting time.

3.1.7. Transfer time costs

Transfer time is related to the passenger walking due to changing between lines or when there are no stations that connects directly with its origin or destination. There are basically two ways of implementing transfer costs. One approach uses a penalty weight or a constant time associated with each transfer unit (Barra et al., 2007; Baaj and Mahmassani, 1990, 1991 and 1995; Pattnaik, Mohan and Tometc, 1998; Shih and Mahmassani, 1994; Shih et al., 1998; Soehodho and Koshi, 1999; Rao et al., 2000;

Tom and Mohan, 2003; Zhao and Ghan, 2003; Zhao, 2006; Zhao and Zeng, 2006 and 2007; Agrawai and Mathew, 2004; Fan and Machemehl, 2004, 2006 and 2008; Petrelli, 2004; Cipriani et al., 2005 and 2012; Mauttone, 2011; Szeto and Wub, 2011). The other approach attaches the proper time cost associated with a complementary network link, i.e., a pedestrian network (Bielli et al., 1998 and 2002; Ceder and Israeli, 1998; Ceder and Wilson, 1986; Chakroborty, 2003; Fernández et al., 2008; Hasselström, 1981; Hu et al., 2005; Israeli, 1992; Lee and Vuchic, 2005; López, 2014; Shimamoto et al., 1993). There is an additional approach which is worth-mentioning despite of being only related to the Network Design phase. García et al. (2006) considers as transfer time costs not only walking time cost between line platforms but also waiting time to board a vehicle in the transferred line platform. The walking times are considered constant, i.e., not depending in the distance between line platforms, whereas waiting at the transferred line platform is computed as the inverse of twice the frequency of the line, which is given as an input to the model.

3.1.8. Vehicle occupancy

Vehicle occupancy refers to the utilization level of the bus capacity. The bus capacity is an input parameter that is fixed according to a maximum number of seated passengers plus a maximum number of standees. The last amount is computed according to an allowable passenger density. The vehicle occupancy is a relevant feature for passengers because it dictates the comfortability of the passengers in the vehicle. The crowder is the vehicle, the less comfortable are the passengers. This feature is implemented using a penalisation term that weights the number of standees in a vehicle going through the segments of the operating line. Surprisingly, this feature is not considered in recent works (from 2003 until present).

3.1.9. Mode disutility

The mode disutility cost allows considering alternative modes of transportation. This cost is implemented using a combined modal splitting assignment model in which the disutility is expressed using a probabilistic function. The vast majority of works employ a multinomial logit function, except Fan and Machemehl (2004), Fan and Machemehl (2006), Fan and Machemehl (2008) in which a nested logit is used. The probabilistic function is usually employed in an iterative procedure where, first, the routes and frequencies of the transportation system are determined and, then, a network evaluation procedure uses the probabilistic function to evaluate several performance indicators of the built lines (see, for instance, Fan and Machemehl, 2004). These indicators are compared to the indicators of the alternative modes of transportation and, according to this comparison, the current network is modified and re-evaluated until some convergence criteria is met. There is only one work (López, 2014) in which the probabilistic function is indirectly expressed as a deterrence function. The author

demonstrates that in the optimal solution of the resulting bilevel program, the modal demand is distributed according to a logit function. Another interesting work, although applied only to network design, is Marín and García-Rodenas (2009) where the authors also use a logit function to represent the modal demand splitting but in a single level problem.

3.2. Modelling features

Tables 3-4 show the main modelling features considered by the literature works. The modelling features are divided into three parts: the features strictly related to the operator, the features strictly associated with the users and the features which correspond to both operator and passenger agents. The terms “strictly related to” and “strictly associated with” refer to the agent which mainly manages these features. The operator is strictly related to Infrastructure Restrictions, Working Lines, Stretch Capacity, Vehicle Fleet Size, Vehicle Capacity and Time Horizon features (shown in columns 3, 4, 6, 7, 8 and 9 of Table 2). Passengers are strictly associated with the % of Satisfied Demand (shown in column 10 of Table 2). The remaining feature, the Express Services, is related to both operator and passenger agents. Like in the preceding table, the coloured tick marks indicate that the paper considers the feature partially (orange coloured tick mark) or totally (green coloured tick mark). In some papers, there are question marks denoting that it is unknown whether the feature is considered. This problem occurs when the author(s) do(es) not mention its use explicitly. In the following subsections, the reader can find the explanation of each modelling feature with references to the literature works that considered these features. Additionally, the alternative implementations of these features are described if any.

3.2.1. Infrastructure budgetary restriction

As explained in the preceding Subsection 3.1.1, infrastructure resource costs are the leading costs for the operator of the system. Therefore, there is a limitation in the number of infrastructure resources that can be used to construct or expand the present public transportation network. Surprisingly, there are only two works that impose such a limitation (López, 2014; Marín et al., 2009). In both works, the number of stations and stretches that can take part of the new railway lines is subject to a infrastructure budget. The infrastructure resource costs and the budget are expressed as the currency value per unit of time. In some works focusing only on Network Design, that feature is more frequently found (see, for instance, Laporte et al., 2007 and 2001; Marín, 2007; Marín and Jaramillo, 2008 and 2009; Marín and García-Rodenas, 2009). The way the feature is modelled is the same as mentioned in the previous two works.

Table 4: Modelling features considered in the literature works (Continued).

Year	Author(s)	Infrastructure Restrictions	Working Lines	Express Services	Stretch Capacity	Vehicle Fleet Size	Vehicle Capacity	Time Horizon	% Satisfied Demand
2003	Chakroborty	?	?						
2003	Ngamchai and Lovell					✓	✓		
2003	Tom and Mohan					✓	✓		
2003	Wan and Lo			✓		✓	✓		
2003	Zhao and Gan					✓	✓		
2004	Agrawal and Mathew					✓	✓		✓
2004	Carrese and Gori					✓	✓		✓
2004	Fan and Machemehl			✓		✓	✓		
2004	Petrelli					✓	✓		✓
2005	Cipriani et al.					✓	✓		
2005	Lee and Vuchic					✓	✓		
2005	Hu et al.			✓		✓	✓		
2006	Fan and Machemehl			✓		✓	✓		
2006	Zhao					✓	✓		
2006	Zhao and Zheng					✓	✓		
2007	Barra et al.					✓	✓		
2007	Borndörfer et al.			✓		✓	✓		
2007	Zhao and Zheng			✓		✓	✓		
2008	Fan and Machemehl			✓		✓	✓		
2008	Fernández et al.			✓		✓	✓		
2009	Pacheco et al.					✓	✓	✓	
2009	Marín et al.	✓				✓	✓		
2011	Mauttone					✓	✓		✓
2011	Szeto and Wub					✓	✓		
2012	Cipriani et al.			✓		✓	✓		
2012	Shimamoto et al.					✓	✓		
2014	López	✓	✓	✓		✓	✓		✓

3.2.2. Working lines

Working lines refer to those lines that are already in operation and that can be considered for an extension of the current working network at no infrastructure resource cost. Under this definition of working lines, there is no literature work that imposes such a constraint, except for the work of López (2014). In this work, the infrastructure resources have a zero-cost and, thus, they have no contribution to the objective function value and to the infrastructure budget limitation, as explained in the Subsections 3.1.1 and 3.2.1, respectively.

3.2.3. Express Service design

Express Service design refers to a specific way that vehicles work on a line, usually when lines are longer (in the sense that lines have many intermediate stations between the terminal stations) and there are high levels of congestion at stations. A vehicle performs a express service when it does not halt at some intermediate stations contained in the line cycle. As shown in the studies of Vuchic (1973) and Ercolano (1984), express services allow decreasing the waiting times experienced by the passengers (see Subsection 3.1.5 and 3.1.6 for an explanation of these concepts). For the point of view of operators, this type of service permits savings in the planning resource costs (see Subsection 3.1.2 for a detailed explanation of these costs). Although state-of-the-art setting frequency models consider this feature (Chiraphadhanakul and Barnhart, 2013; Larraín et al., 2013), models that integrate the network design and the frequency setting problems mislead this feature, except for the work of López (2014).

3.2.4. Stretch capacity

The stretch or link capacity is related to the maximum number of vehicles per unit of time that can go through a segment of a line so that overtaking cannot occur. This feature is commonly known as the minimum headway. The headway is expressed as the difference of two consecutive vehicle arrivals at a given station. Therefore, the headway is inversely proportional to the frequency. Literature works implement this feature in three different ways: 1) A lower bound on the line headway (Wan and Hong, 2003; Fan and Machemehl, 2004, 2006 and 2008; Zhao and Zeng, 2007), 2) An upper bound on the line frequency (Cipriani et al., 2005 and 2012; Borndörfer, 2007; Marín et al., 2009; López, 2014) and 3) A maximum service time at stations (Hu et al., 2005). The work of Fernández et al. (2008) does not explain how this feature is implemented.

3.2.5. Vehicle capacity

As explained in Subsection 3.1.8, the capacity of a public transportation vehicle is regarded as the maximum number of seated passengers plus the maximum number

of standees according to an allowable passenger density. This feature is commonly referred to as the line capacity which is expressed as the product of the line frequency and the capacity of the vehicles operating on the line. The line capacity is limited in two distinct ways. Headway-based approaches constraint the link load factor (Marwah et al., 1993; Baaj and Mahmassani, 1990, 1991 and 1995; Israeli, 1992; Shih and Mahmassani, 1994; Shih et al., 1998; Pattnaik et al., 1998; Petrelli, 2004; Rao et al., 2000; Fan and Machemehl, 2004, 2006 and 2008; Carrese and Gori, 2004; Cipriani et al., 2005 and 2012; Zhao and Ghan, 2003; Zhao, 2006; Zhao and Zeng, 2006 and 2007; Barra et al., 2007; Agrawai and Mathew, 2004; Ngamchai and Lovell, 1993; Tom and Mohan, 2003) which is expressed as follows:

$$L_a = \frac{q_a \cdot h^l}{q_v} \quad (1)$$

where parameter q_a is related to the maximum allowable passengers flow on the link, q_v is the vehicle capacity and h^l is the headway of the line l . On the other hand, frequency-based approaches limit the maximum flow load on the link according to the line capacity (Borndörfer, 2007; Bussieck et al., 1996; Fernández et al., 2008; López, 2014; Mauttone, 2011; Wan and Hong, 2003). The line capacity is expressed as the line frequency times the capacity of the vehicle.

3.2.6. *Vehicle fleet size*

The vehicle fleet size accounts for the maximum number of available vehicles. In general, the vehicles comprised in the fleet are considered to have an acquisition cost. However, López (2014) also considers a subset of vehicles with no acquisition cost due to the fact that this subset of vehicles is already in operation in some working line. This feature is verified using a constraint that limits the total number of vehicles used in the whole set of lines. This number is obtained by means of the product of the line cycle and the frequency of the line.

3.2.7. *Time horizon*

The time horizon or also the planning horizon refers to the maximum amount of time that all the services performed by a vehicle on a line must be accomplished. This feature is usually related to the peak hour of a working day, when the public system is supposed to be most congested. Surprisingly, there are just a few works in the literature that limit the planning horizon (López, 2014; Pacheco et al., 2009; van Nes et al., 1988).

3.2.8. Minimum amount of demand satisfaction

Some works in the literature aim at covering a minimum amount of demand to justify the investment costs of the operator (Agrawai and Mathew, 2004; Carrese and Gori, 2004; Chien et al., 2001; Mauttone, 2011; Petrelli, 2004; van Oudheusden et al., 1987). It is arguable whether this feature can be indirectly considered including the infrastructure resource costs in combination with the mode disutility in the objective function (see Subsections 3.1.1 and 3.1.9 for an explanation of these costs). Anyway, this feature is also mentioned in the present review to not exclude the cited works.

3.3. Solving techniques

This subsection reviews the solving techniques without attaching importance to algorithmic details. Rather than that, the focus is on the utility and quality of the approaches. Tables 5-6 show the five distinct features of each solving technique. They comprise the solving scheme (column 3), the nature of the approach (column 4), the algorithms involved in this approach (column 5), the way in which the line layout is determined (column 6) and the network size which is capable to solve (column 7). The following subsections go into the details of each feature.

3.3.1. Solving scheme

The solving scheme refers to the sequence in which the network design and the frequency setting phases are solved. In a sequential scheme, the network design is first solved and, then, the frequency setting is conducted having fixed the line layout. The simultaneous scheme solves both phases at the same time or modifies one of these phases having computed the other phase in an iterative fashion. The second variant of the simultaneous scheme is the most used in the literature, whereas a sequential scheme was implemented in the earlier works (Dubois et al., 1979; Lampkin and Saalmans, 1967; Silman et al., 1974). Although some other works in the beginnings of 2000 also implement the sequential scheme (Chakroborty, 2003; Hu et al., 2005; Soehodho and Koshi, 1999).

3.3.2. Approach

The term approach is strongly related to the quality of the solution obtained with the algorithms used in each work. A exact approach means that the solution obtained is an optimum of the optimization model stated in that work. A matheuristic approach refers to a quasi-exact approach in which the solution is not optimal but is certainly close to the optimum, or is only optimal in reduced instances of the model. For instance, in López (2014) instances where only one line is under construction can be solved to optimally. However, for instances with multiple lines under construction a matheuristic is used to reach a near-optimal solution. The heuristic approach stands for the works in which

Table 5: Solving techniques used in the literature works (see also the next page).

Year	Author(s)	Solving scheme	Approach	Algorithm(s)	Layout Method	Network size
1967	Lampkin and Saalmans	Sequential	Heuristic	RCA + FSP with RGBSP	Selection	Small
1974	Silman et al.	Sequential	Heuristic	RCA + FSP with GPM	Selection	Small
1979	Dubois et al.	Sequential	Heuristic	NRP + RCA + FSP with GBSP	Selection	Small
1981	Hasselström	Simultaneous	Heuristic	RCA + REA	Select. + Mod.	Medium
1884	Marwah et al.	Simultaneous	Heuristic	NRA + RCA + REA with CLP	Selection	Large
1986	Ceder and Wilson	Simultaneous	Heuristic	RCA + RIA	Select. + Mod.	Small
1987	Van Oudheusden et al.	Simultaneous	Heuristic	CGA + FSP + SCP/SPLP with EA	Selection	Medium
1988	Van Nes et al.	Simultaneous	Heuristic	RCA + REA	Selection	Large
1989	Israeli and Ceder	Simultaneous	Heuristic	RCA + RRA + REA with a CGT	Select. + Mod.	Small
1990	Baaj and Mahmassani	Simultaneous	Heuristic	RCFSA + REA + RIA	Select. + Mod.	Large
1992	Baaj and Mahmassani	Simultaneous	Heuristic	RCFSA + REA + RIA	Select. + Mod.	Large
1992	Israeli	Simultaneous	Heuristic	RCA + RRA + REA with a CGT	Select. + Mod.	Small
1994	Shih and Mahmassani	Simultaneous	Heuristic	RCA + REA + RSA + RIA	Select. + Mod.	Large
1995	Baaj and Mahmassani	Simultaneous	Heuristic	RCFSA + REA + RIA	Select. + Mod.	Large
1995	Israeli and Ceder	Simultaneous	Heuristic	RCA + RRA + REA with a CGT	Select. + Mod.	Small
1996	Bussieck et al.	Simultaneous	Mathuristic	Branch & Bound + VI	Selection	Large
1998	Bielli et al.	Simultaneous	Heuristic	RCA with GA + REA with NN + RIA with GA	Select. + Deter.	Large
1998	Ceder and Israeli	Simultaneous	Heuristic	RCA + RRA + REA with a CGT	Select. + Mod.	Small
1998	Pattanaik et al.	Simultaneous	Heuristic	RCA + REA with GA	Selection	Medium
1998	Shih et al.	Simultaneous	Heuristic	RCFSA + REA + RIA	Select. + Mod.	Large
1999	Soehodo and Koshi	Sequential	Heuristic	RCA + REA + RIA	Select. + Mod.	Medium
2000	Rao et al.	Simultaneous	Heuristic	RCA + REA with GA	Select. + Mod.	Small
2001	Caramia et al.	Simultaneous	Heuristic	REA with NN + RIA with GA	Selection	Medium
2001	Chien et al.	Simultaneous	Heuristic	RCA with GA + RNHSP with GA	Selection	Medium
2002	Bielli et al.	Simultaneous	Heuristic	RCA with GA + REA with NN + RIA with GA	Select. + Mod.	Large
2002	Fusco et al.	Simultaneous	Heuristic	RCA + REA with GA + RIA	Select. + Mod.	Small

Table 6: Solving techniques used in the literature works (Continued).

Year	Author(s)	Solving scheme	Approach	Algorithm(s)	Layout Method	Network size
2003	Chakraborty	Sequential	Heuristic	RCA with GA + FSP with GA	Selection	Small
2003	Ngamchai and Lovell	Simultaneous	Heuristic	RCA + REA + RIA	Select. + Deter.	Small
2003	Tom and Mohan	Simultaneous	Heuristic	RCA + REA with GA	Selection	Medium
2003	Wan and Lo	Simultaneous	Exact	CPLEX Branch & Bound	Determination	Small
2003	Zhao and Gan	Simultaneous	Heuristic	RCA with SA + HSP with FDS	Selection	Large
2004	Agrawal and Mathew	Simultaneous	Heuristic	RCA + REA with GA	Selection	Large
2004	Carrere and Gori	Simultaneous	Heuristic	RCA + MREA + FREA	Select. + Mod.	Large
2004	Fan and Machemehl	Simultaneous	Heuristic	RCA with Yen-KSP + REA + RIA with SMH	Selection	Large
2004	Petrelli	Simultaneous	Heuristic	RCA + REA with GA + RIA	Selection	Large
2005	Cipriani et al.	Simultaneous	Heuristic	RCA + REA with GA	Selection	Large
2005	Lee and Vuchic	Simultaneous	Heuristic	RCA + RIA + REA	Select. + Mod.	Small
2005	Hu et al.	Sequential	Heuristic	RCA with ACA + FSP with GA	Selection	Large
2006	Fan and Machemehl	Simultaneous	Heuristic	RCA with Yen-KSP + REA + RIA with GA	Selection	Large
2006	Zhao	Simultaneous	Heuristic	RCA with SA + HSP with FDS	Select. + Deter.	Large
2006	Zhao and Zheng	Simultaneous	Heuristic	RCFSP with LSA + RIA with GA	Select. + Deter.	Large
2007	Barra et al.	Simultaneous	Exact	RCSFP with CP	Selection	Small
2007	Borndörfer et al.	Simultaneous	Matheuristic	CGA + GH	Selection	Large
2007	Zhao and Zheng	Simultaneous	Heuristic	RCFSP with LSA + RIA with TS, GS, BS	Select. + Deter.	Large
2008	Fan and Machemehl	Simultaneous	Heuristic	RCA with Yen-KSP + REA + RIA with TS	Selection	Large
2008	Fernández et al.	Simultaneous	Heuristic	RCA + FSP with HJA	Selection	Large
2009	Pacheco et al.	Simultaneous	Heuristic	RCA + RIA with LS/TS	Select. + Mod.	Medium
2009	Marín et al.	Simultaneous	Heuristic	RCA + FSP using CPLEX Branch & Bound	Determination	Small
2011	Mauttone	Simultaneous	Heuristic	RCA with PIA + FSP with GRASP	Selection	Medium
2011	Szeto and Wub	Simultaneous	Heuristic	RCA with GA + FSP with NSH	Selection	Small
2012	Cipriani et al.	Simultaneous	Heuristic	RCA + REA with GA	Selection	Large
2012	Shimamoto et al.	Simultaneous	Heuristic	(VAP + RCA + FSP) with NSGA-II	Selection	Small
2014	López	Simultaneous	Matheuristic	RCA with Yen-KCSP + LSA + SBD	Select. + Deter.	Large

no optimum is guaranteed no matter what type of instance of the model is solved. The vast majority of works fall in this category, although some works use mathematical approaches to solve the solving modules (see for instance Hasselström, 1981; van Oudheusden et al., 1987). However, the authors do not demonstrate that the optimum is within the established partition of the solution space. To this end, it seems more appropriate to use exact decomposition techniques as in Marín and Jaramillo (2009) or López (2014).

3.3.3. Algorithm(s)

Most algorithms fall within the category of metaheuristics. To mention some of them, the Greedy Randomized Adaptive Search Procedure (*GRASP*), Simulated Annealing (*SA*) and Genetic Algorithm (*GA*). The last-mentioned metaheuristic is the most used, leaving apart its variant implementations. Within these metaheuristics a constructive heuristic is used to build part of the solution. For instance, in Mauttone (2011) this heuristic is called the Pair Insertion Algorithm (*PIA*) where routes are constructed having fixed their frequencies. The *PIA* is driven by means of the outer *GRASP* metaheuristic.

This subsection does not pretend to provide a detailed explanation of the algorithms. Rather than that, the focus is on the type of partition of the solution space employed. Using this criterion, the algorithms within the category of heuristic approaches are divided into: 1) Two-sequential phases, 2) Two-iterative phases, 3) Three-sequential phases, 4) Three-iterative phases and 5) Four-iterative phases. Being the second subcategory the most used.

In two-sequential approaches, a Route Construction Algorithm (*RCA*) builds the skeleton of the routes and then a Frequency Setting Procedure (*FSP*) assigns frequencies and vehicles to these routes (Chakroborty, 2003; Hu et al., 2005; Lampkin and Saalmans, 1967; Silman et al., 1974). The two-iteration approach has two variants. One variant works in a similar way to the two-sequential approach and the main difference is that both modules interact until some criterion is met (Agrawai and Mathew, 2004; Caramia et al., 2001; Ceder and Wilson, 1986; Hasselström, 1981; Mauttone, 2011; Pattnaik et al., 1998; Pacheco et al., 2009; Rao et al., 2000; Szeto and Wub, 2011; Tom and Mohan, 2003; van Nes et al., 1988; Zhao and Ghan, 2003). In some of these works, the *FSP* may evaluate some other indicators apart from frequencies and, therefore, the module is called as the Route Evaluation Algorithm (*REA*). The other variant is more sophisticated. Initially, a global feasible solution is determined using a Route Construction and Frequency Setting Procedure (*RCFSP*) and, then, new routes are constructed analyzing this global solution using a Route Improvement Algorithm (*RIA*). These routes are evaluated in the following iteration using again the *RCFSP* procedure. Both modules interact until some criterion is met (Chien et al., 2001; Zhao and Zeng, 2006 and 2007).

In three-sequential approaches, A Network Reduction Procedure (*NRP*) is first used to reduce the number of links to be considered in the *RCA* algorithm. The remaining steps are similar to the two-sequential approaches (Dubois et al., 1979; Soehodho and Koshi, 1999). The three-iterative phase approaches have three variants which differ from the type of combination used among the preceding mentioned approaches. One variant combines the first variant of the two-iterative phases approach and the three-sequential phases approach. So, a *NRP* is first used and then the *RCA* and *REA* interact until some criterion is met (Marwah et al., 1993). Another variant extends the first variant of the two-iterative-phases. This extension entails to add the *RIA* algorithm after the application of the *REA* algorithm (van Oudheusden et al., 1987; Israeli and Ceder, 1989; Israeli, 1992; Ceder and Israeli, 1998; Bielli et al., 1998 and 2002; Fusco et al., 2002; Ngamchai and Lovell, 1993; Carrese and Gori, 2004; Fan and Machemehl, 2004, 2006 and 2008; Petrelli, 2004; Lee and Vuchic, 2005; Shimamoto et al., 1993; Israeli and Ceder, 1995). In some of these works, the names of the solving blocks are altered because they are more sophisticated. Moreover, the order in which they are used may be also modified. The remaining variant is the most sophisticated approach. It combines the two variants of the two-iterative approaches in such a way that the *RCFSA* is first called, then the *REA* module and finally the *RIA*. The three solving blocks interact until a criterion is met (Baaj and Mahmassani, 1990, 1991 and 1995; Shih et al., 1998).

Moving on to matheuristic approaches, the literature is very scant. The works of Bussieck et al. (1996) and López (2014) assume a predefined set of routes/corridors that are evaluated within two distinct mathematical programming environments in such a way that the output is the near-optimal set of routes and frequencies. The remaining work of Borndörfer (2007) employs a different scheme. This scheme also assumes a predefined set of routes but then likely fractional routes and frequencies are determined using mathematical programming techniques. The likely fractional routes are then rounded using a greedy heuristic.

Finally, it is mentioned the work of Wan and Hong (2003). To the best of the author knowledge, it is the only work that implements a strictly exact approach. This approach consists in formulating the model as a mixed-integer linear programming problem that is directly solved by CPLEX.

The remaining not mentioned acronyms in column 5 of Table 3 are explained in Table 7 of Appendix 1.

3.3.4. Layout method

The term layout refers to the structure of the line, i.e., which are the stretches (links) and stations of the line, and the way the layout is determined is referred to layout method. The literature on this issue can be classified into the following four categories: selection, selection + modification, determination and selection + determination.

Selection is the leading layout method because it requires less computational effort. This method assumes a fixed layout on a set of candidate lines, determined by a route

construction procedure without considering passengers and frequencies issues, and the aim is to choose a subset of these lines meeting frequency and passenger requirements.

Selection + modification is an extension of the selection method. It consists of the following two stages: a selection stage which selects a preliminary subset of good lines and a modification stage in which the selected lines are improved by inserting/deleting links or merging lines which are similar (see the references on Table 3 where the sixth column contains the label “Select. + Mod.”).

Determination is the hardest computational method because it makes no simplistic assumption of the layout. It considers a set of potential links and stations and the aim is to allocate them to the lines. This is carried out by imposing appropriate constraints in the mathematical programming formulation of the model (see Wan and Hong, and Marín et al., 2009).

Selection + determination is a very rare method which has been only found in López (2014). Its aim is to obtain significant better layout solutions than the ones found by the selection (+modification) method but not spending too much time. It consists of the following two stages: a route construction procedure which determines a set of candidate line corridors (a chain of line segments or stretches) and a determination procedure which allocates stations to them. The latter is carried out by means of a mathematical programming approach.

3.3.5. *Network size*

The network size refers to the biggest instance that can be solved by the solving techniques. This size has been computed counting the number of nodes, links, o-d demand pairs and number of lines under construction of the biggest study case. As shown in column 6 of Table 3, early works are only capable of solving small-sized networks and, as time has gone by, the solvable size of the network has been increased. In the early 80s, Hasselström (1981) succeeded in solving medium-sized networks. One decade after, van Nes et al. (1988) managed to solve large-sized networks. However, the author used a model rather simplistic. Shih et al. (1998) were the firsts in solving a more detailed model in real-sized networks. Despite this success, the model was still far from reality. Moreover, the model was solved heuristically as in the previous mentioned works.

The initial works on matheuristics (Borndörfer, 2007; Bussieck et al., 1996) demonstrated the effectiveness of mathematical techniques in combination with heuristics, although the employed models were rather simplistic, again. Until not very recently, matheuristics have not been demonstrated to solve large instances with more realistic models (López, 2014).

4. Conclusions and further research

This survey has shown the literature works on the integration of the network design and the frequency setting phases in public transportation networks. These phases correspond to the two first stages of the Transit Planning Process (Ceder and Wilson, 1986). The survey has put emphasis on both modelling issues, i.e., objective cost components and constraints; as well as on solving approaches.

Through Tables 1-6 and their corresponding explanations in Subsections 3.1-3.2, we have seen a great variety of works covering different aspects from the point of view of modelling features and solving techniques. However, there are four major concerns. First, non of these works integrates all the mentioned modelling features. Second, many of these modelling features are not fully or properly covered. Third, other key modelling features have been omitted. Finally, the solving techniques do not guarantee an accurate solution, or are limited to the modelling features being considered. In the following subsections, some lines for further research concerning issues 3 and 4 are provided.

4.1. Modelling issues

Modelling issues concern the platform capacity, the operational capacity of stations, the dwell time, the design with multiple demand scenarios and robustness and recovery in Rapid Transit Network Design. All of them affect to both operator and passengers agents and, thus, they are not considered in separate subsections. They are explained in the following subsections.

4.1.1. Platform capacity

The capacity of a platform is related to the maximum number of passengers that a platform can hold while passengers are waiting to board the vehicle. This capacity comes into play in congested scenarios, i.e., in the peak hours. Its implementation is rather cumbersome because there are several variables interconnected, i.e., the operating frequency on the line, the average passenger waiting time at the station and the arrival pattern of the passengers. Additionally, the relationships of these elements are non-linear and non-convex. Codina et al. (2013) have modeled the station capacity in the context of a bus bridging network where a number of lines are given as inputs. The authors imposed the following constraint:

$$\sum_{l \in L_b} \zeta_a^{l,b}(v_a^{b,l}, v_{x(a)}^{b,l}, z^l) \leq \frac{H}{\eta} \bar{N}_b^{pax} \quad (2)$$

where L_b is a set containing the indexes of the lines serving at the station b , $\zeta_a^{l,b}$ is the total passenger waiting time at the station b before boarding a vehicle working on line l . This time depends on the total number of passengers boarding a vehicle serving at

the station b throughout the time period H under consideration ($v_a^{b,l}$), the total number of vehicle waiting in the vehicle serving at the station b ($v_{x(a)}^{b,l}$) and the total number of services on the line l (z^l). The remaining parameters η and \bar{N}_b^{pax} represent the ratio between the passenger queue length exceeded a fraction $1 - \alpha$ of the line and the average queue length and the capacity of the station b , respectively. The authors also define a general formula for computing the total waiting time $\zeta_a^{l,b}$ as follows:

$$\zeta_a^{l,b}(v_a^{b,l}, v_{x(a)}^{b,l}, z^l) = v_a^{b,l} P_a^b(z^l) \xi_a \left(\frac{v_a^{b,l}}{c z^l - v_{x(a)}^{b,l}} \right) \quad (3)$$

where function P_a^b is the average waiting time per passenger and service without congestion effects, ξ_a is a function that considers the congestion and c is a parameter denoting the vehicle capacity. Function P_a^b was approached using the Allen-Cunee's formula (Allen, 1998), whereas function ξ_a was determined empirically using bulk service queue simulation models. These models establish the relationship between bus stop load factor and passenger waiting times. Finally, constraint (2) was included in a mixed-integer non-linear programming problem. This problem was solved using a specific heuristic consisting of a fixed-point iteration algorithm based on the method of successive averages (MSA). The main drawback of this methodology is that it does not consider link capacities (see Subsection 3.2.4 for its explanation). Thus, it is difficult to integrate the network design phase.

4.1.2. Operational capacity of stations

The operational capacity of a station refers to the maximum number of services per unit of time that can be operated at a station. This capacity influences over the operational frequencies of the lines and the dwell times of the vehicles serving at the station. Additional variables may be involved in certain types of bus stations (Codina et al., 2013). Figure 1 shows a type of bus station, known as bay station, in which two queues

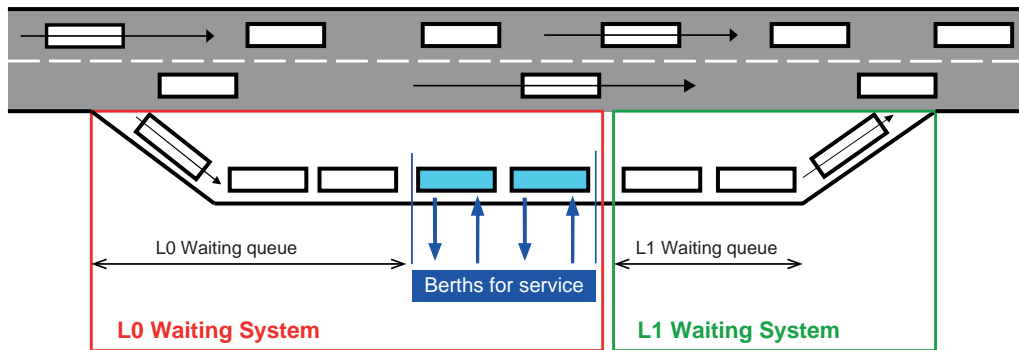


Figure 1: A schematic representation for a bus stop according to Codina et al. (2013).

emerge. One queue represents the waiting time of buses willing to enter the berth place (labeled as \mathcal{L}^0 queue), whereas the other queue models the waiting time of buses willing to exit the berth (labeled as \mathcal{L}^1 queue).

Under this configuration, the following formula applies to the operational capacity of the station:

$$\sum_{l \in L_b} z^l \leq \hat{Z}_b(v, z) \quad (4)$$

where set L_b contains the identifiers of the lines operating at station b , variable z^l indicates the number of services performed on line l and function $\hat{Z}_b(v, z)$ accounts for the following expression:

$$\hat{Z}_b(v, z) \triangleq H \min \left(\frac{(1 - \epsilon)s_b}{\kappa_b(v, z)}, \frac{\mathcal{L}^0}{\eta^0(\kappa_b(v, z) + \omega_b^0(v, z))}, \frac{\mathcal{L}^1}{\eta^1 \omega_b^1(v, z)} \right) \quad (5)$$

where parameter H denotes the planning time horizon, s_b indicates the number of available berth places, $\kappa_b(v, z)$ accounts for the total dwell time, $\mathcal{L}^{0/1}$ stands for the respective queue lengths (i.e., the maximum number of vehicles that can hold the corresponding queues), $\eta^{0/1}$ denotes the occupancy factors at 95 % of the operating time and, finally, $\omega_b^{0/1}(v, z)$ indicates the total waiting time of busses at the respective queues.

Formula (5) can be easily accommodated for railway-based systems. It suffices to omit the quotient expressions inside the big parenthesis which are associated with the bus queues, and to set parameter s_b to 1. In both applications, railway and bus systems, the resulting expressions are not linear because the dwell time $\kappa_b(v, z)$ is in the denominator of the quotient. This limitation was overcome using a specific heuristic as explained in the preceding subsection. Moreover, it was pointed out that this methodology cannot be directly used because the link capacity is omitted.

4.1.3. Dwell time

The dwell time is related to the time in a station spent by the vehicle allowing passengers to board or alight from the vehicle. This time plays also an important role in congested scenarios and in lines with many service stations. The dwell time involves the times on braking and opening the doors when the vehicle enters the station, the passenger times on boarding and alighting when the vehicle is stopped, and the times on closing the doors and accelerating when the vehicle leaves the station.

The computation of passenger times in the dwell time depends on the type of transportation system under consideration. It is also assumed that passengers behave in a

rational manner, i.e., each passenger waits until its predecessor has boarded or alighted. In railway-based systems, first, in-vehicle passengers alight and, then, waiting at-station passengers board. So, only the highest time is added to the dwell time. Whatever the application is, the total type of movement time is divided by the number of vehicle doors dedicated to the movement.

The implementation of the dwell time is rather cumbersome due to non-linearities emerging from the passenger time costs. These costs are related to the alighting, boarding and waiting in-vehicle times. The alighting and boarding times cannot be considered proportional to the number of passengers performing such movements because each passenger does not experience the same time. For instance, the first passenger in alighting from the vehicle starts this movement immediately after the opening of the doors. However, the second passenger needs to wait until the first passenger has alighted and so on. The same reasoning can be done for the boarding movement. To overcome this issue, a portion of the dwell time must be used to weigh the passenger flow associated with these movements. As for the waiting in-vehicle time, the passenger flow related to this waiting must be weighted by the dwell time. So, all these three products are non-linear. The work of Codina et al. (2013), mentioned in the previous subsections, models this feature. Non-linearities are overcome by freezing some of their values in a first optimisation problem and, then, by updating these values, properly. This mechanism is repeated within a fixed-point procedure based on the method of successive averages (*MSA*). This methodology was devised for frequency setting in bus systems but it can be adapted for railway systems with a few changes. As pointed out in the two preceding subsections, the main drawback is that it does not consider link capacities. Thus, it is difficult to integrate the network design phase in the authors approach.

4.1.4. Design with multiple demand scenarios

The literature works have only considered an o-d demand matrix for a given period of the day. This period is usually associated with the peak hours. However, this approach may lead some o-d demand pairs emerging in different periods of the day without coverage. Therefore, different o-d demand matrices should be considered in such a way that the resulting network is consistent with all solution scenarios. Marín and Jaramillo (2008) implement this feature but only for the network design phase. For each period under consideration, a mixed-integer linear programming problem is solved. This problem considers lines being constructed in previous periods. In the first period, some lines already in operation may be taken into account. The infrastructure resource costs used in previous periods are subtracted from the current period under consideration, thus, encouraging passengers to use the already allocated infrastructure. The main drawback of this approach is that the number of lines under construction are not limited. So, if the o-d demand matrices are very different in each period, i.e., different o-d demand pairs appear in each period, an exorbitant number of new lines are likely to be constructed.

4.1.5. Failure to board

The term failure to board applies to congested scenarios where passengers cannot board the first vehicle arriving at their waiting station due to a lack of residual capacity. This feature has been addressed in Kurauchi et al. (2003) and Codina et al. (2013). The first work presents an innovative passenger assignment model that assumes fixed line layouts and operating frequencies, and uses two additional nodes and links accounting for the lack of residual capacity in the vehicle. The additional nodes evaluate the failure to board using a given probability function. Having evaluated this function, the passengers who were unable to board are redirected to the destination, whereas the succeed passengers are transferred to the boarding links. The probability function is expressed using an absorbing Markov chain which is embedded into a hyperpath structure. The solving approach seeks for the minimum hyperpath within a method of successive averages (MSA). This approach was devised for a particular transportation problem and, thus, it cannot be use as a design tool. The other work seems more interesting from the application point of view because it considers the layout of the lines and carries out the frequency setting. The failure to board is indirectly modeled using a function (denoted as ξ_a , where link a accounts for a boarding link) that determines the increment in waiting time due to congestion. The reader is directed to Subsection 4.1.1 for further details.

4.1.6. Robustness in rapid transit network design

Robustness is one of the most complex features from both modelling and computational points of view. It consists of designing a network as much robust as possible so that it is not “very” affected by a vehicle breakdown or an unexpected increase in demand in sections (links) of the network. The robustness issue has been previously considered in Laporte et al. (2011), Marín et al. (2009) and Cadarso and Marín (2012), among others. All these works are based on mathematical programming approaches and the differences rely on the type of robustness measure considered and the way it is incorporated in the model.

In Laporte et al. (2011) and Cadarso and Marín (2012), robustness is only considered from the point of view of the user, i.e., when a failure/congestion occurs in some critical edge, passengers using that edge must have some alternative routes. Laporte et al. (2011) examine separately different scenarios by changing the value of the parameters and using different types of constraints related to robustness. Moreover, they pointed out how the design of the network is affected by each parameter and type of constraint. In contrast, Cadarso and Marín (2012) analysed the different scenarios at the same time and minimized the differences between the optimal network designs in each scenario considering only one type of constraints defined by Laporte et al. (2011).

Marín et al. (2009) extend the concept of robustness to account for the point of view of the operator. A network is robust if a failure or congestion occurring in some critical edge affects the less number of vehicles. To this end, the authors defined an iterative approach in which two mathematical programming problems are solved. The first one

is a network design problem with the same mathematical structure as the one presented in Laporte et al. (2011), the only difference is that the authors make only use of one type of robustness constraint (as in Cadarso and Marín, 2012). The second problem is a frequency setting model with flows expressed by paths (routes) instead of links. In each iteration, alternative routes and planning configurations are sought by fixing to 1 the active routing variables of the previous iterations. The algorithm stops when there is no infrastructure budget. This scheme is repeated twice, one accounting Robustness for the point of view of the user and the other focusing robustness on the point of view of the operator. In this way, a more variety of network designs are found and can be analysed.

All these works can be integrated with the aforementioned features with minor changes. However, algorithmic improvements must be done in order to solve real-sized networks.

4.1.7. Recovery in rapid transit network design

This feature is complementary to Robustness and its aim is to provide an alternative service to those passengers affected by a disruption on their usual transportation system. The literature on this topic have mainly been addressed to some of the final stages of the Transit Planning Process (see, for instance, Cadarso, 2013 or Cadarso and Marín, 2014), and scant literature focus on some of the first stages (see, for instance, Codina et al., 2013).

Cadarso (2013) and Cadarso and Marín (2014) developed an integrated timetable and rolling stock model where the term “rolling stock” refers to vehicle scheduling in Railway systems. In that model, passengers on cancelled services, due to disruptions on some links of their operating lines, are reassigned to new emergency services (*ES*). These *ES* services may take place on the line where the disruption occurred, but the *ES* must begin(end) after(before) the disrupted link. Additionally, an alternative system (the underground) may also carry out some *ES* service as long as part of their line itineraries are close to the disrupted links of the train system.

Codina et al. (2013) devised a Bus Bridging model which provides service to all passengers affected by disruptions on a railway-based system. The model mainly focuses on the frequency setting phase but it can also determine which lines will provide service. Moreover, the model takes into consideration all the main effects of congestion at a bus station, i.e., waiting time to board a vehicle considering lack of residual capacity, waiting time on entering the berth and waiting time on exiting the station (see Subsections 4.1.1, 4.1.2 and 4.1.5 for further details).

Cadarso (2013) and Cadarso and Marín (2014) works cannot being directly integrated into a network design and frequency setting model but some ideas can be taken from. The work of Codina et al. (2013) seems more suitable but the complexity of the resulting model will considerably be increased in views of their solving approach.

4.2. Solving issues

Solving issues are focused on the generation of more attractive line corridors, convergence enhancements of exact decomposition approaches and the non-convexity in variable demand models. The first issue affects both heuristic and exact approaches, whereas the other two issues are strictly related to exact or certain matheuristic approaches. They are explained in the following subsections.

4.2.1. Generation of more attractive line corridors

The generation of a set of input line corridors to the optimization model represents a key aspect for a good network design. To date, state-of-the-art works use a k-shortest path algorithm which determines a preliminary set of line corridors. This set is then reduced, evaluating a certain number of restrictions related to the length of the corridors and, possibly some user behaviour rules (see, for instance, Fan and Machemehl, 2004, 2006 and 2008). This approach may discard a large set of good corridors in the running of the k-shortest path because the restrictions are evaluated afterwards. This drawback is overcome in López (2014). However, there is still an important limitation. The amount of demand is still not considered in the running of the k-shortest path. This limitation affects the in-vehicle waiting time. A k-shortest path algorithm enumerates the line corridors in an increasing fashion. First, it constructs the k-shortest corridor and then seeks for the first least long corridor. At this point, the amount of demand comes into play because part of the enlargement of the previous corridor is only justified if at least one additional o-d demand pair flow uses part of this new corridor. Therefore, the previous allocated o-d demand flows will experience a delay due to boarding and alighting of this (these) additional o-d demand pair(s) within the section of the corridor in which these movements occur.

4.2.2. Convergence enhancements of exact decomposition approaches

This issue is related to the Benders Decomposition (*BD*). The *BD* (Benders, 1962) is a classical decomposition algorithm applied to many large optimization models successfully. This decomposition consists of a reformulation of the model in which two problems called the Master Problem (*MP*) and the SubProblem (*SP*) are iteratively solved until a duality gap is small enough. The *MP* is a relaxation of the original problem in which the interdependencies between the operator and the passengers are discarded and the active dependencies are iteratively appended in the form of Benders cuts. These cuts may be Optimality Benders Cuts (*OBCs*) when the dual of the *SP* has a solution. Otherwise, Feasibility Benders Cuts are added to the *MP*. The *SP* represents the passenger assignment model, thus it is a continuous problem. When the dual form of the *SP* is degenerated, i.e., it has multiple optimal solutions (which is our case), the performance of the algorithm decreases dramatically Magnanti and Wong (1981). To overcome this limitation, the authors in Magnanti and Wong (1981) propose a

new Benders scheme in which an additional problem per iteration is solved to obtain better *OBCs* that enhance the algorithm convergence. This scheme is later improved in Papadakos (2008), so that the generator of *OBCs* is faster to solve. However, the computation of both generators requires an initial *core point*. This point refers to a point strictly in the interior of the feasible region of the *MP*, excluding the *OBCs*. The obtaining of this core point is non-trivial, in general, and the quality of the *OBCs* depends heavily on that point. Recently, it has been demonstrated that good *OBCs* can be obtained from a problem that integrates the *SP* and the generator of *OBCs* Sherali and Lunday (2011). Moreover, the resulting problem does not require a core point but a strictly positive point and a weight factor, which can be easily obtained. However, the quality of the resulting *OBCs* still depends heavily on these two parameters. Thus, this enhancement is not reliable.

4.2.3. *Non-convexity in variable demand models*

The competition among several modes of transportation is correctly formulated as a Bilevel Programming Problem (*BPP*) (López, 2014). The outer level represents a trade-off between operator and passengers agents, whereas the inner level involves only the passenger agent. This *BPP* is solved using an adaptation of the Benders Decomposition (Codina and López, under review). In this adaptation, the Master Problem (*MP*) approaches the original problem iteratively using new types of Benders cuts coming from a more complex SubProblem (*SP*). This *SP* is a reduced *BPP* involving only the continuous variables and their restrictions of the original *BPP*. The two levels of this reduced *BPP* share the same constraints, so the inner level can be first solved and, then, using its solution, a linking constraint is added to the outer level so that it can be solved afterwards. This *BD* encounters serious problems due to inherent non-convexities being raised in the original *BPP*. These non-convexities are detected when non-valid Benders cuts appear (Saharidis and Ierapetritou, 2009). A non-valid Benders cut refers to a cut being generated in the *SP* of current Benders iteration that does not constraint the *MP* (i.e., when the cut is added to the *MP* and the *MP* is resolved, the solution does not change). The authors in Saharidis and Ierapetritou (2009) suggested to add exclusion cuts to the *MP* when a non-valid Benders cut arises. However, the generation of these cuts is rather cumbersome for *NDFSP* problems. Moreover, it requires an exorbitant number of restrictions that slow down the resolution of subsequent *MP* problems.

5. Acknowledgements

The author expresses gratitude to the support of projects TRA2008-06782-C02-02 and TRA2011-27791-C03-01/02 from the Spanish Government.

Appendix 1

Table 7: Description of the literature methods used to solve the Network Design and Frequency Setting Problem.

Method	Description
ACA	Ant Colony Algorithm
BS	Bisection Search
CGA	Corridor Generation Algorithm
CGT	Column Generation Technique
CLP	Continuous Linear Problem
EA	Erlenkotten Algorithm
FDS	Fast Descend Search
FREA	Feeder Route Evaluation Algorithm
FSP	Frequency Setting Procedure
GA	Genetic Algorithm
GBSP	Gradient Based Search Procedure
GPM	Gradient Projection Program
GRASP	Greedy Randomized Adaptive Search Procedure
GS	Greedy Search
HJA	Hooke & Jeeves Algorithm
HSP	Headway Setting Procedure
KCSP	K-Constrained Shortest Paths
KSP	K-Shortest Paths
LS	Local Search
LSA	Line Splitting Algorithm
MREA	Main Route Evaluation Algorithm
NSGA-II	Non-dominated Sorting Genetic Algorithm of Type-II
NN	Neuronal Networks
NRP	Network Reduce Procedure
NSH	Neighborhood Search Heuristic
PIA	Pair Insertion Algorithm
RCA	Route Construction Algorithm
RCFSA	Route Construction and Frequency Setting Algorithm
REA	Route Evaluation Algorithm
RSA	Route Selection Algorithm
RGBSP	Random Gradient Based Search Procedure
RIA	Route Improvement Algorithm
RNHSP	Route Nested and Headway Setting Procedure
RRA	Route Reduction Algorithm
SA	Simulated Annealing
SBD	Specialized Benders Decomposition
SCP	Set Covering Problem
SMH	Several Metaheuristics
SPLP	Simple Plant Location Problem
TS	Tabu Search
VAP	Vehicle Assignment Procedure
VI	Valid Inequalities

References

- Agrawai, J. and Mathew, T. V. (2004). Transit route design using parallel genetic algorithm. *Journal of Computing in Civil Engineering*, 18, 248–256.
- Allen, A. O. (1998). *Probability, Statistics and Queuing Theory*. Academic Press, New York.
- Barra, A., Carvalho, L., Teypaz, N., Cung, V.D. and Balassiano, R. (2007). Solving the transit network design problem with constraint programming. *Proceedings of the 11th World Conference in Transport Research*.
- Baaj, M. H. and Mahmassani, H. S. (1990). TRUST: a Lisp program for the analysis of transit route configuration. *Transportation Research Record*, 1283, 125–135.
- Baaj, M. H. and Mahmassani, H. S. (1991). An AI-based approach for transit route system planning and design. *Journal of Advanced Transportation*, 25, 187–210.
- Baaj, M. H. and Mahmassani, H. S. (1995). Hybrid route generation heuristic algorithm for the design of transit networks. *Transportation Research Part C*, 3, 31–50.
- Benders, J. (1962). Partitioning procedures for solving mixed-variables programming problems. *Numerische Mathematik*, 4, 238–252.
- Bielli, M., Carotenuto, P. and Confessore, G. (1998). A new approach for transport network design and optimization. *Proc., 38th the Conf. Congress of the European Regional Science Association*, Vienna, Austria.
- Bielli, M., Caramia, M. and Carotenuto, P. (2002). Genetic algorithms in bus network optimization. *Transportation Research Part C: Emerging Technologies*, 10, 19–34.
- Borndörfer, R., Grottschel, M. and Pfetsch, M. E. (2007). A column-generation approach to line planning in public transport. *Transportation Science*, 41, 123–132.
- Bussieck, M. R., Kreuzer, P. and Zimmermann, U. T. (1996). Optimal lines for railway systems. *European Journal of Operational Research*, 96, 54–63.
- Cadarso, L. and Marín, A. (2012). Recoverable robustness in rapid transit network design. *Procedia-Social and Behavioral Sciences*, 54, 1288–1297.
- Cadarso, L., Marín, A. and Maroti, G. (2013). Recovery of disruptions in rapid transit networks. *Transportation Research Part E: Logistics and Transportation Review*, 53, 15–33.
- Cadarso, L. and Marín, A. (2014). Recovery of disruptions in rapid transit networks with origin-destination demand. *Procedia-Social and Behavioral Sciences*, 111, 528–537.
- Caramia, M., Carotenuto, P. and Confessore, G. (2001). Metaheuristics techniques in bus network optimization. *NECTAR Conference no 6 European Strategies in the Globalising markets, Transport Innovations, Competitiveness and Sustainability in the Information Age*, 16–18, Helsinki, Finland.
- Carrese, S. and Gori, S. (2004). An urban bus network design procedure. *Transportation Planning*. In: M. Patriksson and M. Labbé (eds.), 64, 177–195.
- Ceder, A. and Israeli, Y. (1998). User and operator perspectives in transit network design. *Transportation Research Record*, 1623, 3–7.
- Ceder, R. B. and Wilson, N. H. (1986). Bus network design. *Transportation Research Part B*, 20, 331–344.
- Cipriani, E., Fusco, G., Gori, S. and Petrelli, M. (2005). A procedure for the solution of the urban bus network design problem with elastic demand. *Advanced OR and AI Methods in Transportation Proc.*, 10th Meeting of the EURO Working Group on Transportation, Publishing House of Poznan Univ. of Technology, Poland, 681–685.
- Cipriani, E., Gori, S. and Petrelli, M. (2012). Transit network design: a procedure and an application to a large urban area. *Transportation Research Part C*, 20, 3–14.
- Codina, E., Marín, A., González, L. and Ramírez, P. (2008). Bus bridging for rapid transit network incidences. *Congreso Latino-Iberoamericano de Investigación Operativa (CLAIO)*, Cartagena, Colombia.

- Codina, E., Marín, A. and López, F. (2013). A model for setting services on auxiliary bus lines under congestion. *TOP*, 21, 48–83.
- Codina, E. and López, F. (Under review). Solving the strategy based congested transit assignment model using smoothing approximations. *Journal of Global Optimization*.
- Chakroborty, P. (2003). Genetic algorithms for optimal urban transit network design. *Computer-Aided Civil and Infrastructure Engineering*, 18, 184–200.
- Chien, S., Yang, Z. and Hou, E. (2001). Genetic algorithm approach for transit route planning and design. *Journal of Transportation Engineering*, 127, 200–207.
- Chiraphadhanakul, V. and Barnhart, C. (2013). Incremental bus service design: combining limited-stop and local bus services. *Public Transport*, 5, 53–78.
- Desaulniers, G. and Hickman, M. D. (2007). Public Transit, chapter 2. *Handbooks in Operations Research and Management Science*, 14.
- Dubois, D., Bell, G. and Llibre, M. (1979). A set of methods in transportation network synthesis and analysis. *Journal of Operations Research Society*, 30, 797–808.
- Ehrgott, M. and Gandibleux, X. (2002). Multiobjective combinatorial optimization-theory methodology, and applications. *Multi-Criteria Optimization-State of the Art Annotated Bibliographic Surveys*, Kluwer Academic Publishers, Dordrecht, 369–444.
- Ercolano, J. (1984). Limited-stop bus operations: an evaluation. *Transportation Research Record*, 994, 24–29.
- Fan, W. and Machemehl, R. B. (2004). Optimal transit route network design problem: algorithms, implementations and numerical results. Research SWUTC/04/167244-1, University of Texas.
- Fan, W. and Machemehl, R. B. (2006). Optimal transit route network design problem with variable transit demand: genetic algorithm approach. *Journal of Transportation Engineering*, 132, 40–51.
- Fan, W. and Machemehl, R. B. (2008). Tabu Search Strategies for the Public Transportation Network Optimizations with Variable Transit Demand. *Computer-Aided Civil and Infrastructure Engineering*, 23, 502–520.
- Farahani, R. Z., Miandoabchi, E. and Szeto, W. Y. (2013). A review of urban transportation network design problems. *European Journal of Operational Research*, 229, 281–302.
- Fernández, J., de Cea, J. and Malbran, H. R. (2008). Demand responsive urban public transport system design: Methodology and application. *Transportation Research Part A*, 42, 951–972.
- Ferropedia (2014a). Infrastructure construction costs. http://www.ferropedia.es/wiki/Costos_de_construcción_de_infraestructura. Last accessed 1 August 2014.
- Ferropedia (2014b). Railway costs: Services. http://www.ferropedia.es/wiki/Costes_del_ferrocarril:_servicios. Last accessed 17 April 2014.
- Fusco, G., Gori, S. and Petrelli, M. (2002). A heuristic transit network design algorithm for medium size towns. *Proceedings of 9th Euro Working Group on Transportation*, 652–656.
- García, R., Garzón-Astolfi, A., Marín, A., Mesa, J. A. and Ortega, F. A. (2006). *Analysis of the Parameters of Transfers in the Rapid Transit Network Design*. Schloss Dagstuhl, ISBN 978-3-939897-00-2.
- Guihaire, V. and Hao, J.-K. (2008). Transit network design and scheduling: a global review. *Transportation Research Part A*, 42, 1251–1273.
- Hasselström, D. (1981). Public transportation planning: a mathematical approach. PhD dissertation, Univ. of Gothenburg, Gothenburg, Sweden.
- Hu, J., Shi, X., Song, J. and Xu, Y. (2005). Optimal design for urban mass transit network based on evolutionary algorithm. *Lecture notes in computer science*. In: L. Wang, K. Chen and Y. S. Ong (eds.), 3611, Springer, Berlin-Heidelberg.
- Israeli, Y. and Ceder, A. (1989). Designing transit routes at the network level. *Proceedings of the First Vehicle Navigation and Information Systems Conference*, IEEE Vehicular Technology Society, 310–316.

- Israeli, Y. and Ceder, A. (1995). Transit route design using scheduling and multiobjective programming techniques. *Computer-Aided Transit Scheduling. Lecture Notes in Economics and Mathematical Systems*. In: Daduna, J.R., Branco, I. and Piax ao, J. (Eds.), Springer-Verlag, Heidelberg 430, 56–75.
- Israeli, Y. (1992). Transit route and scheduling design at the network level. Doctoral dissertation, Technion Israel Institute of Technology.
- Kepaptsoglou, K. and Karlaftis, M. (2009). Transit route network design problem: review. *Journal of Transportation Engineering*, 135, 491–505.
- Kurauchi, F., Bell, M. G. H. and Schmöcker, J.-D. (2003). Capacity constrained transit assignment with common lines. *Journal of Mathematical Modelling and Algorithms*, 2, 309–327.
- Lampkin W. and Saalmans P. D. (1967). The design of routes, service frequencies and schedules for a municipal bus undertaking: a case study. *Operational Research Quarterly*, 18, 375–397.
- Laporte, G., Marín, A., Mesa, J. A. and Ortega, F. (2007). An integrated methodology for the rapid transit network design. *Algorithmic Methods for Railway Optimization*, 4359, 187–199.
- Laporte, G., Marín, A., Mesa, J. A. and Perea, F. (2011). Designing rapid transit network design with alternative routes. *Journal of Advanced Transportation*, 45, 54–65.
- Larraín, H., Muñoz, J. C. and Giesen, R. (2013). How to design express services on a bus transit network. Webseminar on BRT Center for excellence, Santiago de Chile.
- Lee, Y.-J. and Vuchic, V. R. (2005). Transit network design with variable demand. *Journal of Transportation Engineering*, 131, 1–10.
- López, F. (2014). Conjoint design of railway lines and frequency setting under semi-congested scenarios. Thesis Report. Universitat Politècnica de Catalunya Barcelona-Tech, Barcelona.
- Magnanti, T. and Wong, R. (1981). Accelerating Benders decomposition: algorithmic enhancement and model selection criteria. *Operations Research*, 29, 464–484.
- Marín, A. (2007). An extension to urban rapid transit network design. *TOP*, 15, 231–241.
- Marín, A. and Jaramillo, P. (2008). Urban rapid transit network capacity expansion. *European Journal of Operational Research*, 191, 45–60.
- Marín, A. and Jaramillo, P. (2009). Urban rapid transit network design: accelerated Benders decomposition. *Annals of Operation Research*, 169, 35–53.
- Marín, A., Mesa, J. A. and Perea, F. (2009). Integrating robust railway network design and line planning under failures. *Lectures Notes in Computer Science*, 5868, 273–292.
- Marín, A. and García-Rodenas, R. (2009). Location of infrastructure in urban railway networks. *Computers & Operations Research*, 36, 1461–1477.
- Marwah, B. R., Farokh, S., Umrigar, S. and Patnaik, S. B. (1984). Optimal design of bus routes and frequencies for Ahmedabad. *Transportation Research Record*, 994, 41–47.
- Mauttone, A. (2011). Models and Algorithms for the optimal design of bus routes in public transportation systems. Thesis Report, Montevideo.
- Ngamchai, S. and Lovell, D. J. (2003). Optimal time transfer in bus transit route network design using a genetic algorithm. *Journal of Transportation Engineering*, 129, 510–521.
- Pacheco, J., Álvarez, A., Casado, S. and Gonzalez-Velarde, J. L. (2009). A tabu search approach to an urban transport problem in northern Spain. *Computers & Operations Research*, 36, 967–979.
- Papadakos, N. (2008). Practical enhancements to the Magnanti-Wong method. *Operational Research Letters*, 36, 444–449.
- Patnaik, S. B., Mohan, S. and Tom, V. M. (1998). Urban bus transit route network design using genetic algorithm. *Journal of Transportation Engineering*, 124, 368–375.
- Petrelli, M. (2004). A transit network design model for urban areas. In: Brebbia C. A. and Wadhwa L. C. (eds.), *Urban transport X*, WIT Press, U.K., 163–172.
- Rao, K. V., Muralidhar, S. and Dhingra, S. L. (2000). Public transport routing and scheduling using genetic algorithms. *Computer-Aided Scheduling of Public Transport*, Berlin, Germany, 21–23 June 2000.

- Saharidis, G. K. and Ierapetritou, M. G. (2009). Resolution method for mixed integer bi-level linear problems based on decomposition technique. *Journal of Global Optimization*, 44, 29–51.
- Sherali, H. D. and Lunday, B. J. (2011). On generating maximal nondominated Benders cuts. *Annals of Operational Research*, 210, 57–72.
- Shih, M. and Mahmassani, H. S. (1994). A design methodology for bus transit networks with coordinated operations. Tech. Rep. SWUTC/94/60016-1, Center for Transportation Research, University of Texas, Austin.
- Shih, M., Mahmassani, H. S. and Baaj, M. (1998). A planning and design model for transit route networks with coordinated operations. *Transportation Research Record*, 1623, 16–23.
- Shimamoto, H., Schmöcker, J.-D. and Kurauchi, F. (2012). Optimisation of a bus network configuration and frequency considering the common lines problem. *Journal of Transportation Technologies*, 2, 220–229.
- Silman, L. A., Barzily, Z. and Passy, U. (1974). Planning the route system for urban buses. *Computers and Operations Research*, 1, 210–211.
- Soehodho, S. and Koshi, M. (1999). Design of public transit network in urban area with elastic demand. *Journal of Advanced Transportation*, 33, 335–369.
- Spieß, H. and Florian, M. (1989). Optimal strategies: a new assignment model for transit networks. *Transportation Research-Part B*, 23, 83–102.
- Szeto, W. Y. and Wub, Y. (2011). A simultaneous bus route design and frequency setting problem for Tin Shui Wai, Hong Kong. *European Journal of Operational Research*, 209, 141–155.
- Tom, V. M. and Mohan, S. (2003). Transit route network design using frequency coded genetic algorithm. *Journal of Transportation Engineering*, 129, 186–195.
- van Oudheusden, D. L., Ranjithan, S. and Singh, K. N. (1987). The design of bus route systems-An interactive location allocation approach. *Transportation*, 14, 253–270.
- van Nes, R., Hamerslag, R. and Immer, B. H. (1988). The design of public transport networks. *Transportation Research Record*, 1202, 74–83.
- Vuchic, V. R. (1973). Skip-stop operation as a method for transit speed increase. *Traffic Quarterly*, 27, 307–327.
- Wan, Q. K. and Hong, K. Lo. (2003). A mixed integer formulation for multiple-route transit network design. *Journal of Mathematical Modelling and Algorithms*, 2, 299–308.
- Zhao, F. and Ghan, A. (2003). Optimization of Transit Network to minimize transfers. Report BD-015-02. Research Center Florida Department of Transportation.
- Zhao, F. (2006). Large-scale transit network optimization by minimizing user cost and transfers. *Journal of Public Transportation*, 9, 107–129
- Zhao, F. and Zeng, X. (2006). Optimization of transit network layout and headway with a combined genetic algorithm and simulated annealing method. *Engineering Optimization*, 38, 701–722.
- Zhao, F. and Zeng, X. (2007). Optimization of user and operator cost for large scale transit networks. *Journal of Transportation Engineering*, 133, 240–251.

An extension of the slash-elliptical distribution

Mario A. Rojas¹, Heleno Bolfarine² and Héctor W. Gómez³

Abstract

This paper introduces an extension of the slash-elliptical distribution. This new distribution is generated as the quotient between two independent random variables, one from the elliptical family (numerator) and the other (denominator) a beta distribution. The resulting slash-elliptical distribution potentially has a larger kurtosis coefficient than the ordinary slash-elliptical distribution. We investigate properties of this distribution such as moments and closed expressions for the density function. Moreover, an extension is proposed for the location scale situation. Likelihood equations are derived for this more general version. Results of a real data application reveal that the proposed model performs well, so that it is a viable alternative to replace models with lesser kurtosis flexibility. We also propose a multivariate extension.

MSC: 60E05.

Keywords: Slash distribution, elliptical distribution, kurtosis.

1. Introduction

A distribution closely related to the normal distribution is the slash distribution. This distribution can be represented as the quotient between two independent random variables, a normal one (numerator) and the power of a uniform distribution (denominator). To be more specific, we say that a random variable S follows a slash distribution if it can be written as

$$S = Z/U^{\frac{1}{q}}, \quad (1)$$

¹ Departamento de Matemáticas, Facultad de Ciencias Básicas, Universidad de Antofagasta, Antofagasta, Chile. mario.rojas@uantof.cl

² Departamento de Estatística, IME, Universidad de Sao Paulo, Sao Paulo, Brasil. hbolfar@ime.usp.br

³ Departamento de Matemáticas, Facultad de Ciencias Básicas, Universidad de Antofagasta, Antofagasta, Chile. hector.gomez@uantof.cl

Received: August 2012

Accepted: June 2014

where $Z \sim N(0, 1)$ is independent of $U \sim U(0, 1)$ and $q > 0$. For $q = 1$, the standard (canonical) version follows and as $q \rightarrow \infty$, the standard normal distribution follows. The density function for the standard slash distribution is then given by

$$p(x) = \begin{cases} \frac{\phi(0) - \phi(x)}{x^2} & x \neq 0 \\ \frac{1}{2}\phi(0) & x = 0 \end{cases} \quad (2)$$

where ϕ denotes the density function of the standard normal distribution (see Johnson, Kotz and Balakrishnan 1995). This distribution has thicker tails than the normal distribution, that is, it has greater kurtosis. Properties of this distribution are studied in Rogers and Tukey (1972) and Mosteller and Tukey (1977). Maximum likelihood estimation for location and scale parameters is studied in Kafadar (1982). Wang and Genton (2006) develop multivariate symmetric and asymmetric versions of the slash distribution. Gómez, Quintana and Torres (2007) and Gómez and Venegas (2008) propose univariate and multivariate extensions of the slash distribution by replacing the normal distribution by the elliptical family of distributions. Asymmetric versions of this family are discussed in the work of Arslan (2008). Arslan and Genc (2009) discuss a symmetric extension of the multivariate slash distribution and Genc (2007) investigates a symmetric generalization of the slash distribution. Gómez, Olivares-Pacheco and Bolfarine (2009) use the slash-elliptical family to extend the Birnbaum-Saunders (BS) distribution. Finally, Genc (2013) introduces a skew extension of the slash distribution utilizing the beta-normal distribution.

The present paper focuses on extending the slash-elliptical family of distributions considered in Gómez et al. (2007) to a distribution with greater kurtosis, for which purpose it is necessary to replace the uniform distribution by the beta distribution. This gives a family of distributions, containing the slash-elliptical family, with much greater flexibility.

The paper is organized as follows. In Section 2 we present the standard versions of the slash distribution and some of its properties. In Section 3 we propose the extension investigated in the paper, called the extended slash-elliptical family of distributions, and study some of its properties. Section 4, which deals with a real data application, reveals that the extended slash-elliptical distribution can be quite useful in fitting real data and substantially improve less flexible models. Parameter estimation is dealt with by using the maximum likelihood approach. Section 5 introduces a multivariate version of the distribution, and Section 6 presents our main conclusions.

2. Preliminaries

In this section we discuss some properties of the ordinary univariate and multivariate slash distributions, for the sake of notation and comparisons.

We say that a random variable X follows an elliptical slash distribution with location parameter μ and scale parameter σ if its density function is of the form

$$f_X(x; \mu, \sigma) = \frac{1}{\sigma} g \left(\left(\frac{x - \mu}{\sigma} \right)^2 \right),$$

for some nonnegative function $g(u)$, $u \geq 0$, such that $\int_0^\infty u^{-1/2} g(u) du = 1$. We denote $X \sim El(\mu, \sigma; g)$.

In the multivariate setup, a p -dimensional random vector $\mathbf{Y} = (Y_1, \dots, Y_p)^\top$ follows an elliptical distribution with location parameter vector $\boldsymbol{\mu}$ and scale parameter matrix $\boldsymbol{\Sigma}$, which is positive definite, if its density function is given by

$$f_{\mathbf{Y}}(\mathbf{y}) = \boldsymbol{\Sigma}^{-1/2} g^{(p)} \left((\mathbf{y} - \boldsymbol{\mu})^\top \boldsymbol{\Sigma}^{-1} (\mathbf{y} - \boldsymbol{\mu}) \right), \mathbf{y} \in \mathbb{R}^p$$

where $g^{(p)}$ is the density generator function satisfying

$$\int_0^\infty u^{p-1} g^{(p)}(u^2) du < \infty.$$

We use the notation $\mathbf{Y} \sim El_p(\boldsymbol{\mu}, \boldsymbol{\Sigma}; g^{(p)})$. If the moments of each element of the random vector \mathbf{Y} are finite, then it follows that $E(\mathbf{Y}) = \boldsymbol{\mu}$ and $Var(\mathbf{Y}) = \alpha_g \boldsymbol{\Sigma}$, where α_g is a positive constant, as seen for example, in Fang, Kotz and Ng (1990) and Arellano-Valle, Bolfarine and Vilca-Labra (1996).

An extension of the slash model studied in Gómez et al. (2007), called the slash-elliptical distribution, is defined as

$$X = \frac{Z}{U^{1/q}} \tag{3}$$

where $Z \sim El(0, 1; g)$ and $U \sim \mathcal{U}(0, 1)$, Z and U are independent random variables with $q > 0$. We use the notation $X \sim SEl(0, 1, q; g)$. The density function for the random variable $X \sim SEl(0, 1, q; g)$ is given by

$$f_X(x; 0, 1, q) = \begin{cases} \frac{q}{2|x|^{q+1}} \int_0^{x^2} t^{\frac{q-1}{2}} g(t) dt & \text{if } x \neq 0 \\ \frac{q}{1+q} g(0) & \text{if } x = 0. \end{cases} \tag{4}$$

A location-scale extension for the slash-elliptical distribution is given by $X = \sigma \frac{Z}{U^{1/q}} + \mu$, so that its density function can be written as

$$f_X(x; \mu, \sigma, q) = \frac{q}{\sigma} \int_0^1 u^q g \left(\left(\left[\frac{x - \mu}{\sigma} \right] u \right)^2 \right) du, \quad (5)$$

$-\infty < x < \infty$, $\mu \in \mathbb{R}$, $\sigma \in \mathbb{R}^+$ and $q > 0$. We use the notation $X \sim SE\ell(\mu, \sigma, q; g)$.

3. The extended slash-elliptical distribution and its properties

In this section we consider a stochastic representation, the density function (with some graphical representations) and properties for the extended slash distribution.

3.1. Stochastic representation

The stochastic representation of the new distribution is given as

$$X = \frac{W}{T} \quad (6)$$

where $W \sim E\ell(0, 1; g)$ and $T \sim Beta(\alpha, \beta)$ are independent random variables with $\alpha > 0$, $\beta > 0$. We call the distribution of X the extended slash elliptical distribution, and use the notation $X \sim ESE\ell(0, 1, \alpha, \beta; g)$.

3.2. Density function

The following result shows that the density function of the random variable $ESE\ell$, can be generated using the stochastic representation in (6).

Proposition 1 Let $X \sim ESE\ell(0, 1, \alpha, \beta; g)$. Then, the density function of X is given by

$$f_X(x) = \begin{cases} \frac{1}{2B(\alpha, \beta)|x|^{\alpha+1}} \int_0^{x^2} g(u) u^{\frac{\alpha-1}{2}} \left(1 - \frac{u^{1/2}}{|x|}\right)^{\beta-1} du, & \text{if } x \neq 0 \\ \frac{\alpha}{\alpha + \beta} g(0), & \text{if } x = 0 \end{cases} \quad (7)$$

with $\alpha > 0$, $\beta > 0$, and $g(\cdot)$ density generator function.

Proof. From the stochastic representation (6), we have

$$\begin{aligned} W \sim El(0, 1; g) &\Rightarrow f_W(w) = g(w^2) \\ T \sim Beta(\alpha, \beta) &\Rightarrow f_T(t|\alpha, \beta) = \frac{1}{B(\alpha, \beta)} t^{\alpha-1} (1-t)^{\beta-1}, 0 \leq t \leq 1, \end{aligned}$$

in which

$$B(\alpha, \beta) = \int_0^1 t^{\alpha-1} (1-t)^{\beta-1} dt,$$

which can be written as

$$B(\alpha, \beta) = \frac{\Gamma(\alpha)\Gamma(\beta)}{\Gamma(\alpha + \beta)}.$$

Moreover, using the stochastic representation in (6) and the Jacobian transformation approach, it follows that:

$$\left. \begin{matrix} X = \frac{W}{T} \\ Y = T \end{matrix} \right\} \Rightarrow \begin{matrix} W = XY \\ T = Y \end{matrix} \Rightarrow J = \begin{vmatrix} \frac{\partial W}{\partial X} & \frac{\partial W}{\partial Y} \\ \frac{\partial T}{\partial X} & \frac{\partial T}{\partial Y} \end{vmatrix} = \begin{vmatrix} y & x \\ 0 & 1 \end{vmatrix} = y.$$

Hence,

$$\begin{aligned} f_{X,Y}(x,y) &= |J| f_{W,T}(xy,y) \\ f_{X,Y}(x,y) &= y f_W(xy) f_T(y), -\infty < x < \infty, 0 \leq y \leq 1. \end{aligned}$$

Therefore,

$$\begin{aligned} f_X(x) &= \int_0^1 y f_W(xy) \frac{1}{B(\alpha, \beta)} y^{\alpha-1} (1-y)^{\beta-1} dy, \quad -\infty < x < \infty \\ &= \frac{1}{B(\alpha, \beta)} \int_0^1 f_W(xy) y^\alpha (1-y)^{\beta-1} dy, \quad -\infty < x < \infty, \end{aligned}$$

with $f_W(w) = g(w^2)$ as the density function of W . Hence,

$$f_X(x) = \frac{1}{B(\alpha, \beta)} \int_0^1 g(x^2 y^2) y^\alpha (1-y)^{\beta-1} dy, \quad -\infty < x < \infty. \quad (8)$$

a) For $x = 0$,

$$\begin{aligned}
 f_X(x) &= \frac{1}{B(\alpha, \beta)} \int_0^1 g(0) y^\alpha (1-y)^{\beta-1} dy \\
 &= g(0) \frac{B(\alpha+1, \beta)}{B(\alpha, \beta)} \int_0^1 \frac{1}{B(\alpha+1, \beta)} y^{(\alpha+1)-1} (1-y)^{\beta-1} dy \\
 &= g(0) \frac{B(\alpha+1, \beta)}{B(\alpha, \beta)} \\
 &= g(0) \frac{\alpha}{\alpha + \beta}.
 \end{aligned}$$

b) For $x \neq 0$,

$$f_X(x) = \frac{1}{B(\alpha, \beta)} \int_0^1 g(x^2 y^2) y^\alpha (1-y)^{\beta-1} dy.$$

Furthermore, let

$$\begin{aligned}
 u = x^2 y^2 &\Rightarrow y^2 = \frac{u}{x^2} \Rightarrow y = \frac{u^{1/2}}{|x|} \\
 du &= 2x^2 y dy,
 \end{aligned}$$

so that

$$\begin{aligned}
 f_X(x) &= \frac{1}{2x^2 B(\alpha, \beta)} \int_0^{x^2} g(u) \left(\frac{u^{1/2}}{|x|} \right)^{\alpha-1} \left(1 - \frac{u^{1/2}}{|x|} \right)^{\beta-1} du \\
 &= \frac{1}{2B(\alpha, \beta) |x|^{\alpha+1}} \int_0^{x^2} g(u) u^{\frac{\alpha-1}{2}} \left(1 - \frac{u^{1/2}}{|x|} \right)^{\beta-1} du.
 \end{aligned}$$

Then,

$$f_X(x) = \begin{cases} \frac{1}{2B(\alpha, \beta) |x|^{\alpha+1}} \int_0^{x^2} g(u) u^{\frac{\alpha-1}{2}} \left(1 - \frac{u^{1/2}}{|x|} \right)^{\beta-1} du & \text{if } x \neq 0 \\ \frac{\alpha}{\alpha + \beta} g(0), & \text{if } x = 0, \end{cases}$$

concluding the proof. □

3.3. Some special cases

We now consider some special important cases that can be obtained from the general distribution of $X \sim ESE\ell(0, 1, \alpha, \beta; g)$ presented previously.

Example 1 (Slash-elliptical) If X is distributed according to the extended-slash distribution, then $\beta = 1$ (see Gómez et al., 2007). Hence, the pdf of X , can be shown to be given by

$$f_X(x) = \begin{cases} \frac{1}{2B(\alpha, 1)|x|^{\alpha+1}} \int_0^{x^2} g(u)u^{\frac{\alpha-1}{2}} du, & \text{if } x \neq 0 \\ \frac{\alpha}{\alpha+1}g(0), & \text{if } x = 0. \end{cases} \quad (9)$$

Example 2 (Extended-slash) If X is distributed according to the extended-slash (ES) distribution, then $g(u) = \frac{1}{\sqrt{2\pi}}e^{-u/2}$. Hence, the pdf of X can be shown to be given by

$$f_X(x) = \begin{cases} \frac{1}{2\sqrt{2\pi}B(\alpha, \beta)|x|^{\alpha+1}} \int_0^{x^2} e^{-u/2}u^{\frac{\alpha-1}{2}} \left(1 - \frac{u^{1/2}}{|x|}\right)^{\beta-1} du, & \text{if } x \neq 0 \\ \frac{\alpha}{\alpha+\beta}g(0), & \text{if } x = 0 \end{cases} \quad (10)$$

If $\beta = 1$, then one obtains the slash distribution (see Johnson et al., 1995)

Example 3 (Extended-slash-Student- t) If X is distributed according to the extended-slash distribution, then $g(u) = \frac{\Gamma(\frac{1+\nu}{2})}{\Gamma(\frac{\nu}{2})\sqrt{\pi\nu}}(1 + \frac{u}{\nu})^{-\frac{1+\nu}{2}}$. Hence, the pdf of X , is given by

$$f_X(x) = \begin{cases} \frac{\Gamma(\frac{1+\nu}{2})}{2\Gamma(\frac{\nu}{2})\sqrt{\pi\nu}B(\alpha, \beta)|x|^{\alpha+1}} \int_0^{x^2} (1 + \frac{u}{\nu})^{-\frac{1+\nu}{2}} u^{\frac{\alpha-1}{2}} \left(1 - \frac{u^{1/2}}{|x|}\right)^{\beta-1} du, & \text{if } x \neq 0 \\ \frac{\alpha}{\alpha+\beta}g(0), & \text{if } x = 0. \end{cases} \quad (11)$$

If $\beta = 1$, then one obtains the slash-Student- t distribution (see Gómez et al. 2007).

In the following we illustrate graphically the behaviour of the density function of the extended slash-elliptical distribution for α fixed and for the normal and Student- t (with 5 degrees of freedom) and density function generators, respectively.

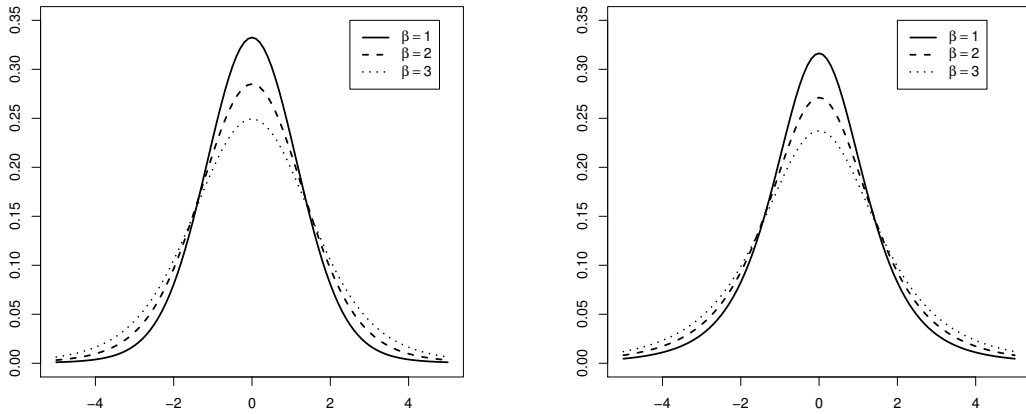


Figure 1: Density functions for the extended slash distributions with normal density generator (left) and Student-t density generator (right), for $\alpha = 5$ and several values of β .

3.4. Moments

Proposition 2 If $X \sim ESE\ell(0, 1, \alpha, \beta; g)$, the r -th moment of X is given by

$$E[X^r] = \frac{\Gamma(\alpha - r)\Gamma(\alpha + \beta)}{\Gamma(\alpha - r + \beta)\Gamma(\alpha)} a_{r/2}, \quad (12)$$

in which

$$a_{r/2} = \int_{-\infty}^{\infty} w^r g(w^2) dw. \quad (13)$$

Proof. From the stochastic representation, $X = \frac{W}{T}$, in which $W \sim E\ell(0, 1; g)$ and $T \sim \text{Beta}(\alpha, \beta)$ are independent random variables, we have

$$E[X^r] = E\left[\left(\frac{W}{T}\right)^r\right] = E[W^r]E[T^{-r}], \quad (14)$$

from which both expectations are known. \square

Corollary 1 Let $X \sim ESE\ell(0, 1, \alpha, \beta; g)$. Then, it follows that

$$E(X) = 0, \quad (15)$$

$$\text{Var}(X) = \frac{(\alpha + \beta - 1)(\alpha + \beta - 2)}{(\alpha - 1)(\alpha - 2)} a_1, \quad \text{for } \alpha > 2. \quad (16)$$

3.5. The location-scale extension

A random variable X following a location scale extended slash-elliptical distribution, which we denote by $X \sim ESE\ell(\mu, \sigma, \alpha, \beta; g)$, can be stochastically represented as

$$X = \sigma \frac{W}{T} + \mu \tag{17}$$

where $W \sim E\ell(0, 1; g)$ and $T \sim Beta(\alpha, \beta)$ are independent random variables, $\alpha > 0$, $\beta > 0$, $\mu \in \mathbb{R}$ and $\sigma > 0$. Some results for the location-scale are considered next. We start by presenting a general expression for the density function, which can be written as:

$$f_X(x) = \frac{1}{\sigma B(\alpha, \beta)} \int_0^1 g\left(\left(\left[\frac{x-\mu}{\sigma}\right]t\right)^2\right) t^\alpha (1-t)^{\beta-1} dt, \tag{18}$$

for $-\infty < x < \infty$.

Proposition 3 *If $X \sim ESE\ell(\mu, \sigma, \alpha, \beta; g)$ then, the r -th moment of X is given by*

$$E[X^r] = \sum_{c=1}^n \binom{r}{c} \sigma^c \mu^{r-c} \frac{\Gamma(\alpha - c)\Gamma(\alpha + \beta)}{\Gamma(\alpha - c + \beta)\Gamma(\alpha)} a_{c/2}, \tag{19}$$

in which

$$a_{c/2} = \int_{-\infty}^{\infty} w^c g(w^2) dw, \quad c = 1, 2, \dots \tag{20}$$

Proof. Notice that

$$\begin{aligned} E[X^r] &= E\left[\left(\sigma \frac{W}{T} + \mu\right)^r\right] \\ &= E\left[\sum_{c=0}^r \binom{r}{c} \left(\sigma \frac{W}{T}\right)^c \mu^{r-c}\right] \\ &= \sum_{c=0}^r \binom{r}{c} \sigma^c \mu^{r-c} E[W^c] E[T^{-c}]. \end{aligned}$$

Therefore,

$$E[X^r] = \sum_{c=0}^r \binom{r}{c} \sigma^c \mu^{r-c} \frac{\Gamma(\alpha - c)\Gamma(\alpha + \beta)}{\Gamma(\alpha - c + \beta)\Gamma(\alpha)} a_{c/2}$$

in which

$$a_{c/2} = \int_{-\infty}^{\infty} w^c g(w^2) dw, \quad c = 1, 2, \dots \quad \square$$

Corollary 2 Let $X \sim ESE\ell(0, 1, \alpha, \beta; g)$, then the kurtosis coefficient (γ_2) is given by:

$$\gamma_2 = \frac{E[(X - E(X))^4]}{(Var(X))^2} = \frac{(\alpha - 1)(\alpha - 2)(\alpha + \beta - 3)(\alpha + \beta - 4) a_2}{(\alpha - 3)(\alpha - 4)(\alpha + \beta - 1)(\alpha + \beta - 2) a_1^2}, \quad \alpha > 4. \quad (21)$$

The kurtosis coefficient depends on the parameters α and β and, moreover, on a_1 and a_2 . Tables 1 and 2 reveal that the values for the kurtosis are greater for the Student-t than for the normal distribution. Note also that for fixed β and α decreasing, the kurtosis coefficient increases, that is, the distance from the normal model gets more pronounced.

Table 1: Kurtosis coefficients for the extended slash-elliptical for $\beta = 1$ and $\alpha > 4$ for normal and Student-t generators.

Normal		Student-t				
$a_1 = 1, \quad a_2 = 3$		$a_1 = \frac{v}{v-2}, \quad a_2 = \frac{3v^2}{(v-4)(v-2)}$				
α	γ_2	α	$v = 5$	$v = 8$	$v = 20$	$v = 100$
5	5.4	5	16.2	8.1	6.075	5.5125
6	4.0	6	12	5.6	4.4999	4.0833
7	3.5714	7	10.7143	5.3571	4.0178	3.6458
8	3.375	8	10.125	5.0625	3.7968	3.4453
9	3.2627	9	9.8	4.9	3.675	3.3347
10	3.2	10	9.6	4.8	3.6	3.2667

Table 2: Kurtosis coefficients for the extended slash-elliptical for $\beta = 3$ and $\alpha > 4$ for normal and Student-t generators.

Normal		Student-t				
$a_1 = 1, \quad a_2 = 3$		$a_1 = \frac{v}{v-2}, \quad a_2 = \frac{3v^2}{(v-4)(v-2)}$				
α	γ_2	α	$v = 5$	$v = 8$	$v = 20$	$v = 100$
5	8.5714	5	25.7143	12.8571	9.6428	8.75
6	5.3571	6	16.0714	8.0357	6.0268	5.4687
7	4.3749	7	13.125	6.5624	4.9218	4.4661
8	3.92	8	11.76	5.88	4.41	4.0017
9	3.6654	9	10.9963	5.498	4.1236	3.7418
10	3.5064	10	10.5195	5.2597	3.9448	3.5795

3.6. Likelihood function

Consider a random sample of size n, X_1, \dots, X_n , from the distribution $ESE\ell(\mu, \sigma, \alpha, \beta; g)$. Then the log-likelihood function for $\boldsymbol{\theta} = (\mu, \sigma, \alpha, \beta)^\top$ can be expressed as

$$\ell(\boldsymbol{\theta}; \mathbf{x}) = -n \log(\sigma) - n \log B(\alpha, \beta) + \sum_{i=1}^n \log(k(x_i, \boldsymbol{\theta})) \tag{22}$$

where $k(x_i, \boldsymbol{\theta}) = \int_0^1 g\left(\left(\left[\frac{x_i - \mu}{\sigma}\right] t\right)^2\right) t^\alpha (1-t)^{\beta-1} dt$.

After differentiating the log-likelihood function, the likelihood equations are given by

$$\frac{\partial \ell(\boldsymbol{\theta}; \mathbf{x})}{\partial \mu} = \sum_{i=1}^n \frac{1}{k(x_i, \boldsymbol{\theta})} k_1(x_i, \boldsymbol{\theta}) = 0, \tag{23}$$

$$\frac{\partial \ell(\boldsymbol{\theta}; \mathbf{x})}{\partial \sigma} = -\frac{n}{\sigma} + \sum_{i=1}^n \frac{1}{k(x_i, \boldsymbol{\theta})} k_2(x_i, \boldsymbol{\theta}) = 0, \tag{24}$$

$$\frac{\partial \ell(\boldsymbol{\theta}; \mathbf{x})}{\partial \alpha} = -n\{\psi(\alpha) - \psi(\alpha + \beta)\} + \sum_{i=1}^n \frac{1}{k(x_i, \boldsymbol{\theta})} k_3(x_i, \boldsymbol{\theta}) = 0, \tag{25}$$

$$\frac{\partial \ell(\boldsymbol{\theta}; \mathbf{x})}{\partial \beta} = -n\{\psi(\beta) - \psi(\alpha + \beta)\} + \sum_{i=1}^n \frac{1}{k(x_i, \boldsymbol{\theta})} k_4(x_i, \boldsymbol{\theta}) = 0. \tag{26}$$

where

$$k_1(x_i, \boldsymbol{\theta}) = \int_0^1 -\frac{2}{\sigma} \left(\frac{x_i - \mu}{\sigma}\right) t^2 g' \left(\left(\left[\frac{x_i - \mu}{\sigma}\right] t\right)^2\right) t^\alpha (1-t)^{\beta-1} dt,$$

$$k_2(x_i, \boldsymbol{\theta}) = \int_0^1 -\frac{2}{\sigma} \left(\frac{x_i - \mu}{\sigma}\right)^2 t^2 g' \left(\left(\left[\frac{x_i - \mu}{\sigma}\right] t\right)^2\right) t^\alpha (1-t)^{\beta-1} dt,$$

$$k_3(x_i, \boldsymbol{\theta}) = \int_0^1 g \left(\left(\left[\frac{x_i - \mu}{\sigma}\right] t\right)^2\right) \log(t) t^\alpha (1-t)^{\beta-1} dt,$$

$$k_4(x_i, \boldsymbol{\theta}) = \int_0^1 g \left(\left(\left[\frac{x_i - \mu}{\sigma}\right] t\right)^2\right) \log(1-t) t^\alpha (1-t)^{\beta-1} dt.$$

and $\psi(z) = \frac{\Gamma'(z)}{\Gamma(z)}$ is the digamma function. Maximum likelihood estimators (MLEs) are obtained by maximizing the above equations. No analytical solution is available for the above equations, so that iterative procedures are required.

3.7. Simulation study

As described next, a simple algorithm can be formulated to generate random deviates from the ES distribution.

- (i) Simulate $W \sim N(0, 1)$
- (ii) Simulate $T \sim \text{Beta}(\alpha, \beta)$
- (iii) Compute $X = \sigma \frac{W}{T} + \mu$

Table 3 shows results of simulations studies, illustrating the behaviour of the MLEs for 5000 generated samples of sizes $n = 50, 100, 150$ and 200 from distribution $ES(\mu, \sigma, \alpha, \beta)$. For each generated sample, MLEs were computed numerically using a Newton-Raphson procedure. Means and standard deviations (SD) are reported. Note that in general, as sample size increases, estimates get close to the parameter values and the empirical standard deviation (SD) gets small, as expected. Therefore, large sample properties of the maximum likelihood estimates seem to hold for moderate sample sizes.

Table 3: Empirical means and SD for the MLE estimators of μ, σ, α and β .

$n = 50$							
μ	σ	α	β	$\hat{\mu}$ (SD)	$\hat{\sigma}$ (SD)	$\hat{\alpha}$ (SD)	$\hat{\beta}$ (SD)
0	1	1	2	0.2374 (0.5218)	1.0090 (0.2029)	1.2248 (0.3946)	2.8790 (1.4356)
0	1	1	5	0.4503 (0.9686)	1.0404 (0.1904)	1.1204 (0.3333)	6.3611 (3.2877)
2	10	1	1	3.1886 (3.1744)	10.5595 (1.6844)	1.3382 (0.4474)	1.6140 (0.8279)
$n = 100$							
μ	σ	α	β	$\hat{\mu}$ (SD)	$\hat{\sigma}$ (SD)	$\hat{\alpha}$ (SD)	$\hat{\beta}$ (SD)
0	1	1	2	0.0374 (0.3259)	1.1333 (0.1613)	1.1930 (0.2213)	2.1900 (0.7484)
0	1	1	5	0.2426 (0.6733)	1.0378 (0.1297)	1.0706 (0.1768)	5.4931 (1.6113)
2	10	1	1	2.1469 (2.4254)	10.1862 (1.2163)	1.0567 (0.2685)	1.1124 (0.4572)
$n = 150$							
μ	σ	α	β	$\hat{\mu}$ (SD)	$\hat{\sigma}$ (SD)	$\hat{\alpha}$ (SD)	$\hat{\beta}$ (SD)
0	1	1	2	0.0234 (0.2742)	1.0393 (0.1090)	1.0441 (0.1753)	2.1387 (0.5938)
0	1	1	5	0.2338 (0.5569)	1.1015 (0.1158)	1.0675 (0.1611)	5.4171 (1.3794)
2	10	1	1	2.0511 (1.6831)	10.0914 (1.0147)	1.0494 (0.1911)	1.0735 (0.3131)
$n = 200$							
μ	σ	α	β	$\hat{\mu}$ (SD)	$\hat{\sigma}$ (SD)	$\hat{\alpha}$ (SD)	$\hat{\beta}$ (SD)
0	1	1	2	0.0023 (0.2376)	1.0366 (0.0946)	1.0389 (0.1433)	2.0983 (0.4803)
0	1	1	5	0.2307 (0.4547)	0.9951 (0.0980)	1.0267 (0.1427)	5.0110 (1.1707)
2	10	1	1	1.9983 (1.4606)	9.9764 (0.8570)	1.0262 (0.1583)	1.0382 (0.2585)

4. Numerical illustration

In the following, we present a real data application using the likelihood approach developed in the previous section. Since a numerical iterative approach is required to achieve the MLE for the $ESE\ell$, we used the function `optim` available in the R system. The specific method is the `L-BFGS-B` developed by Byrd et al. (1995) which allows “box constraint”, that is, each variable can be given a lower and/or upper bound. This uses a limited-memory modification of the quasi-Newton method. Large sample variance estimates can be computed by inverting the Hessian matrix, which can also be computed numerically using R.

The data set considered is from an entomological experiment with a total of 730 ants. The ants were initially at the center of a box covered with sand and they moved toward a visual stimulus located at an angle of 180° degrees from the center of the box rounded to the nearest 10° . The data set was initially analysed in Jander (1957), and further analysed in Batschelet (1981), SenGupta and Pal (2001), Jones and Pewsey (2004) and Gómez et al. (2007).

Table 4 reveals descriptive statistics indicating the data set presents greater kurtosis than a data set typically coming from a normal distribution. Table 5 presents maximum likelihood estimates and corresponding standard deviations for normal (N), slash (S) and extended slash (ES) models. Using the Akaike information criterion (AIC) (see Akaike, 1974), it can be noticed that the extended slash (ES) model presents the smallest AIC. More strong evidence in favour the ES model is provided by the likelihood ratio statistics. Figure 2 (left side) depicts the histogram and graphical representation for estimated normal, slash and extended slash models for the ant data set. As revealed by the plots, the best fit seems the one corresponding to the ES model. Figure 2 (right side) shows the log-likelihood profile for parameter beta. Notice that the MLE is unique for the ant data.

Table 4: Summary statistics for ant data set.

Mean	Standard deviation	Asymmetry	Kurtosis
176.4384	62.64341	-0.2049024	4.575356

Table 5: Parameter estimates for normal, slash and extended slash distributions.

Parameter estimates	N(SD)	S(SD)	ES(SD)
$\hat{\mu}$	176.438 (2.316)	181.425 (1.268)	181.321 (0.094)
$\hat{\sigma}$	62.600 (1.638)	16.804 (1.246)	1.336 (0.108)
\hat{q}	—	1.171 (0.085)	—
$\hat{\alpha}$	—	—	1.907 (0.094)
$\hat{\beta}$	—	—	40.084 (4.719)
Log-likelihood	-4055.670	-3972.111	-3953.321
AIC	8115.339	7950.222	7914.642

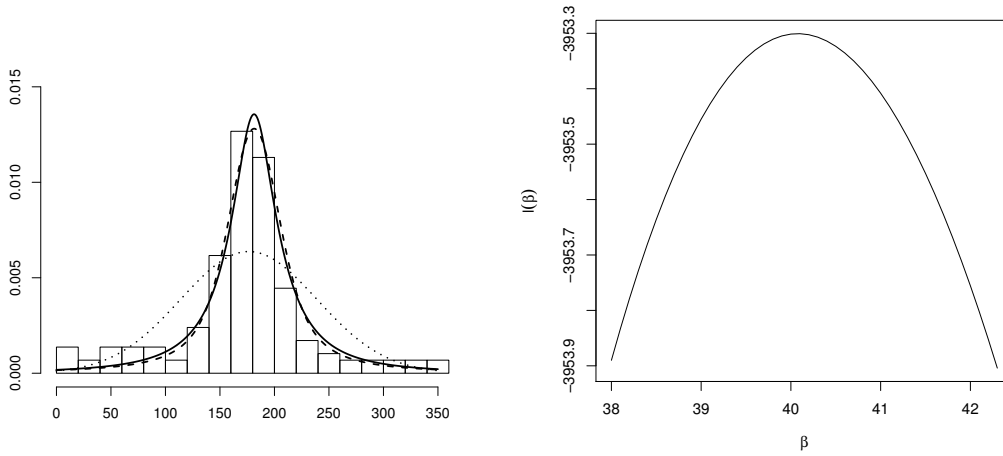


Figure 2: Models fitted by the maximum likelihood approach for the ant direction data set: ES (solid line), S (dashed line) and N (dotted line) (left), the log-likelihood function profile of β for the ant data set (right).

5. Multivariate case

In this section, we introduce a multivariate extended slash-elliptical model and derive some additional results concerning this extension.

The random vector $\mathbf{Y} \in \mathbb{R}^p$ follows a multivariate extended slash-elliptical distribution with location parameter $\boldsymbol{\mu}$, scale parameter matrix $\boldsymbol{\Sigma}$ (positive definite) and shape parameters $\alpha > 0$ and $\beta > 0$, which we denote by $\mathbf{Y} \sim ESEl_p(\boldsymbol{\mu}, \boldsymbol{\Sigma}, \alpha, \beta; g^{(p)})$, if

$$\mathbf{Y} = \boldsymbol{\Sigma}^{1/2} \frac{\mathbf{X}}{U} + \boldsymbol{\mu}, \quad (27)$$

where $\mathbf{X} \sim El_p(\mathbf{0}, \mathbf{I}_p; g^{(p)})$ is independent of $U \sim Beta(\alpha, \beta)$.

Proposition 4 Let $\mathbf{Y} \sim ESEl_p(\boldsymbol{\mu}, \boldsymbol{\Sigma}, \alpha, \beta; g^{(p)})$. Then, the density of \mathbf{Y} is given by

$$h(\mathbf{y}; \boldsymbol{\mu}, \boldsymbol{\Sigma}, \alpha, \beta) = \begin{cases} \frac{\boldsymbol{\Sigma}^{-1/2}}{2B(\alpha, \beta)\gamma^{(\alpha+p)/2}} \int_0^\gamma t^{\frac{\alpha+p-2}{2}} \left(1 - \frac{t^{1/2}}{\gamma^{1/2}}\right)^{\beta-1} g^{(p)}(t) dt & \mathbf{y} \neq \boldsymbol{\mu} \\ \frac{B(\alpha+p, \beta)}{B(\alpha, \beta)} \boldsymbol{\Sigma}^{-1/2} g^{(p)}(0) & \mathbf{y} = \boldsymbol{\mu} \end{cases} \quad (28)$$

where $\gamma = \|\boldsymbol{\Sigma}^{-1/2}(\mathbf{y} - \boldsymbol{\mu})\|^2 = (\mathbf{y} - \boldsymbol{\mu})^\top \boldsymbol{\Sigma}^{-1}(\mathbf{y} - \boldsymbol{\mu})$.

Proof. Using the stochastic representation given in (27), the density function associated with \mathbf{Y} is given by

$$\begin{aligned} h(\mathbf{y}; \boldsymbol{\mu}, \boldsymbol{\Sigma}, \alpha, \beta) &= \int_0^1 u^{\alpha+p-1} f_p(u\mathbf{y}; u\boldsymbol{\mu}, \boldsymbol{\Sigma}) \frac{1}{B(\alpha, \beta)} (1-u)^{\beta-1} du \\ &= \frac{1}{B(\alpha, \beta)} \int_0^1 u^{\alpha+p-1} (1-u)^{\beta-1} \frac{-1/2}{\boldsymbol{\Sigma}} g^{(p)}(\gamma u^2) du. \end{aligned}$$

If $\mathbf{y} = \boldsymbol{\mu}$ then the result follows straightforwardly. On the other hand, if $\mathbf{y} \neq \boldsymbol{\mu}$, after the variable change $t = (\mathbf{y} - \boldsymbol{\mu})^T \boldsymbol{\Sigma}^{-1} (\mathbf{y} - \boldsymbol{\mu}) u^2$, the result follows. \square

Example 4 Considering $g^{(p)}(t) = \frac{1}{(2\pi)^{p/2}} e^{-t/2}$ as the generator function for the multivariate normal model and then using (28), we obtain an extension of the multivariate slash distribution introduced in Wang and Genton (2006).

Proposition 5 *Moreover, if $\mathbf{Y} \sim ESEL_p(\boldsymbol{\mu}, \boldsymbol{\Sigma}, \alpha, \beta; g^{(p)})$, then we have that*

$$E(\mathbf{Y}) = \boldsymbol{\mu} \text{ and } Var(\mathbf{Y}) = \frac{(\alpha + \beta - 1)(\alpha + \beta - 2)}{(\alpha - 1)(\alpha - 2)} \alpha_g \boldsymbol{\Sigma}, \alpha > 2 \tag{29}$$

6. Concluding remarks

This paper introduced an extension of the slash-elliptical distribution considered in Gómez et al. (2007). The distribution is called the extended slash-elliptical distribution. This new distribution is generated as the quotient between two independent random variables, one of them from the elliptical family (numerator) and the other (denominator) a beta distribution with parameters α and β . The resulting slash-elliptical distribution potentially has a larger kurtosis coefficient than the slash-elliptical distribution. We investigated properties of this distribution such as moments and closed expressions for the density function. We also derived likelihood equations for the location-scale version, placing emphasis on the special cases of the generalized slash-normal and generalized slash-Student-t models. The results of a real data application reveal that the proposed model can fit real data well, making it a viable alternative to replace models with lesser kurtosis flexibility. We also proposed a multivariate extension.

Acknowledgments

We thank two referees for comments and suggestions that substantially improved the presentation. The research of H. Bolfarine was supported by CNPq-Brasil. The research of H. W. Gómez was supported by FONDECYT-Chile 1130495.

References

- Akaike (1974). A new look at the statistical model identification. *IEEE Transactions on Automatic Control*, 19(6), 716–723.
- Arellano-Valle, R. B., Bolfarine, H. and Vilca-Labra, F. (1996). Elliptical ultrastructural models. *Canadian Journal of Statistics*, 24(2), 207–216.
- Arslan, O. (2008). An alternative multivariate skew-slash distribution. *Statistics and Probability Letters*, 78(16), 2756–2761.
- Arslan, O. and Genc, A. I. (2009). A generalization of the multivariate slash distribution. *Journal of Statistical Planning and Inference*, 139(3), 1164–1170.
- Batschelet, E. (1981). *Circular Statistics in Biology*. London: Academic Press.
- Byrd, R. H., Lu, P., Nocedal, J. and Zhu, C. (1995). A limited memory algorithm for bound constrained optimization. *SIAM Journal on Scientific Computing*, 16(5), 1190–1208.
- Fang, K. T., Kotz, S. and Ng, K. W. (1990). *Symmetric Multivariate and Related Distributions*. London-New York: Chapman and Hall.
- Genc, A. I. (2007). A generalization of the univariate slash by a scale-mixture exponential power distribution. *Communications in Statistics-Simulation and Computation*, 36(5), 937–947.
- Genc, A. I. (2013). A skew extension of the slash distribution via beta-normal distribution. *Statistical Papers*, 54(2), 427–442.
- Gómez, H. W., Olivares-Pacheco, J. F. and Bolfarine, H. (2009). An extension of the generalized Birnbaum-Saunders distribution. *Statistics and Probability Letters*, 79(3), 331–338.
- Gómez, H. W., Quintana, F. A. and Torres, F. J. (2007). New family of slash-distributions with elliptical contours. *Statistics and Probability Letters*, 77(7), 717–725.
- Gómez, H. W. and Venegas, O. (2008). Erratum to: a new family of slash-distributions with elliptical contours. *Statistics and Probability Letters*, 78(14), 2273–2274.
- Jander, R. (1957). Die optische richtungsorientierung der roten waldameise (*Formica rufa* L.). *Zeitschrift für Vergleichende Physiologie*, 40, 162–238.
- Jones, M. C. and Pewsey, A. (2004). A family of symmetric distributions on the circle. *Technical Report*, The Open University, Department of Statistics.
- Johnson, N. L., Kotz, S. and Balakrishnan, N. (1995). *Continuous Univariate Distributions*, vol. 1, 2nd ed. New York: Wiley.
- Kafadar, K. (1982). A biweight approach to the one-sample problem. *Journal of the American Statistical Association*, 77, 416–424.
- Mosteller, F. and Tukey, J. W. (1977). *Data Analysis and Regression*. Addison-Wesley, Reading, MA.
- Rogers, W. H. and Tukey, J. W. (1972). Understanding some long-tailed symmetrical distributions. *Statistica Neerlandica*, 26, 211–226.
- SenGupta, A. and Pal, C. (2001). On optimal tests for isotropy against the symmetric wrapped stable-circular uniform mixture family. *Journal of Applied Statistical*, 28, 129–143.

New approaches in the chemometric analysis of infrared spectra of extra-virgin olive oils

María Isabel Sánchez-Rodríguez^{1,*}, Elena M. Sánchez-López²,
Alberto Marinas², José M^a Caridad¹, Francisco José Urbano²
and José M^a Marinas²

Abstract

The aim of this paper is to apply new chemometric approaches to obtain quantitative information from near and mid infrared spectra of Andalusian extra-virgin olive oils, using gas chromatography as a classical reference analytical technique. Estimations of the content in saturated, monounsaturated and polyunsaturated fatty acids are given using partial least squares regression from the near and mid infrared data matrices as well as their concatenated matrix. The different estimations are evaluated in terms of goodness of fit (calibration) and prediction (validation), as a function of the number of partial least squares factors in the regression model and the used matrix of data. Furthermore, the nature, systematic or random, of the prediction errors is studied by a decomposition of their mean squared error. Finally, procedures of cross-validation are implemented in order to generalize the previous results.

MSC: 62H25, 62J05, 62Q99.

Keywords: Extra-virgin olive oil, infrared spectroscopy, partial least squares regression, cross-validation.

1. Introduction

Extra-virgin olive oil is an edible oil very much appreciated by its taste and benefits for health. Mediterranean countries (Spain, Italy, Greece, Turkey, Tunisia and Morocco) and Portugal cover 90% of the world production, Spain and Italy being the major producers and consumers. In Spain, Andalusia produces 80% of the national product.

* Corresponding author e-mail: td1sarom@uco.es

¹ Dep. Estadística, Econometría, I.O., Org. Empresas y Ec. Aplicada. University of Córdoba

² Dep. Química Orgánica. University of Córdoba

Received: September 2013

Accepted: June 2014

The composition of olive oil depends on the type and the distribution of the fatty acids present in the triglycerides and on the positions in which these fatty acids are esterified to hydroxyl groups in glycerol backbone. The principal fatty acids of vegetable oils are oleic, linoleic, linolenic, myristic, palmitic and stearic. The last three types are classified as saturated (SAFA), the oleic is monounsaturated (MUFA) and the linoleic and linolenic acids are polyunsaturated (PUFA).

Extra-virgin oil is by definition obtained only from the olive, using solely mechanical or other physical means, in conditions, particularly thermal conditions, which do not alter the oil in any way. It presents a high price of commercialization, which makes it susceptible to adulteration with other cheaper oils, such as hazelnut, sunflower, soybean, maize or refined olive oils (see, for example, Baeten et al. (2005), Gurdeniz and Ozen (2009) and Öztürk et al. (2010)), considerably modifying its quality indices. This makes it necessary to provide fast, reliable and cost-effective analytical procedures which require no or little sample manipulation. In this sense, for several years we have elaborated an extra-virgin olive oils database using diverse spectroscopic techniques such as near and mid infrared (NIR and MIR, respectively). IR techniques provide continuous information (spectra) that is rich in both isolated and overlapping bands and not so obvious to analyse as in the case of gas chromatography (GC). Nevertheless, the application of multivariate statistics to the above-mentioned spectra allows to obtain quantitative information (as the content of oil in diverse compounds) or qualitative (as the geographical origin or the protected designation of origin, PDO) about the olive oil.

There are in the literature diverse examples of application of NIR, MIR or concatenated NIR-MIR spectroscopic techniques to the quantitative and qualitative analysis of olive oils. Thus, for example, Bertran et al. (2000) and Galtier et al. (2007, 2011) classify several olive oils according to different geographical zones and determine the composition in fatty acids and triacylglycerols by using NIR spectra. Baeten et al. (2005) and Gurdeniz and Ozen (2009) study the possible adulteration of olive oils with lower quality oils (such as hazelnut, sunflower or maize) by MIR spectroscopy. Dupuy et al. (2010a, 2010b) and Sinelli et al. (2008) use NIR, MIR and concatenated NIR-MIR spectra to develop quantitative and qualitative studies of olive oil. Sinelli et al. (2010) apply NIR and MIR spectroscopies as a rapid tool to classify extra virgin olive oil on the basis of fruity attribute intensity. Casale et al. (2012) use NIR and MIR spectroscopical data, individually and jointly, to characterize olive oils from an Italian protected designation of origin.

Some of these works determine, using correlation, specially significant IR spectral bands to fit regression models to predict some components of olive oil (see Guillén and Cabo (1997) or Zhang et al. (2012)). Other works, such as Maggio et al. (2011), use partial least squares (PLS) regression to avoid the presence of multicollinearity in the model. PLS regression summarizes the information of a spectral band in some components or latent factors being orthogonal among them and so avoiding multicollinearity, incompatible with the hypothesis of uncorrelation in the general linear model. Other authors, such as Casale et al. (2012) or Dupuy et al. (2010a, 2010b), extract the PLS

components from the complete NIR, MIR or concatenated NIR-MIR spectra, not from the previously selected spectral bands.

The aims of this paper are to revisit the procedures used in the literature to obtain quantitative information of olive oil from the near and mid zones of the infrared spectra and propose new approaches. The goal is to determine the profile in SAFA, MUFA and PUFA fatty acids of diverse extra-virgin olive oils by using the information provided by the NIR, MIR and concatenated NIR-MIR matrices of data, using the values obtained from GC as a reference. The estimations are provided by partial least squares regression models and are compared in terms of goodness of fit (calibration) and prediction (validation), that is, measuring errors that correspond to data used or not used to train the regression model. In addition, a decomposition of the mean squared error of prediction is provided to evaluate the character, systematic or random, of prediction errors (see Sánchez-Rodríguez et al. (2013)). The obtained results are generalized using procedures of cross-validation, based on the design of repetitive algorithms that, for each iteration, modify the partition of the available data set in subsets of calibration and validation. Finally, three-dimensional scatterplots give a global vision for the three types of fatty acids and matrices of data, simultaneously.

The computer programs commonly used in Chemometrics have internally implemented a stopping criterion to determine the number of PLS latent factors to retain in the regression model. But, in this work, the PLS factors are progressively introduced in the model, with the aim of determining the evolution of calibration and validation errors as a function of the number of factors and the estimated fatty acid type. The chemometric software has also cross-validation procedures implemented that change, at each iteration, the learning and the test data sets, and provide a global mean of the calibration and validation errors. On the contrary, in the present work, the procedures of cross-validation have been programmed and show the results corresponding to each iteration. Therefore, the evolution and the variability of the fit and prediction errors can be studied for the successive iterations.

2. Acquisition of data

The studied samples include 128 Andalusian extra-virgin olive oils, collected for four consecutive seasons (from 2007 to 2011) with a ripeness index of 3. The varieties studied are, mainly, 'Arbequina', 'Hojiblanca', 'Picual', 'Lechín', 'Manzanilla', 'Picudo' and 'Royal'. Olive oil was extracted by the producers through a two-phase centrifugation system. The data for the subsequent statistical treatment have been provided by the following analytical chemical procedures:

- **Gas chromatography.** Classical separation technique that leads to discrete information including several usually well-defined, separated peaks from which, on proper integration, the content of various chemical components (for example,

SAFA, MUFA and PUFA fatty acids) can be determined. It will be considered as reference technique in the next studies.

- **Spectroscopical techniques.** Infrared techniques, such as NIR and MIR, generate continuous information, rich in both isolated and overlapping bands attributed to vibration of chemical bonds in different molecules. The use of mathematical and statistical procedures allows us to extract the maximum useful information from data (Berrueta et al. (2007)).

2.1. Gas Chromatography (GC)

The determinations of fatty acid composition by GC-FID, according to the official methods for olive and pomace oil control in the European Union, EU (2011) and the International Olive Council, COI (2001a, 2001b), were performed by the staff of Organic Chemistry of University of Córdoba, using an Agilent 7890A gas chromatograph with a capillary column (SGE FORTE BPX-70 de 50 m × 220 μm × 0.25 μm). The conditions of analysis were as follows: 250 °C of injector temperature, 2 μL of injection volume, 260 °C of detector temperature. The oven temperature was programmed to remain at 180 °C for 15 min and then raised to 240 °C at a rate of 4 °C/min and maintained at this temperature for 5 min.

The triacylglycerol samples (olive oil samples), were initially submitted to a cold transesterification procedure to convert the triacylglycerol into fatty acid methyl esters. This method is indicated for edible oils with acidity index lower than 3.3°. In this process, 0.1 g of olive oil are transferred into a 5 mL volumetric flask. Next, 2 mL *n*-heptane and 0,2 mL of a 2N KOH solution in methanol were added and reaction mixture was vigorously stirred. Finally, the methyl esters were extracted and subject to GC analyses.

2.2. NIR and MIR spectra

NIR and MIR spectra were obtained by the staff of the Organic Chemistry Department of the University of Córdoba within 15 days after reception of the samples which were kept in the fridge so that properties were not modified [Baeten et al. (2003)]. The instruments employed for spectra collection were available at the Central Service of Analyses (SCAI) at the University of Córdoba.

As for NIR instrument, it consisted in a Spectrum One NTS FT-NIR spectrophotometer (Perkin Elmer LLC, Shelton, USA) equipped with an integrating sphere module. Samples were analyzed by transreflectance by using a glass petri dish and a hexagonal reflector with a total transreflectance pathlength of approximately 0.5 mm. A diffuse reflecting stainless steel surface placed at the bottom of the cup reflected the radiation back through the sample to the reflectance detector. The spectra were collected by us-

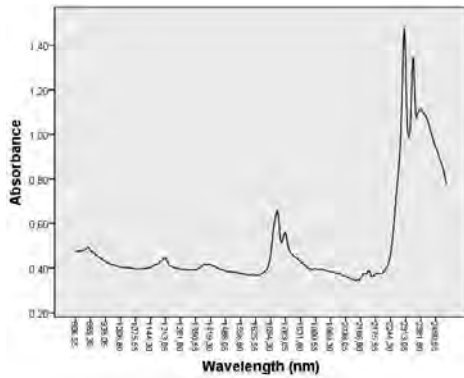


Figure 1: NIR spectrum of an extra-virgin olive oil.

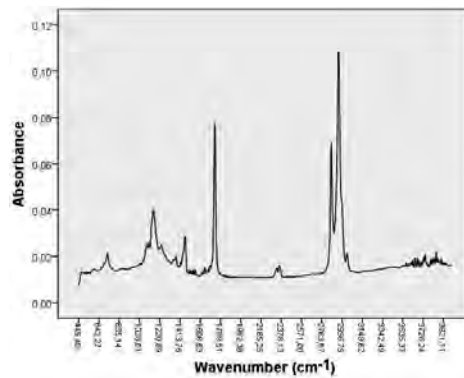


Figure 2: MIR spectrum of an extra-virgin olive oil.

ing Spectrum Software 5.0.1 (Perkin Elmer LLC, Shelton, USA). The reflectance ($\log 1/R$) spectra were collected with two different reflectors. Data correspond to the average of results with both reflectors, thus ruling out the influence of them on variability of the obtained results. Moreover, spectra were subsequently smoothed using the Savitzky-Golay technique, which performs a local polynomial least squares regression in order to reduce the random noise of the instrumental signal. Once pre-treated, NIR data of 1237 measurements for each case (representing energy absorbed by olive oil sample at 1237 different wavelengths, from 800.62 to 2499.64 nm) were supplied to the Department of Statistics (University of Córdoba) in order to be analysed.

Regarding MIR spectra of olive oil samples, they contain both well-resolved ($3100\text{--}1721\text{ cm}^{-1}$) and overlapping peaks ($1500\text{--}700\text{ cm}^{-1}$). Spectra were registered at room temperature in the $600\text{ to }4000\text{ cm}^{-1}$ range on a Tensor 27 FTIR Spectrometer (Bruker Optics, Milano, Italy) coupled to an ATR (Attenuated total reflectance) device consisting in several reflection crystals (ZnSe). Software used was OPUS r. 5,0 (Bruker Optics), the resolution 2 cm^{-1} and 50 scan per sample. The number of measurements for each case was 1843, which were supplied to the Department of Statistics (University of Córdoba) for analysis.

3. Multivariate data analysis

3.1. Selection criteria of regression models

The purpose of this work is to use statistical regression models to determine the profile in fatty acids SAFA, MUFA and PUFA of extra-virgin olive oils obtained by gas chromatography (classical technique used as reference) from the information provided by the IR spectroscopy technique. The regression models are evaluated in terms of goodness-of-fit and predictive capability, using the following measures.

Let y_1, y_2, \dots, y_n be the observations of a dependent variable, Y , and the corresponding predictions, $\hat{y}_1, \hat{y}_2, \dots, \hat{y}_n$, of a regression model. The *mean squared error of calibration*, $\text{MSEC} = \sum_{i=1}^n (y_i - \hat{y}_i)^2 / n$, takes values nearer to 0 for a good fit (calibration). But MSEC is not dimensionless, that is, it depends on the units of measurement of the variable, hence it is useful. It is useful in comparisons of models with variables measured in the same units but not as an absolute goodness of fit measure.

Given the predictions for the future t observations, $\hat{y}_{n+1}, \hat{y}_{n+2}, \dots, \hat{y}_{n+t}$, of a certain regression model, the *mean squared error of the prediction*, $\text{MSEP} = \sum_{j=1}^t (y_{n+j} - \hat{y}_{n+j})^2 / t$, evaluates the predictive capability (validation) of a regression model. The predictive capability of a model is obviously better as MSEP approaches 0, taking into account that MSEC has no upper bound and depends on the measurement units.

As indicated by Berrueta et al. (2007), the ideal situation in the evaluation of the predictive capability of a model is when there are enough data available to create separate test sets completely independent from the model building process (this validation procedure is known as *external validation*). When an independent test set is not available (e.g. because cost or time constraints make it difficult to increase the sample size), MSEP has to be estimated from the data used to train the regression. For this reason, as validation set, part of the original data set is used, avoiding the bias associated to the fact that the same data are used to the fit of the regression model and the evaluation of the predictions). The *cross-validation* procedures are designed to modify the selections repeatedly, using an algorithm that, for each iteration, changes the partition of the original data set into calibration and validation sets.

Besides, in line with the approach introduced by Fisher around 1920 relative to analysis of variance, Sánchez-Rodríguez et al. (2013) described new insights into evaluation of regression models through a decomposition of MSEP to analyse more in depth the causes of the prediction errors. Let \bar{y} and $\bar{\hat{y}}$ be the means of the t future observations and their predictions, s_Y and $s_{\hat{Y}}$ are the corresponding standard deviations and $s_{Y\hat{Y}}$ represents the covariance. Therefore, MSEP can be expressed as

$$\text{MSEP} = \frac{1}{t} \sum_{j=1}^t (y_{n+j} - \hat{y}_{n+j})^2 = (\bar{y} - \bar{\hat{y}})^2 + (s_Y - s_{\hat{Y}})^2 + 2(s_Y s_{\hat{Y}} - s_{Y\hat{Y}}) = E_B + E_V + E_R,$$

or, equivalently, with the identity

$$1 = \frac{E_B}{\text{MSEP}} + \frac{E_V}{\text{MSEP}} + \frac{E_R}{\text{MSEP}} = U_B + U_V + U_R,$$

where U_B is the part of MSEP corresponding to the bias due to the systematic prediction errors; U_V indicates the difference between the variability of the real values and the variability of the predicted values; finally, U_R shows the random variability in the prediction errors.

A model is obviously better as MSEP approaches 0 (taking into account that MSEP is not upper bounded and depends on the unit of measurement). But, using the proposed decomposition, if MSEP shows a great percentage attributable to systematic errors, this aspect indicates that there is some detectable cause causing these deviations in the predictions. This cause must be detected in order to eliminate systematic errors. Thus, a great percentage of MSEP attributable to systematic prediction errors indicates that the model can be improved in some sense. Nevertheless, this improvement is difficult if the predictions generated by a model have a random nature because random errors, with a white noise appearance, are usually inherent to a process.

Definitively, the ideal situation for evaluating the predictive capability of a model is presented when MSEP has a value as close as possible to 0 and besides $U_B = 0$, that is, systematic errors do not exist in the prediction; $U_V = 0$, which indicates that the variability of the real values is the same as that of the predictions; and $U_R = 1$, which corresponds to prediction errors with random nature.

3.2. New methodological approaches in the chemometric analysis of IR spectra

Now, the procedures used in the literature to extract information of olive oil from IR spectra (NIR, MIR and concatenated NIR-MIR) are revised. The different contributions to each technique are conveniently motivated and justified.

- 1. Extraction of the information from the complete IR spectra versus the analysis of some particular IR bands.** There are in the literature many references in which the analysis of IR spectra is made based on the detection of highly informative bands. One such example is the work by Guillén and Cabo (1997), who relate IR spectral bands of edible oils with some chemical functional groups. This approach is based on the *Lambert-Beer Law*, which states that the intensities of the spectral bands are proportional to the concentration of their respective functional groups. The frequencies of some bands, fundamentally the ones associated to the so-called *fingerprint region*¹, are highly correlated to the composition of olive oil. Guillén and Cabo (1997) successfully obtained regression equations to predict the content in SAFA, MUFA and PUFA fatty acids of olive oil from the frequencies of some bands in the fingerprint region (see Table 1). A follow-up study (Guillén and Cabo, 1998) generalized the previous results by regression models that provide relationships between the composition in SAFA, MUFA and PUFA of edible oils and the ratio of absorbance of specific bands of the IR spectra, not necessarily

1. The region $1500\text{-}700\text{ cm}^{-1}$ of the MIR spectra is named *fingerprint region* because this region is highly characteristic of a specific compound. Little changes in the molecular structure frequently cause significant changes in the absorption peaks of this region.

associated to the fingerprint region. Besides, Guillén and Cabo (1999) used the previous regression equations to determine the composition of mixtures of olive oil and other low quality oils (such as sunflower or peanut), using gas chromatography values as references.

There are other works which analyse IR spectra by determining relevant frequency bands. Vlachos et al. (2006) establish the relation between the frequency 3009 cm^{-1} of the IR spectra and the percentage of adulteration of olive oil with low quality oils. Rohman and Man (2010) use PCA and PLS components extracted from the fingerprint region $1500\text{-}1000\text{ cm}^{-1}$ (MIR spectra) to quantitatively and qualitatively analyse extra-virgin olive oils, to detect possible adulteration with palm oil. Nicoletta et al. (2010) select some regions from NIR and MIR spectra to classify, by discriminant analysis, diverse extra-virgin olive oils based on their fruity attribute intensity. Zhang et al. (2012) divide the IR spectra in regions, attending to the absorbance peaks, to establish linear regression equations to detect possible adulteration of vegetables oils with used frying oils.

All the previously cited works determine, by using correlation, highly informative IR spectral regions to predict the composition of olive oil. In general, the determined zones are localized in the mid infrared spectral region (MIR), where the spectral fingerprint is localized.

Our previous study (Sanchez-Rodriguez et al., 2013), from NIR spectral data, compares the estimation results obtained by extracting information from the whole spectra with those provided by some specific NIR bands (either determined by cluster analysis or associated to certain spectral peaks). The best calibration and validation results are obtained from the whole spectra. This is the reason why the present work uses the whole NIR, MIR and concatenated NIR-MIR spectra to

Table 1: Coefficients for IR equations, $\text{Frequency} = a + b\%M$ (%P o %S), and linear correlation coefficients^a (Guillén and Cabo, 1997).

Percentage	<i>a</i>	<i>b</i> (10^{-2})	<i>r</i>
<i>M</i>	3010.40	-7.24	0.9853
<i>P</i>	3004.85	+6.10	0.9492
<i>M</i>	1394.90	+9.90	0.9910
<i>P</i>	1402.61	-8.43	0.9223
<i>M</i>	1100.46	-4.87	0.9908
<i>P</i>	1096.68	+4.43	0.9176
<i>S</i>	2926.04	-6.28	0.8504
<i>S</i>	2855.07	-6.59	0.9565
<i>S</i>	1122.65	-22.65	0.9510
<i>S</i>	724.30	-9.93	0.9924
<i>S</i>	1238.11	+2.33	0.8408
<i>S</i>	1160.20	24.44	0.9989

^a %M, %P and %S represents the percentage of MUFA, PUFA and SAFA, respectively.

predict the content of olive oil in SAFA, MUFA and PUFA fatty acids. As subsequently shown, although in the analysis of spectral bands the most informative zones are localized in the MIR spectral region, the NIR spectra provides better estimations in certain situations when the whole spectral information is used.

- 2. PLS regression versus general linear regression or PCA regression.** The analysis of IR spectra from the detection of relevant wavelength bands to obtain quantitative information (such as the prediction of the content of olive oil in some specific compounds) is based on the matching of some wavelengths with high correlation with the response variable. Then linear regression equations are fit to predict the percentage of the compound as a function of the wavelengths (see, for example, Guillén and Cabo (1997, 1998, 1999), Vlachos et al. (2006), Rohman and Che Man (2010), Zhang et al. (2012)). The selection of a single wavelength could lead to a waste of useful statistical information. But the selection of many wavelengths highly correlated with the dependent variable could cause the presence of multicollinearity among the explanatory variables, incompatible with the hypothesis of uncorrelation in the general linear model. This is why the use of principal component regression (PCA regression) or partial least squares regression (PLS regression) is more interesting. Both methodologies summarize the information of the whole IR spectrum in some latent factors or components, orthogonal among themselves, thus avoiding the possible multicollinearity in the model. These factors are obtained as linear combinations of the independent variables in both methodologies. However, the factors are obtained by maximizing the covariances (or correlations) among the explanatory variables, in PCA regression, and the covariances (or correlations) between the explanatory variables and the dependent one, in PLS regression.

In this work, PLS regression has been selected because a previous one (Sánchez-Rodríguez et al. (2013)) highlights the benefits of PLS regression versus PCA regression in the determination of quantitative information from NIR data. There are also other works indicating that PLS regression is better than PCA regression in the multivariate analysis of NIR or MIR spectral data (see, for example, Frank and Friedman (1993) or Maggio et al. (2011)).

- 3. Progressive introduction of PLS factors in the regression model.** The estimation algorithms that compare the MSEC and MSEF values obtained for PCA and PLS regression or for PCA or PLS discriminant analysis (PCA-DA or PLS-DA) have established, in the chemometric software, a stopping internal criterion to determine the number of factors to retain. This is the case, for example, of the article by Dupuy et al. (2010a) and (2010b), which uses UNSCRAMBLER software version 9.8 from CAMO (Computer Aided Modelling, Trondheim, Norway) and Matlab software from MathWorks in the analysis of NIR, MIR and concatenated NIR-MIR spectra.

The criteria determining the number of factors to retain in PLS regression are diverse. For example, in PCA, the *Kaiser criterion* is the default in most statistical software. It suggests that those principal components with eigenvalues equal to or higher than 1 should be retained, as each eigenvalue represents the variance of the corresponding factor. In PLS analysis, the *criterion of the first increase of the mean squared error of prediction* is considered: the number of latent factors taken into account is

$$h^* = \min\{h > 1 : \text{MSEP}(h+1) - \text{MSEP}(h) > 0\},$$

where $\text{MSEP}(h)$ is the mean squared error of prediction of the regression model with h factors. Gowen et al. (2010) present some measures for preventing the overfitting in PLS calibration models of near-infrared (NIR) spectroscopy data and investigate the simultaneous use of both model bias and variance in the selection of the number of latent factors to include in the model.

The cited criteria have an empirical character and are not unanimously applied. Therefore, the present work does not fix the number of factors. This number is progressively incremented in the PLS regression model and the associated MSEC and MSEP values are compared. As subsequently confirmed, the NIR matrix of data provides better estimations of the content in fatty acids of olive oil than MIR matrix for a lower number of factors whereas the opposite holds true for a higher number of latent factors.

- 4. Procedures of cross-validation.** The procedures of cross-validation are aimed at avoiding the bias associated to the case of using the same data to fit the regression model and to evaluate the corresponding predictions. They are repetitive algorithms that, at each iteration, subdivide the set of original data in the calibration and the validation subsets. The calibration (or fit) set, formed by 80% of the data approximately, is used in the fit of the model and provides the MSEC value as a measure of goodness-of-fit. But the validation (or prediction) set, formed by the remaining 20% of the data, is reserved in the training of the model and so can be used to evaluate its predictive capability with the MSEP value.

The computer programs frequently used in Chemometrics have some cross-validation procedures implemented. They iteratively repeat the selection of calibration and validation sets and provide an average of the MSEC and MSEP values obtained for each iteration. This is the case, for example, of the paper by Rohman and Man (2010), that uses the software TQ AnalystTM Version 6 (Thermo Electron Corporation, Madison, WI); Sinelli et al. (2010), which uses the V-PARVUS package (Forina et al. (2008)); Dupuy et al. (2010b), that uses the UNSCRAMBLER software version 9.8 from CAMO.

But the present work calculates and represents the MSEC and MSEP values obtained for different random selections of the calibration and validation sets, from the NIR, MIR and concatenated NIR-MIR matrices of data. The algorithm has been programmed by using the Matlab software from MathWorks. The graphical representations permit to compare not only the mean MSEC and MSEP values but also their variability in the successive selections. The three-dimensional graphics permit to compare the results for the three type of acids and matrices of data simultaneously.

- 5. Decomposition of the mean squared error of prediction.** With the aim of analyzing the nature of the prediction errors, this work uses a decomposition of the MSEP value in the terms E_B , E_V and E_R , attributable to systematic errors, the difference in variability among the real and the predicted values and random errors, respectively (Section 3.1, Sánchez-Rodríguez et al. (2013)). This decomposition is presented for the predictions for each type of fatty acid (SAFA, MUFA and PUFA) and spectral zone (NIR, MIR and concatenated NIR-MIR), as a function of the number of PLS factors in the regression model. Besides, in the context of cross-validation, this decomposition is also presented for the successive selections of calibration and validation sets. The ideal situation for evaluating the predictive capability of a model is presented when MSEP has a value nearer to 0 and the great percentage of this value is associated to the randomness and the lowest percentage is attributable to systematic errors. This work afterwards highlights that these percentages depend on the type of fatty acid to estimate, the IR spectral zone used for the estimation (NIR, MIR or NIR-MIR) and the number of PLS factors in the regression model.
- 6. Treatment of the spectra in the context of functional data analysis.** A line of future research (see Sánchez-Rodríguez and Caridad (2014)) could consider IR spectra as so-called *data objects* in *object-oriented data analysis* (OODA). This is the particular case of functional data analysis (FDA), in which the data objects of OODA are curves (see the overview by Marron and Alonso (2014)). In this context, multivariate techniques such as PCA or PLS regression, have been extended to the functional case. For example, Aguilera et al. (2010) apply functional PLS and PCA regressions to simulated and spectrometric data, comparing the results with the corresponding discrete ones and concluding that functional PLS regression provides better estimations of the parameter function than functional PCA regression and similar predictions. Preda and Saporta (2005) apply functional regression models to predict the behaviour of shares and conclude that the functional PLS regression model provides the best forecasts evaluating the global model quality by the sum of squared errors. Finally, also the classification techniques, such as logit regression or discriminant analysis, have been successfully extended to the functional case (see, respectively, Escabias et al. (2007) or Preda et al. (2007)).

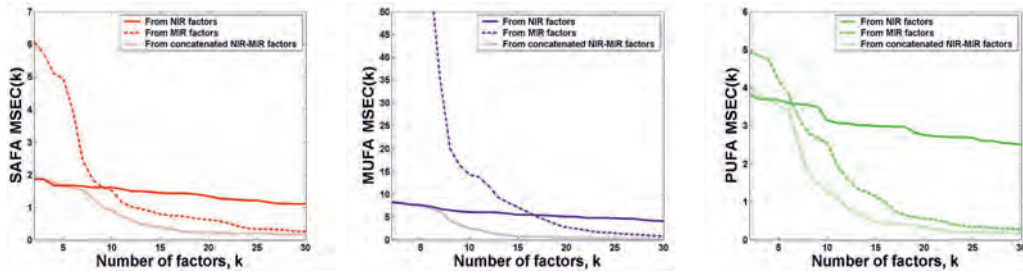
4. Results and discussion

Initially, Section 4.1 deals with the estimation of SAFA, MUFA and PUFA fatty acids of olive oils by PLS regression from the NIR, MIR and concatenated NIR-MIR matrices of data. The results of calibration and validation depend on the number of PLS factors in the regression model. These results are compared for the three matrices of data and types of fatty acids. The randomness of the prediction errors is analysed by a decomposition of MSE. Subsequently, in Section 4.2, the previous results are generalized by using cross-validation procedures, that is, changing iteratively the training and the test data sets. Besides, three-dimensional scatterplots permit to obtain conclusion simultaneously for the three matrices of data or types of fatty acids.

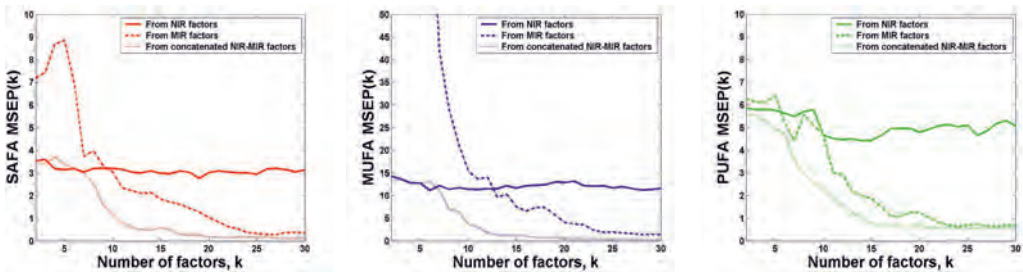
4.1. *Chemometrics from IR data: progressive introduction of PLS factors in the regression model*

NIR and MIR spectroscopies provide $n \times p$ data matrices whose rows refer to an olive oil ($n = 128$, in total) and each column is associated to a wavelength of the spectrum ($p_{\text{NIR}} = 1237$ and $p_{\text{MIR}} = 1843$). The information given by NIR and MIR data is summarized by using PLS regression. Sánchez-Rodríguez et al. (2013) pointed out that this technique, applied directly to the matrix of NIR data, provides a potential methodology to predict the content in fatty acids of olive oil. This paper shows that the results obtained from the whole matrix of data, being considered as a “black box”, are better than the ones obtained with the selection of some spectral peaks or spectral regions by cluster analysis. Besides, PLS regression considerably improves, in this context, the results obtained for PCA regression. As stated above, both PCA and PLS methodologies provide components or factors orthogonal among themselves, thus avoiding the possible presence of multicollinearity in the regression model.

With regard to the rows of the NIR and MIR data matrices, 80% of them, randomly selected, will be used for calibration and the remaining 20%, for prediction or validation. Initially, the NIR matrix of data is considered and PLS components are extracted. Those components will be progressively introduced in the PLS regression models that consider the content in SAFA, MUFA and PUFA fatty acids as explained variables, respectively. For each number of introduced components, the mean squared error of calibration and prediction, MSEC and MSE, are calculated. The same process is repeated considering, secondly, the MIR data matrix and, finally, the concatenated NIR-MIR data matrix. In addition, with the purpose of determining the character, systematic or random, of the prediction errors, a decomposition of MSE obtained by the PLS regression models on NIR, MIR and NIR-MIR matrices (in the U_B , U_V and U_R components) is obtained for each fatty acid.



Figures 3, 4 and 5: MSEC in the estimation of SAFA, MUFA and PUFA from PLS components of NIR, MIR and concatenated NIR-MIR matrices.

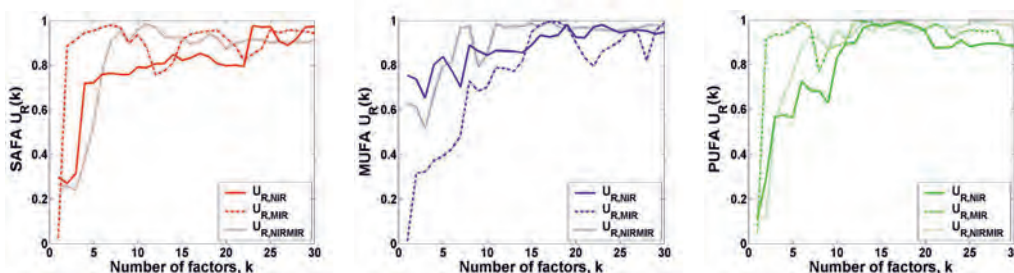


Figures 6, 7 and 8: MSEP in the estimation of SAFA, MUFA and PUFA from PLS components of NIR, MIR and concatenated NIR-MIR matrices.

Figures 3, 4 and 5 represent the MSEC in the estimation of SAFA, MUFA and PUFA acids obtained by successively introducing components in the regression model. These components are obtained on the NIR, MIR and concatenated NIR-MIR matrices of data. These figures show that, for the three types of fatty acids, the NIR (and concatenated NIR-MIR) matrix of data provides better calibration results in regression models with a lower number of PLS factors. But MIR (and concatenated NIR-MIR) matrix supplies better estimations for models with a higher number of factors.

Then, Figures 6, 7 and 8 represent, in the same context, the respective MSEP values. MSEP evaluates the predictive capability of a model, taking into account that the estimations are calculated by using observations that are not included in the fit or calibration of the model. The conclusions in prediction are similar to the ones obtained in calibration: the MSEP values obtained from MIR data are lower than the ones obtained from NIR data when the number of PLS factors in the model is sufficiently high, but not for low values.

Figures 9, 10 and 11 show the U_R term in the decomposition of MSEP for SAFA, MUFA and PUFA acids, respectively. This term corresponds to random prediction errors and, as in the previous graphics, is expressed as a function of the number of PLS components in the model. The figures evidence that the U_R term represents the great



Figures 9, 10 and 11: U_R term of MSEP in the estimation of SAFA, MUFA and PUFA from PLS components of NIR, MIR and concatenated NIR-MIR matrices.

percentage for each case, as this ratio is near to 1. With respect to the comparison of the techniques, there are differences depending on the used NIR, MIR and concatenated NIR-MIR matrices of data and the estimated fatty acid. For a higher number of PLS factors in the model, the three NIR, MIR and NIR-MIR U_R terms are very close to one. But for a lower number of factors, the MIR U_R term is closer to one in the estimation of SAFA and PUFA acids but it is farther from one in the estimation of MUFA acids. In this last case, the NIR matrix of data provides better results.

These results suggest that, under our experimental conditions, a more accurate estimation in calibration and validation of SAFA, MUFA and PUFA content in extra-virgin olive oil (taking GC as the reference technique) is obtained from the NIR matrix for a lower number of PLS factors. For a greater number of PLS factors, the MIR matrix provides the best results. The previous considerations are important as usual chemometric computer programs have internally implemented a stopping criterion to retain a concrete number of PLS factors in the regression model. It is interesting to identify the range of variation of this number to determine the region of the IR spectra, NIR or MIR, that provides better estimations of the different fatty acids. Then, analysing the nature of the prediction errors, the percentage of them attributable to random causes also depends on the region of the IR spectra and the type of acid. The MIR matrix provides, in general, better results in the estimation of SAFA and PUFA acids, irrespective of the number of PLS factors in the model. On the contrary, in the estimation of MUFA acids, NIR matrix supplies better results, also independently of the number of factors.

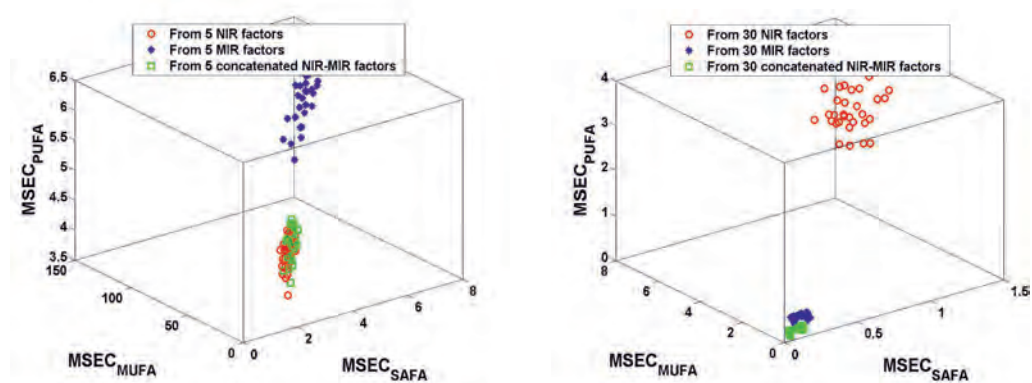
4.2. Cross-validation: generalization of the previous results

In the last subsection, the original data have been subdivided in a single calibration set (containing the 80% of the original data, specifically, 102 out of 128 data) and a single validation set (with the 20%, that is, 26 data). The calibration set is used to train the regression model. The validation set is used to test the model, using data reserved in the fit of the model. With the goal of generalizing the previously obtained results,

procedures of cross-validation are used in this section. They are implemented by a repetitive algorithm that, for each iteration, modifies the partition in calibration and validation subsets of the original data set. For each iteration, MSEC and MSEP are calculated for evaluating, respectively, the goodness-of-fit and the predictive capability of the corresponding model.

More specifically, the cross-validation algorithm has been implemented for 30 iterations, randomly selecting, for each one, the sets considered for calibration and validation. Besides, since the previous section highlights differences depending on the number of PLS factors in the regression model, this section compares the results for a low number of factors, 5, and also for a high number of factors, 30.

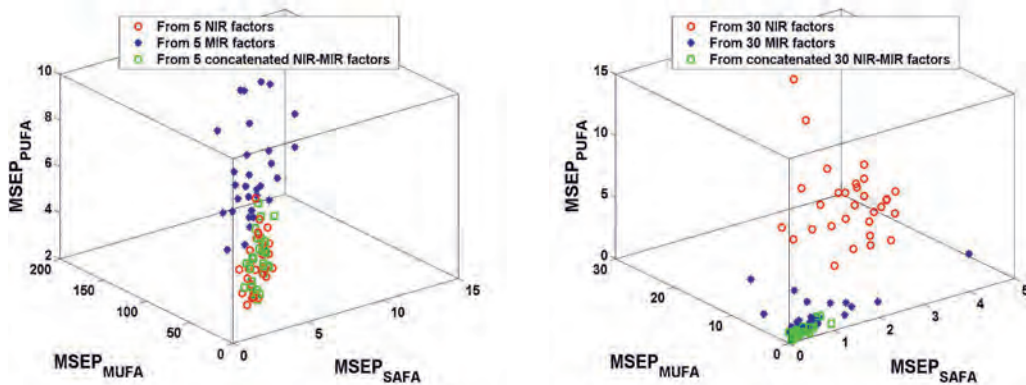
Figures 12 and 13 draw three-dimensional scatterplots for goodness-of-fit or calibration in cross-validation. The point clouds are associated to models with 5 and 30 PLS factors, respectively, representing $MSEC_{SAFA}$, $MSEC_{MUFA}$ and $MSEC_{PUFA}$ in x , y , z axes. Unlike the previously represented figures, these graphics permit to compare, in a global manner, the results obtained for the three types of fatty acids simultaneously. For 5 PLS factors (Figure 12), the MIR point cloud is farther from the origin (0,0,0) than the corresponding to the NIR (and NIR-MIR) data. For 30 PLS factors (Figure 13), the conclusions are the opposite: in this case, the estimations from NIR data are associated with the high MSEC values.



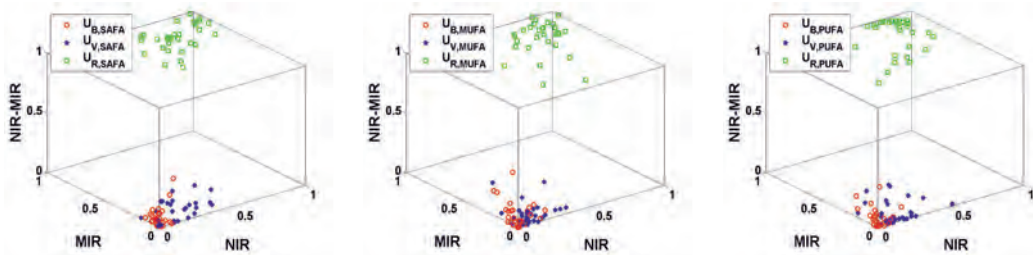
Figures 12 and 13: MSEC obtained by the cross-validation algorithm from NIR, MIR and concatenated NIR-MIR data (for SAFA, MUFA and PUFA) for 5 and 30 factors, respectively.

The same conclusions are obtained for the three fatty acid types, if the models are compared in validation or prediction terms (using MSEP, see Figures 14 and 15). Besides, the variability existing among the MSEP values is higher for the MIR than for the NIR estimations in the models with 5 PLS factors and lower for the models with 30 PLS factors.

Figures 16-18 represent, for each acid type, the decomposition of MSEP in the terms U_B , U_V and U_R obtained, by the cross-validation algorithm, for each iteration. The



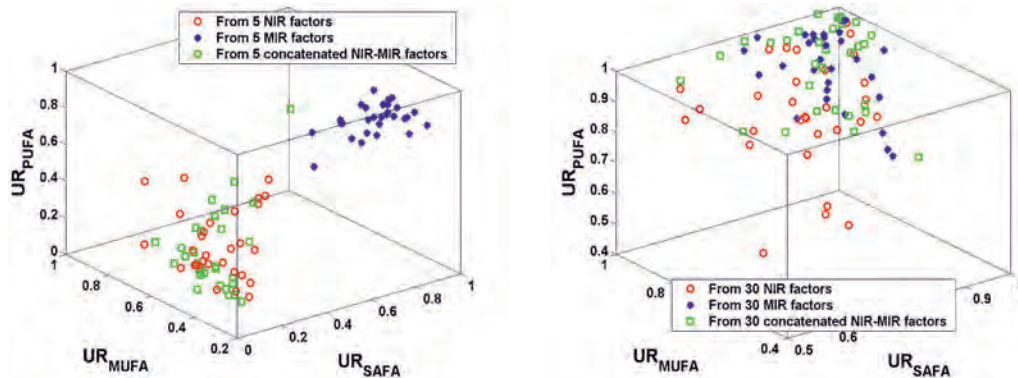
Figures 14 and 15: *MSEP obtained by the cross-validation algorithm from NIR, MIR and concatenated NIR-MIR data (for SAFA, MUFA and PUFA) for 5 and 30 factors, respectively.*



Figures 16, 17 and 18: *Decomposition of MSEP obtained by the cross-validation algorithm in the estimation of SAFA, MUFA and PUFA from PLS components of NIR, MIR and concatenated NIR-MIR matrices, respectively.*

aim is to determine the nature, random or systematic, of the prediction errors. The point clouds represent the values corresponding to NIR, MIR and NIR-MIR matrices in x , y , z axes, respectively. It is evident that, for each case, the component corresponding to random prediction errors, U_R , is associated to the great percentage, as this ratio is near to 1 for NIR, MIR and NIR-MIR axes. This is the suitable situation in the evaluation of the predictive character of a model.

Finally, with the aim to confirm the differences detected previously depending on the number of the PLS factors in the model, Figures 19 and 20 depict the U_R term associated with the models with 5 and 30 factors. The scatterplots represent the values corresponding to $U_{R,SAFA}$, $U_{R,MUFA}$ and $U_{R,PUFA}$ in x , y , z axes, respectively. The results show that the U_R term obtained from the NIR, MIR and concatenated NIR-MIR matrices of data is close to 1 in models with a relatively high number of factors (30). But, in model with a low number of factors, the NIR and NIR-MIR U_R terms are lower, clearly discriminated from the one obtained from the MIR data.



Figures 19 and 20: U_R term of MSEP obtained by the cross-validation algorithm from NIR, MIR and concatenated NIR-MIR data (for SAFA, MUFA and PUFA) for 5 and 30 factors, respectively.

5. Conclusions

In recent years, procedures which permit to determine in a fast and efficient manner the profile of olive oils in different components have been generalized, specially aiming at evaluating quality indexes. In this sense, spectroscopic techniques have been extended. In parallel, multivariate statistics has emerged as a powerful tool to identify and extract the information contained in spectra.

In this work, Chemometrics is applied to data obtained from IR spectra, in the near (NIR) and mid (MIR) zones, and using GC data as a reference. PLS regression models to predict the content in SAFA, MUFA and PUFA fatty acids of olive oil are proposed, using the three NIR, MIR and concatenated NIR-MIR matrices of data. The final conclusion is that the best estimation of calibration or fit and validation or prediction are obtained from the NIR data for lower numbers of PLS factors and from the MIR data for higher numbers of factors. This is important to be taken into account since, usually, chemometric computer programs have a stopping criterion implemented to determine the number of PLS factors to be retained.

These conclusions are generalized via cross-validation procedures. They compare estimations in terms of goodness-of-fit and prediction for different calibration and validation subsets and evidence the desirable main random nature of the estimation errors. Three-dimensional scatterplots confirm the differences among the three fatty acid types and matrices simultaneously.

Then, this study analyses the prediction errors to determine their nature, systematic or random. Also in this case the conclusions depend on the number of PLS latent factors, the type of fatty acid and the matrix of data. These differences are detected by the U_R term, that represents the percentage of randomness in the prediction errors. In general, irrespective of the number of factors in the regression model, the MIR zone provides a

higher value in the estimation of SAFA and PUFA acids. But, in the estimation of MUFA acids, the NIR matrix gives better estimations. In the three-dimensional representation of the U_R term for the three acids and IR zones, this term is always close to 1 for a high number of PLS factors. But, for a low number of factors, the NIR and NIR-MIR U_R terms are clearly lower than the associated to the MIR data.

Acknowledgements

The authors thank the financial support by 'Junta de Andalucía' (Project P08-FQM-3931) and FEDER funds.

References

- Aguilera, A. M., Escabias, M., Preda, C. and Saporta, G. (2010). Using basis expansions for estimating functional PLS regression. Applications with chemometric data. *Chemometrics and Intelligent Laboratory Systems*, 104, 289–305.
- Baeten, V., Aparicio, R., Marigheto, N. and Wilson, R. (2003). *Manual del aceite de oliva*. AMV ediciones, Mundi-Prensa.
- Baeten, V., Fernández Pierna, J. A., Dardenne, P., Meurens, M., García-González, D. L. and Aparicio-Ruiz, R. (2005). Detection of the presence of hazelnut oil in olive oil by FT-Raman and FT-MIR spectroscopy. *Journal of agricultural and food chemistry*, 53(16), 6201–6206.
- Berrueta, L. A., Alonso-Salces, R. M. and Héberger, K. (2007). Supervised pattern recognition in food analysis. *Journal of Chromatography A*, 1158, 196–214.
- Bertran, E., Blanco, M., Coello, J., Iturriaga, H., Maspoch, S. and Montoliu, I. (2000). Near infrared spectrometry and pattern recognition as screening methods for the authentication of virgin olive oils of very close geographical origins. *Journal of Near Infrared Spectroscopy*, 8, 45.
- Casale, M., Oliveri, P., Casolino, C., Sinelli, N., Zunin, P., Armanino, C., Forina, M. and Lanteri, S. (2012). Characterization of PDO olive oil Chianti Classico by non-selective (UV-visible, NIR and MIR spectroscopy) and selective (fatty acid composition) analytical techniques. *Analytical Chimica Acta*, 712, 56–63.
- Commission regulation (EU) No 61/2011 of 24 January 2011 amending Regulation (EEC) No 2568/91 on the characteristics of olive oil and olive-residue oil and on the relevant methods of analysis.
- D'Imperio, M., Mannina, L., Capitani, D., Bidet, O., Rossi, E., Bucarelli, F. M., Quaglia, G. B. and Segre, A. (2007). NMR and statistical study of olive oils from Lazio: a geographical, ecological and agronomic characterization. *Food chemistry*, 105(3), 1256–1267.
- Dupuy, N., Galtier, O., Ollivier, D., Vanloot, P. and Artaud, J. (2010a). Comparison between NIR, MIR, concatenated NIR and MIR analysis and hierarchical PLS model. Application to virgin olive oil analysis. *Analytica chimica acta*, 666(1), 23–31.
- Dupuy, N., Galtier, O., Le Dréau, Y., Pinatel, C., Kister, J. and Artaud, J. (2010b). Chemometric analysis of combined NIR and MIR spectra to characterize French olives. *European Journal of Lipid Science and Technology*, 112(4), 463–475.
- Escabias, M., Aguilera, A. M. and Valderrama, M. J. (2007). Functional PLS logit regression model. *Computational Statistics and Data Analysis*, 51, 4891–4902.
- Frank, I. E. and Friedman, J. H. (1993). A statistical view of some chemometrics regression tools. *Technometrics*, 35(2), 109–135.

- Forina, M., Lanteri, S., Armanino, C., Casolino, C., Casale, M. and Oliveri, P. (2008). *P-PARVUS. Dip. Chimica e Tecnologie Farmaceutiche e Alimentari*, University of Genova, <http://www.parvus.unige.it>.
- Galtier, O., Abbas, O., Le Dréau, Y., Rebufa, C., Kister, J., Artaud, J. and Dupuy, N. (2011). Comparison of PLS1-DA, PLS2-DA and SIMCA for classification by origin of crude petroleum oils by MIR and virgin olive oils by NIR for different spectral regions. *Vibrational Spectroscopy*, 55(1), 132–140.
- Galtier, O., Dupuy, N., Le Dréau, Y., Ollivier, D., Pinatel, C., Kister, J. and Artaud, J. (2007). Geographic origins and compositions of virgin olive oils determined by chemometric analysis of NIR spectra. *Analytica chimica acta*, 595(1), 136–144.
- Gowen, A. A., Downey, G., Esquerre, C. and O'Donnell, C. P. (2010). Preventing over-fitting in PLS calibration models of near-infrared (NIR) spectroscopy data using regression coefficients. *Journal of Chemometrics*, 25, 375–381.
- Guillén, M. D. and Cabo, N. (1997). Characterization of edible oils and lard by Fourier transform infrared spectroscopy. Relationships between composition and frequency of concrete bands in the fingerprint region. *Journal of the American Oil Chemists' Society*, 74(10), 1281–1286.
- Guillén, M. D. and Cabo, N. (1998). Relationships between the composition of edible oils and lard and the ratio of the absorbance of specific bands of their Fourier transform infrared spectra. Role of some bands of the fingerprint region. *Journal of Agricultural and Food Chemistry*, 46, 1788–1793.
- Guillén, M. D. and Cabo, N. (1999). Usefulness of the frequencies of some Fourier transform infrared spectroscopic bands for evaluating the composition of edible oil mixtures. *European Journal of Lipid Sciences and Technology*, 1, 71–76.
- Guillén, M. D. and Ruiz, A. (2003). Edible oils: discrimination by ^1H nuclear magnetic resonance. *Journal of the Science of Food and Agriculture*, 83(4), 338–346. Relationships between composition and frequency of concrete bands in the fingerprint region. *Journal of the American Oil Chemists' Society*, 74(10), 1281–1286.
- Gurdeniz, G. and Ozen, B. (2009). Detection of adulteration of extra-virgin olive oil by chemometric analysis of mid-infrared spectral data. *Food chemistry*, 116(2), 519–525.
- International Olive Oil Council, 200 (COI / T.20 / Doc. no. 24 / 2001a). Preparation of the fatty acid methyl esters from olive oil and olive-pomace oil.
- International Olive Oil Council, 200 (COI / T.20 / Doc. no. 17 / 2001b). Determination of trans unsaturated fatty acids by capillary column gas chromatography.
- Maggio, R. M., Valli, E., Bendini, A., Gómez-Caravaca, A. M., Toschi, T. G. and Cerretani, L. (2011). A spectroscopic and chemometric study of virgin olive oils subjected to thermal stress. *Food Chemistry*, 127, 216–221.
- Marron, J. S. and Alonso, A. M. (2014). Overview of object oriented data analysis. *Biometrical Journal*, 56, doi: 10.1002/bimj.201300072.
- Öztürk, B., Yalçın, A. and Özdemir, D. (2010). Determination of olive oil adulteration with vegetable oils by near infrared spectroscopy coupled with multivariate calibration. *Journal of Near Infrared Spectroscopy*, 18, 191–201.
- Preda, C. and Saporta, G. (2005). PLS regression on a stochastic process. *Computational Statistics and Data Analysis*, 48, 149–158.
- Preda, C., Saporta, G. and Lévêder, C. (2007). PLS classification of functional data. *Computational Statistics*, 22, 223–235.
- Rezzi, S., Axelson, D. E., Héberger, K., Reniero, F., Mariani, C. and Guillou, C. (2005). Classification of olive oils using high throughput flow- ^1H NMR fingerprinting with principal component analysis, linear discriminant analysis and probabilistic neural networks. *Analytica Chimica Acta*, 552(1), 13–24.
- Rohman, A. and Che Man, Y. B. (2010). Fourier transform infrared (FTIR) spectroscopy for analysis of extra virgin olive oil adulteration with palm oil. *Food research international*, 43, 886–892.

- Sánchez-Rodríguez, M. I., Sánchez-López, E., Caridad, J. M., Marinas, A., Marinas, J. M. and Urbano, F. J. (2013). New insights into evaluation of regression models through a decomposition of the prediction errors: application to near-infrared spectral data. *Statistics and Operations Research Transactions (SORT)*, 37(1), 57–78.
- Sánchez-Rodríguez, M. I. and Caridad, J. M. (2014). Modelling and partial least squares approaches in OODA. *Biometrical Journal*, 37(1), 771–773.
- Sinelli, N., Casiraghi, E., Tura, D. and Downey, G. (2008). Characterisation and classification of Italian virgin olive oils by near-and mid-infrared spectroscopy. *Journal of Near Infrared Spectroscopy*, 16, 335–342.
- Sinelli, N., Cerretani, L., Di Egidio, V., Bendini, A. and Casiraghi, E. (2010). Application of near (NIR) infrared and mid (MIR) infrared spectroscopy as a rapid tool to classify extra virgin olive oil on the basis of fruity attribute intensity. *Food research international*, 43, 369–375.
- Vlachos, N., Skopelitis, Y., Psaroudaki, M., Konstantinidou, V., Chatzilazarou, A. and Tegou, E. (2006). Applications of Fourier transform-infrared spectroscopy to edible oils. *Analytica Chimica Acta*, 573–574, 459–465.
- Zhang, Q., Liu, C., Sun, Z., Hu, X., Shen, Q. and Wu, J. (2012). Authentication of edible vegetable oils adulteration with used frying oil by Fourier transform infrared spectroscopy. *Food Chemistry*, 132, 1607–1613.

Exact prediction intervals for future current records and record range from any continuous distribution

H. M. Barakat¹, E. M. Nigm¹ and R. A. Aldallal²

Abstract

In this paper, a general method for predicting future lower and upper current records and record range from any arbitrary continuous distribution is proposed. Two pivotal statistics with the same explicit distribution for lower and upper current records are developed to construct prediction intervals for future current records. In addition, prediction intervals for future observations of the record range are constructed. A simulation study is applied on normal and Weibull distributions to investigate the efficiency of the suggested method. Finally, an example for real lifetime data with unknown distribution is analysed.

MSC: 62G30, 62G32, 62M20, 62F25.

Keywords: Current record values, record range, pivotal quantity, prediction interval, coverage probability.

1. Introduction

Let $\{X_i; i \geq 1\}$ be a sequence of iid continuous random variables each distributed according to cumulative distribution function (cdf) $F_X(x) = P(X \leq x)$ and probability density function (pdf) $f_X(x)$. An observation X_j will be called an upper record value if its value exceeds that of all previous observations. Thus, X_j is an upper record if $X_j > X_i$ for every $i < j$. An analogous definition, with the inequality being reversed, deals with lower record values. The times at which the records occur are called record times.

¹ Department of Mathematics, Faculty of Science, Zagazig University, Zagazig, Egypt

² Department of Mathematics and Statistics, MSA University, Cairo, Egypt

Received: September 2013

Accepted: July 2014

There are some situations wherein upper and lower records are observed together, such as the case of weather data. In these cases, It is quite conceivable to consider lower and upper records jointly, when a new record of either kind (upper or lower) occurs, and these records are called current records. In this paper, we denote them by U_n^c and L_n^c , respectively, and call the n th upper current record and the n th lower current record of the sequence $\{X_n\}$ when the n th record of any kind (either an upper or lower) is observed. It can be noticed that $U_{n+1}^c = U_n^c$ if $L_{n+1}^c < L_n^c$ and that $L_{n+1}^c = L_n^c$ if $U_{n+1}^c > U_n^c$. That is, the upper current record value is the largest observation seen to date at the time when the n th record (of either kind) is observed. According to the definition, $L_0^c = U_0^c = X_1$. For $n \geq 1$, the interval (L_n^c, U_n^c) is then referred to as the record coverage. The record range is then defined by $R_n^c = U_n^c - L_n^c$. The record range may also be defined as the n th record range in the sequence of the usual sample range $R_n = \max(X_1, X_2, \dots, X_n) - \min(X_1, X_2, \dots, X_n)$, where by definition $R_0^c = 0$ and $R_1^c = R_2$. Notice that a new record range is attained once a new upper or lower record is observed (see, Basak, 2000). Both current record values and record range can be detected in several real-life situations. For example, the consistency of the production process is required to meet a product's specifications. If the record range is large, then it is likely that large number of products will lie outside the specifications of the product. Predictions of future upper and lower current records, as well as record range, are of natural interest in this context. Prediction of future events is a problem of great interest and plays an important role in many applications, such as meteorology, hydrology, industrial stress testing and athletic events. Several authors have considered prediction problems involving record values. For example, Ahmadi and Balakrishnan (2004) derived distribution-free confidence intervals to estimate the fixed quantiles of an arbitrary unknown distribution, based on current records of an iid sequence from that distribution. Raqab and Balakrishnan (2008) obtained distribution-free prediction intervals for records from the Y -sequence based on record values from the X -sequence of iid random variables from the same distribution. Raqab (2009) obtained prediction intervals for the current records from a future iid sequence based on observed current records from an independent iid sequence of the same distribution. Ahmadi and Balakrishnan (2011) discussed the prediction of future order statistics based on the current record values. In this paper, we consider two pivotal quantities for the lower and upper current records based on an arbitrary cdf F_X with the same explicit distribution-free (not depending on the cdf F_X). By using these pivotal quantities, prediction intervals of future observations of lower-upper current records and record range are explicitly derived. Moreover, simulation study is applied on normal and Weibull distributions to investigate the efficiency of the suggested method. Finally, an example of real lifetime data is analysed, where it is assumed that the distribution of the data is unknown.

2. Auxiliary results

Houchens (1984) used an inductive argument to derive the pdf of U_n^c , L_n^c and R_n^c , based on an arbitrary cdf F_X , (in the sequel we write $U_n^c \parallel X$, $L_n^c \parallel X$ and $R_n^c \parallel X$ to indicate that these statistics are based on the cdf F_X), respectively by

$$f_{U_n^c \parallel X}(x) = 2^n f_X(x) \left[1 - \bar{F}_X(x) \sum_{k=0}^{n-1} \frac{[-\log \bar{F}_X(x)]^k}{k!} \right], \tag{2.1}$$

$$f_{L_n^c \parallel X}(x) = 2^n f_X(x) \left[1 - F_X(x) \sum_{k=0}^{n-1} \frac{[-\log F_X(x)]^k}{k!} \right]$$

and

$$f_{R_n^c \parallel X}(r) = \frac{2^n}{(n-1)!} \int_{-\infty}^{\infty} f_X(r+x) f_X(x) \left[-\log(1 - F_X(r+x) + F_X(x)) \right]^{n-1} dx, \quad 0 < r < \infty,$$

where $\bar{F}_X(x) = 1 - F_X(x)$.

Houchens (1984) deduced a useful representation for $U_n^c \parallel Y$, when Y has a negative exponential with parameter 2, i.e., $Y \sim \text{EX}(2)$. Namely,

$$U_n^c \parallel Y \stackrel{d}{=} Y_0 + Y_1 + \dots + Y_n, \tag{2.2}$$

where “ $\stackrel{d}{=}$ ” means identical in distribution and Y_i 's are independent random variables such that $Y_0 \sim \text{EX}(2)$ and the remaining $Y_i \sim \text{EX}(1)$. An analogous representation for the lower current record can be easily obtained by noting that

$$\begin{aligned} f_{-U_n^c \parallel X}(x) &= f_{U_n^c \parallel X}(-x) = 2^n f_X(-x) \left[1 - \bar{F}_X(-x) \sum_{k=0}^{n-1} \frac{(-\log \bar{F}_X(-x))^k}{k!} \right] \\ &= 2^n f_{-X}(x) \left[1 - \bar{F}_{-X}(x) \sum_{k=0}^{n-1} \frac{(-\log \bar{F}_{-X}(x))^k}{k!} \right], \end{aligned}$$

which yields

$$-U_n^c \parallel X \stackrel{d}{=} L_n^c \parallel -X. \tag{2.3}$$

Applying (2.3), we get $-U_n^c \parallel Y \stackrel{d}{=} -Y_0 - Y_1 - \dots - Y_n \stackrel{d}{=} Z_0 + Z_1 + \dots + Z_n$, where $Z_0 \sim \text{EX}^+(2)$, $Z_i \sim \text{EX}^+(1), i = 1, 2, \dots, n$, and $\text{EX}^+(\beta)$ is the positive exponential cdf

with parameter β . Thus, by applying again (2.3) and noting that $Y \sim \text{EX}(\beta) \Rightarrow Z = -Y \sim \text{EX}^+(\beta)$, we get

$$L_n^c \parallel Z \stackrel{d}{=} Z_0 + Z_1 + \dots + Z_n,$$

where $Z \sim \text{EX}^+(2)$, $Z_0 \sim \text{EX}^+(2)$ and $Z_i \sim \text{EX}^+(1)$, $i = 1, 2, \dots, n$.

3. Main results

The following theorem is the main result of this article. In what follows we assume that F_X is a continuous cdf with the generalized inverse function $F_X^{-1}(y) = \inf\{x : F_X(x) \geq y\}$.

Theorem 3.1. Let $U_n^c = U_n^c \parallel X$, $L_n^c = L_n^c \parallel X$ and $R_n^c = R_n^c \parallel X$ be the upper current record, the lower current record and the record range based on the cdf F_X , respectively. Furthermore, let $0 < \alpha, \beta < 1$ and $m = 1, 2, \dots$. Then,

1. $\left(U_n^c, F_X^{-1}\left(1 - \bar{F}_X^{1+tm;\alpha}(U_n^c)\right) \right)$ is $(1 - \alpha)\%$ confidence interval for U_{n+m}^c .
2. $\left(F_X^{-1}\left(F_X^{1+tm;\beta}(L_n^c)\right), L_n^c \right)$ is $(1 - \beta)\%$ confidence interval for L_{n+m}^c ,
3. $\left(R_n^c = U_n^c - L_n^c, F_X^{-1}\left(1 - \bar{F}_X^{1+tm;\alpha}(U_n^c)\right) - F_X^{-1}\left(F_X^{1+tm;\beta}(L_n^c)\right) \right)$ is $\gamma\%$ confidence interval for R_{n+m}^c , where $\gamma \geq \max(1 - \alpha - \beta, 0)$ (e.g., $\gamma \geq 0.98$ if $\alpha = \beta = 0.01$).

Theorem 3.1 will follow from the following lemma, which is proved in the Appendix and individually expresses an interesting fact.

Lemma 3.1. Let $U_n^* = U_n^c \parallel Y$ and $L_n^* = L_n^c \parallel Z$, where $Y \sim \text{EX}(2)$ and $Z \sim \text{EX}^+(2)$. Then, for every $m = 1, 2, \dots$, the two pivotal statistics $\bar{T}_m = \frac{U_{n+m}^* - U_n^*}{U_n^*}$ and $T_m = \frac{L_{n+m}^* - L_n^*}{L_n^*}$ have the same pdf $f(t)$, where

$$f(t) = \frac{2^{n-1} m t^{m-1}}{\left(t + \frac{1}{2}\right)^{m+1}} - \sum_{k=0}^{n-1} \binom{k+m}{k} \frac{2^{n-k-1} m t^{m-1}}{(t+1)^{k+m+1}}. \quad (3.1)$$

Remark 3.1. One can easily check that $\int_0^\infty f(t) dt = 1$, by using the two formulas

$$\int_0^\infty \frac{t^N}{(t+a)^M} dt = a^{N-M+1} \sum_{i=0}^N \binom{N}{i} \frac{(-1)^{i+1}}{N-i-M+1}, \quad a > 0,$$

and

$$\sum_{i=0}^N \frac{(-1)^i}{M+i} \binom{N}{i} = \frac{N!(M-1)!}{(M+N)!},$$

for any two positive integers N and M , for which $N < M - 1$.

Proof of Theorem 3.1. On applying Lemma 3.1, we get $P(0 \leq \bar{T}_m \leq t_{m:\alpha}) = 1 - \alpha$, and $P(0 \leq T_m \leq t_{m:\beta}) = 1 - \beta$. Therefore, we get

$$P\left(0 \leq \frac{U_{n+m}^* - U_n^*}{U_n^*} \leq t_{m:\alpha}\right) = P\left(U_n^* \leq U_{n+m}^* \leq U_n^*(1 + t_{m:\alpha})\right) = 1 - \alpha \quad (3.2)$$

and

$$P\left(0 \leq \frac{L_{n+m}^* - L_n^*}{L_n^*} \leq t_{m:\beta}\right) = P\left(0 \geq L_{n+m}^* - L_n^* \geq L_n^* t_{m:\beta}\right) = 1 - \beta \quad (3.3)$$

(note that $L_n^* \leq 0$). Thus, the first two relations of Theorem 3.1 (1. and 2.) follow immediately by applying the transformations $U_n^* = -2 \log(\bar{F}_X(U_n^c))$ and $L_n^* = 2 \log(F_X(L_n^c))$, respectively, on the relations (3.2) and (3.3).

In order to find the confidence interval for the record range we use the two well-known relations

$$P(C_1 C_2) \geq \max(P(C_1) + P(C_2) - 1, 0),$$

for any two events C_1 and C_2 , and

$$\{a + \bar{a} \leq X + Y \leq b + \bar{b}\} \subset \{\bar{a} < X < \bar{b}, a < Y < b\},$$

for any two random variables X and Y , to get

$$\begin{aligned} &P\left(R_n^c = U_n^c - L_n^c \leq R_{n+m}^c \leq F_X^{-1}\left(1 - \bar{F}_X^{1+t_m:\alpha}(U_n^c)\right) - F_X^{-1}\left(F_X^{1+t_m:\beta}(L_n^c)\right)\right) \\ &\geq P\left(U_n^c \leq U_{n+m}^c \leq F_X^{-1}\left(1 - \bar{F}_X^{1+t_m:\alpha}(U_n^c)\right), -L_n^c \leq -L_{n+m}^c \leq -F_X^{-1}\left(F_X^{1+t_m:\beta}(L_n^c)\right)\right) \\ &= \gamma \geq \max(1 - \alpha - \beta, 0). \end{aligned}$$

This completes the proof. □

By using an argument similar to the one applied in Lemma 3.1, the proofs of the following two results are in the appendix.

Lemma 3.2. *The joint pdf's of $U_1^*, U_2^*, \dots, U_n^*$ and $L_1^*, L_2^*, \dots, L_n^*$ are given respectively by*

$$f_{U_n^*, U_{n-1}^*, \dots, U_1^*}(y_n, y_{n-1}, \dots, y_1) = e^{-y_n} [e^{y_1/2} - 1], 0 < y_1 < y_2 < \dots < y_n,$$

and

$$f_{L_n^*, L_{n-1}^*, \dots, L_1^*}(z_n, z_{n-1}, \dots, z_1) = e^{z_n} [e^{-z_1/2} - 1], z_n < z_{n-1} < \dots < z_1 < 0.$$

Lemma 3.2 opens the way for interesting inferential study based on the current records. Actually, by noting that $U_n^* = -2\log(\bar{F}_X(U_n^c \| X))$ and $L_n^* = 2\log(F_X(L_n^c \| X))$, we can obtain the likelihood functions based on the upper and lower current records, respectively, as

$$f_{U_n^c \| X, \dots, U_1^c \| X}(x_n, \dots, x_1) = \frac{\bar{F}_X^2(x_n) F_X(x_1)}{\bar{F}_X(x_1)} \left(\prod_{j=1}^n \frac{2f_X(x_j)}{\bar{F}_X(x_j)} \right), x_1 < x_2 < \dots < x_n$$

and

$$f_{L_n^c \| X, \dots, L_1^c \| X}(x_n, \dots, x_1) = \frac{\bar{F}_X^2(x_n) \bar{F}_X(x_1)}{F_X(x_1)} \left(\prod_{j=1}^n \frac{2f_X(x_j)}{F_X(x_j)} \right), x_n < x_{n-1} < \dots < x_1.$$

The above likelihood functions can be used to obtain the point estimators of any unknown parameters of the cdf F_X , especially if the available data are the current record values.

Lemma 3.3. *Each of the sequence $\{U_n^c \| X\}$ and $\{L_n^c \| X\}$ forms a Markov chain.*

Tables 1, 2 and 3 give the values of $t_{m;\theta}$, where $\int_0^{t_{m;\theta}} f(t) dt = 1 - \theta$, for the values of $n = 2, 3, \dots, 20, m = 1, 2, \dots, 5$ and $\theta = 0.1, 0.05, 0.01$. The calculations in these tables are carried out by Mathematica 8.

Table 1: $P(\bar{T}_m \leq t_{m:0.1}) = P(T_m \leq t_{m:0.1}) = 0.9$.

n	$m = 1$	$m = 2$	$m = 3$	$m = 4$	$m = 5$
2	0.893932	1.64789	2.12161	3.09928	3.81681
3	0.637903	1.15382	1.64826	2.13481	2.61746
4	0.496616	0.887298	1.25887	1.62313	1.98369
5	0.406947	0.720864	1.01764	1.30767	1.59422
6	0.34491	0.607108	0.853803	1.09426	1.33144
7	0.299402	0.524443	0.735349	0.940467	1.14249
8	0.264573	0.461651	0.645749	0.824454	1.00024
9	0.237047	0.41233	0.575618	0.733861	0.88935
10	0.214737	0.37256	0.519236	0.661177	0.80051
11	0.196285	0.339808	0.472924	0.601579	0.727758
12	0.180767	0.312366	0.434205	0.551829	0.667099
13	0.167533	0.289036	0.401353	0.509676	0.615756
14	0.156111	0.268957	0.373128	0.473505	0.571739
15	0.146152	0.251494	0.348617	0.442127	0.533588
16	0.137392	0.236166	0.327132	0.41465	0.500204
17	0.129626	0.222602	0.308145	0.390389	0.470749
18	0.122693	0.210515	0.291243	0.368811	0.444567
19	0.116466	0.199676	0.276101	0.349494	0.421142
20	0.110841	0.1899	0.262458	0.332101	0.400062

Table 2: $P(\bar{T}_m \leq t_{m:0.05}) = P(T_m \leq t_{m:0.05}) = 0.95$.

n	$m = 1$	$m = 2$	$m = 3$	$m = 4$	$m = 5$
2	1.33466	2.36039	3.35038	4.32794	5.29962
3	0.917775	1.58465	2.22095	2.84604	3.46562
4	0.699294	1.18883	1.65183	2.10471	2.55247
5	0.565044	0.950237	1.31202	1.66461	2.01244
6	0.474206	0.791113	1.08708	1.37465	1.6578
7	0.408643	0.677553	0.927536	1.16979	1.4079
8	0.359082	0.592484	0.808619	1.01759	1.2227
9	0.320292	0.526398	0.716627	0.900193	1.08012
10	0.2891	0.473584	0.643377	0.806939	0.967069
11	0.263469	0.430412	0.583685	0.731109	0.875286
12	0.242029	0.394463	0.534115	0.668256	0.799318
13	0.223828	0.364064	0.492298	0.615323	0.735419
14	0.208182	0.338022	0.45655	0.570139	0.680937
15	0.194588	0.315462	0.42564	0.531123	0.633941
16	0.182666	0.29573	0.39865	0.497096	0.592992
17	0.172124	0.278324	0.374878	0.46716	0.556997
18	0.162736	0.262857	0.353783	0.440621	0.525111
19	0.154321	0.249021	0.334935	0.416931	0.49667
20	0.146736	0.23657	0.317995	0.395657	0.471145

Table 3: $P(\bar{T}_m \leq t_{m:0.01}) = P(T_m \leq t_{m:0.01}) = 0.99$.

n	$m = 1$	$m = 2$	$m = 3$	$m = 4$	$m = 5$
2	2.85847	4.79726	6.66544	8.50916	10.3413
3	1.79354	2.91229	3.97659	5.02093	6.05546
4	1.29678	2.06118	2.78104	3.4839	4.17816
5	1.01294	1.58618	2.12161	2.64218	3.15505
6	0.830235	1.28585	1.70856	2.11803	2.52051
7	0.703094	1.07977	1.42729	1.76285	2.09202
8	0.609623	0.929976	1.22414	1.50739	1.78474
9	0.538056	0.816357	1.07087	1.31536	1.55434
10	0.481519	0.727304	0.951294	1.166	1.37557
11	0.435735	0.655671	0.855492	1.04666	1.23301
12	0.397907	0.596827	0.777067	0.949212	1.11681
13	0.366128	0.547641	0.711716	0.868181	1.02035
14	0.339055	0.505923	0.656439	0.799775	0.939036
15	0.315716	0.470098	0.609086	0.741278	0.869594
16	0.295387	0.439003	0.568075	0.690695	0.80962
17	0.277521	0.411761	0.532217	0.646532	0.757316
18	0.261696	0.387699	0.500602	0.607646	0.711309
19	0.247582	0.366292	0.472522	0.573149	0.670533
20	0.234914	0.347123	0.447416	0.542341	0.63415

4. Simulation study

In order to check the efficiency of the presented method in Theorem 3.1, a simulation study is conducted for two important lifetime distributions: *Weibull*[1, 2], with scale and shape parameters 1 and 2, respectively, and *Normal*[0, 1]. For each of these distributions, we generate a random sample of size 100. Moreover, for each of these random samples, the lower and upper current record values are picked up and then the corresponding record ranges are computed. By accident, we got the same number, 12, of current records (lower and upper) for the two random samples (i.e., for the two distributions). Table 4 gives these 12 observed values of $U_n^c \parallel X$ and $L_n^c \parallel X$, as well as $R_n^c \parallel X$, where $X \sim Weibull[1, 2]$, or $X \sim Normal[0, 1]$. Now, we assume that we have only observed the first 9 values of current records (lower and upper) (i.e., 75% of the observed values of the current records) and we want to predict the three next ones (i.e., 25% of the observed values of the current records). Theorem 3.1 enables us to get predictive confidence intervals for these three next values. Tables 5 and 6 give these predictive confidence intervals for $U_{9+m}^c \parallel X$, $L_{9+m}^c \parallel X$ and $R_{9+m}^c \parallel X$, where $m = 1, 2, 3$, for the cdf's $X \sim Weibull[1, 2]$ and $X \sim Normal[0, 1]$, respectively.

Algorithm

Step 1: select the cdf F_X from which the data will come,

Step 2: choose the values of N ,

Step 3: generate a random sample of size N from F_X ,

Step 4: pick up the lower and upper current record values from the observed data and compute the corresponding record range values. Let the number of the observed lower and upper current record values be n . Choose the value of M , which is about 25% of n ,

Step 5: choose a significant coefficient θ and numerically solve the equation

$$\int_0^{t_{m:\theta}} f(t)dt = 1 - \theta, m = 1, 2, \dots, M,$$

using (3.1) (after replacing n in (3.1) by $n - M$) and Mathematica 8,

Step 6: determine the lower and upper bounds of the predictive confidence intervals for $U_{n-M+m}^c \parallel X$, $L_{n-M+m}^c \parallel X$ and $R_{n-M+m}^c \parallel X$, $m = 1, 2, \dots, M$, by using Theorem 3.1 and the step 5.

The presented results in Tables 5 and 6 show that all the true values of $U_{9+m}^c \parallel X$, $L_{9+m}^c \parallel X$ and $R_{9+m}^c \parallel X$, where $m = 1, 2$, are included in their predictive confidence intervals for the two cdf's $X \sim Weibull[1, 2]$ and $X \sim Normal[0, 1]$. Moreover, almost, the true values of these statistics are also included in their predictive confidence intervals for the two cdf's, for $m = 3$. Nevertheless, the length of the predictive confidence interval increases (i.e., we get less accuracy) with increasing the value of m , i.e. the number of the unobserved data is increased. Therefore, we advise predicting no more than one fourth of the data that we have.

Table 4: Current records and record range from Weibull[1, 2] and Normal[0, 1].

Weibull[1, 2]				Normal[0, 1]			
n	U_n^c	L_n^c	R_n^c	n	U_n^c	L_n^c	R_n^c
1	3.84915	3.84915	0	1	-0.187968	-0.187968	0
2	3.84915	0.446312	3.402838	2	-0.187968	-0.35455	0.166582
3	5.64291	0.446312	5.196598	3	0.1652	-0.35455	0.51975
4	5.64291	0.375142	5.267768	4	0.1652	-1.21013	1.37533
5	5.64291	0.192999	5.449911	5	1.40996	-1.21013	2.62009
6	6.1647	0.192999	5.971701	6	1.40996	-1.37108	2.78104
7	10.2282	0.192999	10.035201	7	1.40996	-1.66077	3.07073
8	10.2282	0.108285	10.119915	8	2.07656	-1.66077	3.73733
9	10.2282	0.0235643	10.2046357	9	2.07656	-1.90336	3.97992
10	10.5855	0.0235643	10.5619357	10	2.10684	-1.90336	4.0102
11	12.9219	0.0235643	12.8983357	11	2.10684	-2.15466	4.2615
12	12.9219	0.0202959	12.9016041	12	2.96574	-2.15466	5.1204

Table 5: Predictive confidence intervals for the next three observations of current records and record range from Weibull[1, 2], with different significance levels (SL's) 90%, 95% and 99%.

for $m = 1$	SL = 90%	SL = 95%	SL = 99%
U_{10}^c	(10.2282,12.6528)	(10.2282,13.5042)	(10.2282,15.7315)
L_{10}^c	(0.00818032,0.0235643)	(0.00564575,0.0235643)	(0.00214174,0.0235643)
R_{10}^c	(10.2046357,12.6446)	(10.2046357,13.4986)	(10.2046357,15.7294)
for $m = 2$	SL = 90%	SL = 95%	SL = 99%
U_{11}^c	(10.2282,14.4456)	(10.2282,15.6123)	(10.2282,18.5781)
L_{11}^c	(0.00374765,0.0235643)	(0.00225577,0.0235643)	(0.000621026,0.0235643)
R_{11}^c	(10.2046357,14.4418)	(10.2046357,15.61)	(10.2046357,18.5774)
for $m = 3$	SL = 90%	SL = 95%	SL = 99%
U_{12}^c	(10.2282,16.1157)	(10.2282,17.558)	(10.2282,21.1813)
L_{12}^c	(0.00181212,0.0235643)	(0.000967742,0.0235643)	(0.000200224,0.0235643)
R_{12}^c	(10.2046357,16.1139)	(10.2046357,17.577)	(10.2046357,21.1811)

Table 6: Predictive confidence intervals for the next three observations of current records and record range from Normal[0, 1], with different SL's 90%, 95% and 99%.

for $m = 1$	SL = 90%	SL = 95%	SL = 99%
U_{10}^c	(2.07656,2.43784)	(2.07656,2.55498)	(2.07656,2.84252)
L_{10}^c	(-2.24886,-1.90336)	(-2.36081,-1.90336)	(-2.63544,-1.90336)
R_{10}^c	(3.97992,4.6867)	(3.97992,4.91579)	(3.97992,5.47796)
for $m = 2$	SL = 90%	SL = 95%	SL = 99%
U_{11}^c	(2.07656,2.67961)	(2.07656,2.82774)	(2.07656,3.17785)
L_{11}^c	(-2.47987,-1.90336)	(-2.62134,-1.90336)	(-2.9555,-1.90336)
R_{11}^c	(3.97992,5.15948)	(3.97992,5.44908)	(3.97992,6.13335)
for $m = 3$	SL = 90%	SL = 95%	SL = 99%
U_{12}^c	(2.07656,2.88969)	(2.07656,3.06129)	(2.07656,3.45983)
L_{12}^c	(-2.68049,-1.90336)	(-2.84427,-1.90336)	(-3.22445,-1.90336)
R_{12}^c	(3.97992,5.57018)	(3.97992,5.90556)	(3.97992,6.68428)

5. The case when the cdf F is unknown and real data example

Undoubtedly the lack of knowledge of the distribution of the resulted data in any statistical experiment is the most frequent case. In fact the assumption that the distribution F is known is unreal. However, we can overcome this problem by using the observed data that we have (i.e., X_1, X_2, \dots, X_N) to select a statistical distribution that best fits this data set. Actually, we cannot “just guess” and use any other particular distribution without testing several alternative models as this can result in analysis errors. In most cases, we need to fit two or more distributions, compare the results, and select the most valid model (see Example 5.1). Naturally, the “candidate” distributions we fit should be chosen depending on the nature of our observed data. For example, in the case of a life testing experiment we should fit non-negative distributions such as Gamma or Weibull. Obviously when this procedure is applied, all we need, is that the size N of the observed data to be large enough to carry the necessary identification methods (e.g., build a histogram) and goodness-of-fit tests (e.g., the Kolmogorov-Smirnov test) based on the empirical cdf of X_1, \dots, X_N . In Example 5.1, we consider $N = 130$ realistic observations (cf. Arnold, et al. 1998, Page 49) with unknown distribution. These data yield 14 current records (lower-upper). The first 11 of them resulted from the first 48 observations. Thus, we look for the best distribution F that fits these data (the 48 observations). After that we predict the last three current records and their corresponding record ranges by applying the results of Theorem 3.1 on the first 11 current records and their corresponding record ranges. We find almost all the predictions are accurate even when we select another fitted distribution for the data but with less goodness-of-fit to the data than the first one.

Example 5.1. The following data (read row-wise) represent the average July temperatures (in degrees centigrade) of Neuenburg, Switzerland, during the period 1864-1993 (from Kluppelberg and Schwere, 1995).

```

19.0 20.1 18.4 17.4 19.7 21.0 21.4 19.2 19.9 20.4 20.9 17.2 20.2 17.8 18.1
15.6 19.4 21.7 16.2 16.4 19.0 20.6 19.0 20.7 15.8 17.7 16.8 17.1 18.1 18.4
18.7 18.7 18.4 19.2 18.0 18.7 20.7 19.4 19.2 17.4 22.0 21.4 19.3 16.8 18.2
16.2 15.9 22.1 17.5 15.3 16.5 17.4 17.0 18.3 18.3 15.3 18.2 21.5 17.0 21.6
18.2 18.1 17.6 18.2 22.6 19.9 17.1 17.2 17.3 19.4 20.1 20.1 17.0 19.4 17.5
16.8 17.0 19.9 18.2 19.2 18.5 20.8 19.5 21.1 15.8 21.3 21.2 18.8 22.3 18.6
16.8 18.2 17.2 18.4 18.7 21.1 16.3 17.4 18.0 19.5 21.2 16.8 17.4 20.7 18.4
19.8 18.7 20.5 18.3 18.2 18.2 19.2 20.2 18.2 17.4 19.2 16.3 17.4 20.3 23.4
19.2 20.2 19.3 19.0 18.8 20.3 19.7 20.7 19.6 18.1

```

The above data yield 14 current records. These current records and their corresponding record ranges are presented in Table 7. First, we try to fit the first 48 observations, for several cdf's such as exponential, logistic, Gamma, normal, Weibull, Gumbel, Laplace

and inverse Gamma distributions. The methods of maximum likelihood and moments are used to estimate the parameters of the candidate cdf's. After that we apply the Anderson-Darling, Cramér-von Mises, and Kolmogorov-Smirnov goodness of fit tests to check the fitting of these cdf's. Among these cdf's, we found that only the Gamma, normal and logistic distributions fit these data. Moreover, the *Gamma*[119.277, 0.157808] distribution is the best cdf that fits these data (in the average w.r.t the three applied goodness of fit tests and the two used methods of estimation) the second cdf is *Normal* [18.8229, 1.71722], while the third is logistic distribution *Logistic*[18.8205, 1.01236], see Tables 8-10 and Figures 1-3. The predictive confidence intervals for the next three statistics U_{11+m}^c, L_{11+m}^c and $R_{11+m}^c, m = 1, 2, 3$, for the Gamma, normal and logistic cdf's are represented in Tables 11-13, respectively. These tables show that almost all the true values of the above three statistics are included in the predictive confidence intervals. This result shows that our suggested method is stable regardless the choice of the cdf that fits the data.

Table 7: Current records and record ranges which are resulted from all our data.

n	1	2	3	4	5	6	7	8	9	10	11	12	13	14
U_n^c	19.0	20.1	20.1	20.1	21.0	21.4	21.4	21.4	21.7	22.0	22.1	22.1	22.6	23.4
L_n^c	19.0	19.0	18.4	17.4	17.4	17.4	17.2	15.6	15.6	15.6	15.6	15.3	15.3	15.3
R_n^c	0	1.1	1.7	2.7	3.6	4.0	4.2	5.8	6.1	6.4	6.5	6.8	7.3	8.1

Table 8: Fitting the first 48 observations for gamma cdf.

Distribution/Test-Method	Gamma[α, β]	
Maximum Likelihood	$\hat{\alpha}_{ML} = 119.277$ $\hat{\beta}_{ML} = 0.157808$	
	P-Value	Statistic
Kolmogorov-Smirnov	0.995234	0.0569809
Anderson-Darling	0.977713	0.235002
Cramér-Von-Mises	0.983675	0.0274912
Moments	$\hat{\alpha}_M = 120.149$ $\hat{\beta}_M = 0.156663$	
	P-Value	Statistic
Kolmogorov-Smirnov	0.994289	0.0578043
Anderson-Darling	0.974785	0.241202
Cramér-Von-Mises	0.981763	0.0281783

Table 9: Fitting the first 48 observations for normal cdf.

Distribution/Test-Method	Normal[μ, σ]	
Maximum Likelihood	$\hat{\mu}_{ML} = 18.8229$ $\hat{\sigma}_{ML} = 1.71722$	
	<i>P-Value</i>	<i>Statistic</i>
Kolmogorov-Smirnov	0.994086	0.0579686
Anderson-Darling	0.982812	0.222963
Cramér-Von-Mises	0.987088	0.0261305
Moments	$\hat{\mu}_M = 18.8229$ $\hat{\sigma}_M = 1.71722$	
	<i>P-Value</i>	<i>Statistic</i>
Kolmogorov-Smirnov	0.994086	0.0579686
Anderson-Darling	0.982812	0.222963
Cramér-Von-Mises	0.987088	0.0261305

Table 10: Fitting the first 48 observations for logistic cdf.

Distribution/Test-Method	Logistic[μ, β]	
Maximum Likelihood	$\hat{\mu}_{ML} = 18.8205$ $\hat{\beta}_{ML} = 1.01236$	
	<i>P-Value</i>	<i>Statistic</i>
Kolmogorov-Smirnov	0.98876	0.061264
Anderson-Darling	0.964482	0.260431
Cramér-Von-Mises	0.979247	0.02903
Moments	$\hat{\mu}_M = 18.8229$ $\hat{\beta}_M = 0.946754$	
	<i>P-Value</i>	<i>Statistic</i>
Kolmogorov-Smirnov	0.927317	0.0756047
Anderson-Darling	0.838543	0.409448
Cramér-Von-Mises	0.882778	0.0489246

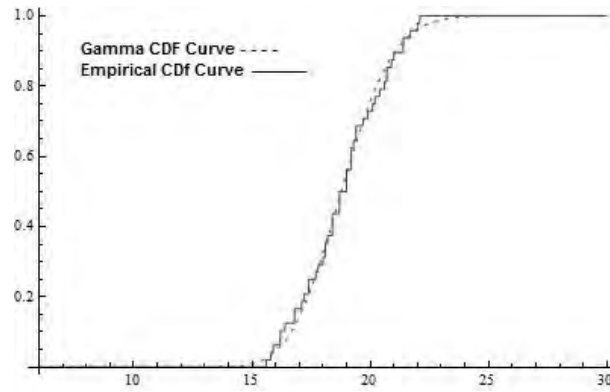


Figure 1: Plot showing the goodness-of-fit for gamma cdf.

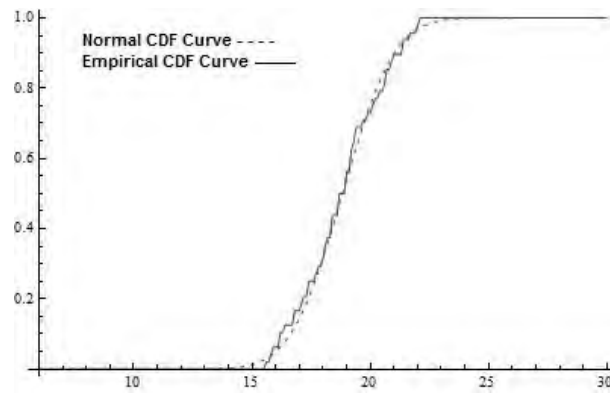


Figure 2: Plot showing the goodness-of-fit for normal cdf.

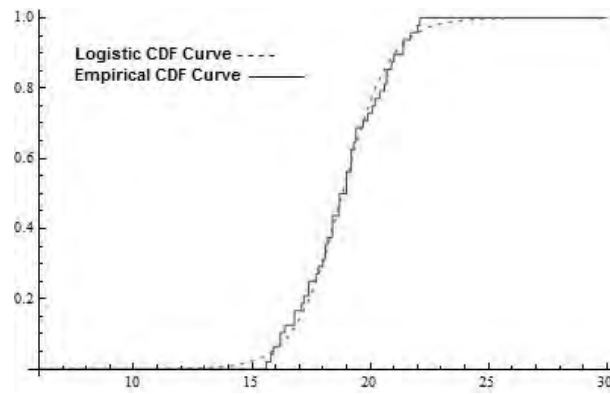


Figure 3: Plot showing the goodness-of-fit for logistic cdf.

Table 11: Predictive confidence intervals for U_{11+m}^c, L_{11+m}^c and R_{11+m}^c , $m = 1, 2, 3$, from $\text{Gamma}[119.277, 0.157808]$.

for $m = 1$	$SL = 90\%$	$SL = 95\%$	$SL = 99\%$
U_{12}^c	(22.1,22.6482)	(22.1,22.8253)	(22.1,23.2593)
L_{12}^c	(15.1588,15.6)	(15.0195,15.6)	(14.6846,15.6)
R_{12}^c	(6.5,7.4894)	(6.5,7.8058)	(6.5,8.5747)
for $m = 2$	$SL = 90\%$	$SL = 95\%$	$SL = 99\%$
U_{13}^c	(22.1,23.021)	(22.1,23.2463)	(22.1,23.7782)
L_{13}^c	(14.8674,15.6)	(14.6945,15.6)	(14.2959,15.6)
R_{13}^c	(6.5,8.1536)	(6.5,8.5516)	(6.5,9.4823)
for $m = 3$	$SL = 90\%$	$SL = 95\%$	$SL = 99\%$
U_{14}^c	(22.1,23.3496)	(22.1,23.6122)	(22.1,24.222)
L_{14}^c	(14.6161,15.6)	(14.4189,15.6)	(13.9732,15.6)
R_{14}^c	(6.5,8.7335)	(6.5,9.1933)	(6.5,10.2488)

Table 12: Predictive confidence intervals for U_{11+m}^c, L_{11+m}^c and R_{11+m}^c , $m = 1, 2, 3$, from $\text{Normal}[18.8229, 1.71722]$.

for $m = 1$	$SL = 90\%$	$SL = 95\%$	$SL = 99\%$
U_{12}^c	(22.1,22.5884)	(22.1,22.756)	(22.1,23.1421)
L_{12}^c	(15.107,15.6)	(14.9494,15.6)	(14.5665,15.6)
R_{12}^c	(6.5,7.4814)	(6.5,7.8066)	(6.5,8.5756)
for $m = 2$	$SL = 90\%$	$SL = 95\%$	$SL = 99\%$
U_{13}^c	(22.1,22.9307)	(22.1,23.1306)	(22.1,23.5979)
L_{13}^c	(14.7762,15.6)	(14.578,15.6)	(14.1147,15.6)
R_{13}^c	(6.5,8.1545)	(6.5,8.5526)	(6.5,9.4832)
for $m = 3$	$SL = 90\%$	$SL = 95\%$	$SL = 99\%$
U_{14}^c	(22.1,23.2219)	(22.1,23.4528)	(22.1,23.9826)
L_{14}^c	(14.4875,15.6)	(14.2586,15.6)	(13.7333,15.6)
R_{14}^c	(6.5,8.7344)	(6.5,9.1942)	(6.5,10.2493)

Table 13: Predictive confidence intervals for U_{11+m}^c, L_{11+m}^c and R_{11+m}^c , $m = 1, 2, 3$, from $Logistic[18.8205, 1.01236]$.

for $m = 1$	$SL = 90\%$	$SL = 95\%$	$SL = 99\%$
U_{12}^c	(22.1,22.77)	(22.1,22.997)	(22.1,23.5757)
L_{12}^c	(14.9403,15.6)	(14.7169,15.6)	(14.1475,15.6)
R_{12}^c	(6.5,7.8297)	(6.5,8.2801)	(6.5,9.4282)
for $m = 2$	$SL = 90\%$	$SL = 95\%$	$SL = 99\%$
U_{13}^c	(22.1,23.2539)	(22.1,23.5578)	(22.1,24.3102)
L_{13}^c	(14.4641,15.6)	(14.1651,15.6)	(13.4251,15.6)
R_{13}^c	(6.5,8.7898)	(6.5,9.3927)	(6.5,10.8851)
for $m = 3$	$SL = 90\%$	$SL = 95\%$	$SL = 99\%$
U_{14}^c	(22.1,23.7001)	(22.1,24.0702)	(22.1,24.9755)
L_{14}^c	(14.0251,15.6)	(13.6612,15.6)	(12.771,15.6)
R_{14}^c	(6.5,9.675)	(6.5,10.409)	(6.5,12.2045)

6. Conclusion

In this paper we focused on the prediction of upper and lower records. The obtained results are useful when people are interested in knowing extreme values on different periods, areas, etc. and their range of variation. Theorem 3.1 suggests a new method to estimate confidence intervals for upper, lower and range records. This new method depends on constructing two pivotal statistics with the same distribution for lower and upper current records. The real data Example 5.1, shows that when the cdf of the data is unknown, this method is applicable with acceptable degree of accuracy, even if we fail to assign the type of the distribution of the data with a high accuracy. It is worth mentioning that the result and the method of the proofs of this paper are quite different from the known results concerning the prediction problems of record values. For example, Ahmadi and Balakrishnan (2004) used only the current records to estimate the fixed quantiles of the given cdf (unknown cdf), while Raqab and Balakrishnan (2008) obtained distribution-free prediction intervals for the usual records (not the current records). Finally Raqab (2009) predicted the current records, by using the two-sample prediction plan, where the variable to be predicted comes from an independent future sample. In this paper, we consider the one-sample prediction plan, where the variable to be predicted comes from the same sample so that it may be correlated with the observed data.

Acknowledgement

The authors would like to thank the anonymous referees for constructive suggestions and comments that improved the representation substantially.

Appendix

Proof of Lemma 3.1. By using (2.2), we get

$$\begin{aligned} P(U_{n+m}^* \leq x | U_n^* = y) &= P(Y_0 + Y_1 + \dots + Y_n + \dots + Y_{n+m} \leq x | Y_0 + Y_1 + \dots + Y_n = y) \\ &= P(Y_{n+1} + \dots + Y_{n+m} \leq x - y | Y_0 + Y_1 + \dots + Y_n = y) = P(Y_{n+1} + \dots + Y_{n+m} \leq x - y). \end{aligned} \quad (1)$$

On the other hand, since $Y_i \sim \text{EX}(1)$, for $i = n + 1, \dots, n + m$, then

$$f_{U_{n+m}^* | U_n^*}(x | y) = f_{Y_{n+1} + \dots + Y_{n+m}}(x - y) = \frac{(x - y)^{m-1}}{(m - 1)!} e^{-(x-y)} I_{(0, \infty)}(x - y), \quad (2)$$

where $I_A(\cdot)$ is the usual indicator function of the set A . Therefore, by combining (1) and (2) with (2.1), we get

$$\begin{aligned} f_{U_{n+m}^*, U_n^*}(x, y) &= f_{U_{n+m}^* | U_n^*}(x | y) f_{U_n^*}(y) \\ &= \frac{(x - y)^{m-1}}{(m - 1)!} e^{-(x-y)} 2^n \left(\frac{1}{2} e^{-y/2}\right) \left[1 - e^{-y/2} \sum_{k=0}^{n-1} \frac{(-\log e^{-y/2})^k}{k!}\right] \\ &= \frac{2^{n-1} (x - y)^{m-1} e^{-(x-y/2)}}{(m - 1)!} \left[1 - e^{-y/2} \sum_{k=0}^{n-1} \frac{y^k}{2^k k!}\right]. \end{aligned} \quad (3)$$

Now, by using the transformation $\bar{T}_m = \frac{U_{n+m}^* - U_n^*}{U_n^*}$ and $W = U_n^*$, we get

$$f_{\bar{T}_m, W}(t, w) = \frac{2^{n-1} w^m t^{m-1} e^{-w(t+\frac{1}{2})}}{(m - 1)!} - \frac{2^{n-1} t^{m-1} e^{-w(t+1)}}{(m - 1)!} \sum_{k=0}^{n-1} \frac{w^{k+m}}{2^k k!}.$$

Thus, we conclude that

$$f_{\bar{T}_m}(t) = \int_0^\infty f_{\bar{T}_m, W}(t, w) dw = \frac{2^{n-1} m t^{m-1}}{(t + \frac{1}{2})^{m+1}} - \sum_{k=0}^{n-1} \binom{k + m}{k} \frac{2^{n-k-1} m t^{m-1}}{(t + 1)^{k+m+1}}.$$

Similarly, we can show, for any $x \leq z \leq 0$, that $P(L_{n+m}^* \leq x | L_n^* = z) = P(Z_{n+1} + \dots + Z_{n+m} \leq x - z)$. Since $Z_i \sim \text{EX}^+(1)$, for $i = n + 1, \dots, n + m$, then

$$f_{L_{n+m}^* | L_n^*}(x | z) = f_{Z_{n+1} + \dots + Z_{n+m}}(x - z) = \frac{(-(x - z))^{m-1}}{(m-1)!} e^{(x-z)} I_{(-\infty, 0)}(x - z).$$

Thus,

$$\begin{aligned} f_{L_{n+m}^*, L_n^*}(x, z) &= f_{L_{n+m}^* | L_n^*}(x | z) f_{L_n^*}(z) \\ &= \frac{2^{n-1} (-(x - z))^{m-1} e^{(x-z/2)}}{(m-1)!} \left[1 - e^{z/2} \sum_{k=0}^{n-1} \frac{(-z)^k}{2^k k!} \right], \quad x \leq z \leq 0. \end{aligned}$$

Now, by using the transformation $T_m = \frac{L_{n+m}^* - L_n^*}{L_n^*}$ and $V = L_n^*$, we get

$$f_{T_m, V}(t, v) = \frac{2^{n-1} (-v)^m t^{m-1} e^{v(t+\frac{1}{2})}}{(m-1)!} - \frac{2^{n-1} t^{m-1} e^{v(t+1)}}{(m-1)!} \sum_{k=0}^{n-1} \frac{(-v)^{k+m}}{2^k k!}, \quad v \leq 0, t \geq 0.$$

Then, we conclude that

$$f_{T_m}(t) = \int_{-\infty}^0 f_{T_m, V}(t, v) dv = \frac{2^{n-1} m t^{m-1}}{(t + \frac{1}{2})^{m+1}} - \sum_{k=0}^{n-1} \binom{k+m}{k} \frac{2^{n-k-1} m t^{m-1}}{(t+1)^{k+m+1}}.$$

This completes the proof. □

Proof of Lemma 3.2. Clearly, (3) yields

$$f_{U_n^*, U_{n-1}^*}(y_n, y_{n-1}) = 2^{n-2} e^{-(y_n - y_{n-1}/2)} \left[1 - e^{-y_{n-1}/2} \sum_{k=0}^{n-2} \frac{(y_{n-1}/2)^k}{k!} \right].$$

On the other hand, by applying the same argument as in Lemma 3.1, we can show that

$$\begin{aligned} &P(U_n^* \leq y_n, U_{n-1}^* \leq y_{n-1} | U_{n-2}^* = y_{n-2}) \\ &= P(Y_{n-1} + Y_n \leq y_n - y_{n-2}, Y_{n-1} \leq y_{n-1} - y_{n-2} | Y_0 + Y_1 + \dots + Y_{n-2} = y_{n-2}) \\ &= P(Y_{n-1} + Y_n \leq y_n - y_{n-2}, Y_{n-1} \leq y_{n-1} - y_{n-2}). \end{aligned}$$

Since, $f_{Y_{n-1}, Y_n}(y_{n-1}, y_n) = e^{-y_{n-1} - y_n}$, we get

$$f_{Y_{n-1}, Y_{n-1} + Y_n}(y_{n-1} - y_{n-2}, y_n - y_{n-2}) = e^{-(y_n - y_{n-2})}, \quad y_{n-2} < y_{n-1} < y_n.$$

Therefore, $f_{U_n^*, U_{n-1}^* | U_{n-2}^*}(y_n, y_{n-1} | y_{n-2}) = e^{-(y_n - y_{n-2})}$, which by using (2.1) implies

$$\begin{aligned} f_{U_n^*, U_{n-1}^*, U_{n-2}^*}(y_n, y_{n-1}, y_{n-2}) &= e^{-(y_n - y_{n-2})} f_{U_{n-2}^*}(y_{n-2}) \\ &= 2^{n-3} e^{-(y_n - y_{n-2}/2)} \left[1 - e^{-y_{n-2}/2} \sum_{k=0}^{n-3} \frac{(y_{n-2}/2)^k}{k!} \right]. \end{aligned}$$

Therefore, by induction we get the claimed result for the upper current records and the result for the lower current records can be proved by applying the same argument. \square

Proof of Lemma 3.3. Since the proof of the lemma for the two sequences $\{U_n^c \parallel X\}$ and $\{L_n^c \parallel X\}$ are very similar, we only prove the lemma for the 1st sequence. For any two positive integers $t < s$, we can easily, by applying the same argument in the proof of Lemmas 3.1, 3.2, to show that

$$\begin{aligned} P(U_s^c \parallel X \leq x_s | U_1^c \parallel X = x_1, \dots, U_t^c \parallel X = x_t) \\ = P(U_s^* \leq x_s^* | U_1^* = x_1^*, \dots, U_t^* = x_t^*) = P(Y_{t+1} + \dots + Y_s \leq x_s^* - x_t^*), \end{aligned}$$

where $x_i^* = -2 \log[\bar{F}_X(x_i)]$, $i = t, s$. Therefore,

$$f_{U_s^c \parallel X | U_1^c, \dots, U_t^c \parallel X}(x_s | x_1, \dots, x_t) = \frac{(x_s^* - x_t^*)^{m-1}}{(m-1)!} e^{-(x_s^* - x_t^*)} I_{(0, \infty)}(x_s^* - x_t^*).$$

This completes the proof. \square

References

Ahmadi, J. and Balakrishnan, N. (2011). Distribution-free prediction intervals for order statistics based on record coverage. *Korean Statistical Society*, 40, 181–192.

Ahmadi, J. and Balakrishnan, N. (2008). Prediction intervals for future records. *Statistics & Probability Letters*, 78, 395–405.

Ahmadi, J. and Balakrishnan, N. (2004). Confidence intervals for quantiles in terms of record range. *Statistics & Probability Letters*, 68, 1955–1963.

Arnold, B. C., Balakrishnan, N. and Nagaraja, H. N. (1998). *Records*. Wiley, New York.

Basak, P. (2000). An application of record range and some characterization results. In: Balakrishnan, N. (ed.) *Advances on Methodological and Applied Aspects of Probability and Statistics*. Gordon and Breach Science Publishers, New York: 83–95.

Houchens, R. L. (1984). *Record Value, Theory and Inference*, Ph. D. Dissertation, University of California, Riverside, CA.

Raqab, M. R. (2009). Distribution-free prediction intervals for the future current record statistics. *Statistical Papers*, 50, 429–439.

Balancing properties: A need for the application of propensity score methods in estimation of treatment effects

Arantza Urkaregi^{1,2}, Lorea Martinez-Indart^{2,3} and José Ignacio Pijoán^{2,3,4}

Abstract

There has been recently a striking increase in the use of propensity score methods in health sciences research as a tool to adjust for selection bias in making causal inferences from observational controlled studies. However, reviews of published studies that use these techniques suggest that investigators often do not pay proper attention to thorough verification of appropriate fulfilment of propensity score adjusting properties. By using a case study in which balance is not achieved, we illustrate the need to systematically assess the accomplishment of the balancing property of the propensity score as a critical requirement for obtaining unbiased treatment effects estimates.

MSC: 62P10, 62J12, 62G10.

Keywords: Propensity score, balancing score, treatment effect.

1. Introduction

In assessing the impact of a clinical intervention an experimental approach through the use of a randomized trial is always regarded as a reference of optimum design leading to the highest quality evidence if properly conducted (D'Agostino and D'Agostino, 2007; Friedman, Furberg and DeMets, 1998). Randomized assignment of alternative interventions minimizes the risk of selection bias (confounding by indication) (Walker, 1996)

¹ Department of Applied Mathematics, Statistics and Operational Research. University of the Basque Country (UPV/EHU). E-mail: arantza.urkaregi@ehu.es

² BioCruces Health Research Institute

³ Clinical Epidemiology Unit-Cruces University Hospital

⁴ Network Biomedical Research Centre for Epidemiology and Public Health (CIBERESP), Instituto de Salud Carlos III, Madrid, Spain

Received: September 2013

Accepted: July 2014

and therefore maximizes internal validity of the causal inferences. Unfortunately, many times ethical, economic or practical reasons impede the use of this experimental design.

The effect of many interventions is instead assessed using observational studies. In non-experimental designs it is necessary to take into account the potential existence of selection bias due to the fact that groups to be compared are not genuinely “comparable” (Grimes and Schulz, 2002). The treatment or intervention any individual receives can be influenced by a mix of measurable and immeasurable factors. We might consider among them, physician preference or belief about the specific effect of a given intervention according to the patient profile, local clinical practice patterns or patient preferences and values. Propensity scores (PS) techniques (Rosenbaum and Rubin, 1983) conform a set of statistical methods devised to minimize this bias.

Although the original paper written by Rosenbaum and Rubin addressed a clinical problem as an example of application, this method has been scarcely used in the health sciences until the last decade. A substantial increase in researchers’ interest in and use of this method has been recently detected (Sturmer et al., 2006).

A search of the term “propensity score” in MEDLINE and EMBASE bibliographic databases permit us confirm this tendency and shows that the number of papers that use this approach keeps exponentially increasing (Figure 1).

By using the PS (the conditional probability of receiving the intervention of interest given the pre-treatment individual covariates) we reduce the multidimensionality of the pre-intervention covariate vector to a single number (scalar) that encapsulates all the original information. All individuals with a given PS are expected to have a homogeneous distribution of relevant baseline characteristics, irrespective of whether or not they have received the intervention of interest. Therefore, it is stated that, conditional on these measured pre-intervention covariates, allocation of interventions can be thought

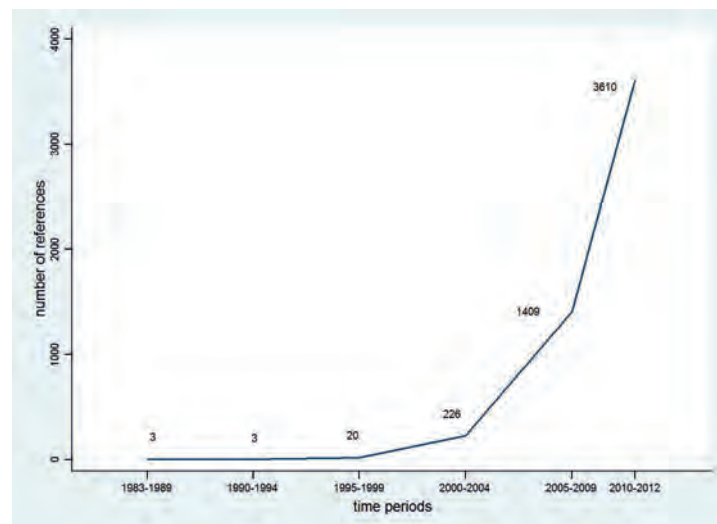


Figure 1: Time distribution of publications that include the “propensity score” term.

of as a random process, similar to what happens in a clinical or community trial (Austin, 2011).

One of the theoretical foundations of the adjusting ability of the PS is that it is a balancing score, (Rosenbaum and Rubin, 1983). It implies both, that PS achieves homogeneous covariate distributions between groups and that given the PS, treatment received and covariates are conditionally independent. However, in many cases, the fulfilment of the balancing property of the empirically estimated PS is not systematically assessed (Weitzen et al., 2004). When this is the case there is no real guarantee that the covariates making for the PS are actually adequately balanced; this can, in turn, lead to unfair comparisons. It has been proved (Rosenbaum and Rubin, 1983) that the PS is a balancing score but authors warned that in certain practical conditions that balance cannot be reached. In this article we present a case study in which proper balance could not be achieved because of the highly deterministic nature (lack of significant uncertainty) of the treatment assignment process. If that happens, PS-based methods should not be used to estimate treatment effects.

Methodology

Data description

We analysed data from a clinical cohort of 4,339 neonates with respiratory problems due to prematurity. Some of them were given pulmonary surfactant, a tensioactive substance which improves the mechanics of breathing. Our aim was to estimate the effect of this medical intervention on probability of death during the first 28 postnatal days.

Estimation of PS

PS is defined as the conditional probability of receiving a given treatment conditional on the observed pre-treatment characteristics of the individual. In our step by step PS estimation process every recorded pre-treatment covariate deemed to be important by clinicians with regard to clinical management and treatment of breathing problems in prematurity and/or early prognosis was first pre-selected. Separate bivariate logistic regression models were then fitted to assess the relationship of each pre-selected covariate firstly with treatment received (pulmonary surfactant) and then with outcome (death in the first 28 days after birth). The PS is ultimately estimated from a multivariable binary logistic regression with treatment received as the dependent variable and predictor variables selected from the previous steps. We first included all physician recommended covariates that were shown to be associated with the outcome in previous bivariate models, irrespective of their relationship with the treatment choice (Brookhart et al., 2006). Then, through a manual, step by step, backward approach, variables that were not statistically significant in the multivariable model were removed until the final estimation model was obtained. Predicted probabilities from this model represent the estimated PS.

After PS estimation, we proceeded to check for the existence and pattern of overlapping (common support) in PS values between individuals in comparing groups. PS methods rely on the so-called “counterfactual or potential outcomes” framework (Oakes and Johnson, 2006). For each individual and intervention, there are two potentially observable outcomes: one if she receives the study intervention and another if she does not receive it. The natural effect of the intervention on the subject would be obtained as the difference between these two potential outcomes. In practice, however, only one outcome can be actually observed as the individual either does or does not receive the intervention of interest. Lacking the natural reference for comparison (the same individual in the counterpart situation), we must ensure a proper comparison group exists as a proxy for this unobservable counterfactual experience.

Ensuring that for each selected interval of PS values there are both treated and untreated individuals (Caliendo and Kopeining, 2008) is a required criterion that comparable experience is available, enabling causal inference and estimation of intervention effects. With real data, it is commonplace to find, especially at the tails of the PS distribution, regions where only treated or untreated individuals are found. This finding affects comparability of groups (also referred to as positivity) and produces biased estimates, based partly on extrapolations (Shadish and Steiner, 2010). To appraise the observed degree of overlapping achieved we used descriptive statistics and graphical tools that help inspect the empirical distributions of estimated PS among each treatment group (histograms and box-plots) and took special care in inspecting the tails of the distributions. Additionally nonparametric density estimators (kernel functions) were used to explore and detect potential non-overlapping regions within the whole range of observed PS.

To ensure estimates based on comparable subjects (Pattanayak, Rubin and Zell, 2011), we excluded neonates from the tail areas where there was no overlapping (all untreated neonates whose PS was smaller than the smallest PS in the treated units and all the treated neonates whose PS was larger than the largest PS in the untreated).

Finally balancing properties of the estimated PS were assessed. This is a two-step process: it should be first checked whether the PS is similarly distributed between treated and untreated groups over defined regions across the PS observed range. If this requirement is fulfilled, then assessment of homogeneity of distributions should additionally be performed for each covariate included in the final PS estimation model over the pre-specified regions of observed PS (Adelson, 2013). Only after these two conditions are met we can accept the empirically estimated PS is working adequately as a balancing score.

To do it in practice we started splitting the observed range of PS values into five blocks of equal size (quintiles) (Rosenbaum and Rubin, 1984) and statistically tested the balance of PS between treated and untreated within each block by the use of nonparametric tests (Kolmogorov-Smirnov test). A statistical significance threshold of 0.01 was chosen to account for the chance effect of multiple comparisons (Benjamini and Hochberg, 1995). If balance in PS was not achieved in a specific block, it was further subdivided into two new blocks of the same size and PS balance between the groups was

Table 1: Pre-selected variables and association with treatment and outcome. DR: delivery room. NEC: necrotizing enterocolitis. RDS: respiratory distress syndrome. PIVH: peri/intraventricular haemorrhage. PDA: patent ductus arteriosus. Only statistically significant or marginally significant associations are shown.

Variables associated with treatment	Variables associated with outcome
Gestational age (week and day) ($p < 0.001$)	Gestational age (week and day) ($p < 0.001$)
Mode of delivery ($p < 0.001$)	Mode of delivery ($p < 0.001$)
Gender ($p < 0.001$)	Gender ($p = 0.033$)
Multiple Birth ($p < 0.001$)	—
Apgar test score at 5 minutes ($p < 0.001$)	Apgar test score at 5 minutes ($p < 0.001$)
Endotracheal intubation in DR ($p < 0.001$)	Endotracheal intubation in DR ($p < 0.001$)
Adrenaline /Epinephrine in DR ($p < 0.001$)	Adrenaline /Epinephrine in DR ($p < 0.001$)
Cardiac Compression in DR ($p < 0.001$)	—
Prenatal corticosteroid use ($p < 0.001$)	Prenatal corticosteroid use ($p < 0.001$)
Conventional Ventilation after leaving DR ($p < 0.001$)	Conventional Ventilation after leaving DR ($p < 0.001$)
High Frequency Ventilation after leaving DR ($p = 0.001$)	High Frequency Ventilation after leaving DR ($p < 0.001$)
NEC surgery ($p < 0.001$)	NEC surgery ($p = 0.04$)
RDS ($p < 0.001$)	RDS ($p < 0.001$)
Pneumothorax ($p < 0.001$)	Pneumothorax ($p < 0.001$)
Focal Gastrointestinal Perforation ($p < 0.001$)	—
PIVH grade 3-4 ($p < 0.001$)	PIVH grade 3-4 ($p < 0.001$)
—	Cystic Periventricular Leukomalacia ($p < 0.001$)
Early Bacterial sepsis and/or meningitis (before day 3) ($p < 0.001$)	Early Bacterial sepsis and/or meningitis (before day 3) ($p = 0.078$)
Major Birth Defect ($p = 0.08$)	Major Birth Defect ($p = 0.025$)
PDA Ligation ($p < 0.001$)	—
Indomethacin/Ibuprofen use ($p < 0.001$)	Indomethacin/Ibuprofen use ($p < 0.001$)

again tested (Dehejia and Wahba, 2002; Pattanayak et al., 2011). We proceeded using this strategy in a systematic way in an attempt to achieve proper balance (for both PS and selected covariates) in all blocks as already described.

Results

Table 1 shows recorded pre-treatment variables and their association to treatment use and/or the outcome of interest. Seventeen variables were identified that behaved as true confounders (associated to treatment decision and outcome of interest). One additional variable (Cystic Periventricular Leukomalacia) showed a strong association with death in the first 28 days but was not related to use of surfactant. Those variables were included in the initial, full model to estimate the PS. Four additional variables that showed only significant association with treatment choice were not included (Brookhart et al., 2006; Austin, 2011). The final model retained 13 variables (Table 2).

Table 2: Variables included in the final model.

Mode of delivery
Gender
Endotracheal intubation in DR
Adrenaline /Epinephrine in DR
Prenatal corticosteroid use
Conventional Ventilation after leaving DR
High Frequency Ventilation after leaving DR
NEC surgery
RDS
Pneumothorax
PIVH grade 3-4
Indomethacin/Ibuprofen (therapeutic)
Gestational Age

Table 3: Minimum and maximum values of estimated PS for treated and untreated groups.

	min	max
Untreated	0.0034	0.9970
Treated	0.0059	0.9997

Summary statistics and distributional graphics (not shown) warned about the existence of lack of overlapping between the groups in both tails of the distribution of estimated PS. Table 3 shows minimum and maximum values of PS for both groups. As a consequence 102 untreated neonates in the lower tail and 104 treated neonates in the upper tail were dropped out of the analysis to obtain estimates in the common support region. This area therefore consisted of 4,133 newborns, out of which 1,971 were given surfactant.

A graphical display of the estimated density functions of PS for treated and untreated individuals illustrated the fact that, even after trimming the tails, the overall degree of overlapping was rather small over the whole range of observed PS values. Most treated newborns had very high PS values whereas most untreated ones had very low PS values (Figure 2).

We then split up the PS in quintiles and evaluated the extent of PS balance between groups (Figure 3). Balance based on statistical significance was obtained only in the first and fifth quintiles. Further splitting up the middle quintiles did not correct for the lack of balance in these regions of the PS values. A last additional subdivision of blocks led to a final division in ten blocks which achieved balance at a significance level $\alpha = 0.01$ but still with apparent uneven distribution of groups (Figure 4).

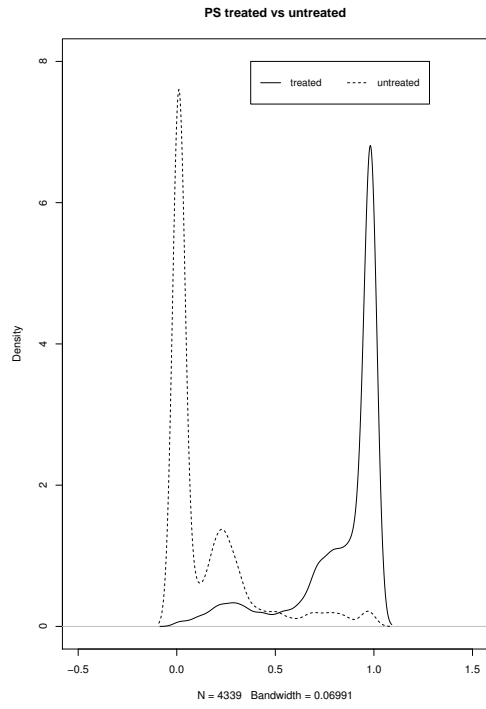


Figure 2: Empirical distribution of PS for treated and untreated newborns (kernel function).

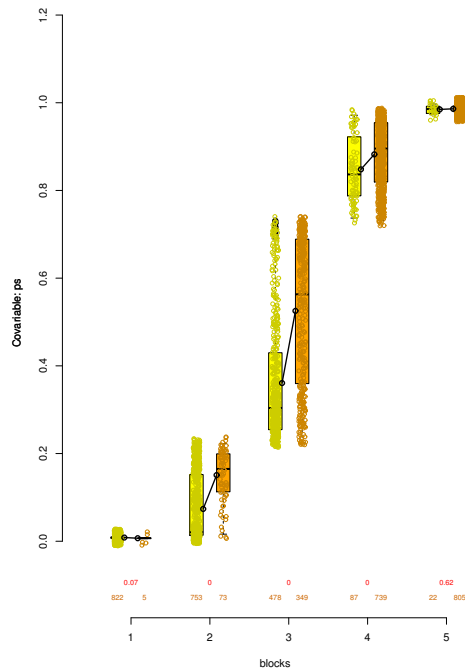


Figure 3: Box-plots of quintiles of estimated PS. Second line over x-axis shows p values (Kolmogorov-Smirnov test of equivalence of distributions). First line, below, displays number of untreated and treated neonates respectively for each quintile.

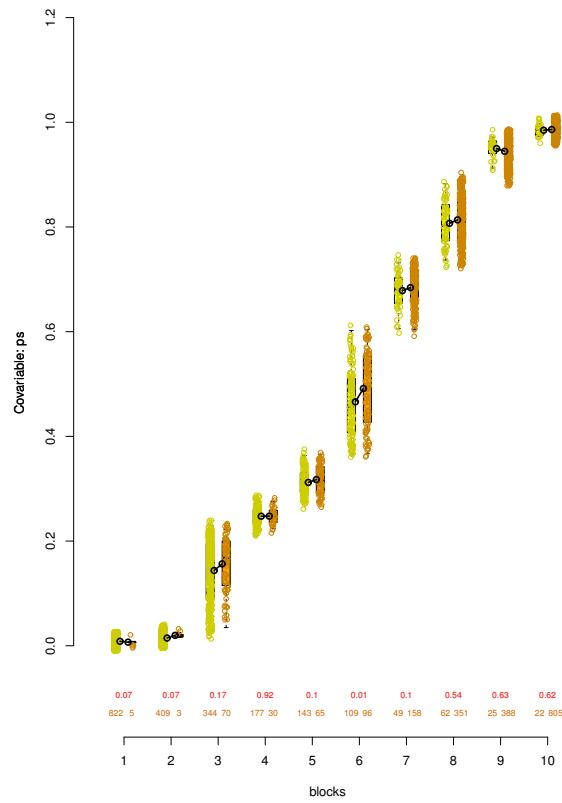


Figure 4: Box-plots of estimated PS split-up in ten subgroups. Second line over x-axis shows p values (Kolmogorov-Smirnov test of equivalence of distributions). First line, below, displays number of untreated and treated neonates respectively for each subgroup (see text for further explanation).

We went on to assess the ability of estimated PS to balance the distributions of individual baseline covariates between treated and untreated. Although reasonable balance seemed to be achieved for some variables, this was not so for some others. Figure 5 displays the comparative distribution of the variable “use of high frequency ventilation after leaving delivery room” showing the scarce number of treated neonates in the lower blocks and the lack of adequate balance in the sixth block ($p < 0.001$).

We decided not to proceed to the effects estimation stage as it was felt our estimated PS did not fulfill the theoretical assumptions required to provide unbiased, reliable adjusted estimates of the effect of surfactant administration on death during the first 28 days after birth.

Discussion

Given the frequent constraints to the conduct of randomized experiments in medicine, it is increasingly common to use observational data to assess the effects of clinical or

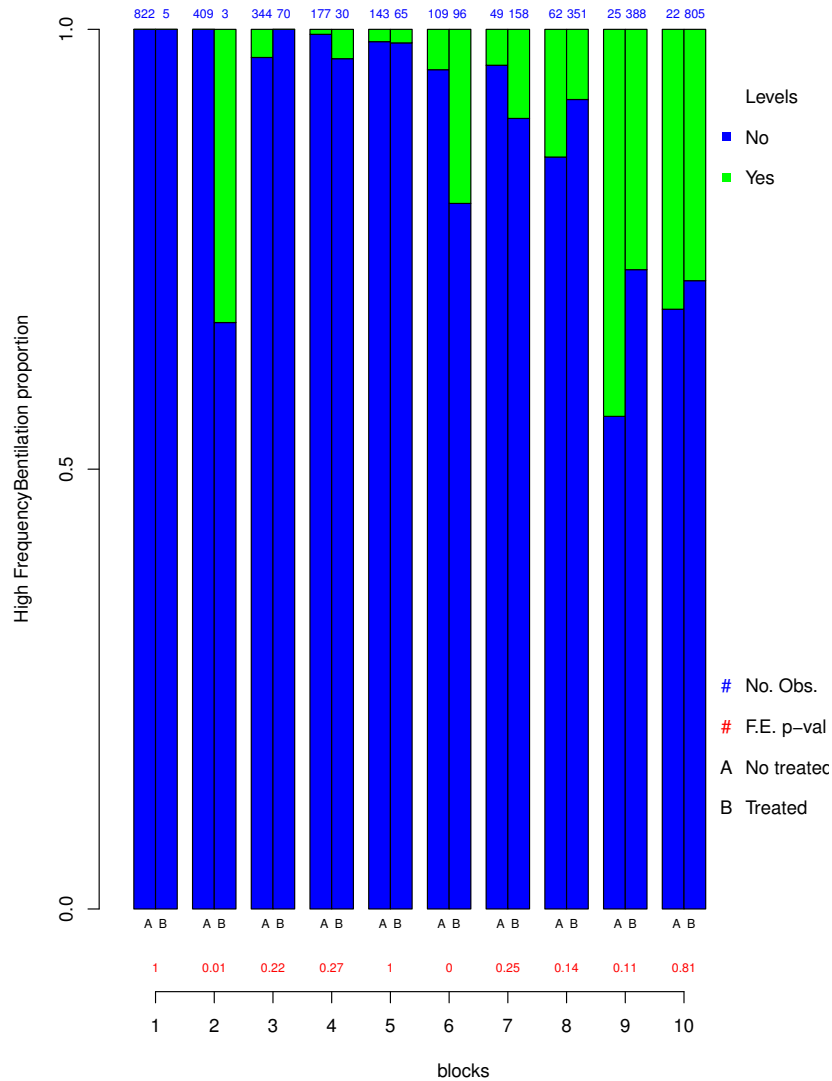


Figure 5: Distribution of the variable “high frequency ventilation” showing the degree of balance achieved across the range of values of estimated PS. Above x-axis p values from exact Fisher test are shown for each block. Above each column, number of individuals is provided for untreated (columns A) and treated newborns (columns B).

public health interventions on relevant health outcomes. In order to minimize the risk of obtaining biased estimates due to existence of unbalanced pre-treatment covariates in the groups to be compared (selection bias), an array of adjustment techniques has been devised (Gang et al., 2012). Among them those based on the PS have been gaining increasing popularity (Sturmer et al., 2006; Klungel et al., 2004). Nowadays there are routines in most popular statistical packages that make it easier to apply PS methods (Klungel et al., 2004; Becker and Ichino, 2002).

Our paper describes, using a case study, the full two-step process that should be undertaken to appropriately check for adequate conditional balance between groups. This process is commonly either not performed or not reported in published applications of these methods. It additionally shows that there may be specific settings where PS based adjustment should not be performed with the available observational data, as the estimated PS does not meet a critical theoretical requirement, namely being a balancing score. We comment on some of the undesired consequences of using PS based adjustment when this requirement is overlooked.

To obtain an empirical PS estimate that behaves as a true balancing score is a key step, dependent on several related factors that should be given proper attention. We would like first to emphasize the need for a correct selection of the covariates to be used in the PS estimation model. This process requires a careful combination of clinical knowledge on the issue at hand, a clearly framed causal pathway that takes into account all relevant information and a comprehensive consideration of the statistical relationships among pre-selected covariates, assignment of treatment and the outcome of interest (Brookhart et al., 2006; Bryson, Dorsett and Purdon, 2013).

One second related aspect is how to best determine that the estimated PS model will make for an appropriate adjustment. As the PS is an estimate of the probability that a given individual receives or not the study treatment and logistic models are commonly used to estimate the PS, it has been common practice to check the adequacy of the model employing standard goodness-of-fit (GOF) diagnostics. In particular, the c-statistic or area under the curve (AUC), an accepted measure of the ability of the model's predicted values to discriminate between positive and negative cases (Midi, Rana and Sarkar, 2010), has been reported in research employing PS adjustment methods (Westreich et al., 2011). High AUC values reflect good predictive performance of the estimated PS model, but the main concern in our setting is not to predict treatment selection but to control for confounding. Theory says that, conditional on PS (as a balancing function of covariates), treatment assignment or choice can be thought of as a random process (conditional independence assumption). If the treatment selection model has an extremely high predictive value, as our case study exemplifies (AUC=0.96), it is difficult to accept this assumption is met. In this model one or more factors strongly determine whether the individual receives or not the intervention under study and therefore it is doubtful that individuals from both treatment groups are "comparable". In this sense, the yield of a high c-statistic in the treatment choice estimation model must raise further concern that poor overlap between treated and untreated patients is likely to be an issue. Therefore it is now recognized that the c-statistic should not be provided as an index supporting the quality of the model. Several GOF statistics and graphical tools have been proposed aimed at specifically checking the adequacy of the PS model as a balancing score (Austin, 2008a).

The degree of overlapping in PS distributions between treated and untreated patients, the third related element, greatly influences comparability and therefore the quality of inference about treatment effect. The positivity principle, one of the key assumptions for causal inference (Westreich and Cole, 2010; Cole and Hernán, 2008), requires the

existence of both treated and untreated subjects at each level of all covariates under consideration. This should also be reflected by the existence of individuals from both treatment groups in all regions of the PS range. However, PS estimated from models with very high predictive abilities will often lead to rather little overlap between treated and untreated (Sturmer et al., 2006). This suggests an inability to make fair comparisons between treated and untreated subjects (Glynn, Schneeweiss and Stürmer, 2006). It has further been shown that there is no association between the value of c-statistic for a given PS model and its ability to balance prognostically important variables between treated and untreated subjects (Austin, Grootendorst and Anderson, 2007).

In our example lack of overlap is small in the tails of PS distribution and therefore it might be considered, at first glance, that overlap is not a big issue (Table 3). However, as Figure 2 shows, most treated patients have very high values of PS whereas most untreated newborns have very low values. This finding supports the notion that, based on our observed pre-treatment covariates, there is low “randomness” (uncertainty) as to whether the patient is to be prescribed surfactant.

Two natural negative consequences of this lack of “conditional randomness” and subsequent absence of appropriate overlap arise: on the one hand, the need to restrict the estimation of treatment effects to a fraction of the study sample where this overlap holds, which in turn influences generalizability of results. On the other hand, the lack of balance achieved by the PS which leads to biased and unreliable effect estimates (Westreich et al., 2011).

If lack of appropriate balance in the PS is found, variables included in the PS estimation model should be carefully reviewed. Detailed assessment of the mechanism relating each variable to treatment choice/assignment and the magnitude of statistical association may help identify baseline covariates that behave as proxies of treatment allocation. If variables of this type are identified, they must be removed from the estimation model and the whole PS building process should start again. Sometimes refinement of the functional form of the regression model estimating PS, including higher order and interaction terms, may help achieve balance (Austin, 2011; D’Agostino and D’Agostino, 2007). Different specifications of our PS model did not provided any real remedy. It may be the case, though, that we have to conclude that the available observational data do not meet the required assumption of randomness of treatment assignment conditioned on a set of observed baseline covariates. This is tantamount to saying that these data are not adequate to obtain valid and reliable estimates of treatment effects.

This is, as far as we know, the first paper that presents a real case study where the balancing property of PS is not achieved. In our case, it was finally agreed to by involved clinicians that frequently treatment assignment decisions were largely determined by implicit clinical decision rules based on general knowledge and routine practice. Accordingly, in order to obtain valid estimates of the effect of surfactant given to premature newborns with respiratory problems further selection of specific subgroups and clinical scenarios where uncertainty about the beneficial effect of this treatment holds true should be sought.

It is expected that current growth in the use of PS methods continues as availability of and access to electronic data is on the rise (Couper and Miller, 2008) and ease of use of menu-driven general statistical packages also increases. There remains debate, however, on a variety of aspects related to the use of propensity score adjusted estimates and further research is warranted if its performance is to be maximized. We can mention, among others, selection of the best approach to obtain estimated PS likely to achieve balance (Imai and Ratkovic, 2014) and choice of a specific set of goodness-of-fit tools aimed at assess extent and quality of covariate balance achieved for each different implementation of the method (Austin, 2008a; Austin, 2009; Belitser et al., 2011). Above all, what is of critical importance is to improve the quality and standards in describing methods used to obtain the empirical PS and to adjust for it, as several articles claim poor and incomplete reporting is common (Austin, 2008b; Shah et al., 2005).

Our case study highlights several important issues: a) the need for careful consideration of whether information contained in available observational data allows for a treatment effect estimation question to be adequately addressed either globally or for some specific subgroup(s) of patients (Austin et al., 2005); b) the requirement that researchers thoroughly verify that the estimated PS truly achieves balance in treatment groups across the range of PS values as well as across levels and categories of the selected pre-treatment covariates. By so doing, clinicians and researchers will ensure that appropriate data and analytical methods are being used to obtain valid answers to focused clinical and public health questions on the causal effect of interventions. These results should help guide clinical practice when a randomized experiment is not feasible.

Acknowledgements

We wish to thank the contribution of doctor Adolf Valls i Soler† in this project and the European Neonatal Network (EURONEONET) supported by grants from the Directorate-General for Health and Consumers (DGSANCO).

This research was supported by the Health Department of the Basque Government (201211008) and Department of Education, Language Policy and Culture of the Basque Government (IT620-13).

References

- Adelson, J. L. (2013). Educational Research with Real-World Data: Reducing Selection Bias with Propensity Scores. *Practical Assessment, Research & Evaluation*, 18(15). Available online: <http://pareonline.net/getvn.asp?v=18&n=15>
- Austin, P. C. (2008a). Goodness-of-fit diagnostics for the propensity score model when estimating treatment effects using covariate adjustment with the propensity score. *Pharmacoepidemiology Drug Safety*, 17, 1202–1217.

- Austin, P. C. (2008b). A critical appraisal of propensity-score matching in the medical literature between 1996 and 2003. *Statistics in Medicine*, 27, 2037–2049.
- Austin, P. C. (2009). Balance diagnostics for comparing the distribution of baseline covariates between treatment groups in propensity-score matched samples. *Statistics in Medicine*, 28, 3083–3107.
- Austin, P. C. (2011). An Introduction to Propensity Score Methods for Reducing the Effects of Confounding in Observational Studies. *Multivariate Behavioral Research*, 46, 399–424.
- Austin, P. C., Mamdani, M. M., Stukel T. A., Anderson G. M. and Tu J. V. (2005). The use of the propensity score for estimating treatment effects: administrative versus clinical data. *Statistics in Medicine*, 24, 1563–1578.
- Austin, P. C., Grootendorst, P. and Anderson, G. M. (2007). A comparison of the ability of different propensity score models to balance measured variables between treated and untreated subjects: a Monte Carlo study. *Statistics in Medicine*, 26, 734–753.
- Becker, S. O. and Ichino, A. (2002). Estimation of average treatment effects based on propensity scores. *Stata Journal*, 2, 358–377.
- Belitser, S. V., Martens, E. P., Pestman, W. R., Groenwold R. H. H., de Boer, A. and Klungel, O. H. (2011). Measuring balance and model selection in propensity score methods. *Pharmacoepidemiology Drug Safety*, 20, 1115–1129.
- Benjamini, Y. and Hochberg, Y. (1995). Controlling the false discovery rate: A practical and powerful approach to multiple testing. *Journal of the Royal Statistical Society, Serie B*, 57, 289–300.
- Brookhart, M. A., Schneeweis, S., Rothmann, K. J., Glynn, R. J., Avorn, J. and Sturmer, T. (2006). Variable selection for propensity score models. *American Journal of Epidemiology*, 163, 1149–1156.
- Bryson, A., Dorsett, R. and Purdon, S. (2002). The use of propensity score matching in the evaluation of active labour market policies. *Policy Studies Institute and National Centre for Social Research. Working paper number 4*. http://eprints.lse.ac.uk/4993/1/The_use_of_propensity_score_matching_in_the_evaluation_of_active_labour_market_policies.pdf Last accessed 13 September 2013.
- Caliendo, M. and Kopeining, S. (2008). Some practical guidance for the implementation of propensity score matching. *Journal of Economic Surveys*, 1, 31–72.
- Cole, S. R. and Hernán, M. A. (2008). Constructing inverse probability weights for marginal structural models. *American Journal of Epidemiology*, 168, 65–664.
- Couper, M. P. and Miller P. V. (2008). Web survey methods-Introduction. *Public Opinion Quarterly*, 5, 831–835.
- D'Agostino, J. R. Jr. and D'Agostino, R. B. Sr. (2007). Estimating treatment effects using observational data. *The Journal of American Medical Association*, 297, 314–316.
- Dehejia, R. H. and Wahba, S. (2002). Propensity Score-Matching methods for nonexperimental causal studies. *The review of Economics and Statistics*, 84(1), 151–161.
- Friedman, L. M., Furberg, C. D. and DeMets, D. L. (1998). *Fundamentals of Clinical Trials*. 3rd ed. Springer, New York.
- Gang, F., Brooks, J. M. and Chrischilles, E. A. (2012). Apples and oranges? Interpretations of risk adjustment and instrumental variable estimates of intended treatment effects using observational data. *American Journal of Epidemiology*, 175, 60–65.
- Glynn, R. J., Schneeweiss, S. and Stürmer, T. (2006). Indications for propensity scores and review of their use in pharmacoepidemiology. *Basic & Clinical Pharmacology & Toxicology*, 98(3), 253–259.
- Grimes, D. A. and Schulz, K. F. (2002). Bias and causal association in observational research. *Lancet*, 359, 248–252.
- Imai, K. and Ratkovic, M. (2014). Covariate balancing propensity score. *Journal of the Royal Statistical Society*, 76, 243–263.

- Klungel, O. H., Martens, E. P., Psaty, B. M., Grobbee, D. E., Sullivan, S. D., Stricker, B. H. Ch. et al. (2004). Methods to assess intended effects of drug treatment in observational studies are reviewed. *Journal of Clinical Epidemiology*, 57, 1223–1231.
- Midi, H., Rana, S. and Sarkar, S. K. (2010). Binary response modelling and validation of its predictive ability. *WSEAS Transactions on Mathematics*, 9, 438–447.
- Oakes, J. M., Johnson, P. J. (2006). Propensity score matching for social epidemiology. In: Oakes, J. M., Kaufman, J. S. editors. *Methods in Social Epidemiology*. John Wiley & Sons, San Francisco.
- Pattanayak, C. W., Rubin, D. B. and Zell, R. (2011). Propensity score methods for creating covariate balance in observational studies. *Revista Española de Cardiología*, 64(10), 897–903.
- Rosenbaum, P. R. and Rubin, D. B. (1983). The central role of the propensity score in observational studies for causal effects. *Biometrika*, 70, 41–55.
- Rosenbaum, P. R. and Rubin, D. R. (1984). Reducing bias in observational studies using subclassification on the propensity score. *Journal of the American Statistical Association*, 79, 516–524.
- Shadish, W. R. and Steiner, P. M. (2010). A primer on propensity score analysis. *Newborn and Infant Nursing Reviews*, 10, 19–26.
- Shah, D. R., Laupacis, A., Hux, J. E. and Austin, P. C. (2005). A comparison of propensity score methods: a case-study estimating the effectiveness of post-AMI statin use. *Statistics in Medicine*, 25, 2084–2106.
- Stuart, E.A. <http://www.biostat.jhsph.edu/~estuart/propensityscoresoftware.html> Last accessed 10 September 2013.
- Sturmer, T., Joshi, M., Glynn, R. J., Avorn J., Rothman, K. J. and Schneeweiss, S. (2006). A review of the application of propensity score methods yielded increasing use, advantages in specific settings, but not substantially different estimates compared with conventional multivariable methods. *Journal of Clinical Epidemiology*, 59, 437–447.
- Walker, A. M. (1996). Confounding by indication. *Epidemiology*, 7, 335–336.
- Weitzen, S., Lapane, K. L., Toledano, A. Y., Hume, A. L. and Mor, V. (2004). Principles for modelling propensity scores in medical research: a systematic literature review. *Pharmacoepidemiology and Drug Safety*, 13, 841–853.
- Westreich, D. and Cole, S. R. (2010). Invited commentary: positivity in practice. *American Journal of Epidemiology*, 171, 678–681.
- Westreich, D., Cole, S. R., Funk, M. J., Brookhart, M. A. and Sturmer, T. (2011). The role of the c-statistic in variable selection for propensity score models. *Pharmacoepidemiology and Drug Safety*, 20, 317–320.

Untangling the influence of several contextual variables on the respondents' lexical choices. A statistical approach

Mónica Bécue-Bertaut^{1,*}, Jérôme Pagès² and Belchin Kostov^{1,3}

Abstract

This work proposes an original textual statistical method to uncover the relationships between opinions, expressed as free-text answers, and respondents' characteristics. This method also identifies the specific links between each characteristic and certain words used in these answers. Promising results are obtained as shown by an application to real data collected to know what health means for non-experts, essential knowledge for effective public health interventions.

MSC: 62P20

Keywords: Aggregated lexical tables, textual analysis, free-text answers, social marketing.

1. Introduction

Open-ended questioning is able to capture information in the form of free-text answers which could not be observed from closed questioning. The usual statistical methodology to deal with this type of answer gives a central role to correspondence analysis (CA; Benzécri, 1973, 1981; Lebart, Salem and Berry, 1998; Murtagh, 2005). However, the direct analysis by CA of the lexical table, crossing respondents (rows) and words (columns), benefit from introducing the respondents' characteristics, such as age and education, to obtain more robust results (Lebart et al., 1998, pp. 103-104). A first and classical way of doing it consists in grouping the respondents from one categorical variable

*The corresponding author will be the first one; her contact address is: Mónica Bécue-Bertaut. Departament d'Estadística i Inv. Operativa. Universitat Politècnica de Catalunya. C/ Jordi Girona 1-3, 08034, Barcelona, Spain. Phone: +34934017031, Fax: +34934015855, e-mail address: monica.becue@upc.edu

¹ Universitat Politècnica de Catalunya, Barcelona, Spain.

² Agrocampus-Ouest, Rennes, France.

³ Transverse group for research in primary care-IDIBAPS, Barcelona, Spain.

Received: March 2014

Accepted: June 2014

and building an *aggregated lexical table* (ALT) crossing categories (rows) and words (columns). CA on this aggregated lexical table (CA-ALT) offers a symmetric approach to the relationships between words and categories allowing for explaining the variability observed among the words by the variability observed among the categories and vice-versa. The attractions/rejections between certain words and certain categories are indicated and visualised on the principal planes.

Considering several categorical variables is frequently required to better understand the variability observed in the lexical choices. An approach similar to CA-ALT consists in building a new variable from crossing all the categories of all the selected variables. In practice, such a cross-tabulation would lead to an unwieldy number of categories when dealing with samples limited to 500 or even 1000 respondents. Furthermore, as a complex network of relationships may exist among the variables, some of these categories would be either empty or with low counts.

When crossing the variables to be considered proves impracticable, three strategies are proposed (Lebart et al., 1998; Garnier and Guérin-Pace, 2010; Cousteaux, 2010). Performing a multiple correspondence analysis on these variables and clustering the respondents from their principal coordinates enables to return to the case of a single categorical variable. The partition into clusters plays the role of a categorical variable and the aggregated lexical table crossing clusters and words is built and then analysed by CA. This strategy, called *working demographic partition* (WDP), highlights the main lexical choices related to the characteristics of the respondents (Lebart et al., 1998, pp. 188-121). However, this strategy presents two main drawbacks. The clustering requires taking several decisions which are not obvious and any direct reference to the variables and categories is lost. This hinders the interpretation of the graphics in terms of relationships between variables/categories and words. A second option consists in applying CA to the multiple aggregated table juxtaposing the aggregated lexical tables built from each categorical variable. This approach has the drawback of not cancelling the associations among the variables and hence possible confusion effects remain. Finally, a direct analysis of the free-answers, that is, CA on the respondents \times words table can be performed. The projection of the categories, at the centroid of the respondents who belong to them, allows for detecting which variables (and which categories) are strongly associated with the words. However, in this case also, the effects of the different variables are merged.

We present here a methodology able to take into account several grouping variables while untangling their respective influence on the lexical choices and avoiding spurious relationships between certain categories and certain words.

The overview of this paper is as follows. Section 2 presents the motivation, based on a case study. In Section 3, the notation is listed. Section 4 recalls the classical methodology to deal with an aggregated lexical table. Section 5 is devoted to the analysis of a multiple aggregated table through classical CA and through the methodology that we propose. The effectiveness of this latter is evaluated in Section 6 on the case study. We conclude in Section 7 with some remarks.

2. Case-study based motivation

In 1989-1990 the Valencian Institute of Public Health (IVESP) conducted a survey to better know the attitudes and opinions related to health for the non-expert population. This information is essential to enhance public health policy. Effective advertising and greater dissemination concerning healthy habits are thus oriented by a deep knowledge of real lifestyles. A sample of 513 residents over 14 years of age was observed. The first question included in the questionnaire “*What does health mean to you?*” required free and spontaneous answers. A priori, the variables *Age group* (*under 21, 21-35, 36-50 and over 50*), *Gender* and *Health condition* (*poor, fair, good and very good health*) were considered as possibly conditioning the respondents’ viewpoint on health. The primary objective is to uncover and describe their complex influence on the ways of defining health. Identifying the different concerns and their relationships with the respondents’ characteristics is aimed at.

3. Notation

For the convenience of the reader, the main notation and terminology are listed and specified here.

N, I, J, K, L	number of occurrences, respondents, words, categories, categorical variables, respectively;
$\mathbf{X} = [x_{ik}]$	$(I \times K)$ two-way two-mode data matrix describing the respondents from K dummy variables issued from coding $L (L \geq 1)$ categorical variables into a disjunctive form. So, $x_{ik} = 1$ if i belongs to category k , otherwise 0;
$\mathbf{Y} = [y_{ij}]$	$(I \times J)$ two-way two-mode data matrix describing the respondents from the frequency of the words that they used to answer an open-ended question. y_{ij} counts the occurrences of word j (column) in respondent i 's answer (row). The grand total of this table is $\sum_{i=1}^I \sum_{j=1}^J y_{ij} = N$, total number of occurrences of the corpus. \mathbf{Y} is called the lexical table (LT);
$\mathbf{P} = [p_{ij}] = \left[\frac{y_{ij}}{N} \right]$	$(I \times J)$ proportion matrix issued from the lexical table. The row margin of \mathbf{P} is the vector $(p_{.1}, \dots, p_{.j}, \dots, p_{.J})^T$ with, for $j = 1, \dots, J$, $p_{.j} = \sum_{i=1}^I p_{ij}$. The column margin of \mathbf{P} is the vector $(p_{1.}, \dots, p_{i.}, \dots, p_{I.})^T$ with, for $i = 1, \dots, I$, $p_{i.} = \sum_{j=1}^J p_{ij}$;

$\mathbf{D}_I = [d_{I_{ii}}] = [p_{i.}]$	$(I \times I)$ diagonal matrix. $d_{I_{ii}}$ is equal to the relative frequency of occurrences corresponding to respondent i 's free answer;
$\mathbf{D}_J = [d_{J_{jj}}] = [p_{.j}]$	$(J \times J)$ diagonal matrix. $d_{J_{jj}}$ is equal to the relative frequency of occurrences of word j in the whole set of free answers;
$\mathbf{Q} = \mathbf{D}_I^{-1} \mathbf{P} \mathbf{D}_J^{-1}$ $= [q_{ij}] = \left[\frac{p_{ij}}{p_{i.} \cdot p_{.j}} \right]$	$(I \times J)$ data matrix analysed by CA.
$\bar{\mathbf{Q}} = \mathbf{D}_I^{-1} (\mathbf{P} - \mathbf{D}_I \mathbf{1} \mathbf{D}_J) \mathbf{D}_J^{-1}$ $= [\bar{q}_{ij}] = \left[\frac{p_{ij} - p_{i.} \cdot p_{.j}}{p_{i.} \cdot p_{.j}} \right]$	$(I \times J)$ data matrix, double-centred form of \mathbf{Q} which can be alternatively considered by CA. $\mathbf{1}$ denotes the $(I \times J)$ matrix with generic term the constant 1. $\bar{\mathbf{Q}}$ describes the weighted deviation between \mathbf{P} and the $(I \times J)$ independence model matrix $\mathbf{D}_I \mathbf{1} \mathbf{D}_J = [p_{i.} \cdot p_{.j}]$;
$\mathbf{Y}_A = \mathbf{Y}^T \mathbf{X} = [y_{jk}]$	$(J \times K)$ two-way two-mode data matrix describing the categories (columns) from the frequency of the words (rows) used in the free answers of the categories' respondents. $y_{A_{jk}}$ is the count of occurrences of word j in category k 's answers. \mathbf{Y}_A is called either <i>aggregated lexical table</i> (ALT; $L = 1$) or <i>multiple aggregated lexical table</i> (MALT; $L > 1$);
$\mathbf{P}_A = [p_{A_{jk}}] = \left[\frac{y_{A_{jk}}}{L \cdot N} \right]$	$(J \times K)$ proportion matrix issued from \mathbf{Y}_A . The row margin of \mathbf{P}_A is the vector $(p_{A_{.1}}, \dots, p_{A_{.k}}, \dots, p_{A_{.K}})^T$ with $p_{A_{.k}} = \sum_{j=1}^J p_{A_{jk}}$, $k = 1, \dots, K$. The column margin of \mathbf{P}_A is the vector $(p_{A_{1.}}, \dots, p_{A_{j.}}, \dots, p_{A_{J.}})^T$ with $p_{A_{j.}} = \sum_{k=1}^K p_{A_{jk}}$ for $j = 1, \dots, J$;
$\mathbf{Q}_A = \mathbf{D}_J^{-1} \mathbf{P}_A \mathbf{D}_K^{-1}$	$(J \times K)$ data matrix built from \mathbf{P}_A and analysed by CA;
$\mathbf{D}_K = [d_{K_{kk}}] = [p_{A_{.k}}]$	$(K \times K)$ diagonal matrix which gathers the terms of the row-margin of \mathbf{P}_A . $d_{K_{kk}}$ is the relative frequency of the occurrences used by the category k 's respondents;
$\mathbf{Q}_A^G = \mathbf{D}_J^{-1} \mathbf{P}_A \mathbf{C}^-$	$(J \times K)$ data matrix built from \mathbf{P}_A where \mathbf{C}^- is the generalized inverse of $\mathbf{C} = \mathbf{X}^T \mathbf{D}_I \mathbf{X}$. This is the data matrix analysed by the methodology that we propose.

4. Classical correspondence analysis on lexical tables

We present CA and the methodology that we developed in terms of our application field. We consider the frequency table \mathbf{Y} and the contextual data matrix \mathbf{X} observed on the same respondents. In this Section the columns of \mathbf{X} are dummy variables corresponding to the categories of only one variable.

In textual analysis, it is usual to apply CA on the lexical table (CA-LT), and on words \times categories tables, called *aggregated lexical tables* CA-ALT.

4.1. Direct analysis of the lexical table CA-LT

As any classical CA, the direct analysis of the lexical table CA(\mathbf{Y}) can be performed in three equivalent ways:

1. As the principal component analysis (PCA) on the following ($I \times J$) data matrix

$$\bar{\mathbf{Q}} = \mathbf{D}_I^{-1} (\mathbf{P} - \mathbf{D}_I \mathbf{1} \mathbf{D}_J) \mathbf{D}_J^{-1} \quad (1)$$

with metric \mathbf{D}_J in the row space (metric \mathbf{D}_I in the column space) and weighting system \mathbf{D}_I on the rows (weighting system \mathbf{D}_J on the columns) (Bécue-Bertaut and Pagès, 2004; Böckenholt and Takane, 1994; Escofier and Pagès, 2008). This PCA is denoted $\text{PCA}(\bar{\mathbf{Q}}, \mathbf{D}_J, \mathbf{D}_I)$. This formulation, besides underlining that what is analysed is the deviation of \mathbf{P} from the independence model matrix, places this method in the general scheme for principal axes methods. We favour here this point of view which allows for generalisations in a more straightforward manner. Equivalently, the ($I \times J$) data matrix

$$\mathbf{Q} = \mathbf{D}_I^{-1} \mathbf{P} \mathbf{D}_J^{-1} \quad (2)$$

can be considered in $\text{PCA}(\mathbf{Q}, \mathbf{D}_J, \mathbf{D}_I)$.

Both $\text{PCA}(\bar{\mathbf{Q}}, \mathbf{D}_J, \mathbf{D}_I)$ and $\text{PCA}(\mathbf{Q}, \mathbf{D}_J, \mathbf{D}_I)$ lead to the same results due to the centring usually performed by a PCA.

2. As the ordinary SVD of $\mathbf{D}_I^{-1/2} \mathbf{P} \mathbf{D}_J^{-1/2} = \mathbf{D}_I^{1/2} \mathbf{Q} \mathbf{D}_J^{1/2}$ completed by further computing to obtain the row and column factors (Böckenholt and Takane, 1994; Greenacre, 1984; Lebart et al., 2006; Legendre and Legendre, 1998).
3. As the two analyses of the row and column profiles matrices through, respectively, the PCA of $\mathbf{D}_I^{-1} \mathbf{P}$, with row metric \mathbf{D}_J^{-1} and weighting system \mathbf{D}_I , and the PCA of $\mathbf{D}_J^{-1} \mathbf{P}$, with row metric \mathbf{D}_I^{-1} and weighting system \mathbf{D}_J (Escofier and Pagès, 2008; Lebart et al., 2006)

4.2. Analysis of an aggregated lexical table CA-ALT

The $(J \times K)$ aggregated lexical table

$$\mathbf{Y}_A = \mathbf{Y}^T \mathbf{X} \quad (3)$$

is built and transformed into the $(J \times K)$ proportion matrix

$$\mathbf{P}_A = \mathbf{P}^T \mathbf{X}. \quad (4)$$

The $(K \times K)$ diagonal matrix \mathbf{D}_K stores the row-margin of \mathbf{P}_A whose generic term is the proportion of occurrences corresponding to category k . In this section, where only one categorical variable is considered, \mathbf{D}_K is equal to $(\mathbf{X}^T \mathbf{D}_I \mathbf{X})$.

From \mathbf{P}_A , the $(J \times K)$ matrix

$$\mathbf{Q}_A = \mathbf{D}_J^{-1} \mathbf{P}_A \mathbf{D}_K^{-1} \quad (5)$$

is computed. Then, CA-ALT is performed through PCA $(\mathbf{Q}_A, \mathbf{D}_K, \mathbf{D}_J)$.

This analysis provides good and robust results which indicate the associations (respectively, oppositions) between words to the extent that they are related to identical (respectively, different) categories of the contextual variable.

4.3. Correspondence analysis as a double projected analysis

We consider the ‘‘inflated’’ $(N \times K)$ matrix $\mathbf{X}_N = [x_{N;n,k}]$ and $(N \times J)$ matrix $\mathbf{Y}_N = [y_{N;n,j}]$ (Legendre and Legendre, 1998, p. 595). \mathbf{X}_N and \mathbf{Y}_N cross the N occurrences and, respectively, the K indicators corresponding to the column-categories of table \mathbf{X} and the J words. If occurrence n corresponds to word j , $y_{N;n,j} = 1$; $y_{N;n,j} = 0$ otherwise. If occurrence n has been pronounced by a respondent who presents category k , $x_{N;n,k} = 1$; $x_{N;n,k} = 0$ otherwise. The $(N \times N)$ diagonal matrix $\mathbf{D}_N[1/N]$ corresponds to the uniform weighting system on the rows. Both the column-words of \mathbf{Y}_N and the column-variables of \mathbf{X}_N are in R^N space.

The proportion matrix \mathbf{P}_A can be rewritten as

$$\mathbf{P}_A = \mathbf{Y}_N^T \mathbf{D}_N \mathbf{X}_N \quad (6)$$

and matrix \mathbf{Q}_A as

$$\mathbf{Q}_A = \mathbf{D}_J^{-1} \mathbf{P}_A \mathbf{D}_K^{-1} = \left(\mathbf{Y}_N^T \mathbf{D}_N \mathbf{Y}_N \right)^{-1} \left(\mathbf{Y}_N^T \mathbf{D}_N \mathbf{X}_N \right) \left(\mathbf{X}_N^T \mathbf{D}_N \mathbf{X}_N \right)^{-1}. \quad (7)$$

Eq. (7) shows that the columns of \mathbf{Q}_A are the \mathbf{D}_N -orthogonal projection of the dummy-columns of $\mathbf{X}_N \mathbf{D}_K^{-1} = \mathbf{X}_N (\mathbf{X}_N^\top \mathbf{D}_N \mathbf{X}_N)^{-1}$ on the subspace of R^N generated by the column-words of \mathbf{Y}_N . Similarly, Eq. (7) shows that the rows of \mathbf{Q}_A are the \mathbf{D}_N -orthogonal projection of the column-words of $(\mathbf{Y}_N \mathbf{D}_J^{-1}) = \mathbf{Y}_N (\mathbf{Y}_N^\top \mathbf{D}_N \mathbf{Y}_N)^{-1}$ on the subspace of R^N generated by the dummy-columns of \mathbf{X}_N .

This viewpoint highlights that CA studies both the variability of the cloud of words, insofar as it is explained by the variability of the categories, and the variability of the cloud of categories, insofar as it is explained by the variability of the words.

$CA(\mathbf{Y}_A)$ is a double-projected analysis because

$$\mathbf{D}_K^{-1} = \left(\mathbf{X}^\top \mathbf{D}_I \mathbf{X} \right)^{-1} \quad (8)$$

is equal to the inverse of the matrix of moments of the second order of \mathbf{X} relative to the origin, i.e., all of the off-diagonal terms are null because the columns of \mathbf{X} are orthogonal.

Note that this rationale places CA in the context of canonical analysis (Saporta, 2006, pp. 212-217).

5. Analysis of a multiple aggregated lexical table

5.1. Classical correspondence analysis on a multiple aggregated lexical table

We may be interested in a broader context, such as a set of L categorical variables ($L > 1$). As the starting point, the multiple aggregated lexical table is built by juxtaposing row-wise the L aggregated lexical table built from the L categorical variables. From now on, \mathbf{Y}_A is used to denote this multiple aggregated lexical table. We follow a rationale akin to that of the former section.

The aggregated lexical table

$$\mathbf{Y}_A = \mathbf{Y}^\top \mathbf{X} \quad (9)$$

is built and transformed into the proportion matrix

$$\mathbf{P}_A = \frac{\mathbf{Y}_A}{L \cdot N} = \frac{\mathbf{P}^\top \mathbf{X}}{L}. \quad (10)$$

Diagonal matrix \mathbf{D}_K stores the row-margin of \mathbf{P}_A whose general term is the proportion of occurrences corresponding to category k . From \mathbf{P}_A , matrix

$$\mathbf{Q}_A = \mathbf{D}_J^{-1} \mathbf{P}_A \mathbf{D}_K^{-1} \quad (11)$$

is computed. Then, PCA ($\mathbf{Q}_A, \mathbf{D}_K, \mathbf{D}_J$) is performed. As in the usual CA, the first eigenvalue is equal to 1 and the corresponding axis is neglected.

The main difference with Section 4.2 is that \mathbf{D}_K is no longer equal to $(\mathbf{X}^T \mathbf{D}_I \mathbf{X})^{-1}$. This latter matrix presents non-null off-diagonal terms because the column-categories of \mathbf{X} are generally not orthogonal when belonging to different variables. It is no longer a double-projected analysis and hence the influence of the associations among the categories of different variables is not filtered.

5.2. CA with a modified metric on a multiple aggregated lexical table

In this section, the dummy columns of \mathbf{X} are centred. To maintain a double projected analysis, the starting point consists in substituting the row space metric \mathbf{D}_K^{-1} by the Moore-Penrose pseudoinverse \mathbf{C}^- of

$$\mathbf{C} = (\mathbf{X}^T \mathbf{D}_I \mathbf{X}) = [c_{kk'}], \quad (12)$$

Matrix \mathbf{C} is the covariance matrix between the columns of \mathbf{X} taking into account that the respondents are endowed with weighting system \mathbf{D}_I .

Note: if $k = k'$, $c_{kk'}$ is equal to the sum of weights of the respondents belonging to this category. If $k \neq k'$ and k and k' belong to the same variable then $c_{kk'} = 0$; if $k \neq k'$ and k and k' belong to different variables, then $c_{kk'}$ is equal to the sum of weights of the respondents belonging both to category k and category k' . \mathbf{C}^- substitutes \mathbf{D}_K^{-1} in the expression of the $(J \times K)$ data matrix

$$\mathbf{Q}_A^G = \mathbf{D}_J^{-1} \mathbf{P}_A \mathbf{C}^-, \quad (13)$$

that will be analysed through PCA ($\mathbf{Q}_A^G, \mathbf{C}, \mathbf{D}_J$).

Metric \mathbf{C}^- operates a multivariate standardisation that not only separately standardises the columns of \mathbf{X} but in addition makes them uncorrelated (Brandimarte, 2011; Härdle and Simar, 2012). To compute $(\mathbf{C}^-)^{1/2}$, \mathbf{C} is diagonalised and the whole of its S_C non-null eigenvalues, all positive, are ranked in descending order and stored in the $(S_C \times S_C)$ diagonal matrix $\mathbf{\Lambda}_C$. S_C is equal to the dimension of the space spanned by the columns of \mathbf{X} , that is, the number of independent dummy-columns of \mathbf{X} . The corresponding eigenvectors are stored in the columns of the $(K \times S_C)$ matrix \mathbf{U}_C . The S_C columns of $\mathbf{X}(\mathbf{C}^-)^{1/2}$, with $(\mathbf{C}^-)^{1/2} = \mathbf{U}_C \mathbf{\Lambda}_C^{-1/2}$, are standardised and uncorrelated. The set of dummy columns of \mathbf{X} is now taken into account through the subspace that they span. Performing PCA ($\mathbf{Q}_A^G, \mathbf{C}, \mathbf{D}_J$) is equivalent to analyse the column-centred multiple aggregated table \mathbf{P}_A through CA with a modified metric \mathbf{C}^- in the row space.

We have called the multiple aggregated lexical table \mathbf{P}_A *generalised aggregated lexical table* (GALT) and the methodology *correspondence analysis on a GALT* (CA-

GALT). This analysis provides the usual PCA results. The S non-null eigenvalues are ranked in descending order and stored in the $(S \times S)$ diagonal matrix Λ . The factors on the row-words and column-categories are stored, respectively, in the $(J \times S)$ matrix \mathbf{F} and $(K \times S)$ matrix \mathbf{G} .

The interpretation of the results of this specific CA follows the usual CA interpretation rules (Escofier and Pagès, 2008; Greenacre, 1984; Lebart et al., 1998). We will only emphasize here the transition relationships. The transition relationships linking \mathbf{F} and \mathbf{G} are expressed in Eq. 15 and Eq. 17 hereafter.

Given that

$$\mathbf{X} \left(\mathbf{X}^\top \mathbf{D}_I \mathbf{X} \right)^{-} \left(\mathbf{X}^\top \mathbf{D}_I \mathbf{X} \right) = \mathbf{X}, \quad (14)$$

the matrix \mathbf{F} is expressed as

$$\begin{aligned} \mathbf{F} &= \mathbf{Q}_A^G \mathbf{C} \mathbf{G} \Lambda^{-1/2} = \mathbf{D}_J^{-1} \mathbf{P}_A \mathbf{C}^- \mathbf{C} \mathbf{G} \Lambda^{-1/2} = \mathbf{D}_J^{-1} \frac{\mathbf{Y}^\top}{N \cdot L} \mathbf{X} \left(\mathbf{X}^\top \mathbf{D}_I \mathbf{X} \right)^{-} \left(\mathbf{X}^\top \mathbf{D}_I \mathbf{X} \right) \mathbf{G} \Lambda^{-1/2} \\ &= \mathbf{D}_J^{-1} \mathbf{P}_A \mathbf{G} \Lambda^{-1/2}. \end{aligned} \quad (15)$$

The matrix \mathbf{G} is expressed as

$$\begin{aligned} \mathbf{G} &= \left(\mathbf{Q}_A^G \right)^\top \mathbf{D}_J \mathbf{F} \Lambda^{-1/2} = \left(\mathbf{D}_J^{-1} \mathbf{P}_A \mathbf{C}^- \right)^\top \mathbf{D}_J \mathbf{F} \Lambda^{-1/2} = \mathbf{C}^- \mathbf{P}_A^\top \mathbf{D}_J^{-1} \mathbf{D}_J \mathbf{F} \Lambda^{-1/2} \\ &= \mathbf{C}^- \mathbf{P}_A^\top \mathbf{F} \Lambda^{-1/2}. \end{aligned} \quad (16)$$

By considering the matrices $\mathbf{Y}_N = [y_{N;n,j}]$ and $\mathbf{X}_N = [x_{N;n,k}]$ defined similarly to those in Section 4.3, but \mathbf{X}_N now comprising the K centred dummy columns corresponding to all the categories of the selected categorical variables, \mathbf{G} can be rewritten as

$$\mathbf{G} = \left(\mathbf{X}^\top \mathbf{D}_I \mathbf{X} \right)^{-} \frac{\mathbf{X}^\top \mathbf{Y}}{N \cdot L} \mathbf{F} \Lambda^{-1/2} = \left(\left(\mathbf{X}_N^\top \mathbf{D}_N \mathbf{X}_N \right)^{-} \mathbf{X}_N^\top \mathbf{D}_N \mathbf{Y}_N / L \right) \mathbf{F} \Lambda^{-1/2} = \mathbf{B} \mathbf{F} \Lambda^{-1/2} \quad (17)$$

Here the $(K \times J)$ matrix $\mathbf{B} = \left(\left(\mathbf{X}_N^\top \mathbf{D}_N \mathbf{X}_N \right)^{-} \mathbf{X}_N^\top \mathbf{D}_N \mathbf{Y}_N / L \right) = [b_{kj}]$ is, except for the scaling coefficient $1/L$, the matrix of regression coefficients (strictly, analysis of variance coefficients given that the regressors are dummy variables) of all the column-words of \mathbf{Y}_N on the regressor column-categories of \mathbf{X}_N . These coefficients are issued from the simultaneous, or multivariate, linear regression of all the column-words of \mathbf{Y}_N on the column-categories of \mathbf{X}_N (Finn, 1974).

Eq. 15 shows that, as in classical CA, a word is placed on axis s , up to a coefficient varying from one axis to the other, at the centroid of the categories that use it, endowing the categories with the weighting system $\left(\frac{p_{Ajk}}{p_{Aj}}, k = 1, \dots, K \right)$.

Eq. 17 reflects that category k is placed on axis s , up to a coefficient varying from one axis to the other, at the centroid of the words, endowing them with the weighting

system $(b_{kj}, j = 1, \dots, J)$. The weight given to word j , equal to b_{kj} , is the coefficient of category k in the regression of column-word j on all the categories. Thus, a category is placed in the direction of the words that the respondents belonging to this category tend to use, all things being equal.

6. Results

From the data presented in Section 2, a multiple aggregated lexical table is built by juxtaposing the three aggregated lexical tables issued from using *age group* (four categories), *gender* (two categories) and *health condition* (four categories) as grouping variables.

We first perform a separate CA on each of the tables involved in the analysis. Then, a classical CA is applied on the multiple aggregated lexical table. Finally, CA-GALT is performed with the three previous variables as contextual variables. The comparison of the results obtained from these last two methods allows for demonstrating the effectiveness of CA-GALT.

6.1. Pre-processing of the data

The 392 respondents having answered the open-ended question are selected. Only the words used at least 10 times are selected because a minimum threshold on the word frequency is required to make the comparisons between free answers meaningful from a statistical point of view (Lebart et al., 1998, p. 104; Murtagh, 2005, chap. 5). The final corpus is composed of 7751 occurrences (corpus length) from 126 different words (vocabulary length).

6.2. Separate correspondence analysis on the lexical table and on the aggregated tables

Table 1 summarizes the results of each analysis through classical indicators that are the global inertia, the Cramer's V^2 and the first eigenvalue. Cramér's V^2 is computed by dividing Φ^2 by $Min(I - 1, J - 1)$, that is with the maximum inertia that the table could present.

The intensity of the relationship between the vocabulary and either the respondents or each of the grouping variables is measured through the inertia Φ^2 (Table 1). The Cramer's V^2 allows for comparing the intensity of the relationships between the rows (either the respondents or the categories of respondents) and the columns (the words) from one table to another.

In all the cases the Cramer's V^2 value is weak. This is a usual feature when analysing a corpus of open-ended answers. The associations between words and respondents/categories develop as small variations among words selected from a common vocabulary

Table 1: Summary of the analyses.

Analysis	Φ^2	Cramer's V^2	λ_1
CA on the lexical table	7.145	0.044	0.246
CA on the by <i>age</i> aggregated lexical table	0.106	0.035	0.063
CA on the by <i>health condition</i> aggregated lexical table	0.071	0.024	0.033
CA on the by <i>gender</i> aggregated lexical table	0.038	0.038	0.038

widely shared by all the speakers of the same language. The individual variability, as measured by the Φ^2 , is huge but manifested through a multiplicity of loosely structured syntagmatic associations. The aggregation of the free answers leads to a weak loss in terms of intensity of the relationship, as evaluated by the Cramer's V^2 , despite the huge decreasing of the inertia. What is lost is mainly the non-structured part of the inertia. Thus, the Cramer's V^2 only decreases from 0.044 to 0.038/0.035 when aggregating the free answers by *gender/age group* while the total inertia Φ^2 dramatically lessens. A slightly more pronounced lowering of the Cramer's V^2 is observed when aggregating the free answers by *health condition*.

The direct analysis visualises the relationships between respondents and words on classical CA graphs (not reproduced here). In this case, the projection of the categories at the centroid of the respondents belonging to them shows that a relationship between the three categorical variables and the vocabulary does exist. The two gender categories are opposed on the first axis while the second axis ranks *age* and *health condition* categories in their natural order. The significance of the positions of the categories is assessed through classical tests (Lebart et al., 1998, pp. 123-128). However, the strong association between *age* and *health condition* trajectories makes it difficult to untangle their real influence on the word choices. We can nevertheless report that the *age* trajectory is more elongated than *health condition* trajectory and that *poor health* lies in a position that distinguishes the *over 50* category from others. This analysis merges the non-explained individual variability, which is always huge in the case of the direct analysis of free-answers, and the variability explained by the multiple belonging to categories of several variables. Therefore it is necessary to complete this initial analysis by others focusing on possible specific associations between categories and words. That being said, this first step can be very useful to suggest interesting grouping variables.

6.3. Classical CA on the multiple aggregated table

CA is applied to the multiple aggregated table. The total inertia is equal to 0.072. *Age group*, *health condition* and *gender* contribute to this total inertia bringing, respectively 49.4%, 33.0% and 17.6% of this total inertia. The first two axes, whose inertia are respectively 0.026 and 0.013, keep together 54.6% of the total inertia.

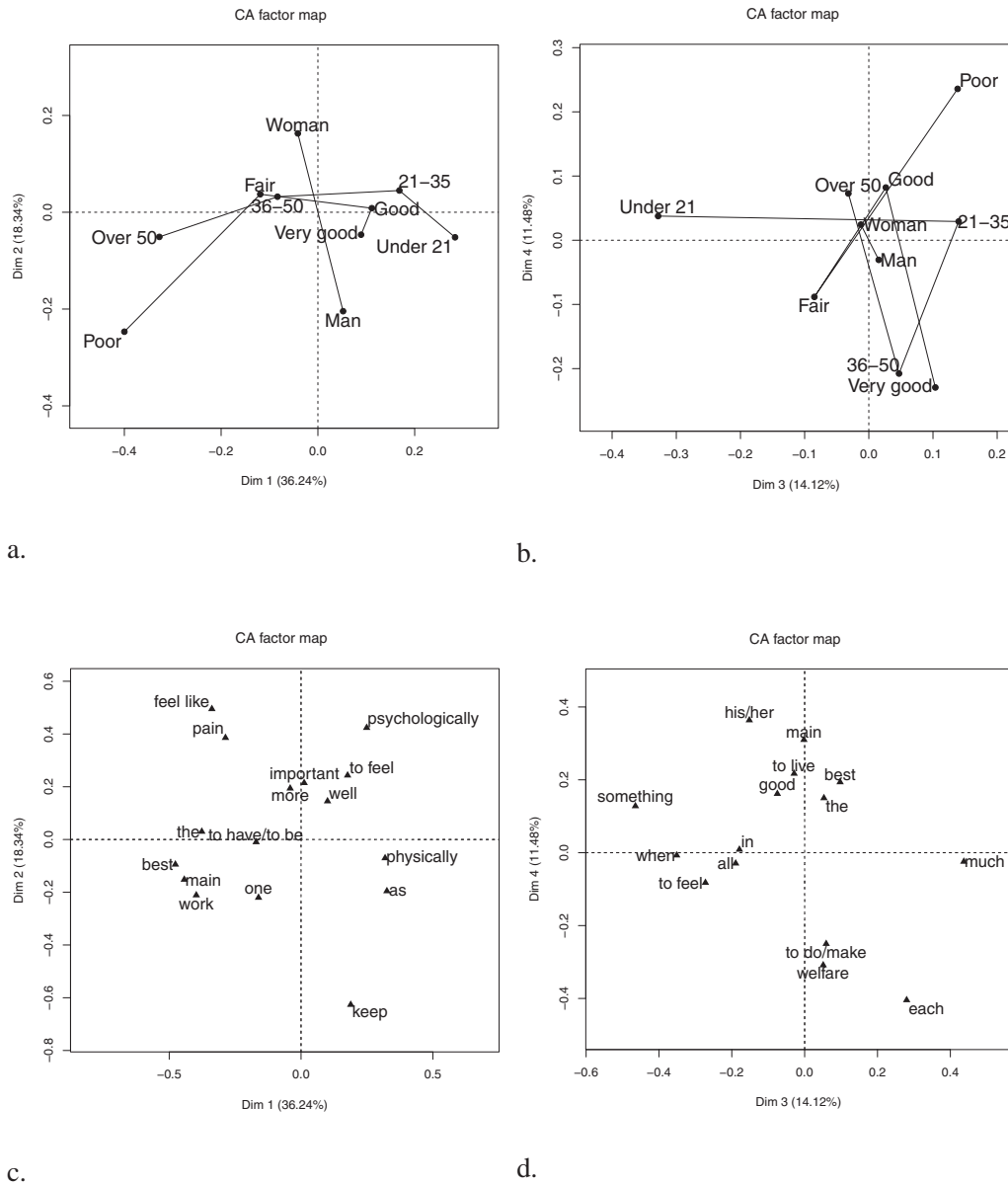


Figure 1: Categories and contributory words on the CA planes (1,2) and (3,4).

Figure 1.a offers the representation of the categories on the plane (1,2). The trajectory of *age group* categories notably follows the first axis, outlining a weak arch effect. This axis ranks, in their natural order, the *health condition* categories except for the inversion between *very good health* and *good health* which lie very close. The extreme categories of this variable, very particularly *poor health*, are opposed to the intermediate categories on the second axis, indicating a more pronounced arch effect than *age group*. However, the main opposition on the second axis concerns the two *gender* categories

Table 2: *age group* × *health condition* frequency of occurrence table.

Age group	Health condition				margin
	Poor	Fair	Good	Very good	
Under 21	0	19	44	8	71
21-35	2	37	81	15	135
36-50	2	34	33	7	76
Over 50	21	49	36	4	110
margin	25	139	194	34	392

so that *age group* and *gender* are practically orthogonal, this in terms of the vocabulary that they use. Regarding the plane (3,4) (Figure 1.b), the third axis shows that young people (*under 21*), besides using words close to those used by the following age group as revealed by axis one, also express themselves with their own words. No clear pattern stands out on the fourth axis.

The words representation (Figures 1.c and 1.d) brings information about the meaning of the oppositions and trajectories, showing for example that the words *the*, *best*, *main* – used in expressions such as (health is) *the best*, *the main* (thing) – and *work* are words both used by the oldest and/or less healthy categories and avoided by the youngest and/or more healthy categories. However, one might wonder if the choice/rejection of these words is related to *age* or to *health condition* or to both.

Table 2 shows that *age group* and *health condition* are strongly associated but still that the association is sufficiently loose as to allow for untangling the influence of both variables on the vocabulary, provided that an adequate method is applied. Precisely, CA-GALT offers a suitable approach because the associations between the variables are cancelled.

6.4. CA-GALT on the multiple aggregated table

CA-GALT is applied on the multiple aggregated table. The total inertia is equal to 0.2067. The first two axes are moderately dominant with eigenvalues equal to 0.0636 (30.81% of the inertia) and 0.0388 (18.78%).

Figures 2.a and 3.a display, respectively, the contextual variables and the words with a high contribution on the CA-GALT first principal plane. These representations are completed by drawing confidence ellipses (Efron, 1979; Lebart et al., 2006). Only the confidence ellipses around the words *the*, *best*, *main* and *work* are represented, because these words are favoured as examples to show the effectiveness of the approach that we propose (Figures 3.c and 3.d). If all the ellipses were drawn, only those around *he/she* and *to be able*, on plane (1,2) and around *to be able* and *from* on plane (1,4) would overlap the centroid.

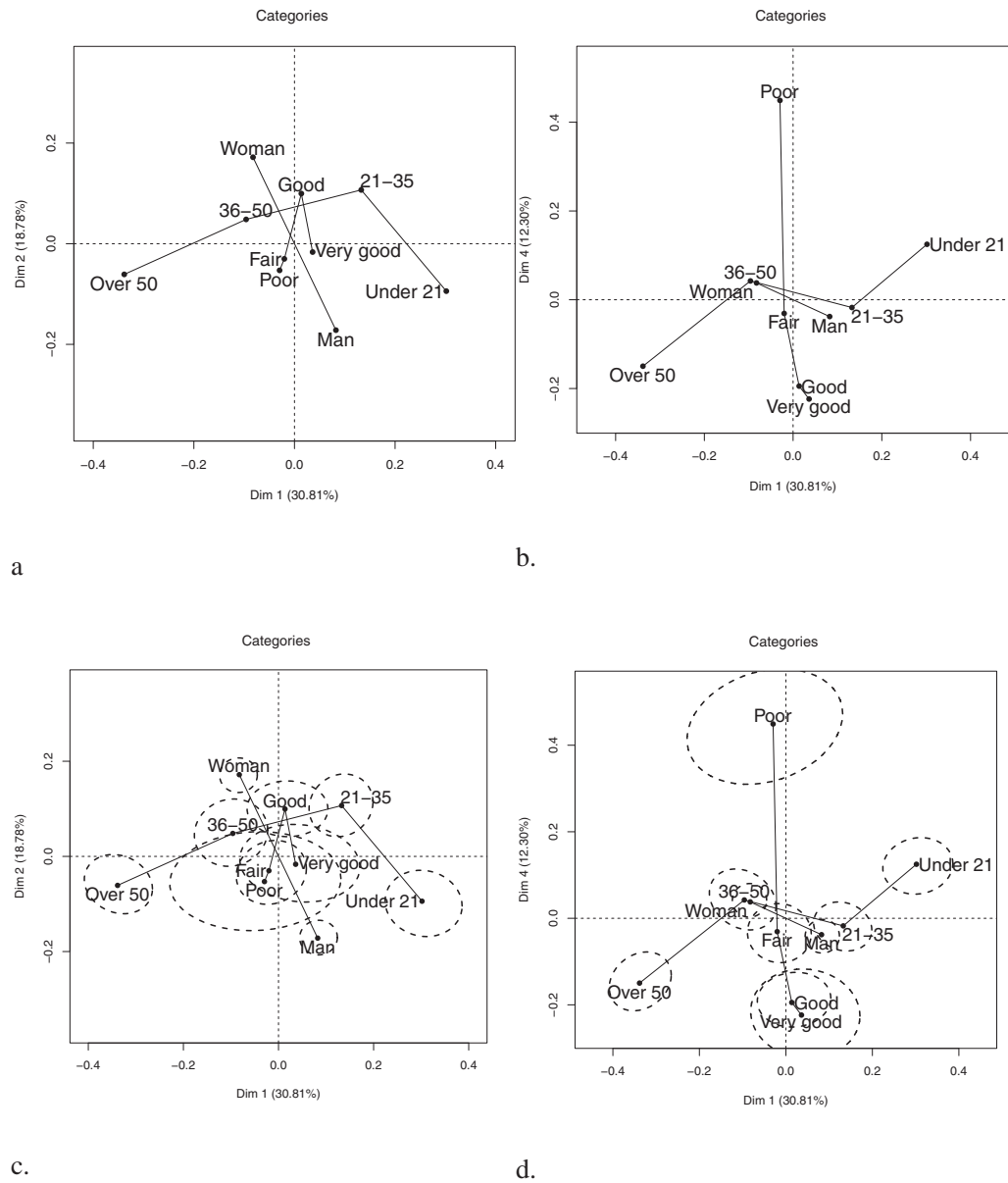


Figure 2: Categories on the CA-GALT planes (1,2) and (1,4) completed by confidence ellipses.

As in the former analysis, the trajectory of *age group* notably follows the first axis. The extreme categories of this variable, *over 50* (at the left); *under 21* (at the right) bring, respectively, 52.1% and 23.1% of this axis inertia. However, *health condition* representation differs. The categories of this variable now lie close to the centroid on the first plane and their confidence ellipses extensively overlap one another (Figure 2.c). Regarding the words, we find again *the*, *best* and *main* with high coordinates at the left

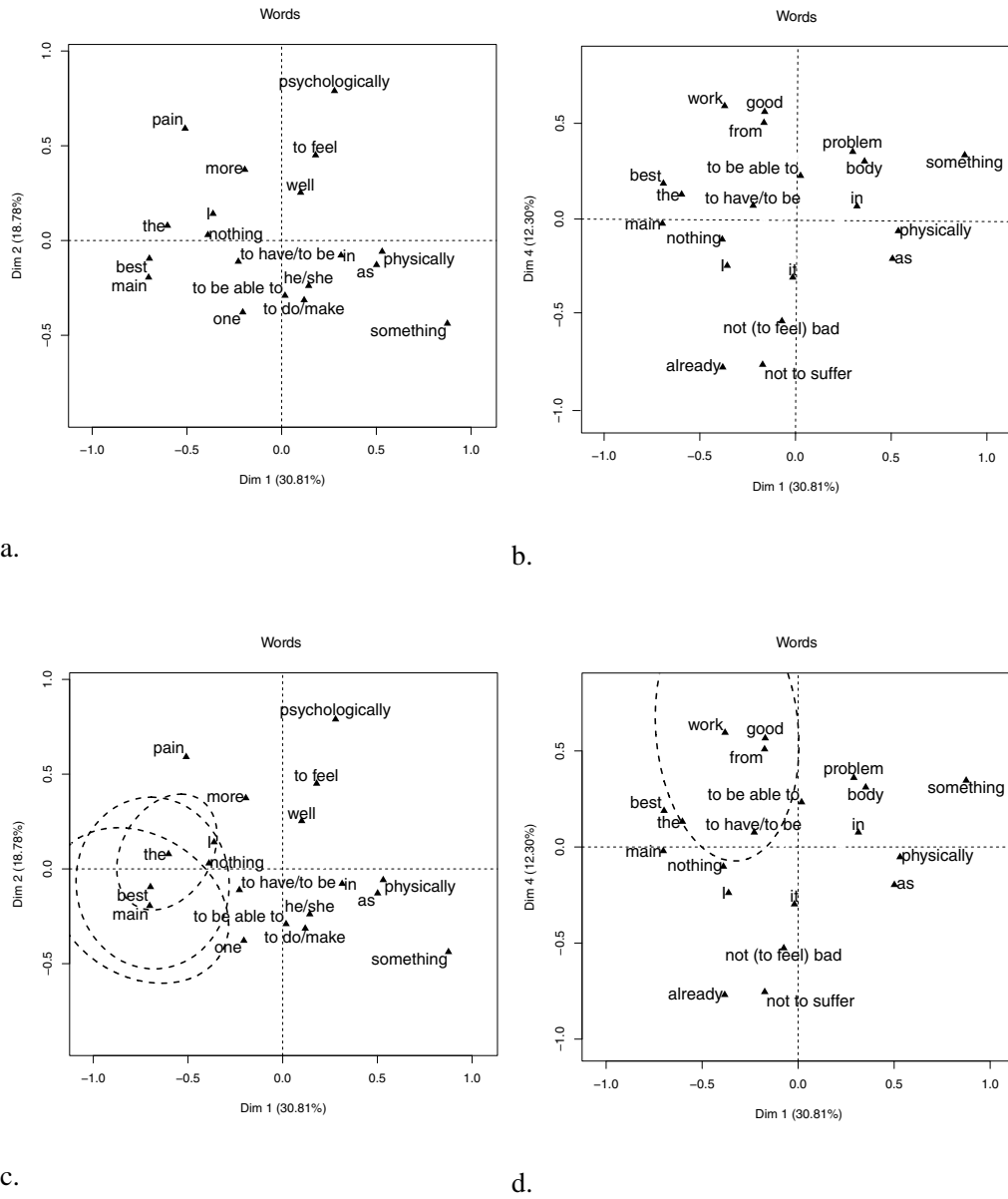


Figure 3: Contributory words on the CA-GALT planes (1,2) and (1,4) completed by confidence ellipses.

of the axis, indicating that they are words both very used by the oldest categories and avoided by the youngest. The word *work* is no more present on this graphic, since it is close to the centroid and thus not a key word for the oldest categories.

We detail neither the second axis, which opposes *Man* and *Woman*, nor the third (not reproduced in the graphic), which highlights the specific use of the vocabulary by the *under 21* respondents. Both axes are close to those computed in the former CA.

The fourth axis turns out to be of interest because of ranking *health condition* categories in their natural order (Figure 2.b). These categories, which provide together 75% of the axis inertia, are well separated, except for the two better health categories whose confidence ellipses overlap (Figure 2.d). The word *work* lies close to *poor health* category in the positive part of the fourth axis (Figures 2.b and 3.b), pointing out a strong association between this word and this category and also little use of this word by the most healthy categories. The word *work* contrasts on the fourth axis with *bad*, *suffer* and *already* which are associated with *good health*, *very good health* and *over 50*. These latter words are used in free answers where health is defined through negative expressions such as *not to feel bad*, *not to be bad*, *not to suffer*, *not to suffer from any disease* or *pain*.

The discrimination between the words associated with *poor health* and those associated with *over 50* that CA-GALT uncovers has to be checked in the data. The variable crossing *age group* and *health condition* is created but grouping similar categories to ensure a minimum membership in every category. This cross-variable allows for comparing the vocabulary from the *health condition* viewpoint at a same age and vice-versa. For each category, the moderate/significant under/over use of the words can be computed from using the test proposed by Lebart et al. (1998, chapter 6). We conserve not only the significant under/over used words ($p\text{-value} < 0.1$) but also the moderate under/over used words ($0.1 < p\text{-value} < 0.16$), because the progression of the use of a word depending on *age* increasing, and of *health condition* decreasing, is also of interest. The results corresponding to the four words (*the*, *best*, *main* and *work*) are summarised in Table 3.

Table 3: *Categories under or over using the words the, best, main and work.*

	<i>Significant under-use</i>	<i>Moderate under-use</i>	Moderate over use	Significant over-use
<i>Word</i>				
<i>the</i>	<21-good/very good health <21 fair health 21-35 fair/poor health		>50 good/very good health	>50 fair health >50 poor health
<i>best</i>	<21-good/very good health	21-35 fair/poor health	>50 good/very good health	>50 poor health
<i>main</i>	21-35 fair/poor health			>50 good/very good health >50 poor health >50 fair health
<i>work</i>	21-35 good health			>50 poor health 36-50 poor/fair health

Table 3 shows that the respondents who do not or barely use the words *the*, *best* and *main* (in expressions such that “*the best/ the main thing*”) differ from those who overuse from the age viewpoint. These words are moderately or significantly overused only by the *over 50* category of respondents with very different health conditions. These three words usage depends on *age*, not on *health condition*, and increases with the former.

We now focus on the word *work*, significantly under-used by the *21-35* with *good health* and significantly overused by the *over 50* with *poor health* and the *36-50* with *poor* or *fair health*, which is the less healthy category for this age group. These results are not as obvious as the former results to allow us to conclude on the effect alone of *health condition* on the selection/rejection of this word. It is more difficult to untangle the influence of *age* and *health condition* in this case because the *poor health* category is almost made up of only *over 50* respondents (21 from 25). Nevertheless, the *over 50* and *36-50* not presenting the worst health condition corresponding to their own age do not over use *work*, even only moderately. This allows for concluding that *health condition* has, at least, a much stronger effect than *age* on the selection of this word.

We can finish telling that CA-GALT is able to untangle the complex influence of *age* and of *health condition* on the lexical choices from differences existing in the data through a *ceteris paribus* analysis.

7. Conclusion

The direct analysis of the lexical table offers valuable visualizations of the associations among the respondents and among the words that also indicate the relationships between respondents and words (Lebart et al., 1998). However, it is necessary to go further and identify the complex relationships between respondents' characteristics and lexical choices. The inclusion of selected categorical variables as explaining variables in the analysis highlights these relationships provided that all the main sources of variability are taken into account. This leads to consider a multiple aggregated lexical table, juxtaposing the aggregated tables built from each selected categorical variable. A specific CA, called CA-GALT, analyses this table while keeping the double projected approach that CA offers. CA-GALT studies the diversity of the vocabulary through the dispersion of the categories and the dispersion of the categories through the diversity of the vocabulary. Thus, the associations and/or oppositions between words acquire their meaning from the categories that they attract or reject and vice versa. The application of the method to a real data set has demonstrated how free-text and closed answers combine to provide relevant information. The influence of each variable on the lexical choices is visualised, avoiding “confusion effect”. The words favoured by the different categories uncover the health-associated concerns related to each variable (*age*, *health condition* or *gender*) in a *ceteris paribus* analysis.

Software note

The R function CaGalt (Correspondence Analysis on Generalised Aggregated Lexical Table) has been developed by the authors. This function will be included in the next release of package FactoMineR (Husson et al., 2007; Lê et al., 2008). Meanwhile, this function can be requested from the authors.

Acknowledgments

This work has been partially supported by the Spanish Ministry of Economy and Competitiveness. Grant ECO2012-35584.

References

- Bécue-Bertaut, M. and Pagès, J. (2004). A principal axes method for comparing multiple contingency tables: MFACT. *Computational Statistics and Data Analysis*, 45, 481–503.
- Benzécri, J.-P. (1973). *L'Analyse des Données. Tome I. L'Analyse des Correspondances*. Dunod, Paris.
- Benzécri, J.-P. (1981). *Pratique de l'Analyse des Données. Tome III. Linguistique & Lexicologie*. Dunod, Paris.
- Böckenholt, U. and Takane, Y. (1994). Linear constraints in correspondence analysis. In: Greenacre, M. J. and Blasius, J. (eds.), *Correspondence Analysis in the Social Sciences*. Academic Press, London.
- Brandimarte, P. (2011). *Quantitative Methods: An Introduction for Business Management*. John Wiley & Sons, Inc., Hoboken, USA.
- Cousteaux, A.-S. (2010). Représentations de la santé et cycle de vie. De la recherche du bien-être au maintien des capacités. *OSC-Notes et Documents N° 2010-01*. http://www.sciencespo.fr/osc/sites/sciencespo.fr/osc/files/nd_2010_01.pdf.
- Efron, B. (1979). Bootstrap methods: another look at jackknife. *The Annals of Statistics*, 7, 1–26.
- Escofier, B. and Pagès, J. (2008). *Analyses Factorielles Simples et Multiples*, 4th Ed. Dunod, Paris.
- Finn, J. D. (1974). *A General Model for Multivariate Analysis*. Holt, Rinehart and Winston, New York.
- Garnier, B. and Guérin-Pace, F. (2010). *Appliquer les méthodes de la statistique textuelle*. CEPED, Paris.
- Greenacre, M. J. (1984). *Theory and Applications of Correspondence Analysis*. Academic Press, New York. (Out-of-print, freely downloadable from www.carme-n.org)
- Härdle, W. and Simar, L. (2012). *Applied Multivariate Statistical Analysis*, 3rd Ed. Springer Verlag, Heidelberg.
- Husson, F., Josse, J., Lê, S. and Mazet, J. (2007). *FactoMineR: Factor Analysis and Data Mining with R*. R package version 1.19.
- Lebart, L., Salem, A. and Berry, L. (1998). *Exploring Textual Data*. Kluwer, Dordrecht.
- Lebart, L., Piron, M. and Morineau, A. (2006). *Statistique exploratoire multidimensionnelle: Visualisation et inférence en fouilles de données*, 4th Ed. Dunod, Paris.
- Legendre, P. and Legendre, L. (1998). *Numerical Ecology*, 2nd Ed. Elsevier Science, Amsterdam.
- Lê, S., Josse, J. and Husson, F. (2008). FactoMineR: An R Package for Multivariate Analysis. *Journal of Statistical Software*, 25, 1–18.
- Murtagh, F. (2005). *Correspondence Analysis and Data Coding with Java and R*. Chapman & Hall, Boca Raton.
- Saporta, G. (2006). *Probabilités, Analyse des Données et Statistique*, 2nd Ed. Technip, Paris.

Selected article from
XIV Conferencia Española
de Biometría 2013

Global hypothesis test to compare the likelihood ratios of multiple binary diagnostic tests with ignorable missing data

Ana Eugenia Marín-Jiménez¹ and José Antonio Roldán-Nofuentes¹

Abstract

In this article, a global hypothesis test is studied to simultaneously compare the likelihood ratios of multiple binary diagnostic tests when in the presence of partial disease verification the missing data mechanism is ignorable. The hypothesis test is based on the chi-squared distribution. Simulation experiments were carried out to study the type I error and the power of the global hypothesis test when comparing the likelihood ratios of two and three diagnostic tests respectively. The results obtained were applied to the diagnosis of coronary stenosis.

MSC: 62P10 (Applications to biology and medical science), 6207 (Data analysis)

Keywords: Global hypothesis test, partial verification, positive and negative likelihood ratio.

1. Introduction

The fundamental parameters to assess the accuracy of a binary diagnostic test are the sensitivity and the specificity. Sensitivity (Se) is the probability of the diagnostic test being positive when the individual has the disease, and specificity (Sp) is the probability of the diagnostic test being negative when the individual does not have the disease. Sensitivity and specificity depend on the intrinsic ability of the diagnostic test to distinguish between individuals with and without the disease. Other parameters to assess the accuracy of a binary diagnostic test are the likelihood ratios (LRs). When the result of the diagnostic test is positive, the likelihood ratio, called positive likelihood ratio (LR^+), is the ratio between the probability of a positive test result in individuals with the disease (Se) and the probability of a positive result in individuals without the disease ($1 - Sp$). When the result of the diagnostic test is negative, the likelihood ratio,

¹ Biostatistics, Department of Statistics, University of Granada, Spain, email: anamarin@ugr.es, jaroldan@ugr.es
Received: March 2014
Accepted: June 2014

called negative likelihood ratio (LR^-), is the ratio between the probability of a negative test result in individuals with the disease ($1 - Se$) and the probability of a negative test result in individuals without the disease (Sp). The LRs only depend on the sensitivity and specificity of the diagnostic test, and their values vary between zero and infinite. When the diagnostic test and the gold standard are independent then $LR^+ = LR^- = 1$, and if the diagnostic test correctly classifies all of the individuals (with or without the disease) then $LR^+ = \infty$ and $LR^- = 0$. A value of $LR^+ > 1$ indicates that a positive test result is more probable for an individual with the disease than for an individual without the disease, and a value of $LR^- < 1$ indicates that a negative test result is more probable for an individual who does not have the disease than for one who has the disease. The LRs quantify the increase in knowledge of the disease presence through the application of the diagnostic test. Let T be the random variable that models the result of the diagnostic test ($T = 1$ when the result is positive and $T = 0$ when the result is negative), let D be the random variable that models the result of the gold standard ($D = 1$ when the individual is diseased and $D = 0$ when this is not the case), and $p = P(D = 1)$ the disease prevalence in the population which is subject to the study. The ratio between the probability that an individual has the disease and the probability that an individual does not have the disease before applying the diagnostic test is

$$\text{Odds pre-test} = \frac{p}{1-p}.$$

After applying the diagnostic test the ratio is

$$\text{Odds post-test}(T) = \frac{P(D = 1|T)}{P(D = 0|T)}.$$

The LRs relate the two previous odds, i.e.

$$\text{Odds post-test}(T = 1) = LR^+ \times \text{Odds pre-test}$$

and

$$\text{Odds post-test}(T = 0) = LR^- \times \text{Odds pre-test}$$

Furthermore, the comparison of the LRs of diagnostic tests has been the subject of different studies. In designs with independent samples, Luts et al (2011) studied a hypothesis test to compare the LRs of two or more binary diagnostic tests studying the effect of sample sizes on the asymptotic behaviour of the proposed test. The hypothesis test proposed by these authors allows us to simultaneously compare the LRs of the diagnostic tests subject to this type of sample design and is based on the chi-squared distribution. For paired designs, Leisenring and Pepe (1998) proposed a *GEE* model

to independently compare the positive LRs and the negative LRs of two diagnostic tests; and Roldán Nofuentes and Luna del Castillo (2007) proposed a hypothesis test to independently and jointly compare the positive LRs and the negative LRs of two diagnostic tests through a likelihood-based approach. Nevertheless, in clinical practice the gold standard is frequently not applied to all of the individuals in a sample, leading to the problem known as partial disease verification (Begg and Greenes, 1983; Zhou, 1993). In this situation, the disease status (whether the disease is present or absent) is unknown for a subset of individuals in the sample, and therefore if the previous parameters are estimated only considering those individuals whose disease status are known, the estimators are affected by what is known as verification bias. The same problem occurs when, in the presence of partial disease verification, the parameters of two (or more) binary diagnostic tests are compared in relation to the same gold standard. When in the presence of partial verification the missing data mechanism is MAR, Roldán Nofuentes and Luna del Castillo (2005) studied a hypothesis test to independently compare the LRs of two binary diagnostic tests. In this article, we extend the results of these authors and we study a hypothesis test to simultaneously compare the LRs of two or more binary diagnostic tests. In Section 2, we propose a global hypothesis test based on the chi-squared distribution to simultaneously compare the LRs of multiple binary diagnostic tests when, in the presence of partial disease verification, the missing data is ignorable. In Section 3, we carry out simulation experiments to study the type I error and the power of the global hypothesis test when simultaneously comparing the LRs of two and of three binary diagnostic tests. In Section 4, the global test is applied to an example and in Section 5 we discuss the results obtained.

2. Global hypothesis test

Let us consider J binary diagnostic tests ($J \geq 2$) that are applied independently to all of the individuals in a random sample sized n , and a gold standard that is only applied to a subset of the n individuals in the sample. Let T_j ($j = 1, \dots, J$), V and D be the random variables defined as: T_j models the result of the j th binary test ($T_j = 1$ when the test result is positive and $T_j = 0$ when it is negative); V models the verification process ($V = 1$ when the individual is verified with the gold standard and $V = 0$ when the individual is not verified with the gold standard); and D models the result of the gold standard ($D = 1$ when the individual has the disease and $D = 0$ when the individual does not have the disease). Let s_{i_1, \dots, i_J} be the number of individuals verified in which $T_1 = i_1, T_2 = i_2, \dots, T_J = i_J$ and $D = 1$; r_{i_1, \dots, i_J} the number of individuals verified in which $T_1 = i_1, T_2 = i_2, \dots, T_J = i_J$ and $D = 0$; and u_{i_1, \dots, i_J} the number of individuals not verified in which $T_1 = i_1, T_2 = i_2, \dots, T_J = i_J$, with $i_j = 0, 1$ and $j = 1, \dots, J$. Let $n_{i_1, \dots, i_J} = s_{i_1, \dots, i_J} + r_{i_1, \dots, i_J} + u_{i_1, \dots, i_J}$ and $n = \sum_{i_1, \dots, i_J=0}^1 n_{i_1, \dots, i_J}$. Let the probabilities be

$$\phi_{i_1, \dots, i_J} = P(V = 1, D = 1, T_1 = i_1, \dots, T_J = i_J)$$

$$\varphi_{i_1, \dots, i_J} = P(V = 1, D = 0, T_1 = i_1, \dots, T_J = i_J)$$

and

$$\gamma_{i_1, \dots, i_J} = P(V = 0, T_1 = i_1, \dots, T_J = i_J)$$

with $i_j = 0, 1$, and it is verified that

$$\sum_{i_1, \dots, i_J=0}^1 \phi_{i_1, \dots, i_J} + \sum_{i_1, \dots, i_J=0}^1 \varphi_{i_1, \dots, i_J} + \sum_{i_1, \dots, i_J=0}^1 \gamma_{i_1, \dots, i_J} = 1.$$

Let $\boldsymbol{\omega} = (\phi_{1, \dots, 1}, \dots, \phi_{0, \dots, 0}, \varphi_{1, \dots, 1}, \dots, \varphi_{0, \dots, 0}, \gamma_{1, \dots, 1}, \dots, \gamma_{0, \dots, 0})^T$ be a vector of size $3 \cdot 2^J$ whose components are the previous probabilities. As the disease status of all the individuals in the sample is not verified with the gold standard, the verification probabilities are defined as

$$\lambda_{k, i_1, \dots, i_J} = P(V = 1 | D = k, T_1 = i_1, T_2 = i_2, \dots, T_J = i_J).$$

Therefore, $\lambda_{k, i_1, \dots, i_J}$ is the probability of selecting an individual to verify the disease status in which $D=k, T_1 = i_1, T_2 = i_2, \dots$ and $T_J = i_J$, with $k, i_j = 0, 1, j = 1, \dots, J$. If the verification process only depends on the results of the J binary tests and does not depend on the disease status, that is to say when $\lambda_{k, i_1, \dots, i_J} = \lambda_{i_1, \dots, i_J} = P(V = 1 | T_1 = i_1, T_2 = i_2, \dots, T_J = i_J)$, this is equivalent to assuming that the verification process is missing at random (MAR) (Rubin, 1976). Assuming that the verification process is MAR and that the parameters of the data model and the parameters of the missingness mechanism are different, the missing data mechanism is called to be ignorable (Schafer, 1997) and all of the parameters of the model can be estimated applying the method of maximum likelihood. Under this assumption, the LR s of the j th diagnostic test are written as

$$LR_j^+ = \frac{(1-p) \left(\sum_{\substack{i_1, \dots, i_J=0 \\ i_j=1}}^1 \frac{\phi_{i_1, \dots, i_J} \eta_{i_1, \dots, i_J}}{\phi_{i_1, \dots, i_J} + \varphi_{i_1, \dots, i_J}} \right)}{p \left((1-p) - \sum_{\substack{i_1, \dots, i_J=0 \\ i_j=0}}^1 \frac{\varphi_{i_1, \dots, i_J} \eta_{i_1, \dots, i_J}}{\phi_{i_1, \dots, i_J} + \varphi_{i_1, \dots, i_J}} \right)}$$

and

$$LR_j^- = \frac{(1-p) \left(p - \sum_{\substack{i_1, \dots, i_J=0 \\ i_j=1}}^1 \frac{\phi_{i_1, \dots, i_J} \eta_{i_1, \dots, i_J}}{\phi_{i_1, \dots, i_J} + \varphi_{i_1, \dots, i_J}} \right)}{p \left(\sum_{\substack{i_1, \dots, i_J=0 \\ i_j=0}}^1 \frac{\varphi_{i_1, \dots, i_J} \eta_{i_1, \dots, i_J}}{\phi_{i_1, \dots, i_J} + \varphi_{i_1, \dots, i_J}} \right)},$$

where $p = \sum_{i_1, \dots, i_J=0}^1 \frac{\phi_{i_1, \dots, i_J} \eta_{i_1, \dots, i_J}}{\phi_{i_1, \dots, i_J} + \varphi_{i_1, \dots, i_J}}$ is the disease prevalence and $\eta_{i_1, \dots, i_J} = \phi_{i_1, \dots, i_J} + \varphi_{i_1, \dots, i_J} + \gamma_{i_1, \dots, i_J}$. The log-likelihood of the observed data is

$$l = \sum_{i_1, \dots, i_J=0}^1 s_{i_1, \dots, i_J} \log(\phi_{i_1, \dots, i_J}) + \sum_{i_1, \dots, i_J=0}^1 r_{i_1, \dots, i_J} \log(\varphi_{i_1, \dots, i_J}) + \sum_{i_1, \dots, i_J=0}^1 u_{i_1, \dots, i_J} \log(\gamma_{i_1, \dots, i_J})$$

Maximizing this function, the maximum likelihood estimators of the probabilities ϕ_{i_1, \dots, i_J} , $\varphi_{i_1, \dots, i_J}$ and γ_{i_1, \dots, i_J} are

$$\hat{\phi}_{i_1, \dots, i_J} = \frac{s_{i_1, \dots, i_J}}{n}, \hat{\varphi}_{i_1, \dots, i_J} = \frac{r_{i_1, \dots, i_J}}{n} \text{ and } \hat{\gamma}_{i_1, \dots, i_J} = \frac{u_{i_1, \dots, i_J}}{n}$$

and, therefore, the maximum likelihood estimators of the LR s of the j th diagnostic test are

$$\widehat{LR}_j^+ = \frac{\left(\sum_{i_1, \dots, i_J=0}^1 \frac{r_{i_1, \dots, i_J} n_{i_1, \dots, i_J}}{s_{i_1, \dots, i_J} + r_{i_1, \dots, i_J}} \right) \left(\sum_{i_j=1}^1 \frac{s_{i_1, \dots, i_J} n_{i_1, \dots, i_J}}{s_{i_1, \dots, i_J} + r_{i_1, \dots, i_J}} \right)}{\left(\sum_{i_1, \dots, i_J=0}^1 \frac{s_{i_1, \dots, i_J} n_{i_1, \dots, i_J}}{s_{i_1, \dots, i_J} + r_{i_1, \dots, i_J}} \right) \left(\sum_{i_1, \dots, i_J=0}^1 \frac{r_{i_1, \dots, i_J} n_{i_1, \dots, i_J}}{s_{i_1, \dots, i_J} + r_{i_1, \dots, i_J}} - \sum_{i_j=0}^1 \frac{r_{i_1, \dots, i_J} n_{i_1, \dots, i_J}}{s_{i_1, \dots, i_J} + r_{i_1, \dots, i_J}} \right)}$$

and

$$\widehat{LR}_j^- = \frac{\left(\sum_{i_1, \dots, i_J=0}^1 \frac{r_{i_1, \dots, i_J} n_{i_1, \dots, i_J}}{s_{i_1, \dots, i_J} + r_{i_1, \dots, i_J}} \right) \left(\sum_{i_1, \dots, i_J=0}^1 \frac{s_{i_1, \dots, i_J} n_{i_1, \dots, i_J}}{s_{i_1, \dots, i_J} + r_{i_1, \dots, i_J}} - \sum_{i_j=1}^1 \frac{s_{i_1, \dots, i_J} n_{i_1, \dots, i_J}}{s_{i_1, \dots, i_J} + r_{i_1, \dots, i_J}} \right)}{\left(\sum_{i_1, \dots, i_J=0}^1 \frac{s_{i_1, \dots, i_J} n_{i_1, \dots, i_J}}{s_{i_1, \dots, i_J} + r_{i_1, \dots, i_J}} \right) \left(\sum_{i_j=0}^1 \frac{r_{i_1, \dots, i_J} n_{i_1, \dots, i_J}}{s_{i_1, \dots, i_J} + r_{i_1, \dots, i_J}} \right)}.$$

Let $\boldsymbol{\eta} = (LR_1^+, \dots, LR_J^+, LR_1^-, \dots, LR_J^-)^\top$ be a vector of size $2J$ whose components are the LR s of each diagnostic test. As the vector $\boldsymbol{\omega}$ is the vector of probabilities of a multinomial distribution, the variance-covariance matrix of $\hat{\boldsymbol{\omega}}$ is $\boldsymbol{\Sigma}_{\hat{\boldsymbol{\omega}}} = \{\text{diag}(\boldsymbol{\omega}) - \boldsymbol{\omega}\boldsymbol{\omega}^\top\}/n$, and applying the delta method (Agresti, 2002) the asymptotic variance-covariance matrix of $\hat{\boldsymbol{\eta}}$ is

$$\boldsymbol{\Sigma}_{\hat{\boldsymbol{\eta}}} = \left(\frac{\partial \boldsymbol{\eta}}{\partial \boldsymbol{\omega}} \right) \boldsymbol{\Sigma}_{\hat{\boldsymbol{\omega}}} \left(\frac{\partial \boldsymbol{\eta}}{\partial \boldsymbol{\omega}} \right)^\top \quad (1)$$

The positive and negative LR s of each one of the J diagnostic tests depend on the same parameters (sensitivity and specificity of the j th diagnostic test) and, therefore, these parameters can be compared simultaneously. The global hypothesis test to compare simultaneously the LR s of the J diagnostic tests is

$$\begin{aligned} H_0 : LR_1^+ = LR_2^+ = \dots = LR_J^+ \text{ and } LR_1^- = LR_2^- = \dots = LR_J^- \\ H_1 : \text{at least one equality is not true.} \end{aligned}$$

This hypothesis test is equivalent to the hypothesis test

$$H_0 : \boldsymbol{\psi} \boldsymbol{\eta} = 0 \text{ vs } H_1 : \boldsymbol{\psi} \boldsymbol{\eta} \neq 0 \quad (2)$$

where $\boldsymbol{\psi}$ is a full range matrix whose dimension is $2(J-1) \times 2J$, and whose elements are known values. For $J = 2$ the matrix $\boldsymbol{\psi}$ is

$$\boldsymbol{\psi} = \begin{pmatrix} 1 & -1 & 0 & 0 \\ 0 & 0 & 1 & -1 \end{pmatrix}$$

and for $J \geq 3$ the matrix $\boldsymbol{\psi}$ is

$$\boldsymbol{\psi} = \begin{pmatrix} \boldsymbol{\psi}_1 & \boldsymbol{\psi}_0 \\ \boldsymbol{\psi}_0 & \boldsymbol{\psi}_1 \end{pmatrix}$$

where $\boldsymbol{\psi}_0$ is a matrix $(J-1) \times J$ with all of the elements equal to 0, and $\boldsymbol{\psi}_1$ is a matrix $(J-1) \times J$ where the elements (i, i) are equal to 1, the elements $(i, i+1)$ are equal to -1 for $i = 1, \dots, J-1$, and the rest of the elements in this matrix are equal to 0. Applying the multivariate central limit theorem it is verified that

$$\sqrt{n}(\hat{\boldsymbol{\eta}} - \boldsymbol{\eta}) \xrightarrow[n \rightarrow \infty]{} N_{2J}(\mathbf{0}, \boldsymbol{\Sigma}_{\boldsymbol{\eta}}).$$

Then, the statistic $Q^2 = (\boldsymbol{\psi} \hat{\boldsymbol{\eta}})^\top (\boldsymbol{\psi} \hat{\boldsymbol{\Sigma}}_{\hat{\boldsymbol{\eta}}} \boldsymbol{\psi}^\top)^{-1} \boldsymbol{\psi} \hat{\boldsymbol{\eta}}$ is distributed according to Hotelling's T-squared distribution with a dimension $2(J-1)$ and n degrees of freedom, where $2(J-1)$ is the dimension of the vector $\boldsymbol{\psi} \hat{\boldsymbol{\eta}}$. When n is large, the statistic Q^2 is distributed according to a central chi-squared distribution with $2(J-1)$ degrees of freedom when the null hypothesis is true, i.e.

$$Q^2 = (\boldsymbol{\psi} \hat{\boldsymbol{\eta}})^\top (\boldsymbol{\psi} \hat{\boldsymbol{\Sigma}}_{\hat{\boldsymbol{\eta}}} \boldsymbol{\psi}^\top)^{-1} \boldsymbol{\psi} \hat{\boldsymbol{\eta}} \xrightarrow[n \rightarrow \infty]{} \chi_{2(J-1)}^2 \tag{3}$$

Alternative methods to the global hypothesis test based on the chi-squared distribution are the following:

1. Comparisons of the paired positive (negative) LR s of diagnostic tests to an error rate of α . This method consists of solving the $2J$ marginal hypothesis tests given by

$$\begin{aligned} H_0 : LR_k^+ = LR_l^+ \text{ vs } H_1 : LR_k^+ \neq LR_l^+ \\ H_0 : LR_k^- = LR_l^- \text{ vs } H_1 : LR_k^- \neq LR_l^- \end{aligned} \tag{4}$$

when $k, l = 1, \dots, J$ and $k \neq l$, each one of them to an error rate of α . Based on the asymptotic normality of the estimators of the LR s, the statistic for hypothesis test (4) is

$$z = \frac{\widehat{LR}_j - \widehat{LR}_k}{\sqrt{\widehat{\text{Var}}(\widehat{LR}_j) + \widehat{\text{Var}}(\widehat{LR}_k) - 2\widehat{\text{Cov}}(\widehat{LR}_j, \widehat{LR}_k)}} \xrightarrow[n \rightarrow \infty]{} N(0, 1)$$

where \widehat{LR} is \widehat{LR}^+ or \widehat{LR}^- and the variances-covariances are obtained from equation (1).

2. Another alternative method to the statistic (3) consists of solving the $2J$ marginal hypothesis tests (4) by applying a method of multiple comparisons, such as the Bonferroni method (1936), the Holm method (1979) or the Hochberg method (1983), which are very easy to apply and which are frequently used in the field of multiple comparisons. The Bonferroni method consists of solving each marginal hypothesis test (4) to an error rate of $\alpha/\{J(J-1)\}$ instead of to an error rate of α . In the Appendix there is a summary of the Holm method and the Hochberg method.

3. Simulation experiments

Monte Carlo simulation experiments were carried out to study the type I error and the power of the global hypothesis test based on the chi-squared distribution (3) and on the alternative methods proposed in the previous section, when simultaneously comparing the LRs of two and of three binary diagnostic tests respectively. The experiments consisted of the generation of 5000 random multinomial samples of size 100, 200, 300, 400, 500, 1000 and 2000. The samples were generated in such a way that for all of them it was possible to estimate the LRs and their variances-covariances. For all of the study we set $\alpha = 0.05$.

3.1. Two diagnostic tests

When simultaneously comparing the LRs of two binary diagnostic tests, as the sensitivity and specificity of each diagnostic test we took the values $\{0.70, 0.75, \dots, 0.95\}$, which are values that frequently appear in clinical practice; as values for the disease prevalence we took $\{10\%, 20\%, 30\%, 40\%, 50\%\}$, and as the verification probabilities we took the values

$$(\lambda_{11} = 0.70, \lambda_{10} = \lambda_{01} = 0.40, \lambda_{00} = 0.10)$$

and

$$(\lambda_{11} = 0.95, \lambda_{10} = \lambda_{01} = 0.60, \lambda_{00} = 0.30),$$

that can be considered to be low and high verification probabilities respectively. The probabilities of the multinomial distributions were calculated applying Vacek's conditional dependence model (Vacek, 1985), i.e.

$$\begin{aligned} \phi_{ij} &= \lambda_{ij} p \left\{ Se_1^i (1 - Se_1)^{1-i} Se_2^j (1 - Se_2)^{1-j} + \delta_{ij} \varepsilon_1 \right\}, \\ \varphi_{ij} &= \lambda_{ij} (1 - p) \left\{ Sp_1^{1-i} (1 - Sp_1)^i Sp_2^{1-j} (1 - Sp_2)^j + \delta_{ij} \varepsilon_0 \right\}, \\ \gamma_{ij} &= (1 - \lambda_{ij}) p \left\{ Se_1^i (1 - Se_1)^{1-i} Se_2^j (1 - Se_2)^{1-j} + \delta_{ij} \varepsilon_1 \right\} \\ &\quad + (1 - \lambda_{ij}) (1 - p) \left\{ Sp_1^{1-i} (1 - Sp_1)^i Sp_2^{1-j} (1 - Sp_2)^j + \delta_{ij} \varepsilon_0 \right\}, \end{aligned}$$

where $\delta_{ij} = 1$ when $i = j$ and $\delta_{ij} = -1$ when $i \neq j$, and ε_1 is the dependence factor (covariance) between the two diagnostic tests when $D = 1$ and ε_0 is the dependence factor (covariance) between the two diagnostic tests when $D = 0$. In general, in clinical practice the two diagnostic tests are usually conditionally dependent on the disease and it is verified that

$$0 < \varepsilon_1 < Se_1(1 - Se_2) \text{ when } Se_2 > Se_1$$

$$0 < \varepsilon_1 < Se_2(1 - Se_1) \text{ when } Se_1 > Se_2$$

and

$$0 < \varepsilon_0 < Sp_1(1 - Sp_2) \text{ when } Sp_2 > Sp_1$$

$$0 < \varepsilon_0 < Sp_2(1 - Sp_1) \text{ when } Sp_1 > Sp_2.$$

If the two diagnostic tests are conditionally independent on the disease then it is verified that $\varepsilon_1 = \varepsilon_0 = 0$.

In Table 1, we show the results obtained for the type I error when comparing the *LRs* of two diagnostic tests with sensitivities equal to 0.90 and specificities equal to 0.80, prevalence is equal to 10% and for intermediate and high dependence factors (ε_1 and ε_0). From the results, the following conclusions are obtained. The global hypothesis test based on the chi-squared distribution has a type I error which, in general terms, fluctuates around a nominal error of 5% especially when $n \geq 1000$, and the type I error is lower than the nominal error for samples of a smaller size. Therefore, the global test based on the chi-squared distribution show the classic performance of an asymptotic tests (the type I error fluctuates around the nominal error starting from a certain sample size). Moreover, the type I error increases when there is a rise in the disease prevalence but without overwhelming the nominal error of 5%, whilst the verification probabilities do not have an important effect upon the type I error (especially with large samples). Regarding the type I error of the method based on the paired comparison to an error rate of 5% (called Method 1 in the tables), its type I error clearly overwhelms the nominal error, above all when $n \geq 300 - 400$ depending on the prevalence and the verification probabilities, and therefore this method may lead to erroneous results. Regarding the methods based on paired comparisons and the application of the Bonferroni method (Method 2), the Holm method (Method 3) and the Hochberg method (Method 4), their respective type I errors are almost identical and show a very similar performance to the type I error of the global test based on the chi-squared distribution. Regarding power, in Table 2 we show the results obtained when the sensitivities are equal to 0.90 and 0.85 and the specificities are equal to 0.80 and 0.75 respectively, prevalence is equal to 10% and also for intermediate and high dependence factors. In general terms, with samples of 500 individuals, the power of the global test is very high (higher than 80%-90%), and the power is greater when the prevalence is greater and also when the verification probabilities are greater. Regarding the power of Method 2, this is greater than that of the global test because its type I error is also greater. As for the powers of Methods 2, 3 and 4, these are very similar to each other and these methods also have a power which is slightly lower than that of the global test, especially when the samples are not very large (in general terms, between 200 and 400 individuals).

Table 1: Type I errors when comparing the LR_s of two diagnostic tests.

$Se_1 = Se_2 = 0.90$ $Sp_1 = Sp_2 = 0.80$ $p = 10\%$ $LR_1^+ = LR_2^+ = 4.5$ $LR_1^- = LR_2^- = 0.125$												
$\lambda_{11} = 0.70$ $\lambda_{10} = 0.40$ $\lambda_{01} = 0.40$ $\lambda_{00} = 0.10$												
$\varepsilon_1 = 0.04$ $\varepsilon_0 = 0.07$												
<i>n</i>	Global test	Method 1	Method 2	Method 3	Method 4	Global test	Method 1	Method 2	Method 3	Method 4	Global test	Method 4
100	0.007	0.010	0.005	0.005	0.005	0.000	0.000	0.000	0.000	0.000	0.000	0.000
200	0.006	0.008	0.005	0.005	0.005	0.001	0.004	0.002	0.002	0.002	0.002	0.003
300	0.005	0.010	0.000	0.000	0.000	0.008	0.010	0.008	0.008	0.008	0.008	0.009
400	0.010	0.020	0.007	0.007	0.008	0.018	0.022	0.015	0.015	0.015	0.015	0.016
500	0.011	0.025	0.009	0.009	0.010	0.013	0.020	0.012	0.012	0.012	0.012	0.013
1000	0.037	0.054	0.027	0.027	0.029	0.014	0.033	0.011	0.011	0.011	0.011	0.012
2000	0.044	0.086	0.040	0.040	0.041	0.025	0.052	0.026	0.026	0.026	0.026	0.027
$\lambda_{11} = 0.95$ $\lambda_{10} = 0.60$ $\lambda_{01} = 0.60$ $\lambda_{00} = 0.30$												
$\varepsilon_1 = 0.04$ $\varepsilon_0 = 0.07$												
<i>n</i>	Global test	Method 1	Method 2	Method 3	Method 4	Global test	Method 1	Method 2	Method 3	Method 4	Global test	Method 4
100	0.004	0.011	0.003	0.003	0.003	0.001	0.002	0.001	0.001	0.001	0.001	0.002
200	0.006	0.022	0.005	0.005	0.006	0.007	0.022	0.010	0.010	0.010	0.010	0.011
300	0.010	0.041	0.011	0.011	0.013	0.007	0.028	0.010	0.010	0.010	0.010	0.011
400	0.025	0.043	0.022	0.022	0.023	0.013	0.036	0.014	0.014	0.014	0.014	0.016
500	0.035	0.053	0.034	0.034	0.034	0.014	0.038	0.015	0.015	0.015	0.015	0.015
1000	0.043	0.080	0.040	0.040	0.042	0.022	0.056	0.022	0.022	0.022	0.022	0.024
2000	0.052	0.098	0.048	0.048	0.051	0.030	0.067	0.023	0.023	0.023	0.023	0.025

Table 2: Powers when comparing the LRs of two diagnostic tests.

$Se_1 = 0.90$ $Se_2 = 0.85$ $Sp_1 = 0.80$ $Sp_2 = 0.75$ $p = 10\%$ $LR_1^+ = 6$ $LR_2^+ = 3.2$ $LR_1^- = 0.12$ $LR_2^- = 0.27$												
$\lambda_{11} = 0.70$ $\lambda_{10} = 0.40$ $\lambda_{01} = 0.40$ $\lambda_{00} = 0.10$												
$\varepsilon_1 = 0.03$ $\varepsilon_0 = 0.05$												
<i>n</i>	Global test	Method 1	Method 2	Method 3	Method 4	Global test	Method 1	Method 2	Method 3	Method 4	Global test	Method 4
100	0.044	0.045	0.023	0.023	0.024	0.036	0.030	0.020	0.020	0.020	0.020	0.020
200	0.166	0.208	0.086	0.086	0.091	0.324	0.261	0.171	0.171	0.171	0.171	0.176
300	0.473	0.492	0.308	0.308	0.322	0.659	0.638	0.466	0.466	0.466	0.466	0.476
400	0.715	0.732	0.560	0.560	0.568	0.841	0.885	0.791	0.791	0.791	0.791	0.799
500	0.874	0.876	0.767	0.767	0.767	0.950	0.968	0.939	0.939	0.939	0.939	0.939
1000	1	0.995	0.992	0.992	0.992	1	1	1	1	1	1	1
2000	1	1	1	1	1	1	1	1	1	1	1	1
$\lambda_{11} = 0.95$ $\lambda_{10} = 0.60$ $\lambda_{01} = 0.60$ $\lambda_{00} = 0.30$												
$\varepsilon_1 = 0.03$ $\varepsilon_0 = 0.05$												
<i>n</i>	Global test	Method 1	Method 2	Method 3	Method 4	Global test	Method 1	Method 2	Method 3	Method 4	Global test	Method 4
100	0.069	0.092	0.039	0.039	0.047	0.131	0.135	0.052	0.052	0.052	0.052	0.069
200	0.340	0.505	0.315	0.315	0.324	0.647	0.748	0.618	0.618	0.618	0.618	0.622
300	0.738	0.809	0.678	0.678	0.680	0.936	0.946	0.901	0.901	0.901	0.901	0.901
400	0.907	0.923	0.856	0.856	0.856	0.922	0.990	0.980	0.980	0.980	0.980	0.980
500	0.974	0.972	0.941	0.941	0.941	0.998	0.998	0.998	0.998	0.998	0.998	0.998
1000	1	1	1	1	1	1	1	1	1	1	1	1
2000	1	1	1	1	1	1	1	1	1	1	1	1
$\varepsilon_1 = 0.06$ $\varepsilon_0 = 0.10$												

3.2. Three diagnostic tests

When simultaneously comparing the *LRs* of three binary diagnostic tests, as the sensitivity and the specificity of each diagnostic test and the disease prevalence we took the same values as in the case of the diagnostic tests, and as verification probabilities we took the values

$$(\lambda_{111} = 0.70, \lambda_{110} = 0.40, \lambda_{101} = 0.40, \lambda_{100} = 0.25, \lambda_{011} = 0.40, \lambda_{010} = 0.25, \\ \lambda_{001} = 0.25, \lambda_{000} = 0.05)$$

and

$$(\lambda_{111} = 1, \lambda_{110} = 0.80, \lambda_{101} = 0.80, \lambda_{100} = 0.40, \lambda_{011} = 0.80, \lambda_{010} = 0.40, \\ \lambda_{001} = 0.40, \lambda_{000} = 0.20)$$

which can also be considered to be low and high verification scenarios. When comparing the *LRs* of three diagnostic tests, the probabilities of the multinomial distributions were calculating applying the Torrance-Rynard and Walter model (1997). In this case, the expressions of the probabilities are:

$$\begin{aligned} \phi_{i_1 i_2 i_3} &= p \lambda_{i_1 i_2 i_3} \left\{ \prod_{j=1}^3 Se_j^{i_j} (1 - Se_j)^{1-i_j} + \sum_{j,k,j < k}^3 (-1)^{|i_j - i_k|} \delta_{jk} \right\}, \\ \varphi_{i_1 i_2 i_3} &= q \lambda_{i_1 i_2 i_3} \left\{ \prod_{j=1}^3 Sp_j^{1-i_j} (1 - Sp_j)^{i_j} + \sum_{j,k,j < k}^3 (-1)^{|i_j - i_k|} \varepsilon_{jk} \right\}, \\ \gamma_{i_1 i_2 i_3} &= p (1 - \lambda_{i_1 i_2 i_3}) \left\{ \prod_{j=1}^3 Se_j^{i_j} (1 - Se_j)^{1-i_j} + \sum_{j,k,j < k}^3 (-1)^{|i_j - i_k|} \delta_{jk} \right\} \\ &\quad + (1 - p) (1 - \lambda_{i_1 i_2 i_3}) \left\{ \prod_{j=1}^3 Sp_j^{1-i_j} (1 - Sp_j)^{i_j} + \sum_{j,k,j < k}^3 (-1)^{|i_j - i_k|} \varepsilon_{jk} \right\}, \end{aligned}$$

with $i_j = 0, 1$, $i_k = 0, 1$ and $j, k = 1, 2, 3$, where δ_{jk} is the dependence factor (covariance) between the j th and the k th diagnostic test when $D = 1$ and ε_{jk} is the dependence factor (covariance) between the j th and the k th diagnostic test when $D = 0$. The dependence factors δ_{jk} and ε_{jk} verifies restrictions that depend on the values of the sensitivities and the specificities of the three diagnostic tests. In order to simplify things, in the simulation experiments it was considered that $\delta_{ij} = \delta$ and $\varepsilon_{ij} = \varepsilon$, and therefore the dependence factors verify the following restrictions:

$$\begin{aligned} \delta &\leq (1 - Se_1)(1 - Se_2)Se_3, \quad \delta \leq (1 - Se_1)Se_2(1 - Se_3), \quad \delta \leq Se_1(1 - Se_2)(1 - Se_3) \\ \varepsilon &\leq (1 - Sp_1)(1 - Sp_2)Sp_3, \quad \varepsilon \leq (1 - Sp_1)Sp_2(1 - Sp_3), \quad \varepsilon \leq Sp_1(1 - Sp_2)(1 - Sp_3). \end{aligned}$$

Table 3: Type I errors when comparing the LR_s of three diagnostic tests.

$Se_1 = Se_2 = Se_3 = 0.90$ $Sp_1 = Sp_2 = Sp_3 = 0.80$ $p = 10\%$ $LR_1^+ = LR_2^+ = LR_3^+ = 4.5$ $LR_1^- = LR_2^- = LR_3^- = 0.125$															
$\lambda_{111} = 0.70$ $\lambda_{110} = 0.40$ $\lambda_{101} = 0.40$ $\lambda_{100} = 0.25$ $\lambda_{011} = 0.40$ $\lambda_{010} = 0.25$ $\lambda_{001} = 0.25$ $\lambda_{000} = 0.05$															
$\delta = 0.004$ $\varepsilon = 0.015$															
<i>n</i>	Global test	Method 1	Method 2	Method 3	Method 4	Global test	Method 1	Method 2	Method 3	Method 4	Global test	Method 1	Method 2	Method 3	Method 4
100	0.001	0.003	0.000	0.000	0.001	0.000	0.001	0.000	0.000	0.001	0.000	0.001	0.000	0.000	0.000
200	0.005	0.022	0.002	0.002	0.014	0.004	0.028	0.001	0.001	0.028	0.001	0.028	0.001	0.001	0.001
300	0.020	0.078	0.012	0.012	0.014	0.004	0.028	0.001	0.001	0.028	0.001	0.028	0.001	0.001	0.001
400	0.036	0.123	0.023	0.023	0.024	0.009	0.053	0.007	0.007	0.053	0.007	0.053	0.007	0.007	0.007
500	0.043	0.140	0.028	0.029	0.032	0.021	0.078	0.011	0.011	0.078	0.011	0.078	0.011	0.011	0.012
1000	0.054	0.199	0.034	0.034	0.040	0.045	0.179	0.035	0.035	0.179	0.035	0.179	0.035	0.035	0.039
2000	0.056	0.216	0.052	0.052	0.057	0.058	0.216	0.048	0.048	0.216	0.048	0.216	0.048	0.049	0.051
$\lambda_{111} = 1$ $\lambda_{110} = 0.80$ $\lambda_{101} = 0.80$ $\lambda_{100} = 0.40$ $\lambda_{011} = 0.80$ $\lambda_{010} = 0.40$ $\lambda_{001} = 0.40$ $\lambda_{000} = 0.20$															
$\delta = 0.004$ $\varepsilon = 0.015$															
<i>n</i>	Global test	Method 1	Method 2	Method 3	Method 4	Global test	Method 1	Method 2	Method 3	Method 4	Global test	Method 1	Method 2	Method 3	Method 4
100	0.010	0.013	0.001	0.001	0.001	0.001	0.004	0.001	0.001	0.004	0.001	0.004	0.001	0.001	0.001
200	0.019	0.077	0.005	0.005	0.007	0.004	0.038	0.003	0.003	0.038	0.003	0.038	0.003	0.003	0.004
300	0.028	0.125	0.013	0.013	0.016	0.012	0.087	0.005	0.005	0.087	0.005	0.087	0.005	0.005	0.006
400	0.032	0.148	0.018	0.018	0.020	0.023	0.125	0.014	0.014	0.125	0.014	0.125	0.014	0.014	0.016
500	0.039	0.161	0.021	0.021	0.024	0.035	0.157	0.019	0.019	0.157	0.019	0.157	0.019	0.019	0.021
1000	0.051	0.204	0.036	0.036	0.039	0.051	0.189	0.039	0.039	0.189	0.039	0.189	0.039	0.040	0.042
2000	0.053	0.221	0.041	0.041	0.046	0.050	0.204	0.037	0.037	0.204	0.037	0.204	0.037	0.037	0.042

In clinical practice, factors δ_{jk} and/or ε_{jk} are greater than zero, and therefore the diagnostic tests are conditionally dependent on the disease status. When $\delta_{jk} = \varepsilon_{jk} = 0$ the three diagnostic tests are conditionally independent on the disease status.

In Table 3, we show the results obtained for the type I error when the three sensitivities are equal to 0.90 and the three specificities are equal to 0.80, prevalence is equal to 10% and for intermediate and high dependence factors (δ and ε). From the results it holds that, in general terms, the type I error of the global hypothesis test performs in a similar way to that obtained when comparing two diagnostic tests (the type I error fluctuates around the nominal error starting from a determined sample size). Regarding the other methods, Method 1 has a type I error that clearly overwhelms the nominal error, and Methods 2, 3 and 4 have a type I error that is slightly lower than that of the global test.

In terms of power, in Table 4 we show the results obtained for sensitivities equal to 0.90, 0.85 and 0.80, specificities equal to 0.85, 0.75 and 0.70 respectively, and prevalence is equal to 10%. In general terms, the power of the global test increases with an increase in the prevalence and/or the verification probabilities, and the power is greater than 80%-90% with samples of 500. Furthermore, Method 1 has a greater power than the global test because (as in the case of the two diagnostic tests) its type I error is greater. Methods 2, 3 and 4 have a power which is slightly lower than the global test, especially for samples of between 100 and 400 individuals.

3.3. Conclusions

From the results of the simulation experiments carried out to simultaneously compare the *LRs* of two and three diagnostic tests respectively, it holds that in general terms the best method to solve this problem of inference is the global test based on the chi-squared distribution, since its type I error performs better around the nominal error than the type I error of each one of the other methods. From these results, the following method is proposed to compare the likelihood ratios of J binary diagnostic tests: 1) Solving the global hypothesis test based on the chi-squared distribution to an error rate of α ; 2) If the global hypothesis is significant to an error rate of α , the investigation of the causes of the significance must be carried out comparing the positive (negative) likelihood ratios of each pair of diagnostic tests applying a multiple comparison method (Bonferroni, Holm or Hochberg) to an error α . Step 2 must be carried out applying a multiple comparison method and not each marginal test to an error rate of α , since the latter has a type I error that clearly overwhelms the nominal error.

4. Application

The results obtained in previous Sections were applied to the diagnosis of coronary stenosis, a disease that consists of the obstruction of the coronary artery and its diagnosis can be made through a dobutamine echocardiography, a stress echocardiography or through a *CT* scan, and as the gold standard a coronary angiography is used. As the coronary angiography can cause different reactions in individuals (thrombosis, heart attack, infections, etc.), not all of the individuals are verified with the coronary angiography. In Table 5, we show the results obtained when applying the three diagnostic tests and the gold standard (T_1 : dobutamine ecocardiography; T_2 : stress echocardiography; T_3 : *CT* scan) to a sample of 2455 spanish males over 45 and when applying the coronary angiography (D) only to a subset of these individuals. The data come from a study carried out at the University Hospital in Granada. This study was carried out in two phases: in the first phase, the three diagnostic tests were applied to all of the individuals; and in the second phase, the coronary angiography was applied only to a subset of these individuals depending only on the results of the three diagnostic tests. Therefore, in this example it can be assumed that the missing data mechanism is *MAR* and the model is ignorable, and therefore the results of the previous sections can be applied. The values of the estimators of the *LRs* are $\widehat{LR}_1^+ = 5.31$, $\widehat{LR}_2^+ = 3.04$, $\widehat{LR}_3^+ = 7.61$, $\widehat{LR}_1^- = 0.13$, $\widehat{LR}_2^- = 0.33$ and $\widehat{LR}_3^- = 0.09$. Applying equation (3) it holds that $Q^2 = 126.20$ (p-value = 0) and therefore we reject the joint equality of the *LRs*. In order to investigate the causes of the significance, the step is to solve the marginal hypothesis tests. In Table 6, we show the results obtained for each one of the six hypothesis tests that compare the *LRs*. Then a method of multiple comparisons (Bonferroni, Holm or Hochberg) is applied and it is found that (with the three methods) the three positive likelihood ratios are different, and the biggest one is that of the *CT* scan, followed by that of the dobutamine echocardiography and finally that of the stress echocardiography. Regarding the negative likelihood ratios, no significant differences were found between that of the dobutamine echocardiography and that of the *CT* scan; whilst the negative likelihood ratio of the stress echocardiography is significantly larger than that of the dobutamine echocardiography and that of the *CT* scan.

5. Discussion

Likelihood ratios are parameters that allow us to assess and compare the performance of binary tests, and technically they are equivalent to a relative risk. In the presence of partial disease verification, the disease status of a subset of individuals in the sample is unknown, and therefore the estimation and comparison of the likelihood ratios of two or more diagnostic tests cannot be made using the existing models (Leisenring and Pepe, 1998; Roldán Nofuentes and Luna del Castillo, 2007), since the results are affected by verification bias. In this article, a global hypothesis test is proposed to simultaneously

Table 5: Data from the study of coronary stenosis.

	$T_1 = 1$				$T_1 = 0$				Total
	$T_2 = 1$		$T_2 = 0$		$T_2 = 1$		$T_2 = 0$		
	$T_3 = 1$	$T_3 = 0$	$T_3 = 1$	$T_3 = 0$	$T_3 = 1$	$T_3 = 0$	$T_3 = 1$	$T_3 = 0$	
$V = 1$									
$D = 1$	457	30	84	5	34	0	7	1	618
$D = 0$	41	23	5	61	16	86	32	95	359
$V = 0$	92	31	85	120	42	195	88	825	1478
Total	590	84	174	186	92	281	127	921	2455

Table 6: Results of the marginal hypothesis tests.

Hypothesis test	z	Two sided p-value
$H_0 : LR_1^+ = LR_2^+$ vs $H_1 : LR_1^+ \neq LR_2^+$	6.24	4.47×10^{-13}
$H_0 : LR_1^+ = LR_3^+$ vs $H_1 : LR_1^+ \neq LR_3^+$	3.30	0.001
$H_0 : LR_2^+ = LR_3^+$ vs $H_1 : LR_2^+ \neq LR_3^+$	7.29	3.06×10^{-13}
$H_0 : LR_1^- = LR_2^-$ vs $H_1 : LR_1^- \neq LR_2^-$	7.53	5.15×10^{-14}
$H_0 : LR_1^- = LR_3^-$ vs $H_1 : LR_1^- \neq LR_3^-$	1.77	0.077
$H_0 : LR_2^- = LR_3^-$ vs $H_1 : LR_2^- \neq LR_3^-$	9.19	0

compare the likelihood ratios of two or more diagnostic tests assuming that the missing data mechanism is ignorable. The assumption of ignorability (Schafer, 1997), which is widely used in this field, means that the selection of an individual to verify the disease status depends only on the results of the diagnostic tests and not on the disease status. This assumption cannot be made from the data observed, but rather depends on how the experiment is conducted. Thus, for example, in two phase studies, if in the second phase the selection of the individuals is made depending on the results of the diagnostic tests, then it can be assumed that the missing data mechanism is ignorable. If the verification process depends on the disease status, the missing data mechanism is not ignorable and the model proposed in this article cannot be applied.

Simulation experiments were carried out to study the type I error and the power of the global test and of other alternative methods, from which the following method was proposed to compare the likelihood ratios of two or more diagnostic tests in the presence of ignorable missing data: 1) Apply the global hypothesis test based on the chi-squared distribution to an error rate of α (equation (3)); 2) If the global hypothesis test is significant to an error rate of α , investigating the causes of the significance solving the marginal hypothesis tests (expression (4)) along with the a multiple comparison method (Bonferroni, Holm or Hochberg). This procedure is similar to the one used in a analysis of variance. Firstly, the global test is solved and then a multiple comparison method is applied. The simulation experiments have also shown that the positive

and negative likelihood ratios cannot be compared independently (Method 1 of the simulation experiments), since the type I error clearly overwhelms the nominal error.

The problem posed in this article can also be solved using the natural log-likelihood ratios. Simulation experiments (similar to those in Section 3 and from the same samples) were carried out using this transformation and it was found that there is no important difference between the results obtained, in terms of type I error and power, and those obtained in Section 3. Therefore, it is recommendable to make the comparison without using this transformation.

Acknowledgements

This research was supported by the Spanish Ministry of Science, Grant Number MTM 2012-35591. We thank the two referees, the Associate Editors (Montserrat Guillén Estany and David Conesa) of SORT for their helpful comments that improved the quality of the paper.

Appendix

Let us suppose that we wish to check K hypothesis tests, H_{0k} vs H_{1k} , with $k = 1, \dots, K$, and let p_k be the p-value obtained by solving each hypothesis test. Let $p_{[1]} \leq p_{[2]} \leq \dots \leq p_{[K]}$ be the p-values in order from the lowest to the highest, so that $p_{[k]}$ is the p-values corresponding to the hypothesis test $H_{0[k]}$ vs $H_{1[k]}$.

The Holm method (1979) consists of the following steps:

- Step 1.** If $p_{[1]} \leq \alpha/K$ then reject hypothesis $H_{0[1]}$ and go to the next step; otherwise finish.
- Step 2.** If $p_{[2]} \leq \alpha/(K-1)$ then reject hypothesis $H_{0[2]}$ and go to the next step; otherwise finish...
- Step K.** If $p_{[K]} \leq \alpha$ then reject hypothesis $H_{0[K]}$ and finish.

The Hochberg method (1988) consists of the following steps:

- Step 1.** If $p_{[K]} \leq \alpha$ then reject $H_{0[k]}$ with $k = 1, \dots, K$ and finish; otherwise go to the next step.
- Step 2.** If $p_{[K-1]} \leq \alpha/2$ then reject $H_{0[k]}$ with $k = 1, \dots, K-1$ and finish; otherwise go to the next step...
- Step K.** If $p_{[1]} \leq \alpha/K$ then reject hypothesis $H_{0[1]}$ and finish.

References

- Agresti, A. (2002). *Categorical Data Analysis*. New York: Wiley.
- Begg, C. B. and Greenes, R. A. (1983). Assessment of diagnostic tests when disease verification is subject to selection bias. *Biometrics*, 39, 207–215.
- Bonferroni, C. E. (1936). Teoria statistica delle classi e calcolo delle probabilità. *Pubblicazioni del R Istituto Superiore di Scienze Economiche e Commerciali di Firenze*, 8, 3–62.
- Hochberg, Y. (1988). A sharper Bonferroni procedure for multiple tests of significance. *Biométrica*, 75, 800–802.
- Holm, S. (1979). A simple sequential rejective multiple testing procedure. Scandinavian. *Journal of Statistics*, 6, 65–70.
- Leisenring, W. and Pepe, M. S. (1998). Regression modelling of diagnostic likelihood ratios for the evaluation of medical diagnostic tests. *Biometrics*, 54, 444–452.
- Luts, J., Roldán Nofuentes, J. A., Luna del Castillo, J. D. and Van Huffel, S. (2011). Asymptotic hypothesis test to compare likelihood ratios of multiple diagnostic tests in unpaired designs. *Journal of Statistical Planning and Inference*, 141, 3578–3594.
- Roldán Nofuentes, J. A. and Luna del Castillo, J. D. (2005). Comparing the likelihood ratios of two binary diagnostic tests in the presence of partial verification. *Biometrical Journal*, 47, 442–457.
- Roldán Nofuentes, J. A. and Luna del Castillo, J. D. (2007). Comparison of the likelihood ratios of two binary diagnostic tests in paired designs. *Statistics in Medicine*, 26, 4179–4201.
- Rubin, D. B. (1976). Inference and missing data. *Biometrika*, 4, 73–89.
- Schafer, J. L. (1997). *Analysis of Incomplete Multivariate Data*. USA: Chapman and Hall/CRC.
- Torrance-Rynard, V. L. and Walter, S. D. (1997). Effects of dependent errors in the assessment of diagnostic test performance. *Statistics in Medicine*, 16, 2157–2175.
- Vacek, P. (1985). The effect of conditional dependence on the evaluation of diagnostic tests. *Biometrics*, 41, 959–968.
- Zhou, X. H. (1993). Maximum likelihood estimators of sensitivity and specificity corrected for verification bias. *Communication in Statistics-Theory and Methods*, 22, 3177–3198.

**Information for authors
and subscribers**

Author Guidelines

SORT accepts for publication only original articles that have not been submitted simultaneously to any other journal in the areas of statistics, operations research, official statistics or biometrics.

Articles should be preferably applied and may include computational or educational elements. Publication will be exclusively in English. All articles will be forwarded for systematic peer review by independent specialists and/or members of the Editorial Board, except for those articles specifically invited by the journal or reprinted with permission. Reviewer comments will be sent to the first corresponding author if changes are requested in form or content.

To submit an article, the author must upload it in **PDF format**.

The article should be prepared in double-spaced **format**, using a 12-point typeface.

The **title page** must contain the following items: title, name of the author(s), professional affiliation and complete address, and an abstract (75100 words) followed by the keywords and MSC2010 classification of the American Mathematical Society.

Before submitting an article, the author(s) would be well advised to ensure that the text uses **correct English**.

Bibliographic references within the text must follow this format: author surname followed by the year of publication in parentheses [i.e., Mahalanobis (1936), Rao (1982b)]. The complete reference citations should be listed alphabetically at the end of the article, with multiple publications by a single author listed chronologically. Examples of reference formats are as follows:

- Article: Casella, G. and Robert, C. (1998). Post-processing accept-reject samples: recycling and rescaling. *Journal of Computational and Graphical Statistics*, 7, 139–157.
- Book: Gelman, A., Carlin, J. B., Stern, H. S. and Rubin, D. B. (2003). *Bayesian Data Analysis*, 2nd Ed. Chapman & Hall / CRC, New York.
- Chapter in book: Engelmann, B. (2006). Measures of a rating's discriminative power-applications and limitations. In: Engelmann, B. and Rauhmeier, R. (eds), *The Basel Risk Parameters: Estimation, Validation, and Stress Testing*. Springer, New York.
- Online article (put issue or page numbers and last accessed date): Marek, M. and Lesaffre, E. (2011). Hierarchical Generalized Linear Models: The R Package HGLMMM. *Journal of Statistical Software*, 39 (13). <http://www.jstatsoft.org/v39/i13>. Last accessed 28 March 2011.

Explanatory footnotes should be numbered sequentially and placed at the bottom of the corresponding page. **Tables and figures** should also be numbered sequentially.

Once the article has been accepted, the journal editorial office will **contact the author** with instructions about this final version, which should be submitted using **LaTeX**. The journal secretary will provide authors with LaTeX templates and appropriate references to the MSC2010 classification of the American Mathematical Society. All the submissions should be handled by RACO (Revistes Catalanes en Accs Obert) website.

New Authors: please register at: <http://www.raco.cat/index.php/SORT/user/register>. Upon successful registration you will be sent an e-mail with instructions to verify your registration.

Submission Preparation Checklist

As part of the submission process, authors are required to check off their submission's compliance with all of the following items, and submissions may be returned to authors that do not adhere to these guidelines.

1. The submitted manuscript follows the guidelines to authors published by SORT
2. Published articles are under a Creative Commons License BY-NC-ND
3. Font size is 12 point
4. Text is double-spaced
5. Title page includes title, name(s) of author(s), professional affiliation(s), complete address of corresponding author
6. Abstract is 75100 words and contains no notation, no references and no abbreviations
7. Keywords and MSC2010 classification have been provided
8. Bibliographic references are according to SORT's prescribed format
9. English spelling and grammar have been checked
10. Manuscript is submitted in PDF format

Copyright notice and author opinions



The articles are licensed under a Creative Commons Attribution-NonCommercial-NoDerivs 3.0 Spain License.

You must attribute the work in the manner specified by the author or licensor (but not in any way that suggests that they endorse you or your use of the work), you may not use the work for commercial purposes and you may not alter, transform, or build upon the work.

Published articles represent the author's opinions; the journal SORT-Statistics and Operations Research Transactions does not necessarily agree with the opinions expressed in the published articles.

SORT Statistics and Operations Research Transactions
Institut d'Estadística de Catalunya (Idescat)
Via Laietana, 58 08003 Barcelona. SPAIN
Tel. +34-93.557.30.76 – Fax +34-93.557.30.01
sort@idescat.cat

How to cite articles published in SORT

Commenges, D. (2003). Likelihood for interval-censored observations from multi-state models. *SORT*, 27 (1), 1-12.

Subscription form

SORT (Statistics and Operations Research Transactions)

Name _____
Organisation _____
Street Address _____
Zip/Postal code _____ City _____
State/Country _____ Tel. _____
Fax _____ NIF/VAT Registration Number _____
E-mail _____
Date _____
Signature

I wish to subscribe to ***SORT (Statistics and Operations Research Transactions)***
for the year 2014 (volume 38)

Annual subscription rates:

- Spain: €40 (4% VAT included)
- Other countries: €44 (4% VAT included)

Price for individual issues (current and back issues):

- Spain: €15/issue (4% VAT included)
- Other countries: €17/issue (4% VAT included)

Method of payment:

- Bank transfer to account number 2100 5000 50 0200051156
IBAN NUM. ES61 2100 5000 5002 0005 1156
- Check made payable to the Institut d'Estadística de Catalunya

Please send this subscription form (or a photocopy) to:

SORT (Statistics and Operations Research Transactions)

Institut d'Estadística de Catalunya (Idescat)

Via Laietana, 58

08003 Barcelona

SPAIN

Fax: +34-93-557 30 01